# Identification of adenovirus E1A gene regions involved in chemosensitisation of prostate cancer cells

Enrique Miranda Rota

A thesis submitted for the degree of Doctor of Philosophy

May 2009

Viral Gene Therapy Unit
Centre for Molecular Oncology and Imaging
Institute of Cancer
Barts and the London School of Medicine and Dentistry
Queen Mary University
Charterhouse Square
London
United Kingdom

# *Declaration*

I hereby declared that the work presented in this thesis is an original work done by the author, Enrique Miranda, at the Centre for Molecular Oncology and Imaging, Barts and the London School of Medicine and Desntistry, Queen Mary University of London. All external sources have been properly acknowledged.

# *Acknowledgements*

I would like to thank Professor Nick Lemoine and Dr. Gunnel Hallden for giving me the opportunity to undertake this project. There are no words to express my gratitude to Dr. Gunnel Hallden; during my time here she has been an inspiring supervisor, showing how a positive attitude and constructive criticism are key skills to keep a team together while doing a great scientific work. I was once told that one's PhD supervisor is the person that more influences one's future scientific career. After this time under her supervision, my motivation to develop a scientific career is higher than ever was before; I could never express with words how grateful I am for this.

I would also like to thank all the members of the group, present and past: Stephan, Chiat, Daniel, Virginia, Katrina, Silvia, Gioia and Maria. We all started at the same time in what it was a new experience for us all: new lab, new country… They are responsible for the great time I have had during my thesis. It has been a pleasure and an honour to meet every one of you, not only professionally but also at a personal level, something that can be said to all members of the Centre for Molecular Onconlogy and Imaging.

I would also like to thank those who encouraged me to become a scientist; my family has always supported me, even though this implied not seeing them as often as we would like to. I also like to thank Dr. Eva Lana Elola, who supported me in those times that were more difficult for me.

# *Abstract*

Replication-selective adenoviruses are promising anti-cancer therapies (virotherapy). Viruses can be engineered to selectively target cancer cells by deleting viral genes involved in cell cycle regulation. These deletions impair replication in normal cells, as the virus cannot overcome cellular checkpoints and pro-apoptotic pathways triggered by the infection. In cancer cells, however, these pathways are often deregulated hence viral propagation is not affected by these deletions. Despite the efforts to maximise potency and selectivity of adenoviruses as therapeutic agents, efficacy was poor when evaluated alone in clinical trials. Enhancement of efficacy was demonstrated in combination with chemotherapy and radiotherapy. A requirement for virus-mediated sensitisation to chemotherapy and enhancement of efficacy is the expression of the early viral gene E1A. However, the exact E1A regions required for increased cell death have not yet been identified. The E1A proteins bind to a variety of cellular factors, including the transcriptional and cell cycle regulators p300/CBP and pRb. This thesis describes the use of replication-selective and replication-defective adenoviruses expressing different mutation of the E1A gene in order to identify regions involved in chemosensitisation of prostate cancer cell lines to two cytotoxic drugs, mitoxantrone and docetaxel. Synergistic interactions were observed with all replication-selective adenoviruses and mitoxantrone in a cell dependent manner. The results obtained indicate that mutations in the p300/CBP binding site, but not pRb, impaired the sensitising activity of E1A to the cytotoxic drugs. Expression of E1A enhanced the arrest in the G2/M phase induced by mitoxantrone and increased the percentage of apoptotic cells in a process dependent on E1A binding to p300/CBP. Deletion of this binding site also attenuated the potency of replicating adenoviruses, indicating that binding to p300/CBP plays a central role in sensitisation to chemotherapy and control of viral cycle in prostate cancer cells.

# *List of abbreviations*

Ab: antibody

Abs: absorbance

Ad: adenovirus

ADP: adenovirus death protein

AR: androgen receptor

ATCC: American Type Tissue Culture Collection

BSA: bovine serum albumin

CAR: coxsackie and adenovirus receptor

CBP: CREB binding protein

CD: cytosine deamidase

Cdk: cyclin-dependent kinase

CI: combination index

CMV: cytomegalovirus

COX2: cyclooxygenase 2

Cyt C: cytochrome C

CR: conserved region

CtBP: carboxy-terminal binding protein

CREB: camp response element binding

CRUK: Cancer Research UK

DHT: dihydrotestosterone

DMEM: Dubelcco's modified Eagle medium

$EC_{50}$: effective concentration at inducing 50% cell death

EGFR: epithelial growth factor receptor

EMT: epithelial messenchymal transition

FCS: foetal calf serum

GFP: green fluorescence protein

h: hours

HAT: histone acetyltransferase

HDAC: histone deacetylase

Ig: immunoglobulin

ITR: inverted terminal repeat

LHRH: Luteinising hormone releasing hormone

min: minutes

mRNA: messenger RNA

NFκB: Nuclear factor κB

NK: natural killer cells

NMR: nuclear magnetic resonance

OD: optical density

orf: open reading frame

P/CAF: p300/CBP associated factor

PCR: polymerase chain reaction

Pfu: plaque forming unit

PIN: prostatic intraepithelial neoplasia

PKA: protein kinase A

PKC: protein kinase C

PKR: protein kinase R

PP2A: protein phosphatase 2A

ppc: particles per cell

pRb: retinoblastoma protein

PSA: prostate specific antigen

PSMA: prostate specific membrane antigen

qPCR: quantitative PCR

rpm: revolutions per minute

s: seconds

SDS: sodium dodecyl sulphate

TBP: TATA-binding protein

$TCID_{50}$: tissue culture inhibitory dose 50%

TF: transcription factor

TK: thymidine kinase

TMRE: tetramethylrhodamine

TNF: Tumour Necrosis Factor

TRAIL: TNF-related apoptosis inducing ligand

TRAM: transcriptional adaptor motif

TRRAP: transactivation/transformation domain protein

vp: viral particles

UK: United Kingdom

# *Table of contents*

# Chapter 1

# *Introduction: Adenoviruses and E1A in gene therapy for prostate cancer*

## 1.1 Prostate cancer

Prostate cancer is the most common malignancy in men and second leading cause of cancer related death in men in Western countries. In the United Kingdom (UK) there are approximately 34000 new cases detected per year, and 10000 death patients per year would die from the disease, making a mortality of 30% (6). It also accounts for 25% of all the malignancies diagnosed in men and approximately the 12% of male deaths from malignant diseases (6). Prostate cancer is a malignancy affecting mostly elder men, with 60% of the cases diagnosed in men aged over 70 years (6). This implies that patients diagnosed with metastatic disease often die from causes not related to prostate cancer. In addition to age, ethnicity is recognised as an important factor in prostate cancer risk. African Caribbean men are more susceptible to this malignancy than Caucasian men, while men of Asian origin have the lowest risk (6, 7). In addition,

black men have a higher risk with development at a younger age, hence increasing the risk of dying from this malignancy. Interestingly, the incidence is 10 times higher in Western industrialised countries than in East Asian countries (8). Therefore the lifestyle, ethnicity and probably diet might contribute to prostate cancer development.

The prostate is a secretory gland, located just below the bladder, surrounding the urethra. Its secretions facilitate sperm mobility and also protects the male urinary and reproductive systems from pathogens (9). Development of the prostate is dependent on androgens, hormones that activate the androgen receptor (AR) expressed in the urogenital mesenchyme, inducing development of the gland (8, 10). In the adult prostate, AR is highly expressed in the stromal and secretory epithelial cells (8, 10).

The prostate is composed of a fibromuscular stroma and a glandular epithelial compartment. The glandular epithelium is composed of three different cell types: basal, secretory luminal and neuroendocrine. Anatomically, the glandular compartment can be divided into a large peripheral area and a small central zone. About 70% of prostatic cancers occur in the peripheral zone (8).

### 1.1.1 Development of prostate cancer

Most prostate cancers are classified as adenocarcinomas, as they occur more frequently in the glands of the peripheral area (8). The earliest precursor of prostate cancer is the prostatic intraepithelial neoplasia (PIN). It is defined as a neoplastic growth of the epithelial layer of cells within the prostatic acini. It is characterised by a loss of the layer of basal cells, although it expressed markers of basal and secretory cells (8). Prostate carcinoma develops due to abnormal cell

growth in PIN thought to be caused by a decrease in the apoptotic rate, since cells still show slow proliferation rates (8). Some reports suggest that only 1.3% of prostate cancer cells enter S-phase per day (11). At this stage, expression of AR and the prostate specific antigen (PSA) are increased. PSA is hence used as a marker for early diagnosis of the malignancy.

Prostate carcinoma is first localised within the gland; usually several foci can be found, varying in their degree of dysplasia and heterogeneity (8). At an early stage, the growth of prostate carcinomas is dependant on androgens, as AR controls growth. The AR is active after binding to hormones such as testosterone. However, the disease becomes androgen independent as it progresses, even though AR is still expressed (8). At a late stage, AR can be activated in the absence of androgens, increasing the growth rate of the tumour. This occurs approximately two years after diagnosis of a localised carcinoma (6). AR can be activated in this case by growth factors or become hypersensitive to androgens (7). In other cases, mutations in the AR alter the affinity or specificity to its ligands and can bind coactivators in a ligand-independent fashion. Gene amplification of the AR has also been reported (8). As a result of these alterations, the malignancy becomes more aggressive (7, 8, 10).

At this late stage, prostate cancers metastasise to local lymph nodes and spread to distal organs in 90% of the cases. A third of prostate carcinomas become invasive, most frequently invading organs such as lung, liver and bone (8). These metastasic tumours are aggressive, with a doubling time faster than that of early stage localised carcinoma.

### 1.1.2 Current treatments for prostate cancer

Treatments depend on the progression of the cancer. A widespread detection of PSA levels has contributed to earlier detection (6, 8). Active surveillance, also called active monitoring or watchful waiting, is now often done after early diagnosis in the UK. Treatment with more invasive therapies can cause side effects and might not increase survival when detection is at an early stage due to the slow growth of prostate cancer and the normally advanced age of the patients (6). If further growth of the tumour is observed, the next treatment could be radiotherapy or surgery. Surgery, also called radical prostatetomy, implies the surgical removal of part or the whole gland. However, this procedure has severe side effects including impotence and urinary dysfunctions (6). Radiotherapy can be administered by external beam irradiation or brachytherapy, also known as sealed source radiotherapy (6). Brachytherapy consists of seeds, small radioactive rods implanted in he prostate that release radiation locally at the tumour site. New therapies are also available for localised prostate cancer, including cryotherapy and high frequency ultrasound therapy, although they are not yet considered standard procedures (6).

Treatments for localised prostate carcinoma are often combined with hormone treatments; prostate carcinoma cells depend on androgens to proliferate, hence hormone depletion reduces the growth rate of tumours. Patients that are not fit enough to receive invasive therapies might be treated by hormone deprivation on its own (6). Androgen deprivation is achieved by orchiectomy or, most commonly, chemical castration. Combination of both treatments can also be used, called total androgen blockade. Orchiectomy is the surgical procedure of castration, while chemical castration is the use of androgen agonists and antagonists to block AR activity. Some chemicals (pituitary downregulators, including goserelin, buserilin and leuprorelin) target the production of

testosterone induced by the luteinising hormone and gonadotropin produced in the pituitary gland while anti androgens stop the testosterone produced in the testicles from getting into cancer cells (6, 12). Flutamide and bicalutamide are examples of anti androgens used currently in the clinic (6). Pituitary down regulators are better known as luteinising hormone releasing hormones (LHRH).

Hormone therapies are the only treatment when prostate carcinoma becomes more aggressive and metastasises to other organs (6). However, it is unclear whether androgen depletion is curative at this stage. At late stage, prostate cells can become hormone independent, so androgen deprivation would only eliminate those hormone dependent, less aggressive cells (8). Chemotherapy can be used as therapy in these cases and has been found efficient in some cases, although ultimately, tumours become resistant to these agents.

#### 1.1.2.1 Chemotherapy in prostate cancer

Chemotherapy has shown efficacy in the treatment of high-risk hormone refractory prostate carcinoma. Most commonly used cytotoxic drugs include mitoxantrone and docetaxel.

Mitoxantrone is a synthetic anthracenedione, was originally synthesised in 1979 as a doxorubicin analogue. The FDA approved mitoxantrone for the treatment of adult acute myeloid leukaemia in 1987, for hormone-refractory prostate cancer in 1996 and for the treatment of multiple sclerosis in 2000 (13). Mitoxantrone has a circulating half-life ranging from 8.9 hours to 9 days and is rapidly taken up by the tissues, persisting in the body for as long as 272 days (13).

Mitoxantrone is a topoisomerase II inhibitor (14) and also intercalates in the DNA, causing cross-linking that together with topoisomerase II inhibition

results in defective DNA repair and apoptosis. Recent studies have shown that mitoxantrone also has an inhibitory effect on microtubule assembly and induces G2/M phase arrest (15). Other biological effects have been described, including electrostatic interactions with DNA, DNA-protein cross-links, prostaglandin byosynthesis and calcium release (16). Mitoxantrone affects both dividing and non-dividing cells and has immunomodulatory effects by suppressing proliferation of macrophages, T and B cells (13). It also decreases the secretion of cytokines, impairs antigen presentation (13) and controls caspase-2 mRNA levels (14). Mitoxantrone is usually administered by rapid intravenous infusion at 3-weekly intervals, although it can also be administered by continous infusion or daily or weekly repeated doses (16). Side effects have been reported after mitoxantrone administration; the most common side effects include drop in the number of white and red blood cells, resulting in higher risk of infections, tiredness and anaemia. Some patients have experienced diarrhoea, loss of hair and mild liver damage (6).

Docetaxel is a taxane that stabilises microtubules and arrests their depolymerisation by binding principally to β-tubulin monomers (17). Consequently, mitosis is impaired and cells are arrested in the G2/M phase. In addition, it inactivates Bcl-2 by phosphorylation. Docetaxel has been shown to induce mitotic catastrophe, an alternative path to cell death (17). Rather than a mode of cell death, mitotic catastrophe is considered an irreversible trigger for cell death, characterised by chromosome missaggregation and imperfect cell division. Adverse effects have been reported after docetaxel treatment, including hypersensitivity reactions, bone marrow suppression, peripheral neuropathy, fluid retention, alopecia and others (18).

Docetaxel is administered in the clinic in combination with prednisolone, or its pro-drug prednisone and is replacing mitoxantrone as the chemotherapy of

choice for prostate cancer, mainly due to cost-benefit ratios rather than other reasons. (18).

### 1.1.3 Alterations in prostate cancer at the cellular level

Chromosomal alterations are not frequent in early stage prostate carcinomas; although deletions of chromosomal segments are observed in early stages, amplifications become predominant at a late stage (19). Decreased copy numbers and loss of heterozygosity of chromosome 8p and 13q are frequently observed in prostate carcinomas, while the most commonly amplified region is 8q, often in metastatic tumours. Loss of 17p and 10q are also observed in late stage carcinomas (8, 19).

At the gene level, loss and mutation of p53 and PTEN have been reported to be involved in the progression of the disease to a more aggressive stage. In addition, loss of 13q implies loss of the retinoblastoma protein (pRb) gene (8). However, there are indications that the role of pRb in prostate cancer progression might not be decisive, as one allele is usually intact. Some reports indicate loss of expression of pRb as prostate carcinomas become more aggressive, although there was not a statistically significant correlation between malignancy and pRb expression (20). Interestingly, other reports showed that loss of expression of p130, a pRb family member, correlated with progression of the disease and that the pRb/p130 ratio could be used as a prognostic tool for prostate carcinoma (21).

Together with loss of these tumour suppressor genes, up-regulated expression of oncogenes has also been observed. Bcl-2, a p53 repressor, is overexpressed in approximately half of the prostate carcinomas (8). Bcl-2 is detected in the epithelium of PIN, but not in normal secretory cells; there are

indications that the AR activity could control expression of Bcl-2 in PIN and early stage carcinomas, suggesting a mechanism that partially explains the dependance on hormones in prostate cancer (8). This is also observed in prostate cancer cell lines; the expression of Bcl-2 in the LNCaP cell line is androgen dependent (8). Overexpression of Ki-67, a known marker for proliferation, has also been reported in prostate carcinomas, showing that its expression correlates with the expression of AR (10). However, it has also been observed that Bcl-2 is deregulated in the absence of AR activity in more advance carcinomas, indicating further alterations in the expression of the oncogene that do not depend on androgens (22).

MYC is another oncogene that is often overexpressed in prostate tumours. Interestingly, MYC is a negative regulator of p27, also found to be down-regulated in prostate cancer (8). The p27 protein is a cyclin-dependent kinase (cdk) inhibitor that blocks phosphorylation of cyclin D1, hence controlling the G1 cell cycle checkpoint (21). Overexpression of MYC together with down-regulation of p27 would therefore inactivate this checkpoint and allow progression to S-phase. In addition, androgen independence of prostate carcinomas correlates with overexpression of MDM2 and cyclin D1 (8, 23).

Other changes at the molecular level correlate with the progression to an androgen independent stage. The expression profiles of different AR coregulators change as the disease progresses to a more undifferentiated and aggressive stage (20, 24). The expression of the transcription factor p300 increases during prostate carcinogenesis and it has been related to an increase in proliferation in androgen independent carcinomas (20, 25). The steroid receptor coactivator Src-1 is also commonly overexpressed in prostate carcinomas; it induces the activation of the AR, promoting proliferation (24).

Gene silencing by methylation is also altered in prostate cancer. Methylation of DNA at cytosines of CpG dinucleotides alters the interactions of

DNA with transcription factors, inhibiting transcription of methylated genes (8). There is evidence that genes such as GSTP1 encoding the glutathione-S-transferase π isozyme, are silenced in prostate cancer by methylation (8). Another example of downregulation by aberrant methylation is the CDKN2 (p16/MTS1), a negative regulator of the G1/S checkpoint; this downregulation is only partially explained by methylation as loss of the 9p chromosome, where this gene is allocated, is also found in prostate carcinomas (8, 26).

## 1.2 Adenoviruses

Adenoviruses were first isolated in 1953 by Rowe and colleagues, who were searching for etiologic agents of acute respiratory infections (1). However, adenoviruses are not the etiologic agents for the common cold and only account for a small portion of respiratory morbidity in the general population (1). Soon it was discovered that there were multiple serotypes with a common complement fixation antigen (27). They were first called adenoid degeneration agents, but in 1956 the name of adenoviruses was adopted, given after the tissue (adenoid) in which they were discovered (1, 27). Today, more than 100 members of the adenovirus group have been identified (1); 51 serotypes are known to infect humans (27). The use of adenoviruses in research led to important discoveries. First, Ad12 was demonstrated to be oncogenic in rodents. Secondly, the splicing of messenger RNA (mRNA) was first observed in adenoviruses (1, 28). In addition, the adenoviral E1A gene has been widely used to investigate cellular mechanisms controlling the cell cycle and its regulation by proteins such as pRb.

Adenoviruses are non-enveloped, icosahedral particles encapsidating a linear, double-stranded DNA genome (29). They constitute the Adenoviridae

family, which is divided into 4 genera Mastadenovirus, Aviadenovirus, Atadenovirus and Siadenovirus; a fifth genus is likely to be added (28). This division is based on the hosts for the viruses within each genus; mastadenovirus infect mammals, aviadenoviruses are found in birds and the other two genera infect a broader range of hosts, including reptiles and amphibians (28). Within each genus, viruses are subdivided into species according to their specific hosts and supplemented with a letter; in the cases of human viruses, they are divided in 6 species: HAdV-A, HAdV-B, HAdV-C, HAdV-D, HAdV-E and HAdV-F, all belonging to the Mastadenovirus genus (28). Each species contains several serotypes of adenoviruses; serotype Ad12 belongs to the HAdV-A species, while Ad2 and Ad5 are classified as HAdV-C viruses.

Although adenoviruses are not responsible for the common cold, infection can lead to acute febrile respiratory disease, pertussis-like syndrome, eye infections, meningoencephalitis and some gastrointestinal disorders (27).

## 1.2.1 Structure of adenovirus

### 1.2.1.1 The viral capsid

The icosahedral protein shell or capsid measures 70 to 100 nm in diameter (1). It comprises 252 capsomeres, of which 240 are hexons and 12 are pentons situated at the vertices of the icosahedral capsid. From each penton a fiber is projected, composed of proteins and traces of carbohydrates (1). There are 11 known proteins forming the viral particle, 7 constituting the capsid and 4 proteins in the core, organising the genomic structure and bridging between capsid and genome (1). The capsid constitutes approximately the 87% of the mass of the adenovirus (1). A diagram of an adenovirus particle can be found in Fig. 1.

The hexon capsomere is composed of three molecules of poplypeptide II (1). The hexon is stabilised by three different proteins: polypeptides VI, VIII and IX. In addition, polypeptides VI and VIII are thought to act as bridges between the capsid and the core components of the virus (1). The structure of the hexon capsomere forms a structure with a hexagonal base with a triangular top facing the outside of the capsid (1). Along the hexagonal bases of each capsomere in the same facet, polypeptide IX stabilises interactions between adjacent hexons. Hexons of adjacent facets are joined by the polypeptide IIIa and polypeptide VI anchors the ring of peripentonal hexons on the inside surface (1).

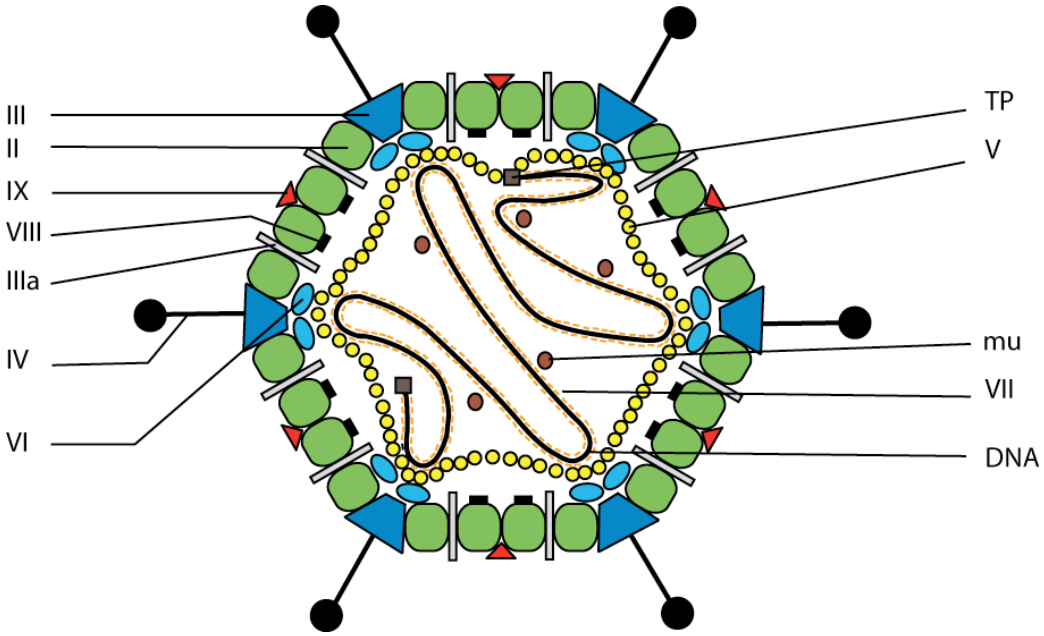


**Fig. 1.** Structure of an adenovirus. The viral DNA is packed with polypeptide VII and stabilise by polypeptide mu and V. The capsid is formed by polypeptide II (hexon capsomeres) and polypeptide III (penton base); polypeptides IIIa, VI, VIII and IX stabilise the capsid structure. A fiber of polypeptide IV, together with the penton base, forms the penton capsomere. Adapted from Shenk, 2001 (1).

The penton capsomere is formed by a penton base and a fiber. The penton base is also an association of a polypeptide. Five molecules of polypeptide III form the penton base. The fiber protein is composed of a trimeric association of polypeptide IV, than in the case of Ad5 is later modified by addition of glucosamine (1). The 40 residues at the amino-terminus of the fiber are embedded in the penton base.

The core of the viral particle contains four known proteins. The structure and organisation of the core remains unclear, and so is the function of some proteins in the core. Protein mu is a small arginine-rich protein found in the core, but its function remains unknown (1). Polypeptide V can bind to the penton base, probably acting as a bridge between the capsid and the core (1). Polypeptide VII is the most abundant protein of the core and acts as a histone-like centre around which viral DNA is wrapped (1). It is also involved in viral chromatin organisation in particles composed of DNA and polypeptide VII (1). The last protein found in the virion core is the terminal protein, attached to the ends of the viral DNA. This protein serves as a primer for DNA replication and mediates attachment of the viral genome to the nuclear matrix (1).

#### 1.2.1.2 Genome organisation

The genome organisation of adenoviruses varies among virus genera; genes common to all modern adenoviruses are located centrally in the genome and are involved in replication, DNA packaging and capsid formation (28). The linear genome of Ad5 contains two identical origins of replication at each terminal repeat (1). A diagram representing the genome organisation of Ad5 can be found in Fig. 2 and a detailed list of genes and proteins coded in Table 1. Near the genome left terminus there is a cis-acting packaging sequence that interacts with

the structural proteins of the capsid during the formation of new virions after infection (1). Viral genes can be classified according to their time of expression after infection, being early, delayed early or late genes. Early genes include E1A, E1B, E2, E3 and E4 coding for different proteins with functions that involve preparation of the infected cell for efficient viral replication and modulation of the host immune response targeting infected cells. Delayed early genes are expressed early after infection but after the expression of early genes; they code for protein IX and IVa2, both involved in transcription of late genes. Late genes are the last viral genes to be expressed, coding for structural proteins and polypeptides that facilitate assembly of new virions. The late genes are divided in five families, termed L1 to L5 (1). Two genes, called virus-associated genes (VA genes I and II) that express short RNA molecules during the translation of viral mRNA (30). The function of all genes will be discussed later in this chapter.

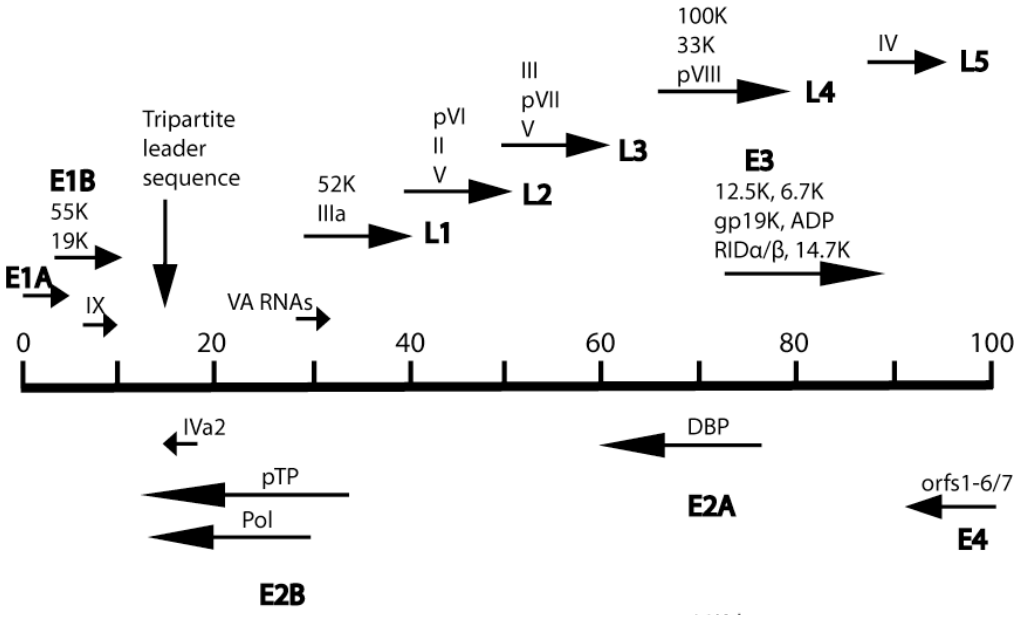


**Fig. 2.** Graphic representation of the Ad5 transcription map. Viral genes are classified in early (E1A, E1B, E2A, E2B, E3 and E4) and late units (L1 to L5); arrows indicate the direction of transcription of each gene. Adapted from Russell, 2000 (2).

Transcription of viral genes is executed by the RNA polymerase II, with the exception of the VA genes, that are transcribed by RNA polymerase III (1). Both strands of the viral DNA are transcribed; the rightward reading strand codes for E1A, E1B, IX, late genes, VA RNA and E3, and the leftward strand codes for E2, E4 and IVa2 genes. The E1B-19K, E1B-55K and protein IX genes are single exon structures (28). Other viral genes, however, are transcribed by splicing; all late genes, including all genes from the L1-52K unit to pVIII and fiber located in the rightward strand, are spliced from the tripartite leader sequence (28). All late mRNA share this sequence, as it facilitates translation (1). Preterminal protein (pTP), the viral DNA polymerase, E1A, E1B, E3 and E4 genes are also spliced. However, transcription of E1A, E1B and E4 is more complex; these genes give rise to several mRNAs and proteins by alternative splicing with different biological functions (28).

## 1.2.2 Viral cycle

### 1.2.2.1 Infection and entry into the cell

Viral infection starts with entry of virus into the cell. This is accomplished by interactions of the viral fiber knob with a cellular protein of the immunoglobulin superfamily, the coxsackie and adenovirus receptor (CAR) (31). CAR is a transmembrane protein that is involved in formation of tight-junctions and cell-cell adhesion complexes (32). Once the fiber knob is bound to CAR, the penton base binds to integrins $\alpha_v\beta_3$ and $\alpha_v\beta_5$ allowing internalisation by endocytosis (1). Internalisation of the virus is a very efficient event, with approximately 85% of the virus that binds to CAR being internalised within 10 minutes (1). The accepted model implies that binding to CAR only serves to

attach the virus particle to the cell, facilitating the interaction with integrins. It was reported that modifications in the CAR binding domain of the fiber impaired infection, while modification of the penton site interacting with the integrins did not affect infection in one study (33). Other researchers showed that the virus cannot be internalised in the absence of $\alpha_v$ integrins (34).

The penton and integrin interaction might not be the only mechanism for viral internalisation. It is possible that the penton base could interact with other integrins through sites that were not mutated in the study. In addition, heparan sulfate glycosaminoglycan and the $\alpha_v\beta_1$ have been implicated in viral attachment and internalisation (35, 36). On the other hand, infection is proportional to CAR expression; overexpression of CAR in transgenic mouse models resulted in an increased infectivity of tissue that was normally poorly infectable (37). The suggestion that CAR only functions as an anchorage protein for adenovirus is based on manipulation of the cytoplasmic and transmembrane domains of CAR. If CAR was also involved in internalisation, truncation of these domains would have an effect on viral entry. However, was demonstrated that expression of the extracellular domain of CAR attached to the cell surface by a glycolipid was sufficient to allow viral infection (38, 39). One of these reports suggested that the absence of cytoplasmic and transmembrane domains actually increased the efficiency of the internalisation, even though the mechanisms remained unclear (38). In addition, alternative modes of infection have been described *in vivo*. It was reported that coagulation factors like Factor X can bind to hexon capsomeres and that this interaction modulates infection of hepatocytes *in vivo* (40).

| | Protein | Function |
|---|---|---|
| **E1A** | (5 isoforms) | Activation of transcription |
| **E1B** | 55K | Inhibition of apoptosis; mRNA transport |
| | 19K | Bcl-2 homolog |
| **E2A** | DBP | DNA binding protein |
| **E2B** | Pol | Viral polymerase |
| | pTP | Primer for DNA replication; attachment to nuclear matrix |
| **E3** | 12.5K | Unknowm |
| | 6.7K | Signal-anchor protein; inhibitor of TRAIL |
| | gp19K | Inhibition of MHC class I presentation |
| | ADP | Virus release |
| | RID | Protection from TNF-mediated apoptosis |
| | 14.7K | Protection from TNF-mediated apoptosis |
| **E4** | Orfs1-6/7 | Activation of transcription; mRNA transport |
| **Delayed early** | IX | Stabilisation of hexon capsomeres |
| | IVa2 | Activation viral late transcription |
| **L1** | 52K | Encapsidation proccess |
| | IIIa | Bridge between penton and hexon |
| **L2** | pVI | Stabilisation: bridge between core and capsid |
| | II | Hexon capsomere |
| **L3** | III | Penton base |
| | pVII | Viral DNA packaging protein |
| | V | Packaging and stabilisation |
| **L4** | 100K | Translation of viral mRNA; encapsidation |
| | 33K | Transcription of late viral genes |
| | pVIII | Bridge between core and capsid |
| **L5** | IV | Fiber protein |
| **VA** | VA RNAs | Interferon antagonism, cellular mRNA block |

**Table 1.** List of viral proteins coded by the different adenoviral genes and their functions during infection. Viral genes are divided into early, delayed early and late genes; early and early delayed genes are involved in transcription, replication of the viral genome and escape from the host's immune system, while late genes are involved in viral mRNA translation and assembly of new viral particles.

After internalisation, the endosome containing the virion is rapidly disrupted and the virus moves quickly to the nucleus by interactions of hexon with microtubules, before the formation of an endosome (1). The virion is dismantled in the lysosome in an organised sequence of event to ensure successful delivery of viral DNA to the nucleus. The regulation of this process is unknown; virions escape the endosome when acidification of this compartment occurs, but this is not related to disassembly of the capsid (1). First, polypeptides IIIa and IV are lost, followed by degradation of polypeptide III and polypeptide VI by viral proteases. At this point, hexon is still bound to viral DNA through polypeptides VI and VIII that are consequently degraded to prepare transport of DNA to the nucleus. Finally, polypeptide IX, the last of the capsid proteins is lost, leaving

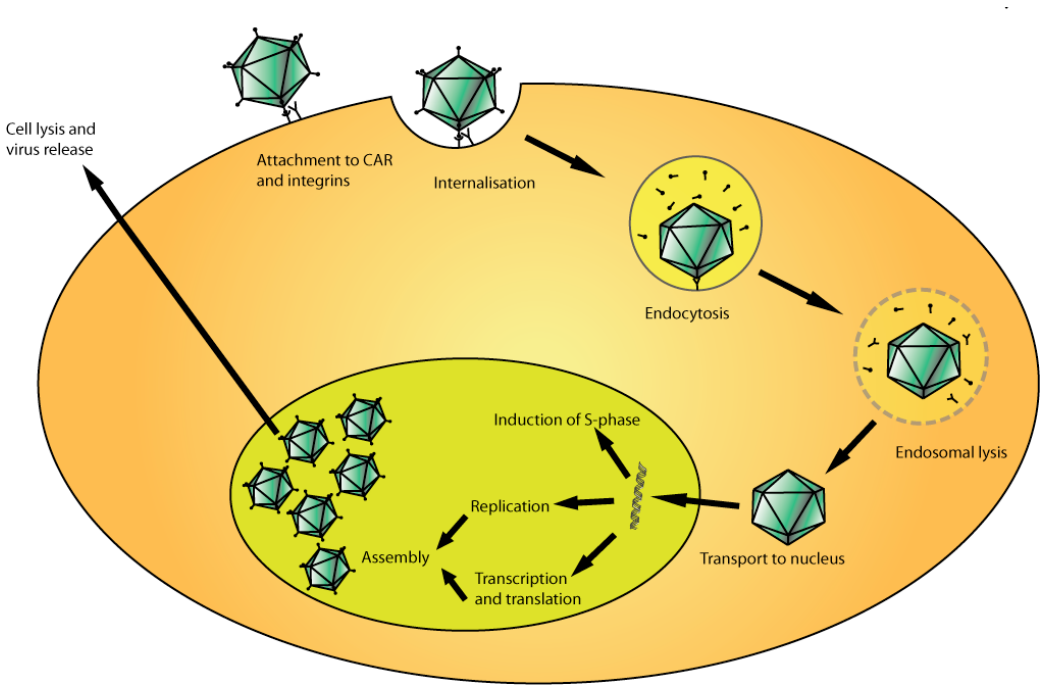


**Fig. 3.** Diagram showing an adenovirus infection cycle. After attachment to CAR and integrins, the viral particle is internalised in an endosome. The particle escapes from the endosome and viral DNA reaches the nucleus of the infected cell. Early viral genes prepare the cell for viral transcription and replication, resulting in the production of new viral particles that are release after lysis of the cell. Adapted from Kanerva *et al*, 2004 (5).

viral DNA free from the hexon (1). Viral DNA is transported to the nucleus through the nuclear pores entering the nucleus in a complex with polypeptide VII. It was thought that polypeptide VII was replaced by cellular histones to form a structure similar to cellular chromatin. However, there is yet no evidence of cellular histones binding to viral DNA. Currently it is believed that polypeptide VII forms a chromatin-like structure with the viral DNA. The terminal protein associates the viral DNA with the nuclear matrix, in a event that is essential for viral replication, as the terminal protein is necessary to activate viral gene expression (1).

#### 1.2.2.2 Activation of viral transcription

Transcription of viral genes is initiated after viral DNA entry to the nucleus and attachment to the nuclear matrix. First, the early viral genes are transcribed and expressed to induce S-phase in the infected cells and enable viral replication by protecting the infected cell from the host immune system and to synthesise viral proteins required for viral DNA replication (1). The first gene to be transcribed is E1A; it is controlled by a constitutively active promoter and codes for five products generated by alternative splicing (1). The two main proteins coded are 13S and 12S that are identical except for an additional 46 amino acid region present only in the 13S protein. All E1A proteins are named based on their respective sedimentation coefficients. The other three proteins coded by the E1A gene (11S, 10S and 9S) are expressed later in the cycle, but their function remains unclear (1). Expression of E1A-9S has only been observed in vitro (4). E1A proteins bind to cellular proteins and modulate their function to induce cellular S-phase entry and activation of the transcriptional machinery. More details about the function and role of E1A in adenovirus infection will be discussed in the next section of this chapter. The expression of E1A and its interactions with cellular proteins induce p53-dependent and p53-independent

apoptosis (1, 3, 41, 42). This is overcome by expression of E1B and E4 proteins; the E1B gene codes for two main proteins, E1B-19K and E1B-55K both with antiapoptotic properties (41, 43).

The E1B-55K protein inhibits p53-dependent apoptosis, while the E1B-19K protein blocks both p53-independent and p53-dependent apoptosis by interacting with BAX and BAK (41, 43). E1B-55K protein inhibits p53-mediated apoptosis by binding directly to p53 and blocking its transcriptional activation (43, 44). In addition, E1B-55K interacts with the E4orf6 viral protein to control viral mRNA export and viral ubiquitin ligase activity (41, 45). E1B-55K acts as a substrate-binding subunit that promotes degradation of p53, a second mechanism of downregulation of p53 by E1B-55K (41, 45). E1B-19K can block apoptosis induced by tumour necrosis factor (TNF), Fas ligand (FasL) or TNF related apoptosis inducing ligand (TRAIL) (41, 43). Deletions of the E1B-19K significantly reduced the viral yield in normal primary cells after TNF treatment (44). E1B-19K can functionally substitute for Bcl-2; activation of E1B-19K differs from Bcl-2 in that E1B-19K is not phosphorylated to be active (43). Although the sequence homology between the E1B-19K and Bcl-2 is weak, there are conserved residues that are common to both the viral and the cellular proteins (43). E1B-19K binds to the proapoptotic members of the Bcl-2 family BAX, BAK, BIK, BNIP1 and BNIP3 (30). The antiapoptotic properties of E1B-19K can mostly be attributed to the ability to bind BAK and BAX; E1B-19K binds BAK and abrogates the interaction with BAX, preventing activation of BAX, mitochondrial pore formation and release cytochrome c (Cyt c) (43). In addition, the E1B-19K protein has been shown to bind the intermediate filaments of the cytoskeleton in the cytoplasm and the nuclear lamina (46); this suggested a role of E1B proteins in regulation of the cytoskeleton that somehow promotes cell survival independent of anchorage, although these mechanisms remain unclear.

#### 1.2.2.3 Viral DNA replication

Viral replication starts when the E2a promoter is activated by E2F and E2 protein is accumulated (1). Viral DNA replication can be divided in two stages; first, replication starts from the terminus of the double-stranded DNA, displacing one of the original strands. Next, the displaced strand is circularised by annealing of the complementary termini; a complementary sequence is synthesised, forming a duplex of parental and daughter strands (1). Cis-Acting sequences within the inverted terminal repeats (ITRs) act as origin of replication (1). The ITRs are formed by three domains; domain A is essential for viral DNA replication, while domains B and C are not required but increase the efficiency of the process. Domains B and C bind to nuclear factor I (NFI) and nuclear factor III (NFIII) respectively and these interactions stabilise the replication complexes bound to the domain A (1). This replication complex is formed by an association of viral proteins coded by the E2 gene, the preterminal protein (pTP) and the DNA polymerase. The pTP binds to the origin of replication, where it is processed by proteolysis to generated the E2-coded terminal protein (TP). In addition, pTP is thought to preserve the integrity of the viral chromosome's terminal sequence during multiple rounds of replication (1). It forms a complex with the E2-coded DNA polymerase to allow replication of the DNA. The pTP binds to a deoxycytidine monophosphate (dCMP) after the polymerase is in place. The pTP-CMP serves a prime start for the polymerase to synthesise the new DNA strand. Another E2-coded protein is needed for chain elongation, the single-stranded DNA-binding protein; its polymerisation is essential for viral DNA strand separation (1). Polymerisation is also necessary for efficient elongation; the polymerase can travel the entire length of the viral chromosome after it has separated from pTP (1). Another nuclear factor, NFII, has been reported to contribute to viral DNA replication; it does not enhance the synthesis of new DNA, hence it must be needed to overcome DNA structural problems after extensive replication (1).

#### 1.2.2.4 Viral mRNA export and translation

One of the consequences of E1A expression is the release of free E2F transcription factor that binds to the promoter of the E2 viral gene, activating transcription of this gene and viral DNA replication. Other viral genes are also able to induce transcription of the viral genome by directing E2F to the E2 promoter (1, 47). Adenoviruses lacking E4orf6/7 do not show attenuated replication, hence this gene is not essential for initiation of transcription (47). However, viruses expressing E4orf6/7 under the control of the CMV promoter in the absence of E1A showed that E4orf6/7 expression was sufficient to displace E2F from pRb and re-direct it to the E2a viral promoter (47). This indicates that E4orf6/7 could act as an auxiliary gene to E1A, to ensure efficient binding of E2F to the E2a promoter. In addition, the E4 gene has shown to modulate apoptosis and control of mRNA export (45, 48-50). Apoptosis by p53-independent mechanisms has been described after expression of E4orf4 (49-51). Apoptosis by E4orf4 does not involve caspase activation but can be reversed by the anti-apoptotic protein Bcl-2 (49) and binding to the phosphatase 2A (PP2A) is a requirement for the induction of apoptosis (50, 51). Interestingly, there is evidence that the E4orf6 can inhibit p53-mediated apoptosis, but not p53-independent, and is able to cooperate with E1A in the transformation of baby rat kidney cells (44, 48). Additional research has shown similar properties for E4orf1 and E4orf3 (50). Some groups have suggested that inhibition of p53-mediated apoptosis by E4orf6 might be caused by the ability of this protein to control mRNA export from the nucleus (44, 52). E4orf6 control the mRNA interacts with pp32/leucine-rich acidic nuclear protein (pp32/LANP) and the complex is exported to the cytoplasm, where binds an AU-rich element (ARE) present within many proto-oncogenic mRNAs (52). E4orf3 and E4orf6 are known to play a role in mRNA export and the control of the alternative splicing of the three major late tripartite leader (51). E4orf6 binds to E1B-55K to control mRNA export; together, they allow nuclear export of late viral mRNAs, block export of cellular mRNA

and induce degradation of proteins like p53 by ubiquitination by E4orf6 ubiquitin ligase activity (45, 53). In fact, an adenovirus expressing a mutant E4orf6 lacking ligase activity was impaired for both ubiquitination of p53 and mRNA export from the nucleus, suggesting that degradation of a specific substrate is responsible for E4orf6/E1B-55K nuclear mRNA export (45).

Expression of adenovirus late genes starts during viral DNA replication, controlled by the major late promoter, activated by E1A proteins late during the infection (1). Late genes are organised into a single large transcription unit that is processed by poly-A site utilisation and alternative splicing by E4 proteins (1). This generates mRNAs classified into 5 families based on the poly-A addition sites, called L1 to L5 (1). Transcription of the late genes is achieved by the contribution of a cellular transcription factor called USF and a viral transcription factor coded by the viral delayed early gene IVa2, also involved in capsid assembly (1, 28). At this point, cellular mRNA fails to accumulate in the cytoplasm, while viral mRNAs are exported from the nucleus by the process mediated by E1B-55K and E4orf6 mentioned earlier in this chapter. Viral mRNA is then translated, but not cellular mRNA; selective translation of viral mRNA is facilitated by the inactivation of protein kinase R (PKR) and the expression of virus-associated RNAs (VA RNAs) (1, 30). VA RNAs are small RNA molecules that accumulate in the cytoplasm and protect viral mRNA from degradation, in addition to other functions, such as protection of the infected cell from interferon-mediated cell death (54). Another mechanism for selective translation of viral mRNA is the inactivation of the helicase activity of eIF-4F. Late viral mRNAs contain a sequence called the tripartite leader sequence, that allows translation by the ribosome in the absence of the helicase activity provided by eIF-4F, essential for translation of cellular mRNA (1). Another viral protein, the 100 K protein of the L4 family, also selectively activates late viral protein synthesis, as viruses with defects in this protein fail to produce viral proteins, even though they are able to block cellular mRNA translation (1).

#### 1.2.2.5 Assembly of new virions

The L4 100K protein is also involved in the assembly of new viral particles. It acts as a scaffold to assemble the three molecules of polypeptide II. Hexon capsomeres and penton base bound to the fiber accumulate in the nucleus to start the assembly of new capsids in a process that could involve L3 proteins. L3 proteins have shown protease activity that could be involved in the modification of structural proteins (1). Empty capsids are formed in a manner that requires interaction with the packaging signal located within the viral DNA. DNA is then encapsidated, beginning with the left end of the viral DNA, in a process that could involve the L152/55K proteins (1).

Viral particles are released after assembly through destruction of intermediate filaments of the cytoskeleton, leaving the cell prone to lysis (1). The action of the E3 11.6Kd protein, known as the adenovirus death protein (ADP), also plays a role in the destruction of the cell and consequent release of the virus, although the exact underlying mechanisms remain unknown (1, 41, 55, 56). E3 genes have also been reported to down-regulate E1A (57, 58). Two E3 proteins, E3-14.5K and E3-10.4K have been described to decrease E1A translation, but not mRNA levels. Consequently, E3 genes appear to be involved in both regulation of the viral cycle and evasion from the immune system (58).

#### 1.2.2.6 Escape from the host's immune system

The E3 genes code for 7 proteins involved in protection of the infected cell from the immune system and in viral release (30). Deletion of these genes has no adverse effect on viral toxicity and replication *in vitro*, but attenuates viral potency *in vivo* (35, 56, 59). The E3 promoter contains binding sites for several transcription factors, one of which is nuclear factor κB (NFκB). NFκB is induced

by TNF, so E3 is expressed in this context (30). It has been shown that the E3-14.7K protein protects from TNF-mediated apoptosis by a mechanism that involves down-regulation of the NFκB transcriptional activity mediated by several cytokines (60). However, other reports showed that E3-14.7K binds to NFκB antagonist to repress apoptosis and induce a NFκB-dependent survival pathway (1, 30). Probably, E3 proteins modulate NFκB activity to promote survival mechanisms and repress apoptosis induced by cytokines. Another E3 complex called RID also protects from TNF-mediated apoptosis; this complex is formed by two E3-coded proteins: RIDα and RIDβ (30). This complex avoids FasL and TRAIL related apoptosis by clearing the corresponding receptors from the cell surface. Another main protein encoded by E3 genes is the E3-gp19K protein that inhibits MHC class I presentation by direct binding and blocking of its transport to the cell surface (30, 61). However, some reports suggest that E3-mediated decreases in MHC class I cell surface presentation is not efficient, cell-dependent and does not prevent from MHC class I recognition at early times of infection (62). Expression of all E3-coded proteins after infection in immunocompetent hosts would allow initial escape from the immune system to achieve efficient viral replication (56).

## 1.3 E1A

E1A is the first gene to be expressed after viral internalisation, controlled by a constitutively active promoter (1). The Ad5 E1A gene starts at nucleotide 499 and ends at nucleotide 1632; it contains two exons, the first at nucleotides 560 to 1112 and the second located at nucleotides 1229 to 1542 (4). The second exon is followed by a stop codon and the poly-A coding region. The E1A gene codes for 5 different proteins (Fig. 4.B) generated from one transcript that is modified alternative splicing (Fig. 4.A) and not by post-translational proteolytic

degradation (63-65). The Ad5 E1A proteins were named based on their sedimentation coefficients (S) of their respective mRNAs: 13S, 12S, 11S, 10S and 9S (63) and contain 289, 243, 217, 171 and 55 amino acids respectively, with molecular weights ranging from 58 to 28 kDa (3, 64). The mRNAs share a common 5' and 3' termini but differ in size of their excised introns; the different mRNA are derived from the larger 13S product by alternative splicing (4, 64). These proteins are encoded in the same reading frame, although because of the structure of the 9S splice junction, the second exon of 9S is read in a different frame (63, 64). Analysis of the residues of E1A proteins of several human serotypes has identified three conserved regions (CRs) (1, 3, 66). These conserved regions, along with arginine at position 2, the PXDLS motif and a short run of basic residues at the C-terminus are regions common in different serotypes (3). The PXDLS together with the basic residues in the C-terminus are highly conserved and some researchers have named that region the conserved region 4 (CR4) (41). The sequence of the PXDLS pentapeptide only changes in one amino acid among different serotypes; in the case of Ad5, the amino acid sequence is PLDLS (41, 67). The other CRs are located within amino acids 40 and 80 (CR1), residues 121 to 140 (CR2) and 140 to 185 (CR3) (1, 4).

The 13S protein is the only E1A product that contains the CR3 and these 46 residues are the only missing in the 12S protein (1, 66). With the discovery of the 11S and 10S product, it was discovered that the CR3 was also present in the 11S product (4, 64). The 11S product lacks the CR1, while the 10S protein lacks both CR1 and CR3. The 9S protein is the only product that lacks all CRs (4). The three-dimensional structure of E1A proteins has yet to be determined, despite numerous efforts by X-ray crystallography and nuclear magnetic resonance (NMR) (42, 68). They contain a high percentage of proline residues that probably limits the formation of secondary structures (42).

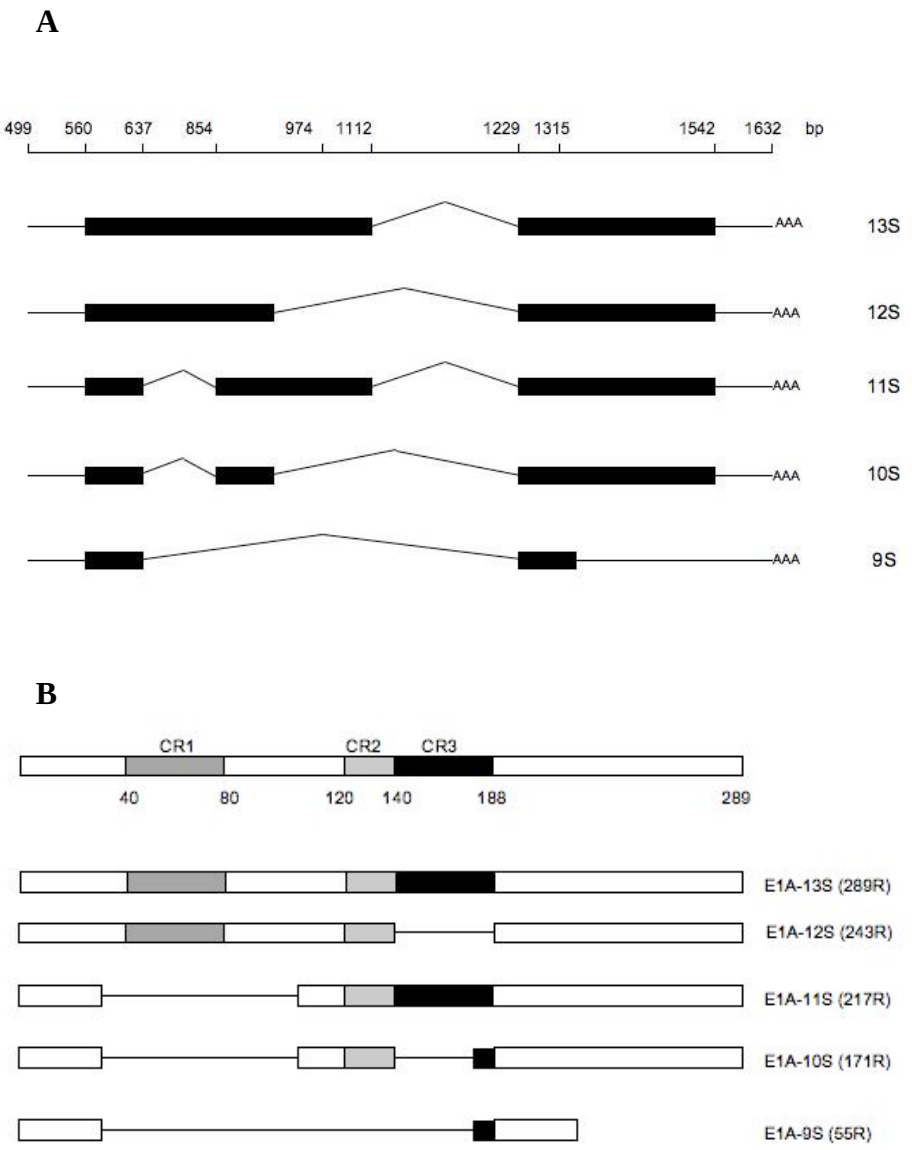


**Fig. 4.** Graphic rtepresentation of the E1A gene and the its products. A) Five E1A mRNA are generated by alternative splicing of the E1A gene. B) Translation of E1A mRNA produces 5 proteins. 13S and 12S are the main regulators of the entry into S-phase; these proteins only differ in the additional CR3 only present in 13S. Adapted from Mymryk, 1998 (4).

In addition, E1A contains segments of linear sequence that mediate protein interactions and that are characterised by local structural plasticity, also called structural disorder (68). This led to the concept that E1A is formed by a series of small modular domains, as deletions of small fragments generally interfere with a small subset of functions without affecting E1A activity globally (68). Although the three-dimensional structure of the complete E1A protein is not known, NMR has been used to resolved the structure of the N-terminal portion of CR3, found to from an α-helix, while CR4 has a series of β-turns (3). Informatical predictions suggest that the N-terminus of E1A contains a α-helix and three regions antiparallel strand (3, 68).

The E1A proteins are acidic, localised in equal amounts in both the cytoplasm and the nucleus and are degraded rapidly, with a half life of 20 to 80 minutes in infected cells (42) It was shown that the half life of 12S is approximately 80 minutes, while that of 13S is only 35 minutes, explaining why the concentration of the 12S protein is similar or greater than the concentration of 13S, despite mRNA levels for 13S being four times greater than for 12S (69).

E1A products are also post-translationally modified. E1A 13S and 12S are phosphorylated at serine residues 89, 96, 132 and 219, while 13S is also phosphorylated at residues 185 and 188 (42). Current evidence indicates that these translational modifications are not essential for E1A activity, although they might modify function since mutations at these sites have modest effects on various E1A activities (4, 42). There is also evidence of E1A modulation by acetylation of a lysine residue; acetylation of Lys-239 in the 12S proteins (Lys-285 in 13S) by p300 and P/CAF decreased the binding affinity of E1A to the carboxy-terminal bindin protein (CtBP) (70).

The different E1A products are not expressed at the same time during infection; 9S mRNA is detected only late during infection, while 13S and 12S are produced both early and late (66). E1A products can be detected already one hour after infection and continue to be expressed at about 90% of its maximal rate through 9 hours after infection (65).

### 1.3.1 Functions of E1A

The main functions of E1A proteins are to activate transcription of viral early promoters for expression of viral proteins and to activate the host cell in order to enter S phase and prevent cell cycle arrest and death, so that the cellular transcriptional machinery is directed towards transcription and translation of viral genes only (1).

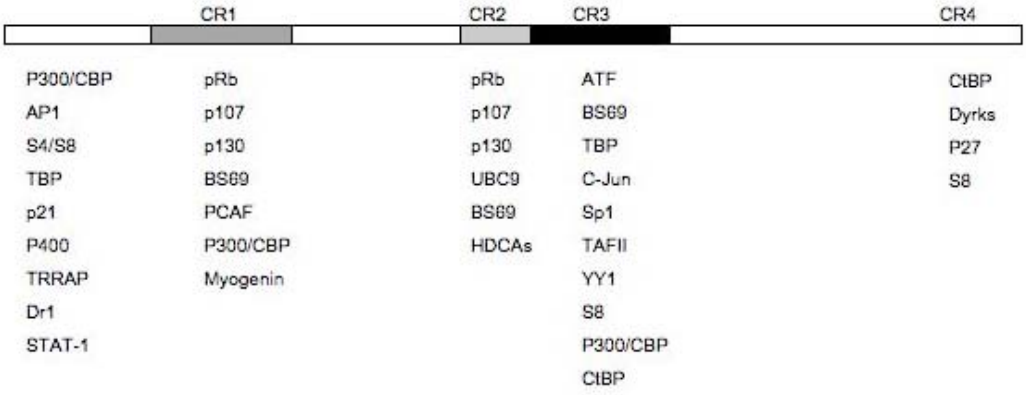


**Fig. 5.** Representation of E1A 13S, indicating the binding sites for the main E1A-interacting proteins. Adapted from Gallimore *et al*, 2001 (3).

#### 1.3.1.1 Entry into S phase

In order to activate the expression of early viral genes, E1A must first generate an optimum environment for transcription (3, 41, 71). E1A expression directs the cell to enter S phase so that the transcriptional machinery of the cell is available for viral transcription. It achieves this by interacting with multiple cellular proteins (Fig. 5) and modulating their function as E1A does not directly bind to DNA (72). The most important E1A interactions are binding to the pRb and the p300/CBP proteins (Fig. 6).

The retinoblastoma protein (pRb) family members, also called pocket proteins, are proteins responsible for cell cycle regulation. In the absence of mitotic stimuli, hypophosphorylated pRb is bound to E2F. In response to growth factors, pRb is phosphorylated by cyclin-dependent kinases (cdk), causing the release of E2F and induction of S phase. E1A can also displace E2F by binding to hypophosphorylated pRb through a LXCXE motif present in the CR2, amino acids 122 to 126 (73). The CR1 can also bind weakly to pRb, so this region was first thought to act as an auxiliary binding site (74, 75). However, the CR1 sequence that binds to pRb is similar to the E2F sequence that contact pocket proteins; for this reason, it has been suggested that E2F is ultimately removed from pRb by competition with CR1, although little is known about this interaction (75-78).

Binding to hypophosphorylated pRb by E1A overrides the phosphorylation-dependent regulation of pRb-E2F complexes. However, the transcriptional activity of pRb is not only regulated by the interactions with E2F. Rb not only represses E2F-dependent transcription, but also recruits histone deacetylases (HDACs), such as HDAC1, and methyltransferases such as HP-1 and SUV39H1, to promoter complexes to inactivate gene expression. In addition, pRb can bind members of the SWI/SNF family of transcripitional regulators

hBRM and BRG1 to induce cell cycle arrest (78). E1A is also able to displace these members of the pRb-associated complex to modulate the transcription of target genes. Interestingly, E1A was reported to overcome transcriptional repression in response to a dominant negative E2F chimaera that was generated by fusing E2F DNA-binding domain to pRb (42). These data indicated that E1A could overcome transcriptional repression independently of E2F release. Consequently, displacement of other members of the repression complex, possibly hBRM and BRG1, is also important for transcriptional regulation.

The interactions between pRb, E2F and E1A might be more complex than originally thought. There are eight E2F family proteins, although only E2F 1 to 5 bind pRb, p130 and p107, with functions varying from transactivation to DNA repair (77). Two independent reports have shown that pRb-E2F1 complexes are not disrupted by E1A expression (77, 79). Rb-E2F2 to 4 complexes were absent in the presence of E1A and so were E2F2 to 4 bound to p107 or 130, even when the expression of E2Fs was increased (79). According to these findings, E1A cannot disrupt the interaction between pRb and E2F1 because of a second binding site in pRb that is specific for E2F1 and does not bind other E2F proteins or E1A. These findings were supported by the detection of pRb-E2F1-E1A complexes (77). Both reports suggested that the interactions between pRb and E2F1 contribute to cell viability in response to DNA damage or E1A, as disruption of pRb-E2F1 complexes increased cellular sensitivity to DNA-damaging agents (77, 79).

Disruption of pRb-E2F complexes by E1A induces cyclins E and A that are important to overcome the G1 checkpoint and enter S phase. These cyclins activate cdk2 that phosphorylates pRb to ensure efficient release of E2F to complete S phase induction and prevent cell cycle arrest (41). E1A binds cdk2 indirectly via interactions with p107 and p130 to modulate their interactions with cyclins A and E, resulting in altered functions of the cyclins (80, 81). The interactions of E1A with the different pocket proteins could regulate different

functions. E1A CR2 binds similarly but not identically to pRb, p107 or 130 and even though the LXCXE residues are important for binding to all three proteins, mutations in adjacent residues resulted in changes in binding affinity to these proteins (73). In addition, the phosphorylation status of these proteins is differentially regulated by E1A. Transfection of U2OS cells with E1A 12S resulted in attenuated hyperphosphorylation of p130 and p107 without affecting the phosphorylation of pRb (82). These results suggested that E1A binds to pRb to induce E2F-dependent transcription while the interactions with other pocket proteins might prevent their hyperphosphorylation, consequently inhibiting cdks. However, E2F-dependent transcription is not only regulated by pRb. In cells lacking pRb a G1-arrest is maintined due to absence of E2F-induced transcription, suggesting that other pocket proteins and/or other cofactors can regulate E2F (76). In addition, E1A binding to pRb is a requirement for E1A-mediated transformation, while interactions with other pocket proteins, such as p130 and p107, are not essential (73, 82).

In general, release of E2F activates E2F-dependent transcription. It has also been shown that E2F can induce apoptosis in growth arrested rodent cells, possibly by induction of the $p19^{ARF}$ gene, repressing the functions of the p53-antagonist MDM2 (HDM2 in humans) (42, 83). However, E1A-mediated apoptosis is not dependent on pRb sequestration, despite p53 stabilisation through E2F induction of $p19^{ARF}$. E1A mutants lacking the pRb-binding region in CR2 are still able to induce apoptosis, showing that the CR2 is not required for E1A-mediated apoptosis (84). Of note, this research did no take into consideration the interactions between pRb and CR1. Interactions of the CR1 and N-terminus of E1A with other cellular factors also induced p53-independent apoptosis. E1A also interacts with the p73 protein and induces apoptosis through p53-independent mechanisms (85). Other mechanisms involve interactions with p21, p400 or regulation of p300/CBP activity by E1A.

Accumulation of p53 after disruption of pRb-E2F complexes can induce members of the Cip/Kip family, like p21 and p27, and the cdk inhibitors from the INK4 family, p16, p15 and others (80, 86). These molecules repress the disruption of pRb-E2F complexes and induce senescence (41). The p21 protein represses cyclin E and ckd2 activities, preventing the disruption of pRb-E2F complexes (87). E1A abrogates activation of p21 by acetylating pRb in a process that involves the acetyltransferase activity of p300. Acetylated pRb forms a complex with MDM2 that binds to p53, inhibiting p53-dependent activation of p21. This process directs p53 towards the induction of apoptosis and might be important for the induction of DNA synthesis (78). Even though at first it is difficult to explain why E1A would induce an apoptotic process that could compromise viability, it is thought that this is a protective mechanism from p21-dependent senescence and G1 arrest, as other viral genes are able to inactive p53-dependent pro-apoptotic pathways (42). It has been reported that E1A directly interacts with p21 to abrogate its growth inhibitory functions and to overcome p21-mediated G1 arrest (88). Interestingly, the N-terminal region of E1A that binds p21 is essential for the induction of apoptosis in DNA-damaged cells after induction of p53 (89).

In addition, p16-dependent senescence requires p16-pRb interactions; without this interaction, p16 induces apoptotic cell death (26). Additional studies in prostate epithelial cells showed that alterations in both p16 and pRb are required to bypass senescence (90). The relief of p16 and p27 induced G1 arrest by E1A requires other regions within CR2 that are independent of binding to pRb. Two motifs within CR2 were found to overcome p16 and p27 activities, a Gly-Phe-Pro motif (GFP motif) and a SDDEDEE motif (80). These motifs are present at the N-terminus of CR2 in close proximity and could be considered as one GFPPSDDEDEE motif. The authors suggested that this region could recruit an additional repressor to target genes; this repressor could potentially be a HDAC, although HDACs bind pRb through a LXCXE motif (80).

The other main protein interacting with E1A is p300, usually in a complex with the CREB-binding protein (CBP), which are transcriptional regulators with histone acetyltransferase activities (HAT). The interactions occur at the N-terminus and at a FPDSVML sequence within the CR1 of E1A (42, 91-94). However, new binding sites for p300/CBP that are required for the transactivating functions of E1A 13S have been found in the CR3 (95). These findings suggest that the regulation of the transcriptional activity of p300/CBP depends on the balance of 13S to 12S, as 12S represses CR3-mediated transcription by binding p300/CBP through the CR1 domain (96).

While the main mechanisms for transcriptional regulation by p300/CBP is through HAT activity, this is not the only mechanism that has been described. There are reports demonstrating the role of p300/CBP in proteasomal degradation of transcriptional regulators located at promoter sites after E1A expression. The p300/CBP complex can bind to the APC/C complex, an ubiquitin E3 ligase. This would target proteins to degradation by the 26S proteasome (97). Interestingly, E1A can bind components of the proteasome such as the S4 and S8 subunits (98). It is possible that E1A interactions with both p300/CBP and the 26S proteasome favour the degradation of the targeted proteins.

E1A can both inhibit p300/CBP HAT activity in some contexts and promote it in others; E1A probably redirects p300/CBP from cellular promoters, hence inactivating transcription, to inactive viral or cellular promoters, where it uses the HAT activity of p300/CBP (3). Activation of the viral E4 promoter requires the recruitment of p300/CBP by E1A 13S, showing that the CR3 region is needed for transcriptional activation, while the CR1 represses it (95). The p300/CBP complex activates transcription by acetylating histone tails or lysine residues of other transcription factors (42). The E1A N-terminus binds to the transcriptional adaptor motif (TRAM) of p300/CBP, thus inactivating HAT activity (99). The TRAM motif can also disrupt the p53-MDM2 complexes,

leading to stabilisation of p53. It is possible that E1A stabilises p53 by using CBP to disrupt this interaction. Other reports have shown that E1A must interact not only with pRb but also with p300 in order to stabilise p53 and induce p53-dependent apoptosis (100). Disruption of pRb-E2F complexes are required for upregulation of p53, but additional interactions of E1A with p300/CBP are required to successfully stabilise p53 (101). However, E1A-mediated apoptosis and the E1A regions involved are more complex and also involve p53-independent pathways. Apoptosis was detected in p53-null cells after expression of E1A; the mechanism was inhibited by co-expression of E1B or treatment with caspase inhibitors, indicating that the mitochondrial apoptotic pathways were implicated (102). Nevertheless, p53-independent apoptosis also required E1A binding to p300 and pRb, according to the results from the research.

E1A can also bind and repress another HAT protein, the p300/CBP associated factor (P/CAF) indirectly in a complex with p300/CBP or by direct interaction with a sequence within the 60 N-terminal amino acids (42). When E1A binds to p300/CBP, it displaces PCAF and inhibits its intrinsic HAT activity (1). Interestingly, PCAF acts as a coactivator of p21 in response to DNA damage-mediated p53 up-regulation and it is possible that the interactions of PCAF with E1A constitute an alternative method for p21 repression. Blockade of p21 activation is not only important for the regulation of phosphorylation of pRb; down-regulation of p21 increases cyclin E and cdk2 activity to ensure the disruption of pRb-E2F complexes and entry to S phase. However, cyclins inactivate p300 through phosphorylation and probably constitutes another checkpoint for G1/S transition. In the presence of p21, cyclins are blocked and p300 can activate transcription. After E1A expression, low levels of p21 should contribute to p300 blockade, but E1A can inhibit cdk-dependent phosphorylation events in p300 and use its HAT activity to control transcription (103). However, other reports suggest that phosphorylation of p300/CBP increases its HAT

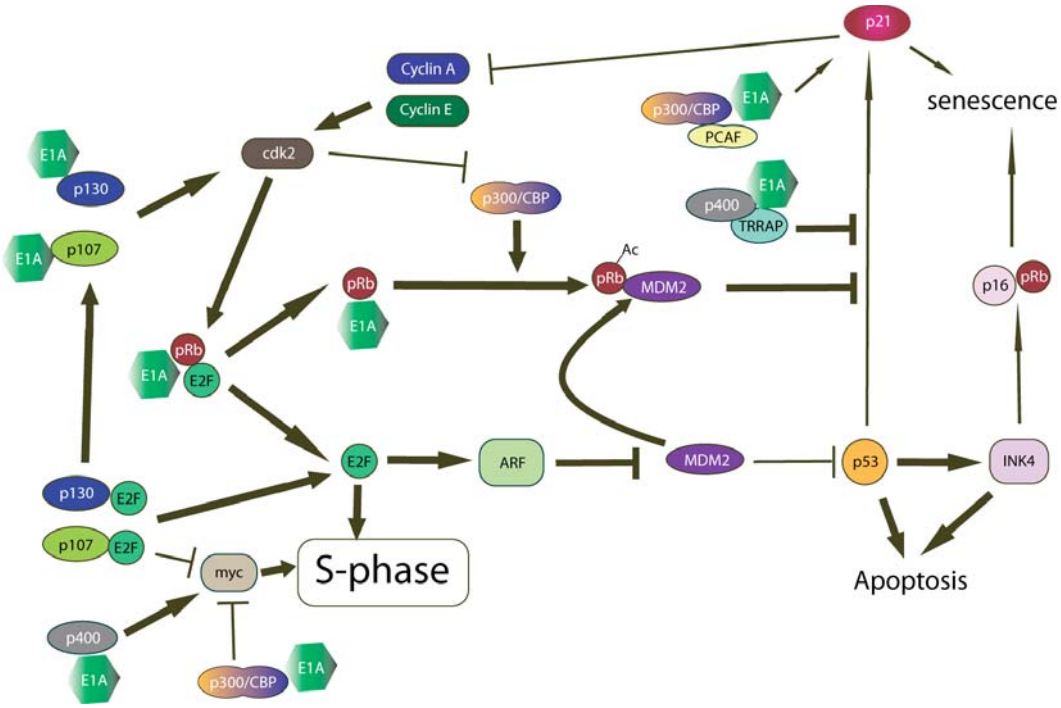


**Fig. 6.** Diagram describing the interactions of E1A with cellular proteins and their downstream consequences. Thick arrows represent events upregulated after expression of E1A; thin arrows represent those events that are downregulated in the presence of E1A. E1A binds to the pRb family members, displacing E2F and inducing upregulation of cdk2, cyclin A/E and entry into S-phase. E2F will also stabilise p53; this can lead to apoptosis or p21/p16-dependent senescence. Senescence is abrogated by E1A binding to p300/CBP and acetylation of pRb, that then binds to MDM2 to inhibit p21 induction. E1A also bind to p400/TRRAP to downregulate p21. The E1B genes will inhibit apoptosis later on in the viral cycle. E1A binding to p300/CBP and p400 is also critical for S-phase induction; p400 allows myc expression and E1A binding to p300/CBP represses transcription of cellular genes involved in regulation of cell cycle checkpoints, hence allowing entry into S-phase.

activity; E1A could form complexes with cyclin E and cdk2 to phosphorylate p300 and increase HAT activity (42, 103).

Besides binding to p300/CBP, E1A interacts with the TATA-binding protein (TBP) to modulate transcription (92). Amino acids 2 to 6 and 20 within E1A are essential for E1A-mediated repression of transcription and binding to TBP and p300/CBP (92). TBP interacts with several transcription factors (TF), like TFIIA, IIB, IIF and RNA polymerase II that are also modified by p300/CBP

dependent acetylation (99, 103). E1A binds to the same region of p300/CBP that interacts with TFIIB and components of the RNA polymerase II holoenzyme complex in order to repress transcription (103). It is likely that p300 serves as a scaffold for the repression of cellular promoters; p300 binds to transcription factors at an active promoter and modulate their function by acetylation, in addition to the acetylation of histones that allow transcription. E1A might prevent the recruitment of p300 to the promoter site by these transcription factors, as E1A interaction with p300 does not abrogate transcription controlled by transcription factors that do not interact with p300 (104).

E1A has other mechanisms for the control of acetylation of histones. The CR4 can interact with CtBP, known to interact with HDACs (105). E1A can compete with HDACs for binding to CtBP and inhibit deacetylation of histones to allow transcription. In addition, absence of the CR4 favours E1A-mediated transformation and impairs the repression of HAT activity of p300/CBP bound to E1A (106). It was demonstrated that CtBP can interact with a protein called CtIP involved in the regulation of tumour suppressor genes like BRCA1 (3, 67). Other reports showed that interactions with CtBP can actually repress E1A transactivation; two different isoforms of CtBP, CtBP1 and CtBP2, were found to repress transcription when bound to E1A, with CtBP2 being the most efficient (107). However, E1A 12S was used in the study and not 13S, that is well known to have higher transactivating activity. Another group found that CtBP1 can bind to CR3 and reduce its transcriptional activity (108). However, the same study showed that E1A 13S but not 12S could activate a CtBP-repressed promoter. This was probably due to the ability of 13S to displace CtBP with the CR4 region while recruiting coactivators at CR3, showing that different E1A proteins modulate transcription differently using the same regulators. In addition, the interactions between E1A and CtBP can also be modulated by interactions of E1A with HAT complexes; E1A can be acetylated at lysine 239, what impairs binding to CtBP, a mechanism that could be involved in gene activation by E1A (70).

Transcriptional regulation by p300 can occur also at the matrix attachment regions, where chromatin binds to the nuclear matrix (109). E1A also interact with other chromatin remodelling factors to alter transcription of cellular genes. The transactivation/transformation domain protein (TRRAP) and p400 interact with E1A at the N-terminus (3, 41, 42). These proteins are known to remodel chromatin to facilitate transcription. TRRAP is a component of three distinct HAT complexes: TIP60, PCAF and GCN5 (110). One of the consequences of E1A-TRRAP interactions is the repression of c-myc and E2F-dependent genes in a process that involves GCN5 HAT activity, although E1A 12S rather than 13S was used in those experiments (110). However, myc expression is essential for S phase induction. The p300/CBP complexes are known to repress myc and contribute to the G0/G1 checkpoint, in addition to p107-E2F complexes near the c-myc promoter site (42, 111). Sequestration of these proteins by E1A, should hence allow the expression of c-myc. The p400 protein also induces myc and it has been shown that E1A interactions with p400 are needed for transformation and repression of p21 (112). E1A promotes the association of p400 with myc that in turn reduces myc ubiquitination and recruits p400 to specific promoters (113). In fact induction of myc and S phase is reduced during the expression of an E1A mutant protein not binding p400 (111). Interestingly, p400 is also involved in E1A-mediated apoptosis, both p53-dependent and p53-independent pathways. The association of p400-TRRAP complexes with p53 has been reported (106); possibly this is another viral mechanism to stabilise p53. In addition, p53 and p400 colocalised at the p21 promoter to repress its expression, providing another viral mechanism to escape p21-mediated senescence (112). Apoptotic mechanisms independent of p53 also required E1A-p400 interactions and there is evidence that binding to p400 is necessary to downregulate the epidermal growth factor receptor (EGFR) to induce apoptosis in cancer cells (114).

#### 1.3.1.2 Regulation of the 26S proteasome

The 26S proteasome is the major non-lysosomal proteolytic machinery in eukaryotes, serving to degrade protein substrates targeted specifically by polyubiquitin modification in an ATP-dependent manner (115, 116). The 26S proteasome is formed by two large macromolecular subunits, the 20S proteasome and the 19S regulatory complex (19S RC). The 20S proteasome degrades non-ubiquitylated proteins in an energy independent manner and contains four heptameric rings arranged into a cylinder with the proteolytic sites facing the inner chamber (115, 116). The 19S RC is formed by a base consisting of six homologous ATPases (S4, S6, S6', S7, S8 and S10b) and three non-ATPases (S1, S2 and S5a), while the lid of the RC is made of eight additional non-ATPase subunits (116).

E1A can regulate the proteasomal activity of the 26S proteasome both in the nucleus and the cytoplasm through binding of E1A to S8 (mammalian ortholog of Sug1) and S4 independently (98, 115). These interactions result in an inhibition of ATPase activity of S4 but not S8. The S8 subunit also has helicase activity that it is not affected by the interaction with E1A (115). The interactions of E1A with the 19S RC inhibit p53 degradation after ubiquitination, while an E1A mutant unable to bind the ATPase complexes failed to do so (115). These data suggest that the N-terminal region of E1A can control the activity of the 26S proteasome by inhibiting ATPase activity of at least one subunit of the 19S RC. The same group also showed that the C-terminal region of E1A was able to bind the 26S proteasome and that the interaction regulated E1A degradation by the 26S proteasome. This process did not require ubiquitination of E1A but phosphorylation in regions rich in P, E, S, and T residues (PEST motifs) (115). The C-terminus of E1A contains five serine residues that can be phosphorylated at positions 227, 228, 231, 234 and 237 to modulate E1A stability. These residues

are phosphorylated by cyclin-dependent kinases, suggesting that E1A activation of cyclins could be a mechanism of self-controlling its own degradation (115).

The interactions with 26S proteasome were later found to be important for the transcriptional activities of the E1A 13S protein. The CR3 can also bind to 20S and S8, interactions that regulate E1A 13S-dependent transcriptional activation and elongation *in vivo* (116). Interestingly, the CR3 from different adenovirus groups binds S8 ans 20S, suggesting a conserved region with biological function. Previous work had already reported the involvement of S8 and its homolog in yeast Sug1 in transcription and recruitment of transcription factors such as Gal4 or TBP (117). The interactions between E1A and 20S are independent of E1A-S8 interactions; in addtion E1A co-precipitated with other subunits of the 19S RC, S2 and S10b, indicating that E1A targets more the whole 19S RC complex. The study of the regulation of the transcriptional activity of CR3 by S8 showed that low levels of S8 enhanced transactivation although binding was not essential. Expression of exogenous S8 at high levels repressed transcriptional activity, but this could also be a consequence of 26S-mediated proteasomal degradation (116). E1A, S8 and 20S were found associated with promoters of other early viral genes, indicating a role for the ATPases in viral transcription. In addition, the CR3 contains PEST motifs that could make E1A 13S more prone to degradation by the 26S proteasome. This is in agreement with the observed half lives of the different E1A proteins, as 13S has a sorter half live than 12S, which lacks the CR3 (3, 116). The proteasome directly controls E1A 13S transactivating activity by proteolytic degradation and indicates that E1A transcriptional activity is directly related to its stability (116). E1A can also modulate the degradation of proteins at the promoter by interactions with p300/CBP. These proteins bind to APC/C, a ubiquitin E3 ligase that targets proteins to the 26S proteaseome (97). Another mechanism involving transactivation activity and ubiquitination of E1A has been described. The BS69 protein has been reported to interact with the CR3 and repress its translational

activity (118). In addition, this protein also bind smaller E1A products through the CR1 and the CR2 (118). Another group showed that interactions between E1A and BS69 inhibit ubiquitination of E1A and consequent ubiquitin-dependent proteosomal degradation through a mechanism that is independent of binding to CR3 (119). E1A can also interfere with the ubiquitin conjugation machinery (E2 enzymes) through interactions of CR2 with UBC9 (3). UBC9 has also been implicated in SUMOylation of proteins and does not necessarily target proteins for degradation but could be involved in protein stability and localisation; the function of E1A-UBC9 interactions is yet unknown (3).

#### 1.3.1.3 Regulation of MHC class I presentation by E1A.

E1A is also known to play a role in the evasion of the immune system, in particular the ability to evade CD8+ cytotoxic T lymphocytes (CTLs) immunity. This role is not shared by all adenovirus groups and it is a major determinant for adenovirus-mediated tumorigenicity. The tumorigenic potential of adenovirus refers to the ability to induce cellular transformation *in vivo* after infection, as it has been demonstrated that Ad5 E1A is also able to transform cells in vitro in cooperation with E1B or activated ras (46, 120). This feature will be discussed later on in this chapter.

It was first thought that tumorigenic potential resided in the ability of certain adenoviruses to down-regulate MHC class I antigen presentation. Viruses like Ad12, known to be tumorigenic, contained a 20 amino acid spacer between CR2 and CR3 not present in non-tumorigenic adenoviruses like Ad5 (3). This region is highly conserved in the highly oncogenic simian Ad7 virus (121, 122). This region is thought to interact with the class I enhancer repression complex, hence decreasing the expression of MHC class I (123). Ad12 E1A may repress MHC class I expression by both inhibiting binding of the activator NFκB and

recruiting the transcription repressor COUP-TFII in a complex with HDACs (123). This was thought to be the reason behind the failure of cells transformed with Ad5 or Ad2 E1A to form tumour in immunocompetent animal models (122). In addition, oncogenic serotypes down-regulate two components of the immunoproteasome, LMP2 and LMP7, that results in a decrease of class I expression (3). This reduces and delays antigen presentation and could serve as an evasive mechanism used by different pathogens (124). However, there is no strong evidence that correlates reduced class I expression and tumorigenicity (121). Hence, tumorigenicity of E1A must involve other components of the immune system. The sensitivity of E1A transformed cells to natural killer cells (NK) mediated death is dependent on the E1A type used; cells transformed with Ad12S are resistant to NK-induced cell death. Contrary, transformation by Ad5 E1A induces tumour rejection irrespective of the changes in MHC class I expression (125). The second factor that favours tumorigenicity of Ad12S but not of Ad5 E1A is the ability of Ad5 E1A to encode CTL-stimulating epitopes that have been found in context with MHC class I antigens (125). In addition, other reports have shown that even though Ad5 E1A does not down-regulate class I presentation on its own, it can cooperate with E3 proteins to enhance an E3-dependent down-regulation of MHC class I antigen expression (61). The interaction of E1A with other transcriptional factors like p300 could also have a role in tumorigenicity and evasion of the immune system, not only in down-regulation of class I presentation. E1A can induce cytolytic susceptibility and tumour rejection by affecting the transcription of genes involved in NK responses through interactions with p300 (126). It has also been shown that E1A can repress the expression of MHC class II by sequestering the transcriptional activator CBP (127).

The role of E1A in evasion of the immune system remains unclear; it can modulate promoters controlled by NFκB-dependent activation and it can modulate the expression of class I antigen alone or in collaboration with E3.

However, E3 also down-regulates translation rates of E1A mRNA during infection and E1A expression is also associated with sensitisation to TNF after NFκB transcriptional activation. Further investigation is needed to elucidate the implications of E1A in immunogenicity and immune response evasion.

### 1.3.2 EMT and transformation

Ad5 E1A first identified as one of the oncogenes present in the adenoviral genome; its expression is sufficient to induce partial transformation of rodent cells and full transformation if co-expressed with E1B or activated ras (42, 120, 128). The ability of E1A to cooperate with other genes to promote transformation has been a useful tool in the research of oncogenic potential of cellular genes. The GLI gene was found to also cooperate with E1A to transform cells, indicating the oncogenic potential of this gene, normally upregulated in gliomas (129). Similar studies were done for the v-src gene; in this case E1A 12S was also able to transform primary epithelial cells in cooperation with v-src although, in contrast to cooperation with ras, loss of the epithelial phenotype was reported (130). This could indicate that the achievement of transformation might involve different pathways that are dependent on the oncogenes used. This work also showed that deletions in E1A p300 binding site abolished transformation in cooperation with E1B or ras but not with v-src, supporting the idea that more than one region could modulate transformation in a cellular-dependent manner.

Transformation of human cells by Ad5 E1A has not been reported, although Ad5 E1A can induce limited cell cycle progression (42). Ad12 E1A has been demonstrated to have the ability to transform human embryonic retinal cells (42). Despite successful immortalisation of rodent cells, Ad5 E1A-expressing failed to form tumours in immunocompetent animals models, as discussed above.

The differences in E1A transformation might not be species-specific as first thought, as later was discovered that expression of E1A suppressed tumorigenesis in a mouse melanoma cell line (131). In fact, E1A has shown anti-oncogenic activity in human cells and it has been used as cancer therapy in clinical trials through delivery of E1A-expressing plasmids in liposomes (132). E1A expression can also reverse the epithelial-mesenchymal transition (EMT) observed in the genesis of carcinomas, contributing to supression of oncogenesis (42). Expression of E1A can indeed induce epithelial characteristics; four human cancer cell lines of non-epithelial origin showed epithelial-like morphology, with epithelial-type adhesion molecules and intermediate filaments containing keratin after retroviral transduction of E1A (133). It is probable that E1A activates epithelial promoters to ensure efficient replication (133).

Transformation of rodent cells is also dependent on the E1A protein used. The 12S protein was able to transform cells at higher efficiency than the 13S protein (134, 135), indicating that CR3 is not required for transformation. Nevertheless, transformation with 12S was sensitive to cold, with very slow transformation and proliferation at 32°C; possibly 13S modulates the transforming activity of 12S (135). Not all E1A proteins have transformation capacity; several reports indicate that E1A 9S is unable to transform cells *in vitro*, either by infection with a 9S-expressing virus or transfection (134, 135). Both CR1 and CR2 have been implicated in the transformation induced by E1A; deletions of amino acids in between these two regions had no effect on transformation, indicating that CR1 and CR2 binding proteins play a role in the immortalisation (120). In addition, mutations in the CR2 impaired the transformation ability of E1A, suggesting that interactions with pRb are needed for complete transformation. Immortalisation requires both control of cell growth through CR2 and DNA synthesis through CR1; these functions are achieved by interactions of CR1 with cellular proteins, in particular p300/CBP (94, 97, 103). Deletions in the N-terminal region and CR1 inhibit DNA synthesis, while this is not observed in

CR2-mutated E1A proteins (71). Interactions between p300 and the APC/C are involved in transformation. E1A targets APC/C-p300/CBP complexes during transformation and modulates the ubiquitin ligase activity of APC/C; E1A mutants unable to bind p300 are unable to fully transform primary rat embryo fibroblasts (97). Binding of E1A to this complex possibly inactivates p300 tumour suppressive abilities. Of note, the expression of E1A in the absence of E1B or ras does not transform but induces apoptosis by mechanisms related to p300/CBP and pRb. In addition, the CR4 also suppresses E1A/ras transformation but enhances E1A/E1B-mediated transformation (97). However, cooperation with v-src did not require p300/CBP but pRb binding but did not show epithelial phenotype (130); this suggests that the status of cellular oncogenes also plays a role in immortalisation and induce changes that are not dependent on E1A expression.

### 1.3.3 E1A in cancer therapy: cancer specificity and sensitisation

E1A is a promising tool for cancer treatment due to its apoptotic properties and have already been used in clinical trials for head and neck, ovarian and breast cancers (132, 136). In the context of viral therapy, E1A can be modified so that it only allows replication in cancer cells but not in healthy cells. Deletions in the N-terminus or the CRs impair interactions with p300 and/or pRb, thus E1A cannot achieve a successful entry into S phase in normal cells. In cancer cells, these pathways are frequently altered, so E1A interactions with these proteins might not be necessary to achieve replication. In cancer cells with deregulated cycle checkpoints due to pRb pathway alterations, E1A does not need to interact with pRb and consequently the CR2 is dispensable (137, 138). This is the rationale for the design of viruses with deletions in the CR2, like the dl922-947 mutant, with a deletion of amino acids 122 to 129; this virus has shown selectivity for cancer

cells and a reduction of potency in normal cells (139). Other mutants with the same deletion, such as AdΔ24, have shown similar results (140). However, deletions in CR2 might not always be specific. Other reports showed attenuation of viral potency in cancer cells when CR2 was deleted, in contrast with deletions of the p300 binding site, which retained potency (141). In this study, CR2-deleted viruses were still capable of inducing S phase in some normal cells but not in others. This was in contradiction with the original description of this E1A deletion that showed higher toxicity than Ad5 in cancer cells (139). More than one deletion can be introduced to improve selectivity; however, deletions of both CR1 and CR2 should compromise viral potency, although there is a report that showed good potency with a double deleted E1A virus (142). However, other reports suggest that deletions in the p300 binding site attenuated potency in glioma cell lines (143). The data from the use of different mutations shows that in some cell lines CR1 deletions improve selectivity and toxicity more than CR2 deletions, but not in others. This suggests that the status of the cell must be taken into account before choosing the E1A fragment to delete. New strategies combine deletions in both E1A and E1B to avoid the attenuation of the E1A double deleted mutants while impairing the antiapoptotic properties of E1B (144, 145).

E1A has another characteristic that makes it a promising gene for therapy; E1A expression can sensitise cancer cells to host immune responses, radiotherapy and chemotherapy. Sensitisation to immune responses is partially due to the interactions with the MHC class I described above. Several reports showed that E1A sensitises cancer cells to TNF-mediated apoptosis, NK cells and macrophages *in vitro* and *in vivo* by interacting with p300 or pRb (146, 147). Sensitisation to radiotherapy has also been reported (148). E1A interacts with pathways involved in the DNA damage response, so it was first thought that it could sensitise to DNA-damaging therapies like radiation or cytotoxic drugs that induce DNA damage. Good sensitisation has been observed to DNA-damaging drugs like gemcitabine or etoposide (145, 149, 150). However, other pathways

might be involved, as good synergistic effects have been reported between E1A and agents targeting the cytoskeleton, like taxol, cisplatin and related cytotoxic drugs (151-154).

The mechanisms and the E1A regions involved remain unclear. There is evidence that down-regulation of Her-2/neu expression after paclitaxel treatment in combination with E1A is important for sensitisation in breast cancer (153). Other report showed that p21 inactivation by E1A was essential for sensitisation to DNA-damaging agents (89). Up-regulation of apoptotic mechanisms, caspase expression and/or downregulation of the PI3K/Akt pathway in response to cisplatin or paclitaxel due to PP2A up-regulation by E1A have also been described (155, 156). There is controversy about the E1A regions responsible for the sensitisation; some studies showed that sensitisation to radiotherapy and DNA damaging agents was dependent on p53, hence E1A must interact with pRb to induce it (157, 158). However, p53 induction was observed in E1A-mediated sensitisation of pRb deficient cells, indicating that in this context the sensitisation was dependent on p53 but not E1A interactions with pRb (138). Sensitisation must not be only dependent on p53, as E1A effectively sensitises cells with non-functional, mutant p53 (138, 151). Possibly, all CRsin E1A play a role in sensitisation; absence of one might not affect E1A-mediated sensitisation depending on the status of the cellular pathways. Interactions with one of the CR could be sufficient to sensitise cancer cells if the pathways interacting with the absent region are deregulated in a way that favours E1A function. Deletion of the N-terminus and CR1 or CR2 totally impaired chemosensitisation to adriamycin in both human and murine fibroblasts, indicating that deletion of more than one domain abrogates sensitisation (138). Although more than one pathway may be involved in E1A-mediated sensitisation, the published evidence suggests that it requires both activation of proapoptotic factors and inactivation of antiapoptotic factors.

## 1.4 Adenoviruses in gene therapy

Over 1340 gene therapy clinical trials had been completed, were ongoing or approved worldwide in 2007. In 1989, one month after the discovery of the cystic fibrosis gene, James Wilson already discuss the prospects of gene therapy to treat this disease by expressing the correct gene using a virus (159, 160). By 1993 the first clinical trials were under way, although the patients did not respond to the treatment (159, 160). The first therapeutic human gene therapy clinical trial was approved in 1990 and involved two children suffering from a form of severe combined immunodeficiency (161), (162). The number of trials has increased every year; in 1996, 116 trials were approved worldwide. However, adverse effects observed in some trials in 1999 and 2002 forced regulatory bodies to critically examine the risk/benefit ratio and to restrict the number of trials while the adverse effects were investigated (161). The adverse effects observed were in some cases due to the vector used, but not always. These cases include development of leukaemia-like complications due to random insertion of retroviral vectors (163) or the death due to a fatal inflammatory resonse after adenovirus delivery in a patient with an ornithine transcarbamylase deficiency (164).

Approximately 66% of clinical trials have addressed cancer, while cardiovascular and inherited monogenic diseases are the other diseases most commonly targeted in gene therapy clinical trials (161). Gene therapy is used in the clinic in different ways. Vectors can be used to deliver a therapeutic gene i*n vivo,* either a gene correcting a genetic deficiency or, in the case of cancer, genes that regulate cell cycle and apoptotic pathways (161, 165, 166). Another approach is to use vector to express antigens in the target tissue that can be recognised by the immune system, called immunotherapy (1, 166). A different approach is to

design viruses that selectively destroy the target of interest, a therapy called oncolytic therapy in the case of cancer treatment (44, 166, 167).

The vectors used in gene therapy can be classified as viral or non-viral vectors. Non-viral vectors are used as an alternative to viruses, due to a greater capacity to harbour therapeutic large DNAs and lower immunogenicity (161, 165). The most commonly non-viral methods of gene delivery are cationic liposomes and “naked” DNA. The first involves a negative-charged lipid molecule transporting the therapeutic DNA; naked DNA means the use DNA directly injected into the target tissue (161, 165). E1A has actually been used as a therapeutic gene on a liposome-based delivery in a phase I clinical trials in breast, ovarian and head and neck cancer (132, 136). E1A therapy proved safe and promising, although efficacy was not reported in this trial. However, viruses are still the vectors of choice for most trials. Adenoviruses are the most commonly used virus in gene therapy, accounting for approximately 25% of all clinical trials to date (161). Retroviruses were the first vectors used in therapy but are currently only used in 22.8% of the trials, due to the adverse effects of viral genome integration in the host genome (161). Another virus is also becoming increasingly popular, the adeno-associated virus (AAV). These vectors are substituting adenoviruses as the vector of choice for the treatment of many diseases. AAVs are now being used in clinical trials for eye diseases in the United Kingdom (168). AAV are also used for the treatment of cystic fibrosis, muscular dystrophies and Parkinson’s disease (168). AAVs are also used for haemophilia and cancer treatment (169). Other viruses are also used, such as herpesvirus, vaccinia virus, reovirus, poliovirus, vesiscular stomatitis virus (VSV) and picornavirus (29, 161, 165, 170).

### 1.4.1 Advantages and disadvantages of adenoviruses as vectors for gene therapy

Adenoviruses are widely used in gene therapy for the advantages over the previously used retroviral vectors. Adenoviruses can infect both dividing and non-dividing cells (1, 171) and do not integrate in the host genome, avoiding the adverse effects observed with retroviruses (161). The adenoviral replicative cycle is lytic, hence infected cells burst as soon as new viral particles are fully formed; an advantage especially promising for cancer treatment, enabling fast spread of virus at the tumour site. In addition, adenoviruses generate a high amplification of progeny, up to $10^5$ new viral particles per infected cell, enhancing the rapid spread of viral particles locally at the tumour site (1, 172, 173). Adenoviruses are also easy to design, manipulate and produce in large quantities and can accommodate relatively large segments of DNA, up to 7.5 kilobases (kb) (173).

Although these advantages have made adenoviruses promising vectors for gene therapy, there are some disadvantages. Not all cell types can be infected, as their natural tropism are epithelial cell types (1). Adenoviruses are also highly immunogenic, inducing both humoral and cell-mediated immune responses (1, 171). Despite adverse effects and the death of a patient in a clinical trial in 1999 (173), data from the latest clinical trials has proven that adenoviruses are safe (167, 173). Most adult humans have already been exposed to Ad2 and Ad5, so the immune system can recognised viral proteins as antigens and the presence of neutralising antibodies is a challenge for multiple administration of adenoviral therapy (173). Another problem when using adenovirus in the clinic is the high viral uptake by the liver after intravenous administration. Viral particles enter the hepatocytes due to the interactions of the hexon with coagulation factors that allow infection in the liver (40).

### 1.4.2 Achievement of cancer specificity

There is ongoing research to optimise safety and efficacy of adenovirus. They include a variety of mechanisms, from detargeting adenovirus fiber to the construction of gutless vectors, adenoviruses expressing a gene of interest but no viral genes that therefore need a helper virus that provides viral proteins for DNA synthesis (1, 171). Other strategies include the use of promoters controlled by irradiation or tissue-specific proteins like the AR for prostate cancer therapy (166, 173) or cyclooxygenase-2 (COX2) dependent promoters for colorectal and pancreatic cancer (174). The main strategies to improve efficacy for cancer gene therapy are fiber and capsid modification, use of tissue-specific promoters and oncolytic viruses with deletions in viral genes that only allow replication in cancer cells. The design of the virus can also be optimised for particular therapies, as the different modifications available have different effects on potency and cancer selectivity (175). In addition, all these strategies can be combined in an attempt to maximise potency and specificity; one example is the Ad5/3cox2LΔ24 virus, with a COX2 promoter driving a CR2-deleted E1A gene and fiber knobs from Ad3 (176).

#### 1.4.2.1 Fiber modifications

Failure to reach the target tumour site is partially caused by uptake of virus in other tissues, specially the liver, and attachment of viral particles to erythrocyes (40, 177). This is due to interactions between the hexon and the fiber knob with coagulation factors that can hence influence the attachment of the virus by CAR-independent mechanisms (177). Fiber knob modifications have been considered a promising approach to enhance successful target of the tumour and hexon

modifications as an approach to avoid liver blood factor X dependent transduction of hepatocytes in the liver.

Modifications of the fiber can be classified in two categories; one approach is the replacement of Ad5 fiber by that of another serotype and a second approach is to modify the fiber so it binds receptors different from CAR. Replacement by another serotype fiber can be total or partial; there are reports of Ad5 fiber knob substitution by that of Ad3 (178). Ad5 modified viruses expressing the Ad35 fiber have also been constructed, targeting CD46 rather than CAR (179). These viruses have been further modified in order to optimise binding to their new receptor. These modifications included the molecular optimisation of the fiber to increase its affinity, like in the case of Ad5/35++ that expressed a Ad35 modified fiber (179), or the addition of the RGD motif to the fiber knob of Ad5/3 (180). The RGD motif (arginine-glycine-asapartic acid motif) binds to RGD-binding integrins, mainly $\alpha_v\beta_3$ (181). Other domains have been inserted at the fiber knob; some strategies involved the used of proteins such as immunoglobulins (Igs) bridging between the knob and the cellular receptor. In this case, a protein binding Igs is attached to the fiber knob; then the viral capsid can bind an Ig targeting a specific receptor (182).

#### 1.4.2.2 Deletion of viral genes

Oncolytic viruses have shown promising results in clinical trial, especially when they are combined with chemo or radiotherapy. This is due to the lack of cross-resistance between cytotoxic agents and viruses and the improvements in the cancer-specificy of these viruses. Specificy of these viruses is based on small deletions of viral genes that are essential to viral replication in normal cells, but dispensable in cancer cells as the interacting pathways are deregulated. Even though new research is focused on deletions in the E1A gene as previously

described, other viral genes have also been altered to achieve cancer selectivity. Deletion in the E3 gene were suggested for therapy as these genes are not essential for viral replication and its absence would allow for insertion of transgenes of interest. However, those initial experiments did not consider the effect of these deletions in an immunocompetent model. It was soon demonstrated that E3 gene manipulations significantly attenuated the potency of oncolytic viruses in the context of a fully functional immune system (56).

The other gene that was originally deleted was the E1B-55K; this generated the *dl*1520 mutant, also known as Onyx-015. It contains an 827 bp deletion and a point mutation that generates a premature stop codon preventing the expression of a truncated form of E1B-55K (183, 184). This virus was generated to selectively replicate in cancer cells with p53 deficiencies, as E1B-55K inhibits p53-dependent apoptosis. Infection of healthy cells would induce p53-dependent apoptosis that could not be block by viral genes. Hence, an infected normal cell would induce a p53 response resulting in growth arrest or apoptosis without replication (183). However, further research showed that the lack of E1B-55K was not sufficient to abrogate replication in cells with dysfunctional p53 pathway (185). It has also been shown that *dl*1520 can override cell cycle checkpoints that are dependent on p53-interacting proteins and this induces mitotic catastrophy and endorreduplication in p53 expressing cells (185, 186). The mechanisms for selective replication of *dl*1520 are not fully understood, but they are not dependent on p53 functional status. Some groups have proposed that the cause for selectivity might reside in the nature of the mutation within p53; the research showed that replication of *dl*1520 varied among cells expressing different p53 mutations, indicating that loss or gain of specific p53 functions might be important in the replication of Onyx-015 (187). E1B-55K is also involved in mRNA transport in collaboration with E4orf6, so this interaction could play a role in the selectivity. It could also explain the attenuation in potency of this virus compared to Ad5. Due to these disadvantages, other mutations in the

E1B will be tested in the clinic; deletions of E1B-19K have shown good cancer selectivity and sensitisation to chemotherapy without the attenuation of potency observed for *dl*1520 (145, 154).

Onyx-015 was the first adenovirus to undergo a clinical trial for cancer treatment (188). Since 1996, it has been used in a variety of clinical trials for different malignancies and it is now an approved therapy in China (161, 188). Phase I clinical trials have shown good safety data, with toxicity being well tolerated at the highest feasible doses (189, 190). This virus has been administered as single agent both intratumourally and intravenously; toxicity was well tolerated, with flu-like symptoms as the most common adverse effects (183, 189). However, efficacy was minimal in head and neck cancer clinical trials after multiple injections, with 14% of the patients showing partial regression of the tumours (183, 191). Data from these trials showed good correlation between viral replication and mutated status of p53 that also correlated with tumour regression (191). The outcome of these trial, however, was that the deletion of E1B-55K and the E3B region in this virus severely attenuated its potency and the modulation of the immune response that could explain the poor efficacy observed in addition to the variability of mutation in p53 (188, 191). However, new clinical trials have combined the Onyx-015 virus with chemo and radiotherapy; results were promising in patients with head and neck cancers after intratumoural administration and in colorectal liver metastases after hepatic arterial administration (188, 189). Onyx-015 was also used in a phase I clinical trial for solid tumours in combination with enbrel, a recombinant dimmer of the TNF-α receptor (192). This trial showed no significant adverse effect of the combination and higher detection of viral DNA when Onyx-015 was combined with enbrel treatment. In addition, a new phase I clinical trial started in 2008 combining Onyx-015 with systemic chemotherapy, doxorubicin and cisplatin, in patients with advanced sarcomas (193). The outcomes of the different trials have shown that adenoviruses can safely be combined with chemo- or radiotherapy, resulting

in a synergistic interaction of the two combined treatments. Combination therapies are now a more promising therapeutic strategy than the use of adenovirus as single treatment, due to the synergy observed in the mentioned trials.

### 1.4.3 Gene therapy in prostate cancer

Gene therapy is now a promising alternative to the lack of effective treatments for hormone-refractory prostate carcinomas. Gene therapy was first administered to a prostate cancer patient in 1994 and ten years later 61 clinical trials were registered on the Office of Biologic Activities Human Gene Transfer Protocol List (166). These clinical trials involved the use of viruses alone or in combination with chemotherapy or radiotherapy. The most commonly used viral vector used has been adenovirus, although vectors like retroviruses, adeno-associated viruses and vaccinia virus have also been tested (166). The strategies used can be categorised into corrective or cytolytic therapy. Corrective therapy involved the use of viral vectors to expressed a tumour suppressor gene mutated in prostate cancer such as p53 or p16; it can also involve the use of silencing RNA to down-regulate the expression of oncogenes often overexpressed in prostate carcinomas such as Hdm-2, myc and Bcl-2 (166, 194, 195). Cytolytic therapy has been more widely used than corrective therapy; it involves the use of viral vectors that selectively destroy cancer cells. Three different approaches have been exploited to achieve tumour destruction by gene therapy: immunotherapy, prodrug converting enzyme delivery and oncolytic therapy. Immunotherapy aims to enhance the recognition of tumour cells by the immune system, increasing histocompatibility complex class I (MHC I) presentation or stimulation of lymphocytes to recognise cancer cells (166, 170). The major disadvantage of this approach is the cost and technical expertise required. As adenoviruses are easy to

manipulate and produce, they represent a good vector for delivery of prodrug-converting enzymes. The virus would be administered in combination with a non-toxic pro-drug that is converted to an active toxic drug in infected cells. The most commonly used enzymes for the treatment of prostate carcinoma are the herpes simplex virus thymidine kinase (TK) in combination with ganciclovir and the cytosine deaminase (CD) together with 5-fourocytosine (5-FC) (166, 167). These two enzymes have also been used in combination in the same virus, the Ad5-CD/TKrep, used in 5 clinical trials for prostate cancer and osteosarcoma (166, 167, 196). The expression of enzymes is controlled by the promoter of the cytomegalovirus (CMV) and it has proved to be clinically safe after a five-year follow-up of one clinical trial (197). PSA and PSMA specific enhancers and promoter are used to drive the expression of the TK gene in the AdIU1 adenovirus in order to achieve specific expression of the enzyme in prostate tissue (196). Efficiency of the pro-drug converting enzymes can also be modified and optimised; second generation adenoviruses expressing optimised enzymes are now in clinical trials, like the Ad5-yCD/*mut*$TK_{sr39}$*rep*-ADP. This virus expresses optimised CD, TK and the adenovirus death protein (ADP) at high levels, improving efficiency of the virus and it is now in clinical trials (198).

The last type of cytolytic therapy involves the use of oncolytic viruses. These are viruses with deletions in genes that are essential for viral replication in healthy cells, but that can be spared in cancer cells due to cellular aberrations in pathways controlling cell cycle. These viruses are often combined with chemotherapy or radiotherapy, as synergistic interactions between these treatments have been reported (199, 200). Cancer specificity can also be achieved by the use of tissue-specific promoters, like in the case of the AdIU1 virus described above. In fact, the same group also develop the Ad5-PSME-E1A virus, with E1A under the control of the same enhancer of prostate-specific PSMA expression (PSME), claiming better prostate cancer specificity than with the use of the PSA promoter (201). The CG7060, previously called CN706 and CV706

was one of the viruses using the PSA promoter-enhancer element to control E1A expression (202). Another virus evaluated in clinical trials is the CG7870 adenovirus, previously called CV787 (202). This virus uses the rat probasin promoter to control E1A and the PSA promoter enhancer to control E1B expression. The use of this virus by intraprostatic delivery is now in phase II clinical trials and it is now in a phase I clinical trial for intravenous administration for treatment of metastatic tumours (202). The adverse effects reported in this trial showed mild to moderate flu-like symptoms; even though phase I trials are designed to test safety rather than efficacy, this trial showed a decrease in PSA levels of treated patients, being the first time that this is achieved after intravenous administration (202). There are reports that this virus can also synergise with drugs like docetaxel *in vitro* and *in vivo* (199).

Even though gene therapy is already being tested for the treatment of prostate carcinomas, there is room for improvement of the vectors used. In the case of adenoviral vectors, it is known that the AR attenuates Ad5 replication (203). Research shows that AR and E1A are mutual inhibitors, and this interaction attenuates replication in AR-positive prostate cancer cells. Construction of viruses expressing a chimeric E1A-AR fusion protein has been proposed as an alternative to overcome this negative interaction of AR and E1A (203). Other factor that affects the success of adenoviral gene therapy is the expression of the receptor that viruses bind to. Expression of CAR is often reduced in carcinomas compared to healthy tissue and there are indications that CAR down-regulation correlates with the progression of the disease, even though the function of CAR remains unclear (204).

# *Aims of this thesis*

This thesis aimed to elucidate the regions within E1A that are essential for chemosensitisation of prostate cancer cells. Using a variety of adenoviruses, both replication-competent and deficient, with partial deletions in the E1A gene the aim was to find regions that are essential for sensitisation to cytotoxic drugs. Two different drugs currently used in prostate cancer treatment, mitoxantrone and docetaxel, would be combined with the viruses mentioned in order to investigate the efficiency of the combination treatments with drugs with different mechanisms of action. At a molecular level, this thesis aimed to find mechanisms involved in the E1A-mediated senstisation and the effects of the combination treatments in apoptosis induction, cell cycle and expression of proteins related to cell death, survival and cycle control.

This work aimed to provide a better understanding of E1A-mediated senstisation that allow for the improvement of future oncolytic adenoviruses for the treatment of prostate cancer in combination with chemotherapy.

# Chapter 2

# *Materials and methods*

## 2.1 Cell lines

### 2.1.1 Human cell lines

The human embryonic kidney cell line HEK293 was obtained from the Cancer Research UK Central Cell Service (Clare Hall, CRUK, Middlesex, UK). JH293 cells were obtained by clonal selection of HEK293 cells for optimisation of viral titration (Clare Hall). The human non-small cell ephitelial lung carcinoma cell line A549 was obtained from the American Type Tissue Culture Collection (ATCC). Three human prostate cancer cell lines were used: the DU145 cell line derived from brain metastasis, the PC3 cell line derived from bone metastasis and the 22Rv1 cell line derived from a human prostate carcinoma xenograft serially propagated in nude mice after castration. The three human prostate cancer cell lines were obtained fron the ATCC. All human cell lines were maintained at 37˚C and 5% $CO_2$ in Dulbecco's Modified Eagle Medium (DMEM; CRUK) supplemented with 10% foetal calf serum (FCS; Sigma-Aldrich, Chemie, Germany). A detailed description of the characteristics of the human prostate cancer cell lines used can be found in Table 2.

| | PC3 | DU145 | 22Rv1 |
|---|---|---|---|
| **AR** | - | - | + |
| **Origin** | Bone metastasis | Brain metastasis | CWR22 xenograft |
| **Morphology** | Epitheloid | epitheloid | epitheloid |
| **PSA RNA** | - | - | + |
| **PSA protein** | - | - | - |
| **p53** | - | mutated | + |
| **pRb** | + | mutated | + |
| **Bcl-2** | + | - | + |
| **p300** | + | + | + |
| **CBP** | + | + | + |
| **E2F** | + | + | + |
| **p21** | + | + | + |
| **p63** | - | - | - |
| **HDM-2** | + | + | + |
| **c-SRC** | + | + | + |
| **PTEN** | - | + | + |
| **p38** | + | + | + |
| **p-p38** | + | + | + |
| **Akt** | + | + | + |
| **p-Akt** | + | - | + |
| **Erk-1** | + | + | + |
| **p-Erk-1** | - | + | + |
| **Erk-2** | + | + | + |
| **p-Erk-2** | - | + | + |
| **JNK-1** | + | + | + |
| **Chk-2** | + | + | + |
| **Cyclin D1** | + | + | + |
| **Cyclin E** | + | + | + |
| **Caspase 3** | + | + | + |
| **PKA** | + | + | + |
| **PKC** | + | + | + |

**Table 2.** Alterations of cellular genes involved in cell cycle control found in the human prostate cancer cell lines used in this thesis. Status of these proteins was obtained from ref. (26, 205-208).

### 2.1.2 Murine cell lines

The murine prostate carcinoma cell line RM-1 (209) was a kind gift from Dr. Thompson (Houston, TX, USA). RM-1 cells were maintained at 37˚C and 5% $CO_2$ in DMEM supplemented with 10% FCS. The murine adenocarcinoma cell line TRAMPC was a kind gift from Dr. Vassaux (London, UK). TRAMPC cells (210) were maintained at 37˚C and 5% $CO_2$ in DMEM supplemented with 20% FCS, 1 nM dihydrotestosterone (DHT) and 5 μg/ml insulin (Sigma-Aldrich, Suffolk, UK).

## 2.2 Viruses

### 2.2.1 Replication-selective

Replication-selective oncolytic adenoviruses with mutations in the CR1 and CR2 regions of E1A were evaluated. In addition to the following deletions, all E1-mutant adenoviruses had the E3B gene deleted; *dl*1101 has a deletion of amino acids 4 to 25, *dl*1102 has a deletion of amino acids 26 to 35, *dl*1104 has a deletion in amino acids 48 to 60, *dl*1107 has a deletion of amino acids 111 to 123, *dl*1108 has a deletion of amino acids 124 to 127. *dl*922-947 has a deletion of amino acids 122 to 129 in CR2 region. Onyx-015 (*dl*1520, with a deletion in the E1B-55kDa gene) was also evaluated. Wild type Ad5 was used as a positive control whereas *dl*312 (E1-deleted virus) was used as negative control. Replication incompetent AdGFP, with GFP expression cassette under control of the CMV promoter replacing E1 and with intact E3 region, was also used as control. These viruses are described in more detail in Table 3 and Fig. 7.

| | Nucleotide deletion | Amino acid deletion | Comments |
|---|---|---|---|
| **Ad5** | None | None | Wild type |
| ***dl*312** | 448-1349 | 1-289 | No E1A protein |
| ***dl*1101** | 569-634 | 4-25 | Does not bind p300 or p400 |
| ***dl*1102** | 635-664 | 26-35 | Does not bind p400 |
| ***dl*1104** | 701-739 | 48-60 | Does not bind p300 |
| ***dl*1107** | 890-928 | 111-123 | Does not bind pRb or p130 |
| ***dl*1108** | 929-940 | 124-127 | Does not bind pRb, p130 or p107 |
| ***dl*922-947** | 923-946 | 122-129 | Does not bind pRb, p130 or p107 |
| **AdGFP** | 448-1349 | 1-289 | GFP gene under control of CMV protomer replacing E1A |

**Table 3.** Description of replication-selective adenoviruses used in this thesis, and the *dl*312 and AdGFP viruses used as controls for the assays. Detailed information of all E1A mutations can be found in Mymryk et al, 1998 (4).

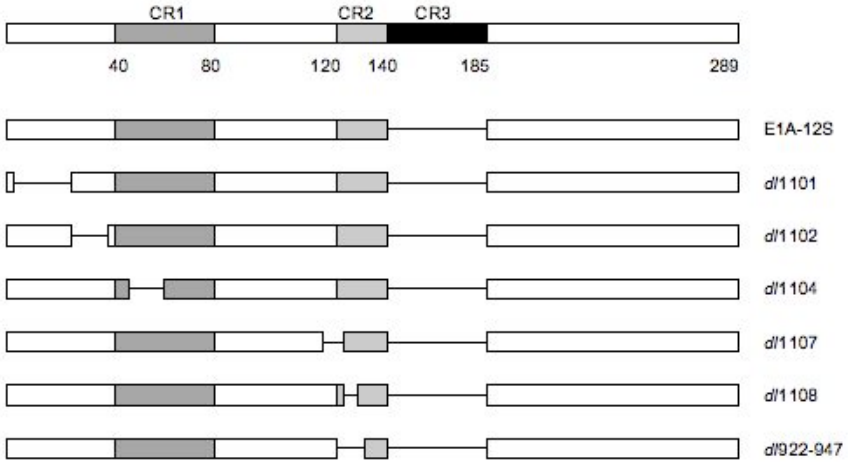


**Fig. 7.** Diagram of E1A deletions of the replication selective adenoviruses used in this thesis. They all expressed E1A mutants based on the E1A-12S protein.

## 2.2.2 AdE1A-12S mutants

### 2.2.2.1 Extraction E1A

A549 cells were seeded in a 6-well plate at $1x10^4$ cells/well and Ad5 was added 24h later at a concentration of 100 particles per cell (ppc) in 2 ml of 2% FCS DMEM. Medium was removed 20h after infection and RNA was extracted from cells using 1ml of Trizol® Reagent (Invitrogen, Carlsbad, CA). RNA was purified using 0.2 ml of chloroform and centrifugation at 12000x *g* for 15 min at 4˚C using an Eppendorf Centrifuge 5415R (Eppendorf, Cambridge, UK). The phase containing RNA collected and RNA precipitated with isopropanol and centrifuged for 10 min at 12000x *g*. The pellet was washed with 75% ethanol, centrifuged at 7500x g for 5 min and resuspended in RNAse-free distilled water. The RNA concentration was quantified using a Nanodrop® ND-1000 Spectrophotometer (Labtech International Ltd, East Sussex, UK), measuring the absorbance ratio 260 nm/280 nm.

cDNA was synthesised from the mRNA using the TaqMan Reverse Transcription Reagents and oligo(dT) primers (Applied Biosystems, Foster City, CA) as described by the manufacturer. E1A cDNA was amplified by PCR, using the Advantage 2 PCR Kit (Clontech, Mountain View, CA). 30 cycles of PCR were performed; each cycle included 30 s at 94°C and 2 min at 68°C. Primers purchased from Sigma-Aldrich were designed using DNA Strider 1.3f13 software (CEA, France); forward primer started with an inserted restriction site for BssH II and reverse primer with a site for Xho I. Primer sequences are shown in Table 4.

#### 2.2.2.2 Cloning of E1A-12S cDNA

PCR products were separated by agarose electrophoresis in a 2% agarose gel and E1A-12S cDNA was extracted from the gel using QIAquick Gel Extraction Kit (Qiagen, West Sussex, UK). Purified E1A cDNA was cloned into pCR2.1-TOPO vector (Invitrogen) to generate pCR2.1-TOPO-12S. TOP10 chemically competent bacteria (Invitrogen) were transformed with pCR2.1-TOPO-12S and cultured overnight at 37˚C in agar plates containing 50 μg/ml of ampicilin (Sigma-Aldrich). Bacterial clones were selected and cultured overnight at 37˚C in brooth containing 50 μg/ml of ampicilin. Qiagen Spin Miniprep Kit (Qiagen) was used to extract the pCR2.1-TOPO-12S plasmid. Sequencing was done and determined as 100% homology and correct orientation of E1A-12S cDNA in the vector. All sequence analysis was performed by the Genome Centre at the Institute of Cancer (London, UK).

#### 2.2.2.3 Construction of AdE1A-12S virus

pCR2.1-TOPO-12S was digested with Kpn I and Xho I (New England Biolabs (NEB), UK) to extract E1A-12S and cloned into a pShuttle-CMV vector (Stratagene, TX, USA) previously linearised with the same restriction enzymes. Quick Ligation Kit from New England Biolabs was used for the ligation reaction, following manufacturer's instructions. pShuttle-CMV-12S was transformed into TOP10 chemically competent bacteria cultured in brooth containing kanamycin (Sigma-Aldrich) at 50 μg/ml and amplified by maxiprep preparation. pShuttle-CMV-12S was linearised with Pme I (NEB, UK) and recombined with pAdEasy-1 plasmid (Stratagene) by transfection in BJ5183 electrocompetent bacteria (Stratagene). Electroporation was done with Biorad's Gene Pulser II system (Biorad laboratories, Hercules, CA, USA), at 2.500V, 200 Ohms and 25 μF. Cells were cultured over night in agar plates containing 25 μg/ml of kanamacyin and 25

μg/ml of streptomycin. Selected colonies were collected and cultured in bacterial brooth containing 75 μg/ml of kanamycin and 50 μg/ml of streptomycin. pAdE1A-12S plasmid was extracted using Qiagen miniprep kit and TOP10 electrocompetent bacteria (Invitrogen) were transformed as previously described. Transformed bacteria were seeded in agar plates containing kanamycin at 25 μg/ml and culture overnight at 37˚C. Maxiprep of selected clones was done to extract the pAdE1A-12S plasmid.

5 μg of pAdE1A-12S was linearised with Pac I (NEB); 2 μg of digested plasmid used to transfect JH293 cells with Fugene 6 Transfection Reagent (Roche; Basel, Switzerland), according to manufacturer's instructions. 10 days after transfection, cells and medium were harvested and freeze-thawed three times in $N_2$ (l). HEK293 cells in 20 ml of DMEM (10% FCS) at 70% confluency in a T75 flask were infected with 2ml of the supernatant of transfected JH293 cells. HEK293 cells and medium were collected 2 days after infection and freeze-thawed three times to release virions from the cells. Supernatant was collected by centrifugation and stored at -80˚C; this represented the primary expansion of the virus.

HEK293 cells grown in DMEM supplemented with 10% FCS were grown in a multiple-layer cell factory CF-10™ (Fisher Scientific, Leicestershire, UK). When 80% confluency was reached, 7 ml of primary expansion previously collected was used to infect HEK293 cells; infection was maintained in DMEM supplemented with 2% FCS for 72h. Infected HEK293 were collected when cytopathic effects of infection were seen as detachment of cells, then centrifuged for 10 min at 2000 rpm using a Sigma 6K15 centrifuge (Sigma, Germany) at 4˚C and resuspended in PBS. Pellets were collected again by centrifugation at 1000 rpm for 10 min, resuspended in 10 mM Tris-HCl (pH 8.0) and freeze/thawed three times; the suspension was centrifuged for 10 min at 6000 rpm at 4˚C. The supernatants containing the viruses were layered onto caesium chloride (CsCl) for

purification. 10 ml of a 1.25 g/ml $CsCl_2$ solution were placed in a 3.5" ultracentrifuge tube (Beckman, UK). Carefully, 7.6 ml of a 1.4 g/ml solution of CsCl was added at the bottom of the tube, avoiding mixing the two solutions of CsCl to create a density gradient. The virus-containing supernatants from the CF-10™ were carefully layered on top of the $CsCl_2$ gradient in 4 tubes and centrifuged at 25000 rpm for 2h at 15˚C using a Beckman SW32Ti swing-out rotor in an Optima LE-80K ultracentrifuge. Three bands were visible after centrifugation: the top corresponding to cellular debris, the middle band corresponding to empty viral particles and the lowest band containing encapsulated infectious viral particles. Ultracentrifuge tubes were pierced with a 19G needle fitted in a 10 ml syringe and the lowest band was aspirated. The band containing the virus was then layered onto 3 ml of a 1.35 g/ml solution of CsCl in a 2" ultracentrifuge tube (Beckman) and centrifuged at 40000 rpm at 15˚C for 15h using a combination of a Beckman SW55Ti swing out rotor in an Optima LE-80K ultracentrifuge. Virus was extracted from the ultracentrifuge tube using a 19G needle as described above and the volume was made up to 12 ml with TSG buffer (96 mM NaCl, 0.5 mM $NaHPO_4$, 2.8 mM, KCl, 0.3 mM $MgCl_2$, 0.5 mM $CaCl_2$, and 30% (v/v) glycerol. The virus/TSG mixture was injected into a slide-a-lyzer (3-15ml, Pierce) using a 18G needle supplied. The slide-a-lyser was placed in the float provided and transferred to a 5 L beaker containing 2 L of dialysis solution (10 mM Tris-HCl pH 7.4, 1 mM $MgCl_2$, 150 nM NaCl, 10% (v/v) glycerol and distilled $H_2O$). The beaker was placed on a magnetic stirrer at 4˚C for 24h. After dialysis, virus was removed using a syringe, aliquoted and stored at -80˚C.

#### 2.2.2.4 Generation AdE1A-12S deletion-mutants

Generation of E1A-1102, E1A-1104 and E1A-1108 cDNA was done by gene splicing by overlapping extension PCR (SOEing PCR). This method consists on the amplification of two fragments of the gene of interest with primers that

overlap. These two fragments are then fused together, generating a deletion of the original gene. Primers were designed to generate the deletions corresponding to E1A-1102, E1A-1104 and E1A-1108 and are described in Table 4. For each mutant two independent PCR reactions were done, with primers corresponding to the 5' of E1A and the 3'primer of the each mutation and the 5'primer of the mutation and the 3' end of E1A. PCR reactions were done with a PTC-200 Peltier Thermal Cycler (MJ Research, BioRad). PCR products were separated by electrophoresis in a 2% agarose gel and purified using QIAquick Gel Extraction Kit (Qiagen). Fragments were quantified and mixed at equal molarity in a final concentration of 1ng/μl. A PCR cycle (96˚C for 6 min, 55˚C for 2 min, 72˚C for 3 min) without primers was run with the mix to fuse the fragments, using Advantage 2 PCR Kit (Clontech, Mountain View, CA). Next E1A forward and reverse primers were added to the PCR reaction and PCR reaction was then completed (30 cycles). The generated E1A mutant cDNA was cloned into pCR2.1-TOPO vector and viruses were produced as described above.

### 2.2.3 Viral DNA extraction

DNA from each $CsCl_2$-purified virus was extracted using the QIAmp DNA Blood Mini Kit (Qiagen). 20 μl of proteinase K (Qiagen) was mixed with 200 μl of virus. 200 μl of Buffer AL, supplied with the extraction kit, was then added, followed by incubation at 56˚C for 10 min in the heat block. 200 μl of ethanol were added to the sample, mixed by pulse-vortexing for 15 s, and transferred to a QIAmp spin column in a 2 ml collection tube. After centrifugation for 1 min at 6000x *g*, the QIAmp spin column was transferred to a new collection tube. 500 μl of Buffer AW1 (supplied) was added to and then sample was centrifuged at 6000x *g* for 1 min wash bound viral DNA. 500 μl of Buffer AW2 (supplied) was added and the column was centrifuged at 20000x *g* for 3 min. With

| | | Sequence | binding site in Ad5 genome |
|---|---|---|---|
| E1A | Forward | GCGCGCACCATGAGACATATTATCTGCC | 5’448 |
| | Reverse | CTCGAGTTATGGCCTGGGGCGTTTAC | 3’1349 |
| set 1 | Forward | CCCGGTGAGTTCCTCAAGAGGCCAC | 5’476 |
| | Reverse | CCGGACCCAAGGCTCTCTGCTCCGGCTGCTCGGGC | 3’853 |
| set 2 | Forward | GTAATGTTGGCGGTGCAGGAAGGGATTG | 5’767 |
| | Reverse | GGGTCCCCCGTATTCCTCCGGTGATAATGAC | 3’1029 |
| set 3 | Forward | GTGTTCGCTTTGCTATATGAGGACCTGTGGC | 5’1069 |
| | Reverse | CCTCGATACATTCCACAGCCTGGCGACGCCCACC | 3’1453 |
| set 4 | Forward | CCTGTGATTGCGTGTGTGG | 5’1554 |
| | Reverse | GACAACAGTAGCAGGCGATTC | 3’2124 |
| set 5 | Forward | GCATCTGTGGAGAGCGGTTGTGAGACAC | 5’2073 |
| | Reverse | GCGCCAGCAGATCAAGCTCATTAGCGC | 3’2440 |
| set 6 | Forward | GCTTAATGACCAGACACCGTCCTGAGTG | 5’2383 |
| | Reverse | GCACCAAGTGATCGGGCCTCAGCTCC | 3’3434 |
| set 7 | Forward | CACCCTCACGCTCATCTGCAGCCTCATCACTGTGG | 5’29915 |
| | Reverse | CTTCAGACGGTCTTGCGCGCTTCATCTGC | 3’31038 |
| set 8 | Forward | CGCTGGGGTCGCCACCCAAGATGATTAGG | 5’28715 |
| | Reverse | GAGTAGGGTACAGACCAAAGCGAGCACTG | 3’29135 |
| Hexon | Forward | GGACAGGCCTACCCTGCTAAC | 5’21564 |
| | Reverse | TGCTGTCAACTGCGGTCTTG | 3’21618 |
| 1102 | Forward | CAGCTGATCGAAAGCCATTTTGAACCACCTACCCTTCACG | 5’664 |
| | Reverse | TTCAAAATGGCTTTCGATCAGCTGGTCCAAAAGACTGG | 3’635 |
| 1104 | Forward | CACGAACTGTATGCGGTTTCGCAGATTTTTCCCG | 5’739 |
| | Reverse | CTGCGAAACCGCATACAGTTCGTGAAGGGTAGGTGGTTC | 3’701 |
| 1108 | Forward | ATCGATCTTACCGGCTTTCCACCCAGTGACGACG | 5’940 |
| | Reverse | GGGTGGAAAGCCGGTAAGATCGATCACCTCCGGT | 3’929 |
| 18S | Forward | CGCCGCTAGAGGTGAAATTC | N/A |
| | Reverse | CATTCTTGGCAAATGCTTTCG | N/A |

**Table 4.** Description of primers used in this thesis, indicating their respective sequence and the binding nucleotides in the Ad5 genome. Primer sets 1 to 8 were used for characterisation of viral E1A-mutants after production, while hexon and 18S primers were used for qPCR.

the column placed in a sterile eppendorf tube, 70 µl of distilled $H_2O$ were added and the column was centrifuged at 6000x *g* for 1 min. The collected filtrate contained purified viral DNA.

## 2.2.4 Viral particle count determination

### 2.2.4.1 Particle determination by optical density (OD)

Dialysis buffer used for virus purification and lysis buffer (1% SDS, 0.04 M Tris-HCl pH 7.4 in $dH_2O$) were prepared; 300 µl of each CsCl-purified virus was used for particle count determination by the optical density assay. Two samples were prepared for each virus:

Sample 1: 100 µl of virus, 100 µl of dialysis buffer, 200 µl lysis buffer.
Sample 2: 200 µl of virus, 200 µl of lysis buffer.

Samples were vortexed and incubated at 56˚C for 10 minutes in a heat block, vortexed 3 times and allowed to cool at room temperature for 10 minutes. 600 µl of distilled H2O was added to each sample and absorbance at 260 nm ($OD_{260}$) was measured using a Beckman DU520 spectophotometer; $OD_{260}$ of sample 1 should be below 0.02 and above 0.05 for sample 2, ensuring accuracy of the assay. The number of viral particles (vp/ml) was calculated using the following conversion factor:

$$vp/ml = OD_{260} \text{ x dilution factor x } 1.12 \text{ x } 10^{12}$$

Sample 1 had a dilution factor of 10; sample 2 had a dilution factor of 5. The coefficient factor $1.12x10^{12}$ was calculated based on virion total protein and

$OD_{260}$, assuming that 87% of total dry weight of Ad5 is protein and that Ad5 molecular mass of $2.3x10^7$ D (211).

#### 2.2.4.2 Particle determination by Pico Green Assay

Pico Green particle determination was done using the Quanti-iT Pico Green dsDNA Assay Kit (Invitrogen) and the Tecan Infinite F200 plate reader (Tecan. Mannedorf, Switzerland). 1:10 and 1:100 dilutions of virus stock were prepared with TE buffer containing 0.5% SDS. Standard dilutions of Lambda DNA provided with the kit were also prepared, from 500 ng/ml to DNA-free standard sample in 5-fold serial dilutions. 100 µl of each dilution was transferred to well of a 96-well plate. Each sample was analysed in triplicate. 100 µl of a 1:200 dilution of the Pico Green reagent was added to each sample and emission at 535 nm after excitation at 485 nm was measured using the Magellan V6.3 software (Tecan). Using the fluorescence measurements from the Lambda DNA serial dilutions, a DNA concentration vs fluorescence graph was constructed with GraphPad Prism software and DNA concentration in virus samples were calculated according to the generated graph and to the dilution factor for each sample. Vp/ml were calculated on the basis that 1 µg DNA was equivalent to $2.7x10^{10}$ vp.

### 2.2.5 Virus titration assay: $TCID_{50}$

The $TCID_{50}$ assay (tissue culture inhibitory dose 50%) is a limiting dilution assay that enables the absolute quantification of any infectious particles in the test sample. The assay used in our lab was based on the original Karber-Speaman equation modified as described by O'Reilley (212).

JH293 cells were seeded in 96-well plates at $1x10^4$ cells/well in 200 µl of DMEM supplemented with 10% FCS. 24h after seeding, virus was diluted in FCS free DMEM to $1x10^{-7}$ of the stock and 20 µl was used to infect each well of the first row on the 96-well plate. Serial dilutions within the same plate from each well of the first row to the second row and so until the seventh row (row G), as last row (row H) was left uninfected as a control of the assay. Cytopathic effect (CPE) 11 days post-infection was scored and the number of wells with CPE in each row were counted and used in the following equation to calculate the $TCID_{50}$ value:

$$\text{Log } TCID_{50} = A - D\,(S - 0.5)$$

A = Log of the highest dilution showing CPE in more than 50% of the wells
D = Log of the dilution factor.
S = summation of the proportion of positive wells in each row.

Quantification of infectious particles was expressed as plaque forming units per ml (pfu/ml). This was calculated by adjusting the Log $TCID_{50}$ to the volume used to infect the wells to obtain Log $TCID_{50}$/ml and multiply this value by the coefficient factor 0.69. According to the Poisson distribution, the proportion (p) of wells not receiving infectious units at a given dose is $e^{-\mu}$, where µ is the concentration of infectious viral particles at that dose. As, $TCID_{50}$ is the dose at which 50% of the wells are infected (p =0.5), meaning that $0.5=e^{-\mu}$, therefore µ=0.69. A more detailed explanation of the mathematics behind these equations can be found in ref. (212).

Viral particles/plaque forming units (vp/pfu) ratio was determined for each purified virus. All viruses used in these thesis had a vp/pfu ratio lower than 50.

## 2.3 Cell viability

### 2.3.1 Dose-response to drug

Docetaxel (Taxotere®, Aventis, Dagenham, UK) is a drug in the taxoid class that binds to microtubules, promoting their assembly and hence preventing cells from dividing, resulting in ultimate cell death. Mitoxantrone (Onkotrene®, Baxter, Norfolk, UK) is a synthetic anthacenedione that suppresses tumour growth by intercalation into cellular DNA and inhibition of topoisomerase II.

$1x10^4$ cells for the DU145 and PC3 cell lines or $2x10^4$ cells for 22Rv1 were seeded in each well of 96-well plates. Cells were exposed 24h later to serial dilutions of docetaxel or mitoxantrone, starting at 200 μM and diluting 1:5 down to 0.1 nM. Media alone and untreated cells were used as control. MTS assay kit Cell Titre 96 $AQ_{ueous}$ Non-Radioactive Cell Proliferation Assay (Promega, WI, USA) was used to determine cell viability 6 days after treatment.

The MTS assay is a colorimetric method for determining cell viability, by using the tetrazolium compound (3-(4,5-dymethylthiazol-2-yl)-5-(3-carboxymethoxyphenyl)-2-(4-sulphophenyl)2H-tetrazolium; MTS) combined with phenazine methosulphate (PMS), an electron coupling reagent. Mitochondrial enzymatic activity of viable cells reduces MTS to formazan, that is water-soluble. The number of living cells is directly proportional to the concentration of formazan in the sample, determined by the absorbance at 490nm. MTS, PMS and DMEM were mixed before addition to the wells (80 μl DMEM, 20 μl MTS, 1 μl PMS per well) and media in the wells was decanted and replaced by the MTS-reagent mixture. Absorbance at 490 nm was measured after 3h of incubation at 37˚C and 5% $CO_2$, using a OpsysMR plate reader (Dynex Technologies Inc, Chantilly, US). Absorbance values for wells with media alone

were subtracted from cell wells (background value of MTS mixture in the absence of cells) and values were expressed as percentages of the absorbance of untreated cells (100% viable cells) according to the following formula:

$$\% \text{ cell death} = 100 - \left[ \frac{Abs_{sample} - }{Abs_{untreated} - Abs_{media}} \right] \times 100$$

Dose-response curves were constructed using GraphPad Prism version 4.0a for Macintosh (GraphPad Software, San Diego CA, USA). The $EC_{50}$ values, efficient concentration killing 50% of the cells, was calculated from the equations of the sigmoidal curves generated by GraphPad Prism software.

### 2.3.2 Dose-response to viruses

$1x10^4$ cells for the DU145 and PC3 cell lines or $2x10^4$ cells for 22Rv1 per well in 96-well plates. Cells were exposed 24h later to 5-fold serial dilutions of each virus, starting at a concentration of $1x10^5$ particles per cell (ppc), down to 0.05 ppc. Cell viability was determined by the MTS assay 6 days after infection, as described above.

## 2.4 Infectability

### 2.4.1 Infectability of prostate cancer cell lines

$2x10^5$ cells (DU145 and PC3 cell lines) or $4x10^5$ cells (22Rv1 cell line) were seeded per well in 6-well plates. Cells were infected with the non-replicating AdGFP at 0, 10, 100 or 1000 ppc in 1ml of FCS free DMEM 24h after seeding. Medium was replaced after 2h with DMEM supplemented with 2% FCS. Cells were collected by trypsinisation 24, 48, 72 and 96h post-infection and washed with DMEM supplemented with 10% FCS to remove the remaining trypsin. Cells were recovered by centrifugation and resuspended in PBS supplemented with 2% FCS. GFP-positive cells were quantified using a benchtop argon laser flow cytometer (FACSCalibur; Becton Dickinson, Cowley, UK) with Cell Quest Pro Software (Becton Dickinson). Green fluorescence was detected at 525 nm using the fluorescence channel 1 (FL-1), with $1x10^4$ cells adquired in total.

### 2.4.2 Infectability in combination with drugs

$2x10^5$ cells (DU145 and PC3 cell lines) or $4x10^5$ cells (22Rv1 cell line) were seeded per well in 6-well plates. 24h later, cells were infected with AdGFP at 2.5, 10 or 100 ppc respectively in 2 ml of DMEM, supplemented with 2% FCS or in 2 ml of DMEM with 2% FCS and mitoxantrone at 50 nM. A second set of samples for each cell line were infected with AdGFP at 100 ppc in 1 ml serum-free DMEM. 2h later medium was removed and replaced by 2 ml of 2% FCS DMEM or with 2ml of 2% FCS DMEM containing mitoxantrone at 50 nM. The number of GFP-expressing cells was quantified by flow cytometry 48h after treatment and expressed as a percentage of total cell number, as described above.

## 2.5 Replication

$2x10^5$ cells/well of the prostate cancer cell lines were seeded in 6-well plates in 2 ml of DMEM supplemented with 10% FCS. Medium was decanted 24h later and cells were infected with each virus at 100 ppc in 1 ml of serum-free DMEM. Medium was replaced by 2 ml of DMEM supplemented with 2% FCS. Cells were harvested with a sterile plastic scrapper at 24, 48 and 96h and collected together with the respective media from each well. Samples were freeze/thawed 3 times in $N_2$ (l) and the supernatant was collected after centrifugation at 1000 rpm for 5 min. Replicating viral particles in each sample was determined by the limiting dilution $TCID_{50}$ assay. Replication of Ad5 was also measured in the presence of mitoxantrone; cells were infected for 2h and media was replaced with DMEM (2% FCS) containing mitoxantrone at 10 or 50 nM.

### 2.5.1 Hexon quantification

The hexon gene was used to quantify viral DNA amplification by qPCR as an indirect method to assess viral replication of Ad5, *dl*1102, AdE1A-1102, *dl*1104, AdE1A-1104, *dl*1108 and AdE1A-1108. Cells were infected with these viruses at 100 ppc for 2h, as described above. DNA was extracted 3, 24,48 and 72h after infection.

#### 2.5.1.1 DNA extraction

DNA was extracted from infected prostate cancer cell lines at the time points mentioned above. Media was removed from the wells and cells were washed with PBS and harvested by scraping with a sterile plastic scrapper in 200 µl of PBS. The Qiagen DNA Blood Extraction Kit (Qiagen) was used for extraction of DNA, as described in section 2.2.3. DNA was quantified using nanodrop and concentration for each sample was adjusted to 5 ng/µl using sterile distilled $H_2O$.

#### 2.5.1.2 qPCR

Hexon copy number was quantified by qPCR, using a 7500 Real Time PCR System and Power SYBR® Green PCR Master Mix (Applied Biosystems). 2 µl of each sample was used in the qPCR reaction in a total volume of 20 µl containing the SYBR green solution and primers at a concentration of 10 µM. The forward and reverse primers for hexon amplification are shown in Table 4. Purified Ad5 DNA was used to generate standard dilutions of known concentrations of viral particles for a standard curve. Ad5 DNA was diluted to a concentration of 9847 pg/µl, equivalent to $5x10^8$ viral particles, assuming that mass of 1 particle is approximately $3.9x10^{-5}$ pg. DNA was then serially diluted 1:10 down to $9.8x10^{-5}$ pg/µl, equivalent to 5 viral particles. 2 µl was used in each reaction to generate a standard curve.

The hexon copy number at 3h post-infection was used as a reference for viral particles that had entered the cells prior to viral replication and genome amplification. Hexon copy number at later time points was expressed as the ratio of the 3h value for each virus in each cell line, showing an increase in viral genomes over time.

## 2.6 Transfections

E1A-12S cDNA was cloned into pcDNA3.1(+) (Invitrogen) by digestion of pCR2.1-TOPO-12S and pcDNA3.1(+) with Kpn I and Xho I (NEB). Fragments were separated by agarose electrophoresis and ligated as previously described to generate pcDNA-12S. Plasmid was amplified by transformation of TOP10 chemically competent bacteria under ampicilin selection and maxiprep preparation.

The pcDNA-GFP plasmid was used for optimisation of the transfection protocol for each one of the reagents used. GFP expression in transfected prostate cancer cell lines was analysed by flow cytometry as described in section 2.4.1; this was done for all transfection reagents and the different conditions used for each one in order to determine the most efficient reagent to transfect prostate cancer cell lines.

Human and murine prostate cancer cells were seeded in 6-well plates at $2x10^5$ cells/well and 24h later were transfected with pcDNA-12S or pcDNA-GFP with different transfection reagents. Cells were trypsinised and collected in PBS 48h after transfection to be analysed for GFP expression by flow cytometry.

### 2.6.1 Genejuice

2 μg of plasmid were mixed with 6 μl of GeneJuice Reagent (Novagen; Darmstadt, Germany) in 100 μl of serum-free DMEM. The mix was incubated at room temperature for 15 min and then added to the cells.

### 2.6.2 Jetpei-RGD

Three different conditions were used for transfection with JetPEI-RGD (Poly-Plus, Illkirch, France). 2 μg of plasmid were diluted in 100 μl of NaCl at 150 mM. 4, 6 or 8 μl of JetPEI-RGD solution were diluted in 100 μl of NaCl in a separate tube. JetPEI-RGD mix was added to the DNA dilution, resulting in DNA:JetPEI-RGD ratios of 1:2, 1:3 or 1:4. The mixtures were incubated at room temperature for 15 and 30 min for all ratios tested, followed by addition to the cells. Transfection at DNA:JetPEI-RGD ratio of 1:2 with 15 minutes of incubation showed best transfection efficiency, based on GFP-expressing cells 48h after transfection with pcDNA-GFP.

Prostate cancer cell lines were also transfected with this reagent in 96-well plates. Cells were seeded at $1x10^4$ cells/well in 200 μl of DMEM, 10% FCS. 24h later, cells were transfected with pcDNA-12S or pcDNA-GFP, using 0.125 μg diluted in 10 μl of NaCl and 0.25 μl of JetPEI-RGD in10 μl of NaCl per well. The order of addition of the reagents and the incubation times were the same as for transfection in 6-well plates.

### 2.6.3 Fugene 6

Fugene 6 Transfection Reagent (Roche, Basel, Switzerland) was used at 2 different DNA to Fugene 6 ratios, 1:3 and 1:6. 2 μg of plasmid was mixed with 6 or 12 μl of Fugene 6 reagent in 100 μl of DMEM, free of FCS and antibiotics. The mixtures were incubated at room temperature for 15 min and added to cells maintained in DMEM supplemented with 2% FCS. A ratio of 1:3 (DNA:Fugene 6) showed the best transfection efficiency.

### 2.6.4 TransIT

Mirus TransIT Prostate Transfection Reagent (Cambridge Bioscience, Cambridge, UK) was the only transfection reagent specifically designed to transfect prostate cells. It contained two different reagents, TransIT-Prostate Reagent and Boost Reagent, that were combined at different ratios with 2 or 3 µg of plasmid DNA to achieve optimal transfection efficiency. The conditions used are described in the following table (Table 5):

| | TransIT-Prostate Reagent (µl) | Boost Reagent (µl) |
|---|---|---|
| Ratio 1 | 4 | 0 |
| Ratio 2 | 4 | 4 |
| Ratio 3 | 4 | 8 |
| Ratio 4 | 6 | 4 |

**Table 5.** Different combinations of TransIT-Prostate Reagent and Boost Reagent used together with 2 and 3 µg of plasmid DNA for transfection of pcDNA-12S and pcDNA-GFP using the Mirus TransIT-prostate transfection reagent

TransIT-Prostate Reagent was added directly into 200 µl of DMEM (FCS free). After 15 minutes incubation at room temperature, 2 or 3 µg of plasmid DNA was added to the diluted transfection reagent and the mix was incubated for 15 minutes at room temperature. Then Prostate Boost reagent was added to the mix and after 15 minutes of incubation at room temperature the mix was transferred to the cells. Best transfection efficiency was obtained with 2 µg of DNA, 6 µl of TransIT-Prostate Reagent and 4 µl of Boost Reagent.

### 2.6.5 Effectene

0.4 µg of plamid was diluted in 100 µl of buffer EC, provided with the Effectene transfection kit (Qiagen). 3.2 µl of enhancer solution (provided with the kit) was added and mixture was incubated for 5 minutes at room temperature. After incubation, 10 µl of Effectene transfection reagent was added to the samples, followed by incubation at room temperature for 10 minutes. DMEM supplemented with 10% FCS was added to each sample and then transferred to the cells, maintained in 1 ml of DMEM supplemented with 10% FCS.

### 2.6.6 Clone selection after JetPEI-RGD transfections.

Human prostate cancer cells were transfected with JetPEI-RGD as described above. 48h after transfection, media was replaced by DMEM (10% FCS) containing geneticin G418 (Sigma-Aldrich) at 800 µg/ml. Cells were maintained under these conditions for a week until successful selection was achieved. Stably transfected cells were maintained in DMEM supplemented with 10% FCS and G418 at 400 µg/ml.

## 2.7 Retroviruses

### 2.7.1 Construction plasmids

Amphotropic phoenix cells (ATCC) were used for retrovirus production. Cells were grown in DMEM, supplemented with 10% FCS, containing hygromycin (Sigma-Aldrich) at 300 μg/ml and diphtheria toxin (Sigma-Aldrich) at 1 μg/ml for a week to ensure the selection of cells able to package retroviral particles.

Phoenix cells were seeded in 10 cm dishes at 70% confluency were transfected with pLPC-12S or pLPC-GFP (kind gifts by Dr. Pilar Martin-Duque, Zaragoza, Spain) using FUGENE 6 kit (Roche, Basel, Switzerland). The pLPC-12S plasmid contained the retroviral packaging signal, the adenovirus E1A-12S cDNA under the control of the CMV promoter and a puromycin-resistance gene. The pLPC-GFP was used for the construction of a control retrovirus expressing GFP. Media was changed to 6 ml of DMEM supplemented with 10% FCS 24h after transfection. Again 24 h later, medium was collected and replaced by 6 ml of fresh DMEM supplemented with 10% FCS. 24h later, medium was collected and dish discarded. The collected medium containing each retrovirus was filtered with a 0.45 μM filter and diluted 1:2 in 10% FCS DMEM and 12 μl of polybrene (Sigma-Aldrich) at 8 mg/ml was added to a final concentration of 10 μg/ml before storage at -80ºC.

### 2.7.2 Retroviral transduction of prostate cancer cells and clone selection

Human and murine prostate cancer cell lines were seeded at $2x10^5$ cells/well in 6-well plates in DMEM supplemented with 10% FCS. 24h later, media was replaced by a 1:2 dilution of retrovirus stock in DMEM (10% FCS). 48h post-infection, media was replaced by DMEM (10% FCS) containing 2 μg/ml of puromycin (Sigma-Aldrich). Cells were treated under these conditions for a week to ensure total selection of infected cells. In addition, percentage of cells infected with the GFP-expressing retrovirus was analysed by flow cytometry as described for infectability assays with AdGFP. Infectability was analysed before and after selection with puromycin.

## 2.8 Combination treatments

### 2.8.1 Synergy

$1x10^4$ cells of each prostate cancer cell line were seeded in 96-well plates and treated after 24 h with different combinations of virus and drug at constant ratios of 62.5, 12.5, 2.5 or 0.5 ppc/nM. One row of the plate was used for each combination; single agent treatment with drug or virus was also performed on each plate and each experiment was set up in triplicate. Untreated cells and wells containing medium alone were used as controls. MTS reagent was added to wells 6 days after treatment and absorbance was used to quantify cell death as described in section 2.3.1. Dose-response curves of each treatment (single or combinations) were constructed with GraphPad Prism to generate $EC_{50}$ values. Isobolograms

were constructed to determine synergistic interactions and combination indexes (CI) using Microsoft Excel as described by the mathematical formula:

$$CI = \frac{vcEC_{50}}{vEC_{50}} + \frac{dcEC_{50}}{dEC_{50}}$$

CI<0.8 = synergistic interaction

0.8<CI<1.2 = additive interaction

1.2<CI = antagonistic interaction

Where $vEC_{50}$ is the $EC_{50}$ of virus alone, $dEC_{50}$ is the $EC_{50}$ of drug alone, $vcEC_{50}$ is the $EC_{50}$ of the virus in combination with the drug and $dcEC_{50}$ is the $EC_{50}$ of the drug in combination with virus.

### 2.8.2 Fixed concentrations of virus and drugs

Prostate cancer cell lines were treated with a combination of fixed concentrations of mitoxantrone and replication-selective adenoviruses. Mitoxantrone at 10 nM, was the concentration chosen based on dose-response studies in each cell line, as it induced no more than 10% cell death in 22Rv1, PC3 and TRAMPC cell lines. Mitoxantrone was combined with two viral doses inducing less than 25% or 50% cell death. These viral doses were selected for each cell line based on the dose-response studies to each virus. Concentrations of mitoxantrone and viruses selected are shown in

Table 6.

| | Dose | PC3 (ppc used) | 22Rv1 (ppc used) | TRAMPC (ppc used) |
|---|---|---|---|---|
| **Ad5** | 1 | 83.1 | 1.01 | 1500 |
| | 2 | 193.8 | 2.2 | 4250 |
| ***dl*312** | 1 | 83.1 | 1.01 | 1500 |
| | 2 | 193.8 | 2.2 | 4250 |
| ***dl*1101** | 1 | 690 | 2.85 | 2100 |
| | 2 | 1683 | 6.4 | 14027 |
| ***dl*1102** | 1 | 281 | 0.64 | 2870 |
| | 2 | 659.7 | 1.6 | 7798 |
| ***dl*1104** | 1 | 846 | 27 | 2720 |
| | 2 | 2589 | 31.5 | 13187 |
| ***dl*1107** | 1 | 42.5 | 0.85 | 1350 |
| | 2 | 260.8 | 1.7 | 4233 |
| ***dl*1108** | 1 | 13.7 | 0.53 | 2130 |
| | 2 | 111.9 | 0.88 | 4365 |
| ***dl*922-947** | 1 | 112 | 0.42 | 1140 |
| | 2 | 365.5 | 0.74 | 3336 |

**Table 6.** Viral particles used to infect PC3, 22Rv1 and TRAMPC cells in combination with mitoxantrone at 10 nM.

The PC3 and TRAMPC cells were seeded in 96-well plates at $1x10^4$ cells/well and the 22Rv1 cells at $2x10^4$ cells/well in 200 µl of DMEM supplemented with 10% FCS. 24h later media was decanted from the plates and replaced by DMEM with 2% FCS. Viruses and mitoxantrone were diluted in DMEM (2% FCS) to a concentration 10x of that selected for treatment and then 10 µl were added to the cells. Cells were treated with mitoxantrone at 10 nM, viruses at the chosen doses or a combination of both in a total volume of 100 µl of

DMEM supplemented with 2% FCS. Cell viability was analysed by MTS assay 6 days after treatment as previously described.

### 2.8.3 Sensitisation: dose-response to drugs in the presence of fixed concentrations of virus

The third type of combination of drugs and viruses consisted of the addition of a fixed dose of virus to cells treated with serial dilutions of mitoxantrone or docetaxel, in order to study changes in sensitivity to these drugs during combination with viruses.

#### 2.8.3.1 Sensitisation by replication selective viral mutants

The 22Rv1, PC3 and TRAMPC cells were seeded in 96-well plates as previously described. Cells were exposed 24h later to serial dilutions of mitoxantrone, starting at 8 μM and diluting 1:5 down to $4x10^{-3}$ nM, alone or in combination with fixed doses of each replication-selective adenovirus in a total volume of 100 μl of DMEM supplemented with 2% FCS. The viral doses used are described in

Table 6. Cell viability was analysed by MTS assay 6 days after treatment. Virus alone was used as control and cell viability was adjusted to subtract the effects of virus alone. $EC_{50}$ value for each treatment was calculated using GraphPad Prism 4.0 and expressed as a percentage of the $EC_{50}$ value of mitoxantrone as single treatment.

#### 2.8.3.2 AdE1A-mutants

22Rv1, PC3 and DU145 cells were seeded in 96-well plates as previously described. 24h later, cells were exposed to 1:5 serial dilutions of mitoxantrone or docetaxel, starting at 8 μM and finishing at $4x10^{-3}$ nM in the presence or absence of different concentrations each AdE1A-mutant, in 100 μl of DMEM supplemented with 2% FCS. Viral concentration inducing no cell death or inducing less than 30% cell death were individually chosen for each cell line based on the dose-response studies to the AdE1A-12S mutant. DU145 cells were treated with drugs in combination with 2 doses of viruses, 10 and 100 ppc. Three viral concentrations were used in PC3 cells: 10, 50 and 100 ppc. For 22Rv1 cells, 1, 2.5 and 10 ppc were used in combination with the drugs. Cells were also treated with drugs or viruses alone. Cell viability was analysed 6 days after treatment by MTS assay; $EC_{50}$ value for each treatment was calculated using GraphPad Prism 4.0 and expressed as a percentage of the $EC_{50}$ value of each drug as single treatment.

### 2.8.4 E1A RT-qPCR

#### 2.8.4.1 Replication selective viruses

PC3 cells were seeded in 6-well plates at $2x10^5$ cells/well in 10% FCS DMEM. 24 later, media was replaced by 1 ml DMEM (2% FCS) with Ad5 at a concentration of 100 ppc. Infection was allowed for 2h and then virus was replaced by 2ml of DMEM (2% FCS) or DMEM (2% FCS) containing mitoxantrone at 10 or 50 nM or docetaxel at 0.1 or 1nM. RNA was extracted from the sample 24 and 48h post-infection using Trizol (Invitrogen) and cDNA was

generated from the RNA of each sample as previously described in section 2.2.2.1 for the generation of E1A-12S cDNA. 2 µl of cDNA sample was used to quantified E1A in each sample by qPCR and each reaction was carried out in a total volume of 20 µl with Power SYBR® Green PCR Master Mix and primers for E1A at a concentration of 10 µM. Cellular 18S RNA was also quantified as control for the reaction. Samples were diluted 1:1000 in distilled $H_2O$ and 2 µl was used for the quantification of 18S. Primers for E1A and 18S are described in Table 4. E1A mRNA quantity in each sample was normalised to 18S RNA.

#### 2.8.4.2 AdE1A-mutants

DU145, PC3 and 22Rv1 cells were seeded in 6-well plates at $2x10^5$ cells/well for DU145 and PC3 or $4x10^5$ cells/well for 22Rv1 cells in 10% FCS DMEM. Two conditions were tested 24h after seeding: in one condition, cells were infected with AdE1A-12S virus at 100 ppc for 2h in 1 ml of serum-free DMEM, and then virus was removed and DMEM (2% FCS) or DMEM (2% FCS) containing mitoxantrone at 50 nM was added to the cells. In the second condition tested cells were were infected with 2.5 (22Rv1), 10 (DU145) or 100 ppc (PC3) in the presence or absence of mitoxantrone at 50 nM; virus was not removed during the length the assay. mRNA was extracted from each sample and cDNA constructed as previously described. E1A and 18S were quantified by qPCR as described above; E1A expression was normalised to 18S expression.

## 2.9 Western blotting

### 2.9.1 Whole cell extract preparation

Prostate cancer cells were seeded in 6-well plates as previously described. For detection of viral proteins, cells were infected with virus at 100 ppc for 24h. For detection of E1A after transfection, cells were transfected and whole cell lysates recovered 24, 48, 72h or 7 days after transfection. For protein detection in combination assays with Ad5, cells were infected for 2h with virus at 100 ppc and then mitoxantrone at 10 nM or docetaxel at 0.1 nM was added to the cells, in 2% FCS DMEM. Whole cell lysates were harvested 24 and 48h after infection. For the detection of proteins during combination of mitoxantrone with AdE1A-mutants, prostate cancer cells were treated with mitoxantrone at 50 nM, each AdE1A-mutant at 2.5 ppc (22Rv1), 10 ppc (DU145) or 100 ppc (PC3), or a combination of both in 2% FCS DMEM. Whole cell lysates were recovered at 24, 48 and 72h.

For harvesting of cell lysates, medium was removed from the wells and cells were washed with PBS. PBS was removed and 100 µl of lysis buffer (25 mM Tris-HCl pH 8, 150 mM NaCl, 1% NP-40 (v/v), 1% sodium deoxycholate (w/v), 0.1% SDS (w/v) and protease inhibitor) were added to each well. Cells were then scraped, recovered and incubated on ice for 30 min. Cells were centrifuged at 14000 rpm for 10 min using an Eppendorf Centrifuge 5415R, lysates were collected and stored at -80˚C.

### 2.9.2 Protein quantification

Protein concentrations in the whole cell extracts were quantified using the Bradford Protein Assay (BioRad). Protein was quantified by diluting 5 µl of whole cell extract in 1 ml of BioRad reagent diluted 1:5 in distilled $H_2O$. In addition, 1, 2, 5, 10 and 15 µl of bovine serum albumin (BSA; Sigma-Aldrich) at 1µg/µl were diluted in 1 ml of diluted BioRad reagent. Absorbance of samples at 595 nm was measured using a Beckman DU520 spectophotometer. A stantard curve of absorbance vs concentration was constructed for the different concentrations of BSA and the protein concentration in each sample was calculated using this graph.

Whole cell lysates were diluted to a concentration of 1 µg/µl with distilled $H_2O$ and 5x loading buffer (5% SDS, 250 mM Tris-HCl pH7.5, 5mM EDTA, glycerol (50%by volume) and Bromophenol Blue); samples were stored at -80˚C prior to use and heated to 100°C for 5 min before separation by electrophoresis.

### 2.9.3 SDS polyacrylamide gel electrophoresis and protein detection

20 µl of each sample was loaded onto 10%, 12% or 15% polyacrylamide gels prepared with a Hoefer SE-400 western blot system (Amersham Biosciences, Bucks, UK). PageRuler Prestained protein ladder (Fermentas UK, York, UK) was also loaded on the gels. Separation of proteins by electrophoresis took place at 120V for 90 min in Tris-Glycine SDS PAGE buffer. Proteins were then transferred onto nitrocellulose membranes provided with the iBlot system (Invitrogen) following manufacturer's protocol.

Membranes were blocked with 5% (w/v) non-fat milk and 0.01% Tween-20 in PBS for 2h at room temperature. Membranes were washed for 10 min in TBS-Tween buffer and primary antibody was added to the membranes as described in

Table 7. Primary antibody was incubated with the membrane overnight at 4˚C, removed and the membrane was washed with TBS-Tween for 10 min at room temperature. Secondary antibody was added to the membrane and incubated for 30 min. Membrane was then washed 3 times with TBS-tween for 10 min.

Detection of protein was done by chemoluminescent detection of horseradish peroxidase-conjugated secondary antibody using the ECL Western Blotting Detection Reagent (Amersham Biosciences, UK). Signal was visualised with Super RX Fuji Medical X-Ray Film (Fujifilm; Düsseldorf, Germany) developed in a Curix 60 Developer (Agfa, Middlesex, UK).

## 2.10 Cell cycle analysis

$2x10^5$ cells (DU145 and PC3 cell lines) or $4x10^5$ cells (22Rv1 cell line) per well were seeded in 6-well plates in DMEM supplemented with 10% FCS. 24h later, cells were treated with mitoxantrone at 50 nM, each AdE1A-mutant at 2.5 ppc (22Rv1), 10 ppc (DU145) or 100 ppc (PC3), or a combination of both in DMEM supplemented with 2% FCS. Attached cells were recovered by trypsinisation after 24, 48 or 72h of treatment. Cells were washed with PBS and recovered by centrifugation at 1700 rpm for 3 min and fixed in 1 ml of 70% ethanol. 24h later, cells were centrifuged and ethanol was decanted. Pellets were washed with PBS and recovered by centrifugation, then diluted in 50 µl of RNAse

A at 100 µg/ml and finally 200 µl of propidium iodine (PI) at 50 µg/ml was added.

| Antibody | Type | Species | Conditions | Supplier |
|---|---|---|---|---|
| E1A | Primary | Rabbit | 1:1000 in 1.5% BSA TBS-tween, 4˚C, O/N | Santa Cruz |
| Hexon | Primary | Rabbit | 1:500 in 1.5% BSA TBS-tween, 4˚C, O/N | Ab Frontier |
| Bcl-2 | Primary | Rabbit | 1:500 in 1.5% BSA TBS-tween, 4˚C, O/N | Santa Cruz |
| Caspase 3 | Primary | Mouse | 1:500 in 1.5% BSA TBS-tween, 4˚C, O/N | AbCam |
| p21 | Primary | Mouse | 1:500 in 1.5% BSA TBS-tween, 4˚C, O/N | Cell Signalling |
| p53 | Primary | Mouse | 1:500 in 1.5% BSA TBS-tween, 4˚C, O/N | Santa Cruz |
| Androgen receptor | Primary | Rabbit | 1:500 in 1.5% BSA TBS-tween, 4˚C, O/N | Santa Cruz |
| Tubulin | Primary | Mouse | 1:20000 in 1.5% BSA TBS-tween, 4˚C, O/N | Sigma |
| Anti-rabbit-HRP | Secondary | Goat | 1:2000 in TBS-tween, 30 minutes, RT | Dako |
| Anti-mouse-HRP | Secondary | Goat | 1:1000 in TBS-tween, 30 minutes, RT | Dako |

**Table 7.** Antibodies used for protein detection in this thesis. RT = room temperature; O/N = overnight. Antibodies providers are Santa Cruz Biotechnology (CA, USA), Ab Frontier (Seoul, Korea), AbCam (Cambridge, UK), Cell Signalling® Technology (MA, USA), Sigma (MO, USA), Dako (Cambridge, UK).

Samples were analysed by flow cytometry using the Benchtop argon laser flow cytometer (FACSCalibur; Becton Dickinson, Cowley, UK) with Cell Quest Pro Software (Becton Dickinson, Cowley, UK). Gates for sub-G1, G1, S and G2/M phase were set based on the cell cycle profile of untreated cells. Percentage of cells in each cell cycle phase was determined for each sample and histograms were constructed using GraphPad Prism 4.0 sfotware.

## 2.11 Caspase inhibitors

### 2.11.1 Inhibition of sensitisation

22Rv1, DU145 and PC3 cells were seeded in 96-well plates, $1x10^4$ cells/well for DU145 and PC3 and $2x10^4$ cells/well for 22Rv1 cells in 200 µl of 10% FCS DMEM. 24h later, cells were treated with serial dilutions of mitoxantrone as single treatment or in combination with 2.5 ppc (22Rv1), 10 ppc (DU145) or 100 ppc (PC3) of each AdE1A-mutant in 2% FCS DMEM, as previously described for sensitisation assays with these viruses in section 2.8.3.2. In addition, cells were also treated with serial dilutions of AdE1A-12S, AdE1A-1102, AdE1A-1104 or AdE1A-1108 viruses in 100 µl of DMEM (2% FCS) or DMEM (2% FCS) containing mitoxantrone at 50 nM. This treatment was done in the presence or absence of the pan-caspase inhibitor z-VAD-FMK (Calbiochem, La Jolla, CA, USA) at a final concentration of 25 µM. Medium was decanted from the plates 3 days after treatment and cell viability was measured by the MTS assay as described in section 2.3.1. $EC_{50}$ values for the drug or each virus in each condition were calculated using GraphPad Prism 4.0 software and expressed as

the ratio of the $EC_{50}$ for the combination treatment compared to mitoxantrone alone.

## 2.12 Analysis of mitochondrial depolarisation

22Rv1, DU145 and PC3 cells were seeded in 6-well plates and 24h later treated with mitoxantrone at 50 nM, AdE1A-mutant viruses or a combination of both as described for the cell cycle analysis. Medium and cells were recovered at 24, 48, 72 and 96h for analysis of mitochondrial depolarisation ($\Delta\Psi$) with tetramethylrhodamine ethyl ester (TMRE) as a measure of apoptotic death. TMRE enters the mitochondria of healthy non-apoptotic cells and is trapped inside, being released when mitochondrial depolarisation occurs.

Cells were recovered by centrifugation at 1700 rpm for 3 minutes, washed with PBS and recovered again by centrifugation. Pellets were diluted in 500 µl of PBS and 40 µl of TMRE (Invitrogen) at 1 µM were added followed by incubation at 37ºC for 20 minutes. Cells were then recovered by centrifugation, washed with PBS and recovered again. Pellets were diluted in 500 µl of PBS and 50 µl of 4',6-diamidino-2-phenylindole (DAPI; Molecular Probes, Eugene, Oregon, USA) solution at 1µg/ml was added to each sample. Samples were analysed by flow cytometry using the FSR flow cytometer (Becton Dickinson). Fluorescence channel 2 FL-2) was used to measure TMRE intake by cells and FL-4 to measure DAPI. Cells were gated using Cell Quest Software (Becton Dickinson) and separated into live cells, proapoptotic cells and dead cells based on the intake of TMRE and DAPI. Percentage of live proapoptotic cells was determined and data was presented using the GraphPad Prism software.

## 2.13 Statistical analysis

Sample data were statistically analysed by t-test for parametric samples when only two data sets were compared. For comparison of more than two data sets, ANOVA was performed and each sample was indidually compared to the control sample using the t test with the Bonferroni's correction. The Bonferroni's correction addresses the problem of multiple comparisons to avoid familywise error rate. The correction consists on multiplying the p-values obtained in each comparison by the number of comparison made with all the data sets.

# Chapter 3

# *Effects of E1A-mutated replication selective adenoviruses and cytotoxic drugs in prostate cancer cell lines.*

## 3.1 Effects of adenovirus mutants in prostate cancer cell lines.

### 3.1.1 Deletion of p300 binding region of E1A attenuated viral toxicity in prostate cancer cell lines.

In order to evaluate the potential of replication-selective adenoviruses in the treatment of prostate cancer, we examined the toxicity of these viruses as single agents. The human prostate cancer cell lines DU145, 22Rv1 and PC3 and the murine prostate cancer cell lines TRAMPC and RM1 were infected with serial dilutions of different Ad5 replicating E1A-deletion mutants, starting at a concentration causing 100% cell death down to concentrations that had no toxic effects on the cells. Dose-response curves were generated and the effective

concentrations inducing 50% cell death ($EC_{50}$ values), expressed as number of particles per cell (ppc), were calculated to determine viral potency in each cell line for each virus (Fig. 8). The murine cell lines were significantly more resistant to Ad5-induced death than the human cell lines. TRAMPC and RM1 cells had $EC_{50}$ values 1000-fold higher than those of 22Rv1 or DU145 and 10 fold higher than that of PC3 cells.

PC3 cells were more resistant to viral toxicity than the other human cell lines tested, with an $EC_{50}$ value of 104.1 ppc for Ad5. DU145 cells had an $EC_{50}$ value of 6.9 ppc for the wild-type virus, while the 22Rv1 cells were the most sensitive, with an $EC_{50}$ value of 1.4 ppc. A similar trend was observed when E1A-mutant viruses were tested; cell lines resistant to Ad5 toxicity were also more resistant to the mutant viruses tested. Sensitivity to each mutant was different while the order of potency was similar in all human cell lines. Toxicity was attenuated in viruses expressing mutant E1A proteins unable to bind p300 (*dl*1101 and *dl*1104), with significantly higher $EC_{50}$ values compared to Ad5 in each cell line.

The other E1A-mutant viruses tested were as efficient as Ad5 in inducing cell death in all human cell lines. Similar results were obtained in the murine cell lines RM1 and TRAMPC; cell death induced by *dl*1101 and *dl*1104 mutants was attenuated as compared to Ad5, with significantly increased $EC_{50}$ values. The E1A-mutant *dl*1107 also showed statistically significant attenuation of toxicity in RM1 cells.

Additionally, potency of the E1A-deletion mutants was compared to the well-established attenuated efficacy of the E1B55K-deleted replication-selective mutant *dl*1520. As expected, the toxicity of this virus was significantly attenuated in all prostate cancer cells except in the murine cells TRAMPC and RM1.

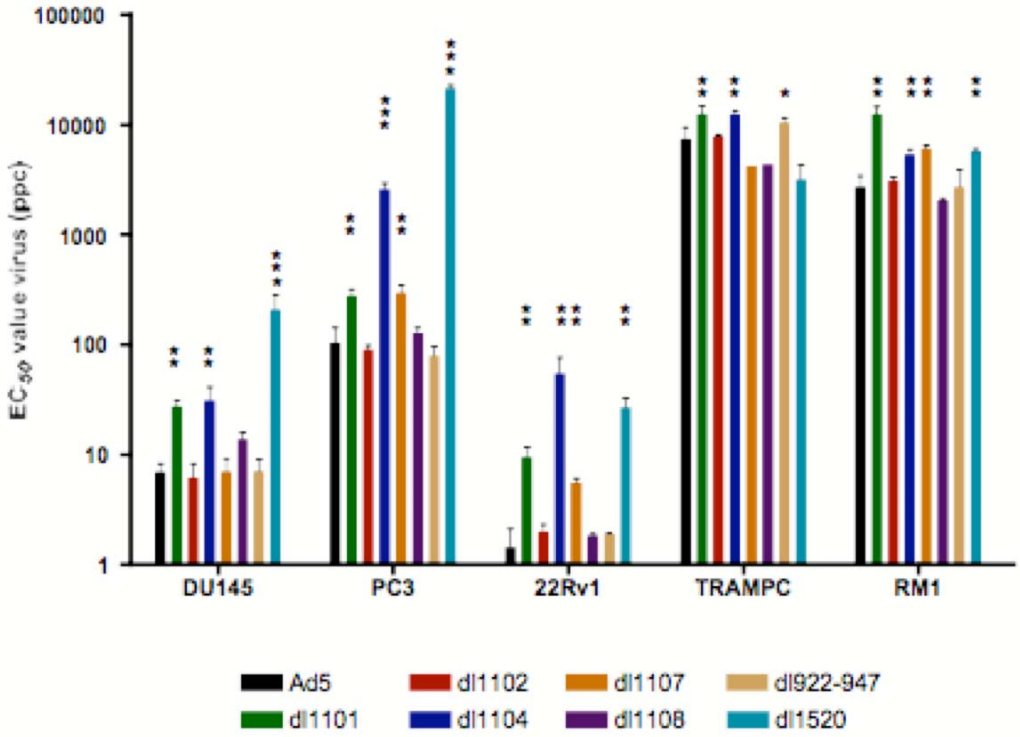


**Fig. 8.** $EC_{50}$ values (ppc) for Ad5, the corresponding E1A-mutants and the *dl*1520 mutant in three human (DU145, PC3 and 22Rv1) and two murine prostate cancer cell lines (TRAMPC and RM1). Bars show average and standard deviation of 3 independent experiments. ANOVA and t test with the Bonferroni correction were used to statistically analyse the data and compare $EC_{50}$ values of each virus to that of Ad5 within each cell line; significant p-values are shown, $p<0.05$ (*), $p<0.01$ (**) or $p<0.001$ (***). A more deatailed explanation of the statitic tests used can be found in the Materials and Methods section.

To confirm that the differences observed in $EC_{50}$ values were not due to a low number of active viral particles in our virus stocks, the ratios of viral particle/plaque forming unit (vp/pfu) were calculated for each virus tested (Table 8). Only viruses with a vp/pfu ratio below 50 were used in these studies. All ratios were within standard range (3 to 30 vp/pfu), with little variation that did not explain the observed differences in potency; therefore, differences in $EC_{50}$ values were likely the result of the mutation in each virus and the corresponding gene alterations in the cancer cell lines.

| | ***vp/ml*** | ***pfu/ml*** | ***vp/pfu ratio*** |
|---|---|---|---|
| **Ad5** | 6.16E+11 | 3.10E+10 | 19.9 |
| ***dl1101*** | 1.00E+12 | 1.19E+11 | 8.4 |
| ***dl1102*** | 1.59E+12 | 1.19E+11 | 13.4 |
| ***dl1104*** | 3.90E+12 | 4.30E+11 | 9.1 |
| ***dl1107*** | 9.00E+11 | 5.80E+10 | 15.5 |
| ***dl1108*** | 2.50E+12 | 6.80E+11 | 3.7 |
| ***dl922-947*** | 3.62E+12 | 6.80E+11 | 5.3 |
| ***dl1520*** | 1.05E+12 | 7.59E+10 | 13.8 |

**Table 8.** Viral titres, particles/ml (vp/ml) and plaque forming units/ml (pfu/ml), and ratios (vp/pfu) for Ad5 and the corresponding E1-deletion mutants used in this and future studies.

### 3.1.2 Resistance to viral toxicity correlated with poor infectability.

To determine whether the different sensitivity to virus-induced cell death of each cell line was caused by differences in infectivity, cells were infected with 10, 100 or 1000 ppc of a non-replicating GFP-expressing Ad5 virus (AdGFP). GFP-expressing cells were quantified by flow cytometry 48h after infection (Fig. 9).

All cell lines expressed GFP in a dose-dependent manner, suggesting that cellular uptake of virus was directly proportional to the AdGFP dose. The human cell line 22Rv1 showed the highest percentage of GFP expression at all viral concentrations tested, with more than 30% of cells infected at 100 ppc and nearly

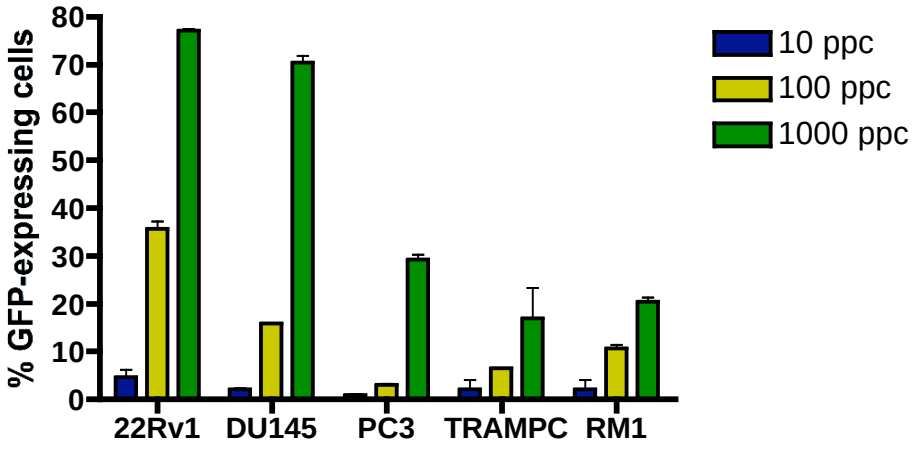


**Fig. 9.** Percentage of GFP-expressing cells 48h post-infection with 10, 100 or 1000 ppc of a non-replicating AdGFP. The murine cell lines TRAMPC and RM1 and the human cell line PC3 were less infectable than 22Rv1 and DU145 cells. Data presented as percentage of total cells expressing GFP with standard deviation (n=3).

80% of cells expressing GFP at 1000 ppc. AdGFP virus successfully infected DU145 cells, with approximately 70% of cells expressing GFP at 1000 ppc. The PC3 cell line was the only human cell line tested that showed poor infectability; only 30% of cells were expressing GFP at 1000 ppc.

Both murine cell lines were poorly infectable, with approximately 20% of cells infected at 1000 ppc. Murine cells were infected to levels similar to those of PC3 cells, thus poor infectability was not the cause of resistance to viral toxicity in murine cells, as PC3 cells were more sensitive to virus-induced cell death despite their poor infectability (Fig. 9).

### 3.1.3 Ad5 efficiently replicated in human but not in murine prostate cancer cell lines.

To determine if differences in viral toxicity correlated with replication efficiency, the level of replication of Ad5 was assessed in each cell line at 24, 48, 72h and 96h post-infection (Fig. 10). Wild type adenovirus failed to replicate in the murine cell lines TRAMPC and RM1, explaining the resistance to viral toxicity in these cells. Replication was observed in all human cell lines with the amount of virus produced significantly increased 48h after infection and continued to increase up to 96h after infection. Ad5 replication was more efficient in DU145 cells, producing approximately 7500 pfu/cell after 96h. 22Rv1 cells were also able to support high levels of replication, with approximately 1500 pfu/cell 96h post-infection. PC3 was the only human cell line that supported viral replication poorly, being significantly lower than in DU145 or 22Rv1 cells.

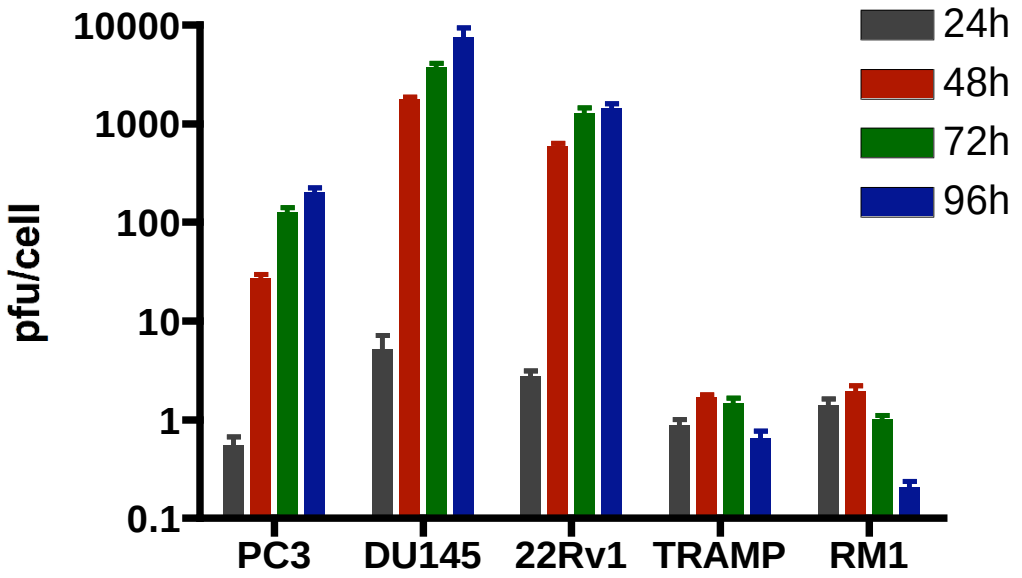


**Fig. 10.** Replication of Ad5 in prostate cancer cell lines over time. Cells were infected with 100 ppc for 2h and production of virus (pfu/cell) was determined by the $TCID_{50}$ assay at the indicated time points. Amplification of virus was seen after 48h of infection and peaked at 96h in human prostate cancer cell lines; no amplification of virus was observed in the murine cell lines, indicating that Ad5 did not replicate in these cells. Average and standard deviation of 2 independent experiments.

## 3.2 The PC3 cell line showed higher resistance to cytotoxic drugs currently used for prostate cancer treatment.

To investigate whether prostate cancer cell lines were sensitive to the cytotoxic drugs commonly used in the clinic, cells were treated with serial dilutions of mitoxantrone or docetaxel, dose-response curves were generated and $EC_{50}$ values for the drugs were determined in each cell line (Fig. 11).

All cell lines were more sensitive to docetaxel than to mitoxantrone. Sensitivity to mitoxantrone was similar for all tested cell lines except for the PC3 cells that were significantly more resistant to this drug (Fig. 11). The $EC_{50}$ value for mitoxantrone in PC3 cells was 160.5±23 nM, while the values in other cell lines varied from 50 to 70 nM. Similar trends were seen with docetaxel with the PC3 cells being more resistant than other tested prostate cancer cell lines. The 22Rv1 cells were the most sensitive cells to docetaxel, with an $EC_{50}$ value of 3.6±1.9 nM.

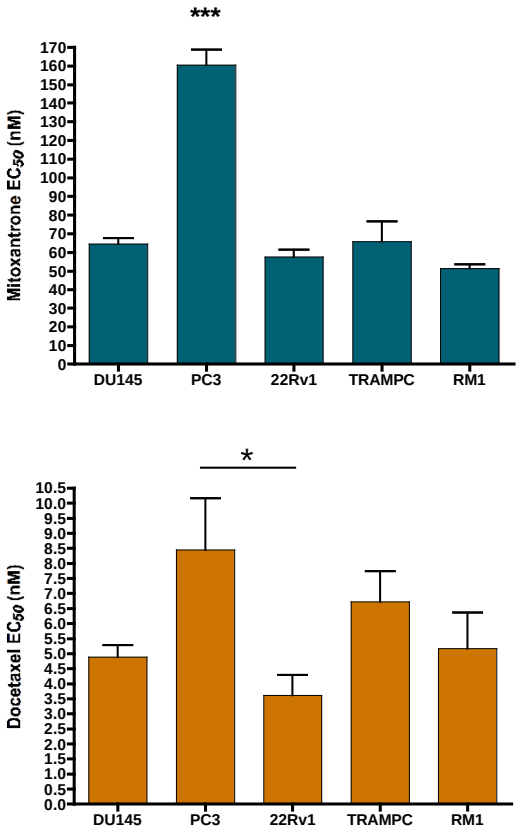


**Fig. 11.** Toxicity of mitoxantrone (A) and docetaxel (B) in prostate cancer cell lines expressed as the $EC_{50}$ value for each drug (nM). Data was analysed by ANOVA and t test with Bonferroni's correction were used to compare data from each cell line with those of the other cell lines. The human prostate cancer cell line PC3 was significantly more resistant to mitoxantrone than the other cell lines used, $p<0.001$ (***). PC3 cells were also significantly more resistant to docetaxel than 22Rv1 cells, $p<0.05$ (*). Bars represent an average of 5 to 9 independent experiments with standard deviation.

## 3.3 Enhancement of cancer cell killing by combining treatments of chemotherapy and replication-selective adenoviruses.

To explore whether combination of viruses and drugs could sensitise prostate cancer cell lines to the cytotoxic effects of mitoxantrone, different combination studies were designed to investigate interactions between the E1A-mutant adenoviruses and mitoxantrone. By testing different combinations, these studies would enable us to elucidate what deletions in the E1A-gene might affect chemo-sensitisation.

### 3.3.1 The magnitude of the synergistic effects with mitoxantrone and adenoviruses in prostate cancer cells was cell line dependent.

The first combination tested was designed to elucidate the possible synergistic interaction between viruses and cytotoxic agents. This assay enabled us to determine whether virus and drug acted in synergy, greater than the additive effect of each treatment used independently, or antagonistic, less than the additive effect of each agent alone. The human PC3, 22Rv1 and murine TRAMPC cell lines were treated with serial dilutions of mitoxantrone and replicating Ad5 or E1A-mutant adenoviruses combined at four constant ratios of 0.5, 2.5, 12.5 and 62.5 ppc/nM. $EC_{50}$ values and combination indexes (CI) were calculated to determine synergistic ($CI \leq 0.8$), additive ($0.8 < CI < 1.2$) or antagonistic interactions ($CI \geq 1.2$) (Table 9). An example of how CIs were calculated is shown in Fig. 12 and Fig. 13.

**A**

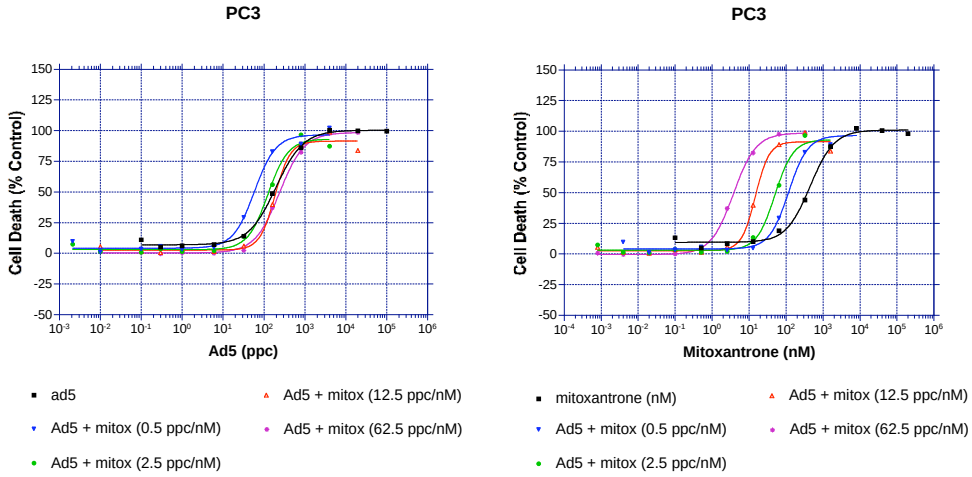


**B**

| Treatment | $EC_{50}$ value for virus (ppc) | $EC_{50}$ value for mitoxantrone (nM) |
|---|---|---|
| Ad5 | 193.8 | N/A |
| Mitoxantrone | N/A | 443.9 |
| Ad5 + mitox (0.5 ppc/nM) | 58.1 | 116.1 |
| Ad5 + mitox (2.5 ppc/nM) | 124.0 | 48.6 |
| Ad5 + mitox (12.5 ppc/nM) | 284.4 | 14.7 |
| Ad5 + mitox (62.5 ppc/nM) | 237.6 | 3.7 |

**Fig. 12.** Example of isobologram construction: determination of $EC_{50}$ values for virus and drug at every combination ratio. PC3 cells were treated with Ad5 and mitoxantrone as described in materials and methods and dose-response curves were constructed independently for the virus and the drug at different concentrations (A). $EC_{50}$ values were calculated from the dose-response curves for virus and mitoxantrone at every combination ratio using Prism Software (B).

**A**

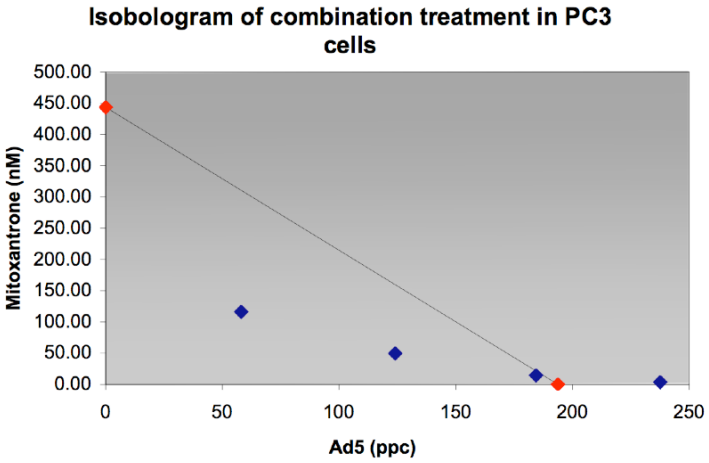


**B**

$$CI\ (0.5ppc/nM) = \frac{58.1}{193.8} + \frac{116.1}{443.9} = 0.56$$

| Treatment | Combination index (CI) |
|---|---|
| Ad5 + mitox (0.5 ppc/nM) | 0.56 |
| Ad5 + mitox (2.5 ppc/nM) | 0.75 |
| Ad5 + mitox (12.5 ppc/nM) | 0.98 |
| Ad5 + mitox (62.5 ppc/nM) | 1.23 |

**Fig. 13.** Example of isobologram construction: determination of combination indexes. $EC_{50}$ values obtained from Fig. 12 were used to construct an isobologram of the combination (A). The X-axis indicates $EC_{50}$ values for Ad5 for each combination ratio; the Y-axis representes the $EC_{50}$ values for mitoxantrone. Both values for each ratio intersect in a blue point that represents that particular combination ratio. The red points indicate the $EC_{50}$ value for virus or drug as single agents. Data points below the line linking these values indicate a synergistic interaction between virus and drug; points above the line indicate antagonism. Using the mathematical formula described in the materials and methods section, combination indexes (CI) were obtained for quantitative measure of the interactions. The calculation of the CI for the first ratio tested is given as example, using the $EC_{50}$ values calculated in Fig. 12 (B): synergisctic ($CI \leq 0.8$), additive ($0.8 < CI < 1.2$) or antagonistic ($CI \geq 1.2$).

In PC3 cells, combinations with mitoxantrone resulted in clear synergy in at least two out four ratios for all mutants except for *dl*1108 that, similar to Ad5, showed synergy only at the lowest virus to drug ratio. CI values for all other E1A-mutants were lower than for Ad5. The *dl*1108 and the *dl*1107 mutants were the only viruses that interacted antagonistically with mitoxantrone, with CI values higher than 1.2 in one to two of the ratios tested. Synergy in PC3 for all ratios was only achieved in combinations with the *dl*1102 or *dl*1104 mutants; the *dl*1104 mutant showed the best synergistic interactions with mitoxantrone, with CI values of 0.09 and 0.18 for the 2.5 and 12.5 ppc/nM ratios respectively. The *dl*1107 mutant also showed very low CI values for three of the combinations, while at a ratio of 62.5 ppc/nM antagonistic effects were observed (Table 9). The E1A-deleted virus *dl*312 was also used, but CI values could not be determined as the dose-response curve could not be constructed due to the severe potency attenuation of this mutant. The *dl*1520 mutant, with an intact E1A gene but lacking E1B-55K, showed better synergistic interactions than Ad5, indicating than deletions in the E1B gene could improve the synergistic interactions between viruses and mitoxantrone.

No synergy was observed for mitoxantrone and the E1A-mutants in the 22Rv1 cell line, except with the *dl*922-947 mutant at the lowest ratio (0.5 ppc/nM). Synergy between Ad5 and drug was only obtained at one of the four ratios tested; treatment at other ratios only resulted in additive effects (2.5 and 62.5 ppc/nM) and antagonism at the lowest ratio (Table 9). Interactions with the drug did not improve in combination with the *dl*1520 mutant compared to Ad5, as observed in PC3 cells, possibly indicating that functional status of different cellular pathways might have an important role in chemosensitisation.

PC3: combination index: viral mutants and mitoxantrone

| | 1 | 2 | 3 | 4 | |
|---|---|---|---|---|---|
| Ratio (ppc/nM) | 0.5 | 2.5 | 12.5 | 62.5 | |
| Ad5 | 0.68 ± 0.16 | 0.92 ± 0.24 | 0.93 ± 0.07 | 1.01 ± 0.31 | *n=3* |
| *dl1101* | 0.49 ± 0.13 | 0.62 ± 0.28 | 0.99 ± 0.20 | 1.09 ± 0.21 | *n=3* |
| *dl1102* | 0.69 ± 0.07 | 0.7 ± 0.21 | 0.88 ± 0.05 | 0.81 ± 0.02 | *n=3* |
| *dl1104* | 0.64 | 0.09 | 0.18 | 0.57 | *n=1* |
| *dl1107* | 0.25 | 0.31 | 0.63 | 1.51 | *n=1* |
| *dl1108* | 0.78 | 1.36 | 1.12 | 1.83 | *n=1* |
| *dl922-947* | 0.91 | 0.36 | 0.43 | 1.2 | *n=1* |
| *dl1520* | 1.27 | 0.16 | 0.21 | 0.52 | *n=1* |

TRAMP-C: combination index: viral mutants and mitoxantrone

| | 1 | 2 | 3 | 4 | |
|---|---|---|---|---|---|
| Ratio (ppc/nM) | 0.5 | 2.5 | 12.5 | 62.5 | |
| Ad5 | 0.89 ± 0.13 | 0.75 ± 0.09 | 0.86 ± 0.10 | 0.77 ± 0.25 | *n=3* |
| *dl1101* | 0.99 ± 0.19 | 0.96 ± 0.25 | 0.98 ± 0.32 | 0.74 | *n=3* |
| *dl1102* | 0.8 ± 0.45 | 0.79 ± 0.19 | 0.74 ± 0.33 | N/A | *n=3* |
| *dl1104* | 0.99 | 1.17 | 1.42 | 0.66 | *n=1* |
| *dl1107* | 1.02 | 0.6 | 0.51 | 1.12 | *n=1* |
| *dl1108* | 1.11 | 1.36 | 1.03 | N/A | *n=1* |
| *dl922-947* | 0.61 | 0.76 | 1.13 | 1.07 | *n=1* |
| *dl1520* | 0.56 | 0.53 | 1.22 | 0.9 | *n=1* |

22Rv1: combination index: viral mutants and mitoxantrone

| | 1 | 2 | 3 | 4 | |
|---|---|---|---|---|---|
| Ratio (ppc/nM) | 0.5 | 2.5 | 12.5 | 62.5 | |
| Ad5 | 1.58 | 1.22 | 0.76 | 1 | *n=1* |
| *dl1101* | 1.22 | 1.39 | 1.39 | 1.33 | *n=1* |
| *dl1102* | 1.13 | 1.46 | 1.24 | 1.18 | *n=1* |
| *dl1104* | 1.36 | 1.25 | 1.17 | 1.32 | *n=1* |
| *dl1107* | 1.49 | 1.15 | 1.63 | 1.89 | *n=1* |
| *dl1108* | 1.15 | 1.57 | 1.68 | 1.43 | *n=1* |
| *dl922-947* | 0.59 | 0.95 | 1.22 | 1.34 | *n=1* |
| *dl1520* | 0.99 | 0.97 | 1.35 | 0.89 | *n=1* |

**Table 9.** Combination indexes (CI) of the different combinations of mutant adenoviruses or Ad5 with mitoxantrone in PC3, TRAMPC and 22Rv1 cells. Values below 0.8 represent clear synergy: values between 0.8 and 1.2 indicate additive effect. Values over 1.2 indicate antagonistic effect of the combination. Number of times the experiment was repeated is indicated (n).

The effects of combination of mitoxantrone and E1A-mutant adenoviruses in the murine TRAMPC cells resulted in additive effects at most combination ratios. Ad5 and the *dl*1101 and *dl*1102 mutants showed CI values close to 0.8 at all ratios tested, indicating additive effects with a trend towards synergy. As observed in PC3 cells, the *dl*1520 mutant had better CIs than Ad5, even though both viruses express wild type E1A proteins. Synergistic interactions were observed with the other mutants at one or two of the ratios used. The mutant

*dl*922-947 showed low CI values at the two lowest ratios used, while the *dl*1107 mutant showed better interactions at 2.5 and 12.5 ppc/nM ratios. The *dl*1104 mutant showed synergy with mitoxantrone at the higher ratio tested, although it acted antagonistically with the drug at one of the ratios (Table 9).

These data indicated that synergistic interactions between viruses and mitoxantrone were not only dependent on the specific deletions within E1A in each mutant but also on E1B-deletions (*dl*1520 mutant) and the gene expression profile of each cell line, possibly due to the functional status of pathways controlling cell survival and/or apoptosis. Combinations of viruses and drug in PC3 cells resulted in good synergistic interactions with almost all the mutants tested, while these interactions were mostly antagonistic in 22Rv1 cells. The *dl*1108 mutant was the only virus that did not show synergistic interactions in any of the cell lines tested although other mutant viruses with smaller deletions in the same pRb-binding region, *dl*1107 and *dl*922-947, were able to act in synergy with mitoxantrone.

### 3.3.2 Combination of mitoxantrone and viruses at fixed concentrations showed that sensitisation was dependent on both the respective cell line and the concentration of mitoxantrone or viruses.

Based on the synergy studies a more simplified experimental set up was used to further evaluate the response to viral mutants in combination with mitoxantrone. The 22Rv1, PC3 and TRAMPC cell lines were treated with fixed concentrations of drug and virus. Concentrations of mitoxantrone that induced less than 10% cell death were combined with two viral doses that killed less than 25% or 50% of the cells (Fig. 14); these doses were determined for each cell line

from dose response curves obtained during the analysis of viral toxicity. Observations of supra-additive effects (synergistic effects) on cell death in response to the combination treatments suggested that cell killing efficacy was improved. The murine TRAMPC cells showed higher supra-additive effects than the human cell lines 22Rv1 and PC3, despite the poor replication and infectivity previously observed with adenoviruses in this cell line (Fig. 9 and Fig. 10). There was an increase in cell death for all combinations tested with mitoxantrone and low levels of Ad5, E1A-deletion mutants and the E1B55K-deleted virus in TRAMPC cells. This increase was higher with the *dl*922-947 and *dl*1520 mutants than with Ad5. At the higher concentrations of virus, only the *dl*1107 mutant failed to induce supra-additive effects in combination with the drug. These results were slightly different from the findings reported in the previous section, with improved cell killing using the fixed concentrations conditions. No supra-additive effect was observed with the E1A-deleted mutant *dl*312, indicating that E1A expression is required for chemosensitisation.

In the human cell lines the combination treatments did not result in significant supra-additive effects; no increase in cell death was observed with any adenovirus in 22Rv1 and PC3 cells when mitoxantrone was combined with the lower viral concentrations. Higher concentrations of viruses resulted in small supra-additive effects in 22Rv1 cells; all E1A-mutant adenoviruses with the exception of the *dl*1108 mutant, were able to induce a small increase in cell death compared to the theoretical additive effect. However, 22Rv1 cells were very sensitive to virus-induced cell death and the viral concentrations tested induced a higher percentage of cell death than expected, that could have affected the results, as seen for the *dl*1108 and *dl*922-947 mutants. The use of fixed concentrations of viruses and mitoxantrone showed similar results as the synergy studies, suggesting that 22Rv1 cells were more resistant to chemosensitisation by adenovirus E1A than other prostate cancer cell lines.

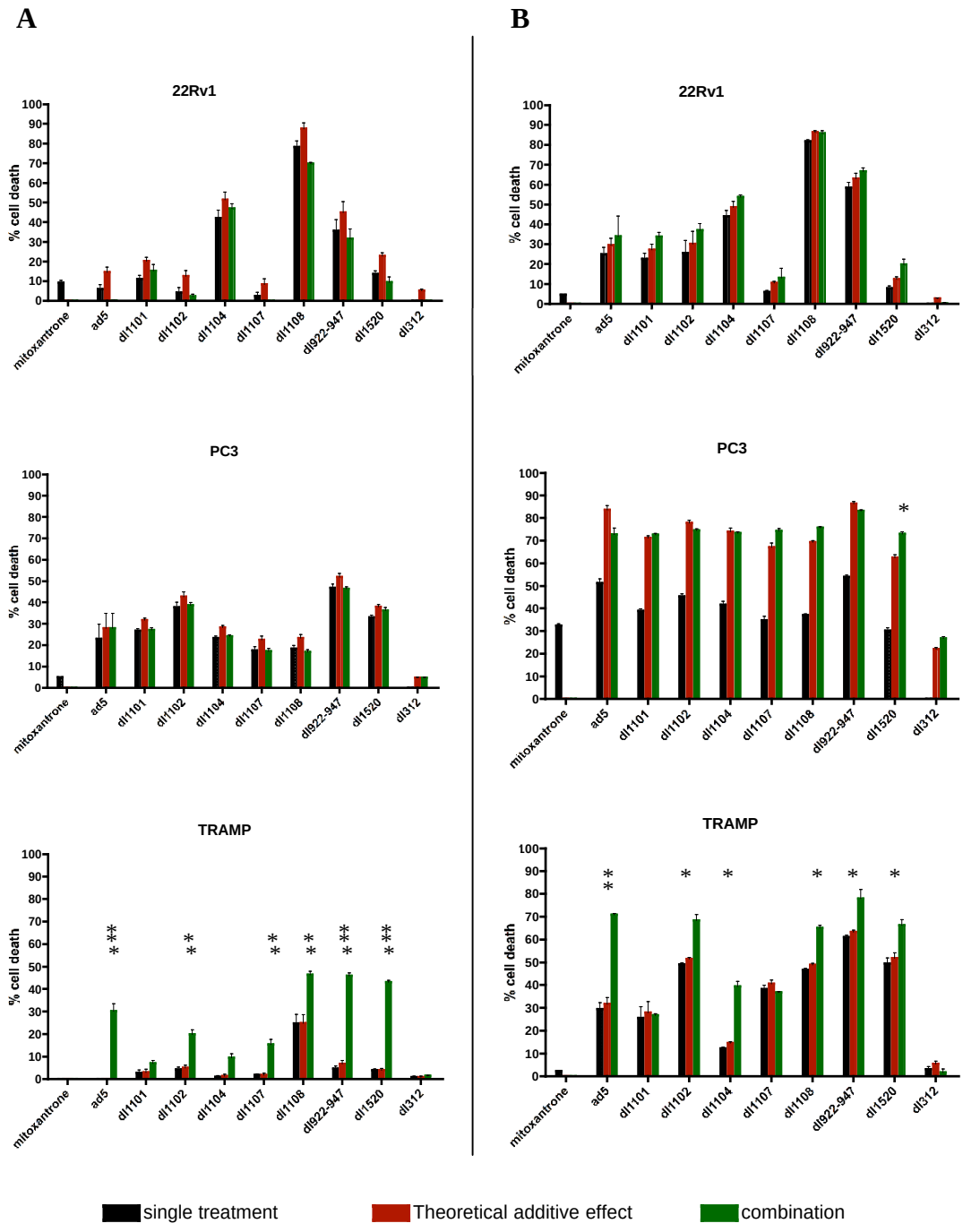


**Fig. 14**. Effects on cell viability by mitoxantrone, E1A-mutant adenoviruses or combination of both at a low dose (A) or a high dose (B) of the respective viruses. Viral doses used can be found in Fig. 15.B. Bars in black indicate the percentage of cell death caused by each agent as a single treatment; red bars indicate the theoretical additive cell death when combined and the green bars represent the observed cell death induced by the combination of mitoxantrone with each virus. Statistical analysis consisted on t-test comparing the percentage of cell death of the combination with the theoretical additive value for each virus; $p<0.05$ (*), $p<0.01$ (**), $p<0.001$ (***). Data is an average of 3 independent experiments with standard deviation.

The effects of combination treatments in the PC3 cells at the higher viral dose showed no significant increase in cell death, with the exception of the *dl*1520 mutant that increased cell death by 10% ($p<0.05$). The *dl*1107 and *dl*1108 mutants also showed an increase in cell death in combination with mitoxantrone but was less than 5% compared to the theoretical additive value of drug and virus alone and was not significant difference. At the lower viral dose no additional increase in cell death in response to the combination treatment was detected, rather additive or less than additive effects were observed. The data from the PC3 cells in this study was in contrast to the findings in the previous section demonstrating clear synergy at specific ratios with several mutants (Table 9). It is likely that the sensitising interactions required doses of drug and virus different from the selected concentrations as we previously observed in the synergy studies that not all combination ratios resulted in synergistic interactions. This hypothesis is supported by the differences in the level of sensitisation observed in TRAMPC; a low dose of virus was more effective at killing cells in combination with mitoxantrone than the highest dose used.

### 3.3.3 Sensitisation to mitoxantrone by replication-selective E1A-mutant adenoviruses varied among cell lines.

To resolve whether combination treatments with the various mutants and mitoxantrone could induce supra-additive (synergistic) increases in cell death, further studies and improvements of test conditions were necessary. To optimise the possibility of identifying supra-additive effects on cell death, prostate cancer cell lines were treated with mitoxantrone to generate dose-response curves with and without the addition of viruses at fixed concentrations inducing less than 25% or 50% cell death alone. $EC_{50}$ values for mitoxantrone were calculated for each cell line under all conditions and results were expressed as percentages of the

$EC_{50}$ value for mitoxantrone alone (Fig. 15). This assay enabled the combinations of numerous drug concentrations with the viruses, hence optimising the possible determination of cell death mechanisms.

Sensitisation by E1A-mutant adenoviruses was more effective in the human cell lines 22Rv1 and PC3 than in the murine cell line TRAMPC; the majority of E1A-mutants caused a significant reduction in the $EC_{50}$ value for mitoxantrone in both human and murine cell lines. Ad5 reduced the $EC_{50}$ values for mitoxantrone to a level that was statistically significant compared to drug alone in all cell lines, while *dl*312, lacking the E1A gene, failed to induce sensitisation to mitoxantrone in any cell line.

As previously observed during the study of synergistic interactions between viruses and mitoxantrone, adenovirus infection showed good ability to sensitise PC3 cells to this drug. All replication-selective mutants tested induced sensitisation to chemotherapy, although with the *dl*922-947 and *dl*1107 mutants the reduction in $EC_{50}$ value was not statistically significant with any of the doses tested. These mutants showed a greater reduction in $EC_{50}$ values for mitoxantrone at the lower doses. The *dl*1104 mutant showed similar sensitisation effects with both concentrations. Only the *dl*1102 mutant was able to induce a reduction greater than 50% of the EC50 value at the highest dose tested. However, in the 22Rv1 cells the *dl*1102 mutant was the only mutant that failed to reduce the $EC_{50}$ values for mitoxantrone. The mutants *dl*1108 and *dl*922-947, unable to bind to different members of the pRb family, showed similar sensitising effects, with reductions of $EC_{50}$ value of approximately 30% compared to value of drug alone. The *dl*1101 and *dl*1104 mutants showed better sensitisation in this cell line than *dl*1108 or *dl*922-947. Interestingly, the *dl*1107 mutant failed to sensitise these cells to mitoxantrone at the lower dose used, but it showed the best reduction of $EC_{50}$ value at the highest dose, with a reduction in $EC_{50}$ value of 80% with respect to drug alone.

**A**

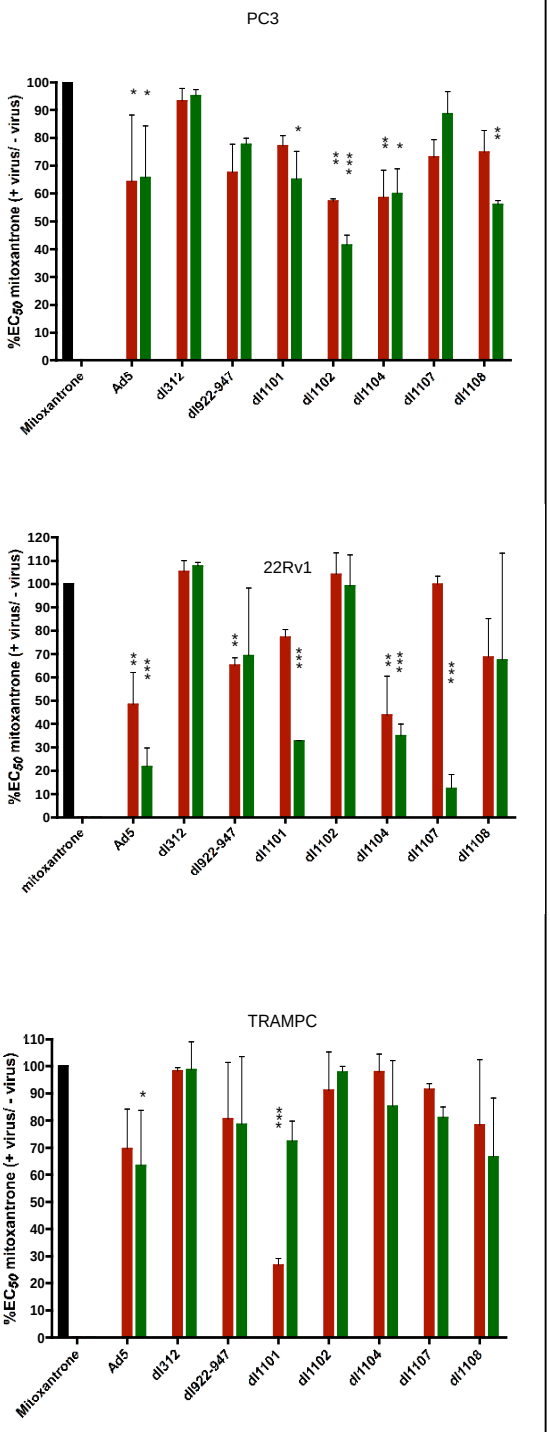


**B**

| PC3 | Dose | Viral particles (ppc) | % cell death |
|---|---|---|---|
| **Ad5** | 1 | 83.1 | 25.13 |
| | 2 | 193.8 | 49.37 |
| **dl312** | 1 | 83.1 | -11.1 |
| | 2 | 193.8 | -10.68 |
| ***dl1101*** | 1 | 690 | 35.45 |
| | 2 | 1683 | 53.41 |
| ***dl1102*** | 1 | 281 | 18.56 |
| | 2 | 659.7 | 35.78 |
| ***dl1104*** | 1 | 846 | 22.13 |
| | 2 | 2589 | 45.42 |
| ***dl1107*** | 1 | 42.5 | 15.44 |
| | 2 | 260.8 | 32.89 |
| ***dl1108*** | 1 | 13.7 | 10.97 |
| | 2 | 111.9 | 25.05 |
| ***dl922-947*** | 1 | 112 | 35.46 |
| | 2 | 365.5 | 50.55 |

| 22Rv1 | Dose | Viral particles (ppc) | % cell death |
|---|---|---|---|
| **Ad5** | 1 | 1.01 | 28.45 |
| | 2 | 2.2 | 63 |
| **dl312** | 1 | 1.01 | -13.02 |
| | 2 | 2.2 | -15.2 |
| ***dl1101*** | 1 | 2.85 | 10.9 |
| | 2 | 6.4 | 49.13 |
| ***dl1102*** | 1 | 0.64 | 3.82 |
| | 2 | 1.6 | 25.05 |
| ***dl1104*** | 1 | 27 | 59.55 |
| | 2 | 31.5 | 73.29 |
| ***dl1107*** | 1 | 0.85 | 49.83 |
| | 2 | 1.7 | 57.07 |
| ***dl1108*** | 1 | 0.53 | 8.49 |
| | 2 | 0.88 | 26.76 |
| ***dl922-947*** | 1 | 0.42 | 56.15 |
| | 2 | 0.74 | 79.28 |

| TRAMPC | Dose | Viral particles (ppc) | % cell death |
|---|---|---|---|
| **Ad5** | 1 | 1500 | 2.53 |
| | 2 | 4250 | 51.26 |
| **dl312** | 1 | 1500 | 0.34 |
| | 2 | 4250 | 0.678 |
| ***dl1101*** | 1 | 2100 | 28.11 |
| | 2 | 14027 | 38.47 |
| ***dl1102*** | 1 | 2870 | 8.78 |
| | 2 | 7798 | 11.25 |
| ***dl1104*** | 1 | 2720 | 9.13 |
| | 2 | 13187 | 15.81 |
| ***dl1107*** | 1 | 1350 | 38.84 |
| | 2 | 4233 | 51.37 |
| ***dl1108*** | 1 | 2130 | 23.44 |
| | 2 | 4365 | 33.49 |
| ***dl922-947*** | 1 | 1140 | 2.98 |
| | 2 | 3336 | 34.66 |

**Fig. 15.** Sensitisation to mitoxantrone by replication-selective E1A-mutant adenoviruses. A) Histograms representing decreases in $EC_{50}$ values for mitoxantrone in combination with a low dose of virus (red bars) or high dose (green bars) compared to mitoxantrone alone (black bar). Data is an average of 3 independent experiments with standard deviation; ANOVA and t test with Bonferroni's correction were used to statistically analyse the data, statistically significant results are shown as $P<0.05$ (*), $P<0.01$ (**) and $P<0.001$ (***). B) Table showing number of viral particles chosen as described in materials and methods for each E1A-mutant adenovirus for combination studies with mitoxantrone; cell death induced by viruses alone is shown as percentrage of untreated cells for low dose (dose 1) or high dose (dose 2) as used for combination studies.

This was the only experimental setting that showed sensitisation to mitoxantrone in 22Rv1 cells; however, good sensitisation correlated with high cell death due to viral infection. Even though virus-mediated cell death was taken into account for the calculation of the $EC_{50}$ values in combination treatments, the high percentage of cell death made these data unreliable and subjected to high variability due to the small number of surviving cells.

In the TRAMPC cells the E1A-mutant adenoviruses did not induce significant reductions in $EC_{50}$. Only the *dl*1101 mutant induced a great reduction in $EC_{50}$ value at the lower viral concentration tested; at the highest dose tested, this virus induced a reduction of 30% in $EC_{50}$ value, similar to the sensitisation effect observed with Ad5 at the two doses tested and with the *dl*1108 mutant at the highest concentration tested. The *dl*922-947 mutant also induced a small reduction in $EC_{50}$ value, while the other mutants tested did not decrease the $EC_{50}$ value for mitoxantrone.

This experimental design was likely to be the most useful to study sensitisation by E1A-mutant viruses, as it allowed to combine viruses with decreasing concentrations of drug. The studies resulted in a more reproducible decrease of $EC_{50}$ values that could not be observed when fixed concentration of virus and drug were used. In addition, it is a simplified design compared to the laborious synergy studies and even though it did not provide information about the interactions, such as CI values, it allowed to determine what E1A-mutant viruses could chemosensitise prostate cancer cell lines to mitoxantrone. Sensitisation was cell-dependent, with the 22Rv1 cells being more difficult to sensitise than the other cell lines tested; even though we reported in a previous section that viruses unable to bind p300 were attenuated in potency, they were still able to sensitise prostate cancer cell lines to cytotoxic drugs. It is also possible that the high percentage in cell death observed after viral infection might

have had an effect in the sensitisation to drugs or in the outcome of the assays, as the observed cell death by virus alone, in particular in 22Rv1 cells, was higher than expected.

## 3.4 Changes in viral protein expression and replication when viral mutants were combined with cytotoxic drugs.

The following results were generated to determine if the presence of cytotoxic drugs had effects on viral gene expression, replication and infectivity. Combination treatments resulted in sensitisation of the prostate cancer cell lines and in order to better understand the interactions between virus and drug, we analysed the effects that the presence of drug had on adenovirus infection. As mitoxantrone and virus were added at the same time, it is possible that changes in viral protein expression were due to an increase in infectivity, and increase in viral transcription or a combination of both.

### 3.4.1 Effects on viral protein expression in response to cytotoxic drugs.

To determine if the enhanced cell death in response to combination treatments of virus and cytotoxic drugs was caused by increased viral gene expression, early and late viral proteins, E1A and hexon respectively, were analysed by western blotting. DU145 and PC3 cells were infected with Ad5 and treated with mitoxantrone at 10 nM or docetaxel at 0.1 nM (both <<EC50 value) and proteins were extracted 24 and 48h post-infection (Fig. 16). These cell lines were chosen as they showed best sensitisation after adenovirus infection than 22Rv1 cells or murine prostate cancer cell lines.

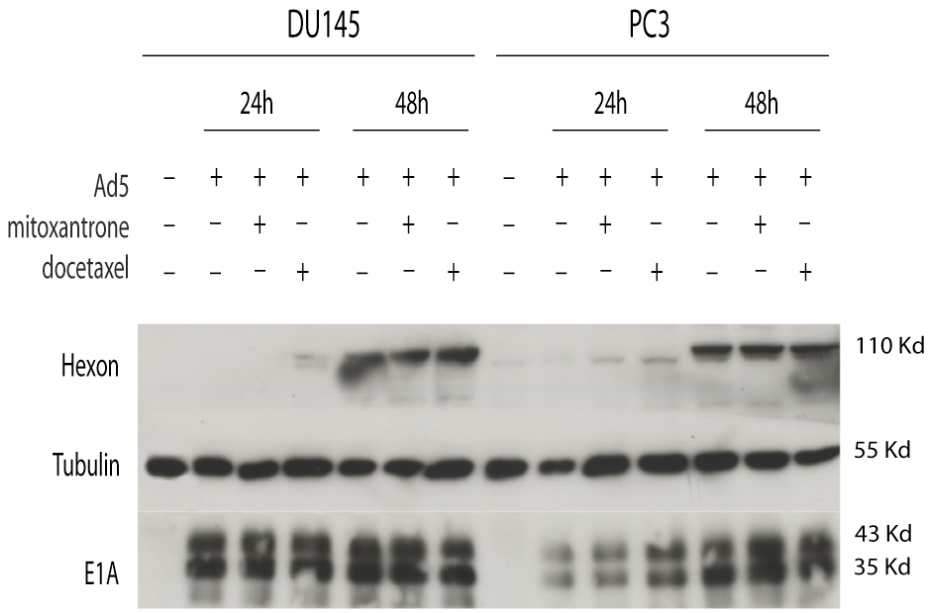


**Fig. 16.** Hexon and E1A expression in PC3 and DU145 was analysed by western blotting. Earlier expression of hexon was observed in both cell lines when Ad5 was combined with mitoxantrone at 10 nM or docetaxel at 0.1nM. Increased E1A expression was observed in PC3 cells in response to both drugs. Representative data of 2 independent experiments.

The level of E1A after Ad5 infection was higher in DU145 than in PC3 cells as expected from the infectivity and replication data. E1A expression remained unchanged in DU145 cells infected with Ad5 in combination with mitoxantrone or docetaxel. However, hexon expression was observed already at 24h post-infection at very low levels in these cells when Ad5 was combined with docetaxel but not with mitoxantrone or when given alone. Hexon expression was increased with all treatments at 48h after infection.

In the PC3 cells E1A expression was increased after 24h in combination with both mitoxantrone and docetaxel. Hexon expression was detected already after 24h in the presence both drugs but not with virus alone. Levels of hexon were similar with all treatments at 48h, while combination of Ad5 with mitoxantrone showed a small increase in E1A at this time point. This data

suggested that the enhanced killing effect observed in combination treatments could be due to an increased rate in viral replication or to the pro-apoptotic properties of E1A, further enhanced by an increase in expression.

### 3.4.2 Levels of viral mRNA increased in the presence of mitoxantrone.

To assess whether the changes in viral protein expression were paralleled by similar changes in mRNA levels, E1A transcripts were quantitated by qPCR at 24 and 48h post-infection with and without mitoxantrone and docetaxel

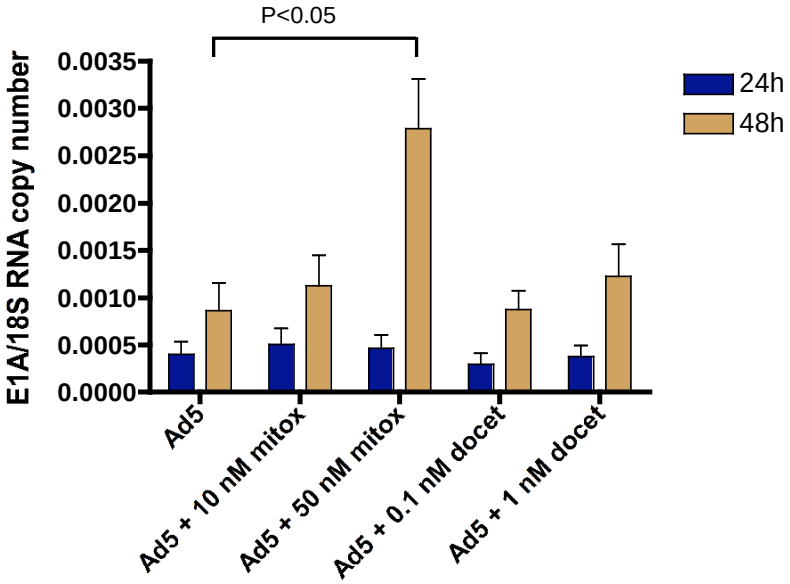


**Fig. 17.** PC3 cells were infected for 2h with Ad5 at 100 ppc, followed by addition of medium only or containing mitoxantrone at 10 and 50 nM or docetaxel at 0.1 and 1 nM. Determination of E1A mRNA expression levels by qPCR showed an increase in E1A mRNA levels over time with all conditions; E1A mRNA levels increased significantly at 48h in the presence of mitoxantrone at 50 nM compared to infected cells in the absence of drugs (t-test, $P<0.05$). Data represents average and standard deviation of 3 independent experiments, presented as E1A-copy numbers normalised to 18S cDNA for each sample

combinations (Fig. 17). PC3 cells were infected with Ad5 for 2h and then treated with two different concentration of mitoxantrone or docetaxel. E1A mRNA levels did not change significantly at 24h post-infection in the presence of drugs; however, there was a significant increase in E1A expression at 48h when cells were treated with mitoxantrone at 50 nM. Small increases in E1A were also observed with a lower dose of mitoxantrone and with docetaxel at the highest dose tested. These data together with the western blot results indicated that E1A expression increased in the presence of cytotoxic agents; the small increase observed by western blot correlated with small increases in mRNA when mitoxantrone was used at a concentration of 10 nM. We also observed that treatment with a higher dose of mitoxantrone significantly increased the levels of E1A mRNA. Therefore we decided to use mitoxantrone at 50 nM for further studies, as it allowed for significant changes in viral gene expression.

### 3.4.3 Mitoxantrone affected infectability of prostate cancer cell lines.

The increase in viral protein expression could be caused by an increase in transcription rate or by increased virus uptake in the presence of the chemotherapeutic drugs. To determine whether virus uptake was enhanced in the presence of drugs, 22Rv1, DU145 and PC3 cells were transduced with a replication defective GFP-expressing adenovirus in the presence of mitoxantrone at 50 nM. The virus was not removed from the medium to mimic the conditions of the sensitisation assays to mitoxantrone (Fig. 14 and Fig. 15). In addition, a lower number of viral particles were used; 22Rv1 cells were infected with 2 ppc, while DU145 and PC3 cells were transduced with 10 and 100 ppc respectively. The use of 100 ppc, as in the replication studies, would have resulted in 100% infection after 48h when virus was not removed. Number of transduced cells was

determined by quantification of GFP-expressing cells after 48h by flow cytometry. The percentage of transduced cells in 22Rv1 and PC3 cells only showed a small increase, approximately 3%, which was not enough to be considered statistically significant. Interestingly, the percentage of GFP-expressing cells almost doubled in DU145 cells (Fig. 18.A).

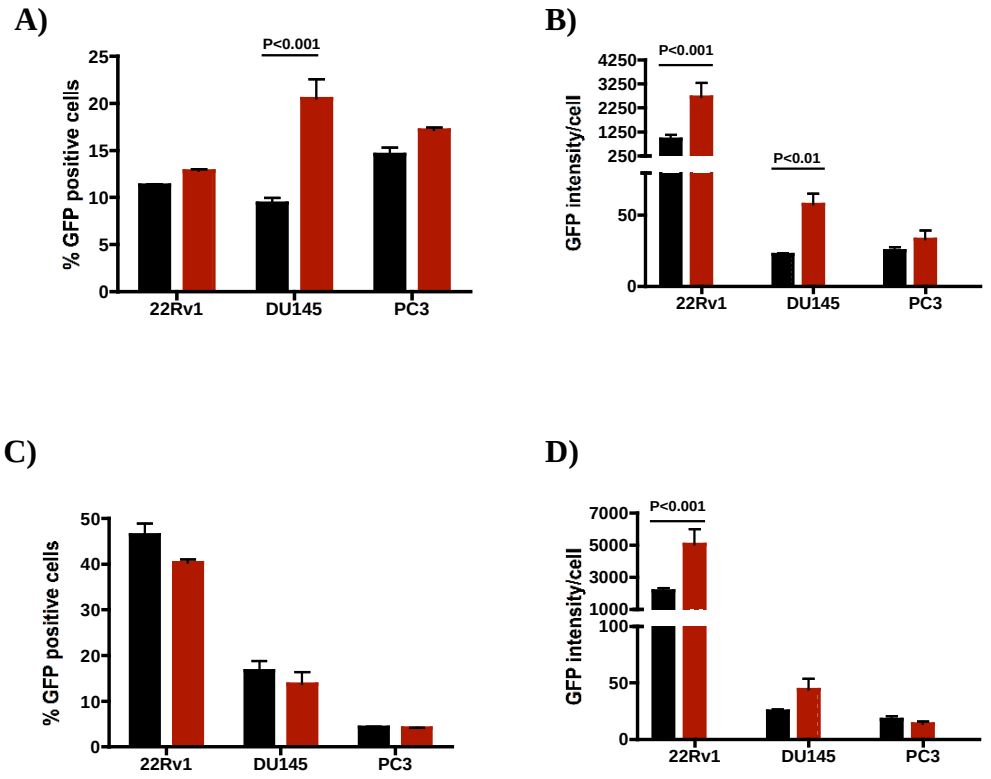


**Fig. 18.** Analysis of effects of mitoxantrone treatment on adenoviral transduction of human prostate cancer cells. Cells were treated with AdGFP in the presence or absence of mitoxantrone at 50 nM during 48h (A, B) or transduction was only allowed for 2h, followed by replacement of virus with media with or without mitoxantrone (C, D). Combination of mitoxantrone and AdGFP virus resulted in an increase in the percentage of transduced cells in DU145 cells with 10 ppc, but the increase was not significant in PC3 cells infected with 100 ppc and 22Rv1 cells infected with 2.5 ppc (A). Under these conditions, presence of mitoxantrone increased the GFP intensity/cell in 22Rv1 and DU145 cells (B). When these cell lines were transduced with 100 ppc for 2h and virus was replaced by medium only or medium containing mitoxantrone at 50 nM, no increase in the percentage of transduced cells was detected in any cell line (C) although GFP intensity/cell increased (D). The data represents the average and standard deviation of 3 independent experiments, statistically significant results are indicated with their corresponding P-value, obtained by t-test analysis within each cell line.

Brightness intensity, measured by the geometric median of GFP expression in each cell line, was also analysed as an indication of GFP expression in individual cells; in the absence of mitoxantrone, 22Rv1 cells showed a higher GFP intensity per cell than other prostate cell lines. In the presence of mitoxantrone, GFP expression per cell increased significantly in 22Rv1 and DU145 cells, but not in PC3 cells (Fig. 18.B).

These cell lines were also transduced with 100 ppc of AdGFP for 2h in the presence or absence of mitoxantrone, followed by removal of virus and incubation in medium containing mitoxantrone at 50 nM. No significant changes in the number of transduced cells were observed after 48h with or without mitoxantrone (Fig. 18.C). However, an increase in GFP intensity per cell was observed for 22Rv1 and DU145 cells (Fig. 18.D). Overall, this data suggests that mitoxantrone increased viral infection when virus was not removed after 2h; it is possible that mitoxantrone treatment increased the number of CAR receptors and integrins over time, thus allowing a higher percentage of transduction. In addition, the brightness per cell increased in both experimental conditions, indicating that more GFP protein was produced in transduced cells when mitoxantrone was present and suggesting that CMV-GFP transcription might be upregulated in combination treatments.

### 3.4.4 Viral replication decreased in the presence of mitoxantrone.

We next assessed whether viral replication was affected by the presence of mitoxantrone. Since we observed an increase in viral proteins at earlier time points, it was possible that viral replication was also affected. DU145 and PC3

cells were infected with Ad5 at 100 ppc for 2 hours as described in the Materials and Methods section.

Viral replication was decreased over time after infection with Ad5 in combination with mitoxantrone at 10 or 50 nM; this was observed in both DU145 and PC3 cells (Fig. 19.A). The extent of the decrease also correlated with the concentration of drug, with a greater decrease with mitoxantrone at 50 nM. Differences between Ad5 alone or in combination with the drug at both doses were highly significant at 72h ($P<0.001$). This decrease in replication could have been caused by cell death induced by the presence of the chemotherapeutic agent; a decrease in the number of cells due to the toxic action of mitoxantrone would result in a reduction on the number of cells that could be infected by new virions over time.

To elucidate this, we measured the percentage of cell death occurring under the conditions of the replication assays (Fig. 19.B). Cell death was measured at 24, 48 and 72h after treatment with virus in the presence or absence of mitoxantrone. Cell death induced by viral replication in DU145 reached 15% of cells after 72 hours, similar percentages were observed after treatment with mitoxantrone at 10 nM. This percentage was significantly higher in combination with Ad5. Cell death observed with the higher concentration of mitoxantrone reached 60% and increased in the presence of Ad5. The effects of mitoxantrone were similar in PC3 cells, with an observed cell death of 16% and 23% at 10 and 50 nM respectively; however, the combination of mitoxantrone and Ad5 resulted in increased cell death at 24 and 48h, but no differences were observed at 72h between the combination and mitoxantrone alone. We concluded that the resulting decrease in viral replication in the combination treatments was likely due to the toxic effect of the drug, reducing the number of cells that the virus could infect.

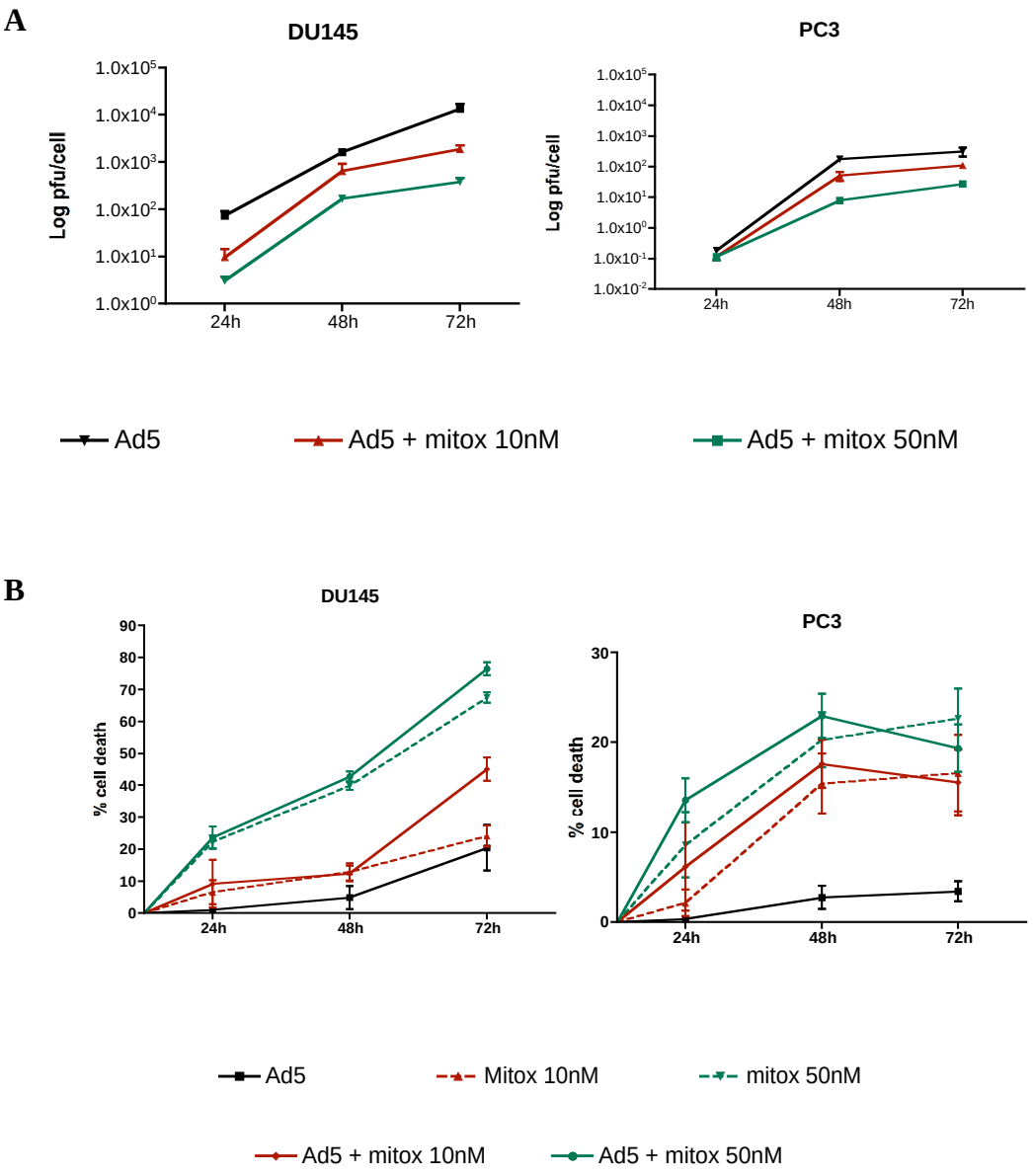


**Fig. 19.** Assesment of replication of Ad5 in DU145 and PC3 in the presence of two concentrations of mitoxantrone. Viral replication was monitored over time by the TCID50 method. Production of new virions was reduced in the presence of mitoxantrone in both human prostate cancer cell lines (A). The decrease in replication correlated with the cell death associated with the cytotoxic effects of the drug (B). Data expressed as average with standard deviation of 3 independent experiments.

The data is this chapter indicated that deletions of the p300/CBP binding site in E1A (*dl*1101 and *dl*1104 mutants) attenuated viral potency compared to Ad5 and other E1A-deletion mutants. All mutants showed sensitising abilities in prostate cancer cell lines; the efficiency of sensitisation was dependent on cell line and the doses of viruses and drugs used, suggesting that cellular alterations might determine or influence the efficiency of E1A-mediated chemosensitisation, in addition to the mode of administration, as we observed that sensitisation was not achieved under all conditions tested with these viruses. We concluded that E1A expression is essential for sensitisation, as the *dl*312 mutant that lacks E1A did not have an effect in chemosensitisation. However, other viral genes might also play a role. Interestingly, we observed higher infectability of prostate cancer cells treated with mitoxantrone that resulted in higher expression of E1A.

# Chapter 4

## *Expression of E1A proteins using plasmids and retroviral vectors.*

In addition to E1A, both E1B and E3 viral genes are expressed early during infection with the replication-selective E1A-mutant adenoviruses used in the previous chapter. Proteins coded by these genes are involved in cell cycle regulation and virus-induced cell death mechanisms. To assess the role of E1A and the different E1A mutations in the absence of other viral proteins and viral replication, the E1A gene was isolated and cloned into non-replicating vectors.

### 4.1 Cloning of E1A gene

Lung carcinoma A549 cells were infected with Ad5 in order to synthesise E1A cDNA. First RNA was extracted from the cells 20h post-infection and cDNA

generated from mRNA using TaqMan® Reverse Transciption Reagent as described in materials and methods. E1A cDNA was amplified using primers targeting the beginning and end of the complete gene. Several bands were obtained by PCR with specific primers, as shown in Fig. 20. These bands corresponded to cDNA derived from mRNA coding for the different E1A proteins reported to be produced during infection: 13S, 12S, 11S, 10S and 9S.

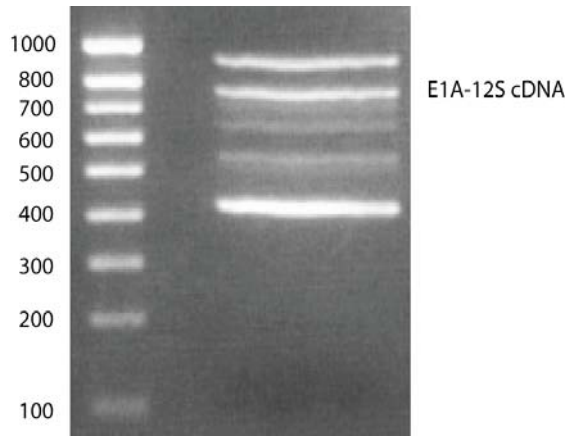


**Fig. 20.** E1A cDNA obtained from RNA extracts of Ad5 infected A549 cells after separation in 2% agarose gel. Bands correspond to the expected cDNAs representing the different E1A proteins expressed during infection. The E1A-12S band was extracted and purified to be cloned into pcDNA-3.1(+) plasmid.

To avoid potential transcriptional activation by the E1A CR3 region present in the E1A-13S protein, we selected the E1A-12S cDNA for further studies. Hence, the band corresponding to the E1A-cDNA was extracted and purified from the agarose gel as described in material and methods. This cDNA was cloned into a TOPO-CR4 vector for cloning and sequencing. Data regarding sequencing of E1A cDNA used during this thesis can be found in the appendix section (chapter 9). The verified E1A-12S cDNA was cloned into a pcDNA-3.1(+) plasmid.

## 4.2 Assessment of transfectability of prostate cancer cell lines.

Prostate cancer cell lines are known to be difficult to transfect. Five commercially available reagents were used to optimise transfection conditions in the prostate cancer cell lines used in this thesis. Fugene 6, Gene Juice and Effectene are reagents widely used for transfection of cell lines of different origins. The Prostate TransIT transfection kit from Mirus Bio Corporation had been demonstrated to have improved efficacy in different prostate cancer cell lines. JetPEI-RGD was indicated for the transfection of cell lines of epithelial origin that were poorly transfectable.

The pEGFP-C2 (described in Materials and Methods) plasmid was used to determine efficacy of each reagent in five prostate cancer cell lines. The percentage of GFP-expressing cells was determined by flow cytometry 48h after transfection (Fig. 21).

Effectene was the only reagent tested that failed to transfect any of the cell lines. GeneJuice and Fugene 6 reagents showed transfection efficiencies of up to 50% and 40% for 22Rv1 cells respectively. Different transfection conditions were tested with Fugene 6 in order to optimise the transfection efficiency; the results shown in Fig. 21 correspond to the optimised protocol for transfection with this reagent, consisting of DNA:reagent ratio of 3:1 for 48h without replacing the medium in the wells. These conditions showed an efficiency similar to that obtained with the prostate-specific reagent Prostate TransIT from Mirus. Transfections with this kit were also optimised to improve efficiency, using 3 μl of IT reagent and 2μl BR reagent with 2 μg of DNA for 48h to obtain the best results, shown in Fig. 21.

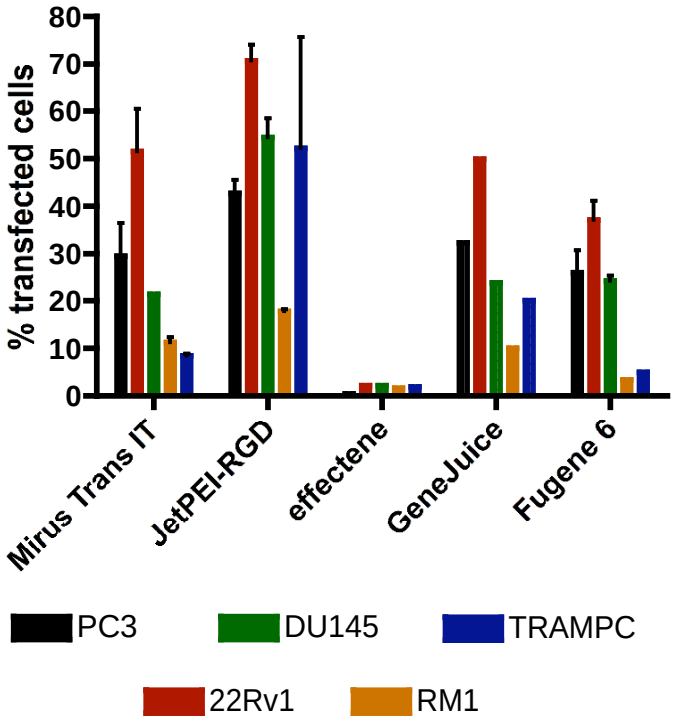


**Fig. 21.** Percentage of GFP-expressing cells 48h after transfection of pEGFP-C2 using different commercially available transfection reagents. Date presented as averages of 2 experiments with standard errors.

Highest transfection efficacies were achieved with JetPEI-RGD. Despite being designed to transfect prostate cancer cell lines, the TransIT Mirus reagent was less effective than JetPEI-RGD in all cell lines used. JetPEI-RGD was the only commercial kit that succesfully transfected more than 40% of cells of the human cell lines; this reagent also showed the best transfection efficiencies for the murine cell lines RM1 and TRAMPC. RM1 cells were not transfected at satisfactory levels with any reagent used, although JetPEI-RGD was the only reagent that resulted in more than 15% of transfected cells. However, this reagent showed very good transfection of TRAMPC cells. Jet-PEI-RGD showed the best

efficacy of the reagents tested and was therefore chosen for further transfection experiments.

### 4.2.1 Effects of E1A in drug toxicity using a plasmid as expression vector.

The human prostate cancer cell lines 22Rv1, PC3 and DU145 were transiently transfected with pcDNA-12S or pcDNA-GFP, then seeded in 96-well plates and treated with serial dilutions of mitoxantrone or docetaxel to generate dose-response curves (Fig. 22). No significant sensitisation to the drugs was observed in 22Rv1 cells. Decreases in $EC_{50}$ values for both mitoxantrone and docetaxel were observed in DU145 and PC3 cells. However, sensitisation caused by transfection with pcDNA-GFP in both cell lines and by mock-transfection in PC3 cells was also observed. These results could be explained by the high cell death and slow growth rate observed in transfected cells after seeding in 96-well plates. Next, to minimise cell death due to handling of transfected cells, transfections with pcDNA-12S or pcDNA-GFP were performed directly in the 96-well plates before treatment with mitoxantrone or docetaxel. The high percentages of cell death induced by the transfection protocol, almost 70% in 22Rv1 cells (Fig. 23) made data of dose-response studies to drugs difficult to reproduce, highly variable, and not comparable with data from untransfected cells.

In addition, transient transfection did not achieve a constant expression of E1A during the length of the dose-response assays. As shown in Fig. 24 expression of E1A in 22Rv1 cells was detectable at 72h post-transfection but not after 7 days. In the sensitisation studies cells were treated with mitoxantrone or docetaxel for 4 to 6 days, and consequently sensitising effects induced by E1A might not have been detectable in cells transfected with E1A-expressing plasmids in contrast to cells infected with virus, where E1A expression was maintained over time.

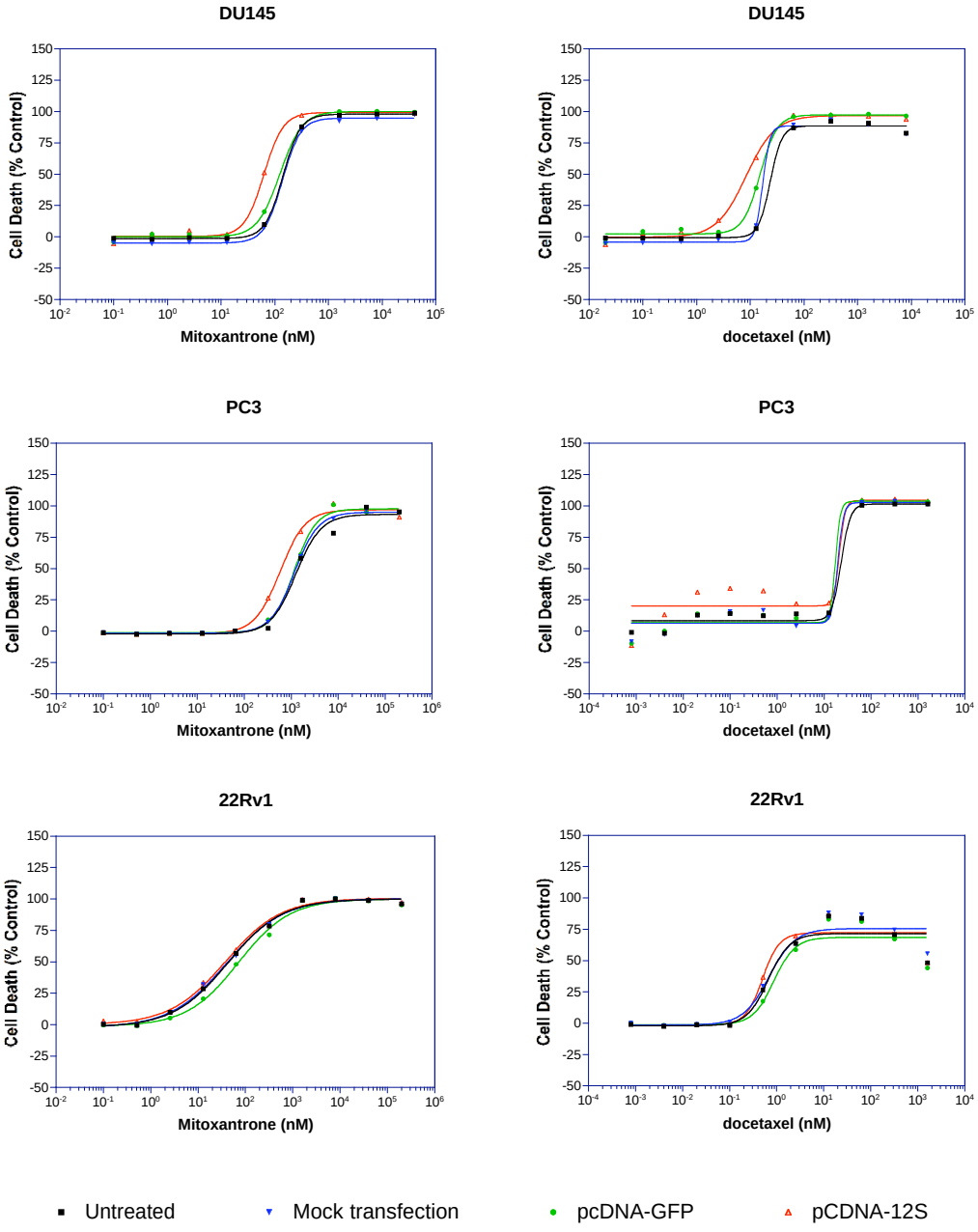


**Fig. 22.** Dose response curves to mitoxantrone and docetaxel of DU145, PC3 and 22Rv1 cells transfected with pcDNA-12S, pcDNA-GFP, mock transfected or untransfected. Toxicity to drugs increased with expression of E1A in DU145 and PC3 cells. Mock transfection and GFP expression also induced sensitisation to drugs, although cell death induced by transfection protocol could influence these results.

Based on the described results, transient transfection was considered a not reliable and reproducible method to achieve E1A expression in prostate cancer cell lines. We considered the selection of stably transfected clones as an alternative to transient transfection. Transfected cells were selected with geneticin as described in Material and Methods in order to obtain E1A-expressing clones. Same selection was done in cells transfected with a plasmid expressing GFP as control. Resistant clones showed a very slow growth ratio compared to parental cell lines, both in E1A and GFP transfected clones. In addition, E1A expression was lost after one passage in culture while geneticin resistance was maintained (Fig. 24).

Taken together, these data indicated that transfection was not suitable to study E1A effects on drug toxicity in prostate cancer cell lines; transient transfection showed high cell death induced by the transfection protocol. The attempts to select E1A-expressing clones showed a reduced growth rate that made this cells difficult to compare to their parental cell lines.

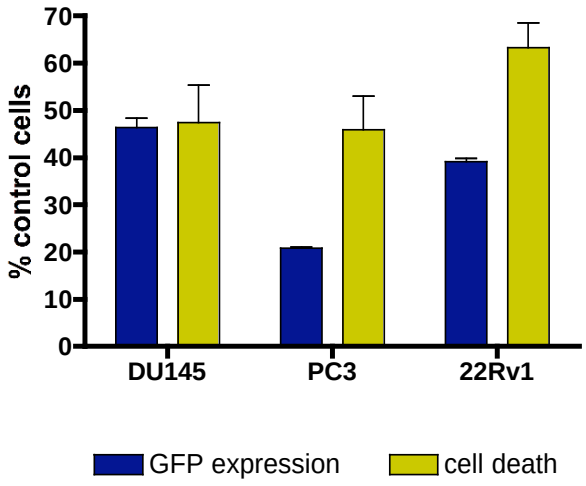


**Fig. 23.** Histogram showing percentages of cell death (yellow) induced by the transfection protocol and the percentage of transfection achieved, expressed as percentage of GFP-expressing cells 48h after transfection (blue). Averages of 3 independent experiments with standard deviations.

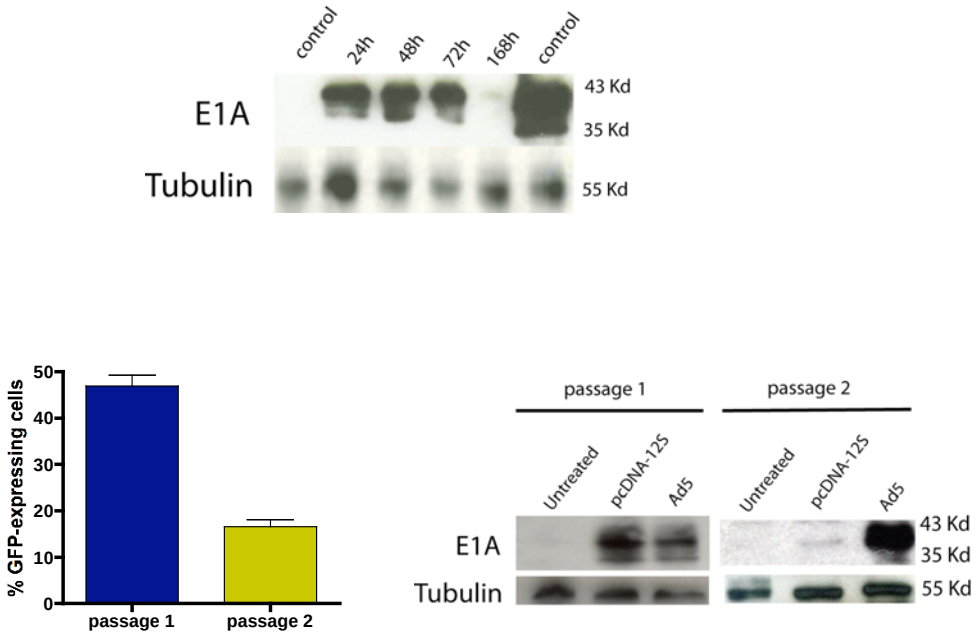


**Fig. 24.** Changes in E1A expression levels over time after transfection. A) 22Rv1 cells were transfected with pcDNA-12S and E1A expression was monitored over time by western blot. E1A was detected up to 72h post-transfection, but not after 7 days. 22Rv1 cells infected for 48h with Ad5 were used as positive control for E1A detection. B) Decrease in percentage of GFP-expressing cells one passage after transfection of 22Rv1 cells selected by G418; averages and standard deviation of 3 experiments. C) Expression of E1A was lost one passage after transfection of 22Rv1 cells determined by western blotting.

## 4.3 Use of retroviruses to generate E1A-expresssing prostate cancer cell lines.

Transient transfection and selection of clones was not a successful method to express E1A in prostate cancer cell lines. In order to generate cells that stably expressed E1A rather than transient expression resulting in poor E1A expression in the above studies, retroviral transduction was evaluated as an alternative. Amphotropic retroviruses with the E1A gene were generated using Phoenix cells, as these cells produced viruses capable of transducing human and murine cell lines.

| | before puromycin selection | | after puromycin selection | |
|---|---|---|---|---|
| | % GFP-expressing cells | *SD* | % GFP-expressing cells | *SD* |
| **PC3** | 2.64 | *0.23* | 65.65 | *0.81* |
| **22Rv1** | 6.25 | *3.00* | 52.49 | *1.74* |
| **DU145** | 2.50 | *3.29* | 76.82 | *4.18* |
| **RM1** | 5.28 | *0.29* | 41.95 | *1.04* |
| **TRAMP-C** | 4.54 | *1.88* | 42.21 | *0.35* |

**Table 10.** Percentages of GFP expressing cells after retrovirus transduction. Expression of GFP was very low after infection with GFP-retrovirus in all prostate cancer cell lines. Selection of infected cells with puromycin for 3 days significantly increased the percentage of GFP-expressing cells (n=3).

E1A-12S cDNA was inserted in the pLPC plasmid to construct retroviruses expressing E1A and control viruses expressing GFP.

Prostate cancer cell lines were very resistant to retrovirus transduction (Table 10). Succesfully transduced cells were selected with puromycin as described in materials and methods. Good level of selection resulting in enrichment of GFP expressing cells was achieved as shown by infection with GFP expressing retroviruses and analysis by flow cytometry (Table 10).

### 4.3.1 Expression of E1A with retroviral vectors and its effects on sensitisation to cytotoxic drugs.

Cell viability was not affected by the E1A expression and were similar to the parental cell lines (Fig. 25). Expression of E1A-12S was determined by western blotting in cells transduced with retrovirus and selected with puromycin (Fig. 26). DU145 and TRAMPC cells expressing E1A-12S were exposed to serial

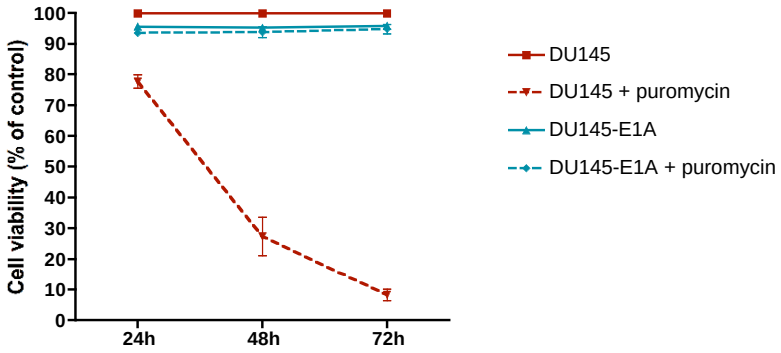


**Fig. 25.** Cell viability was similar to untreated cells in DU145 cells infected with a E1A-expressing retrovirus and selected with puromycin. Transduced cells showed a similar growth rate to parental cells both in the presence (dotted blue) and the absence (blue) of puromycin, while untreated cells were killed by the selection agent (dotted red). Data represent the average and standard deviation of 3 independent experiments.

dilutions of mitoxantrone or docetaxel to determine whether expression of E1A would decrease the $EC_{50}$ value for the drugs compared to parental cell lines (Fig. 26). E1A expression sensitised these cells to both chemotherapeutic drugs; mitoxantrone at 28.2 nM killed 50% of DU145 parental cells, while the concentration required to obtain the same effect in E1A-expressing DU145 cells was 10.2 nM. A similar sensitisation effect was observed with docetaxel, with $EC_{50}$ values of 1.3 nM in the parental DU145 cells and 0.37 nM in the E1A-expressing cells. This effect was also observed in the murine TRAMPC cells; E1A expression reduced the $EC_{50}$ value for mitoxantrone from 135.1 nM to 80.8 nM and the value for docetaxel decreased from 11.25 nM to 4.4 nM.

This study was repeated after further passaging of the E1A expresing cells to determine reproducibility of the sensitisation. However, E1A expression was lost in the retrovirus-transduced prostate cancer cells even though puromycin resistance was maintained (Fig. 27). After one passage of the cells E1A expression was not detectable by western blot, whereas cells grew at a normal rate in puromycin-containing medium. E1A expression was monitored after each

passage, showing great decreases in expression levels from one passage to the next, compromising the reproducibility of the data. Consequently, retroviral infection as an alternative to transfection was not feasible, resulting in similar difficulties and loss of E1A expression observed with transfection protocols.

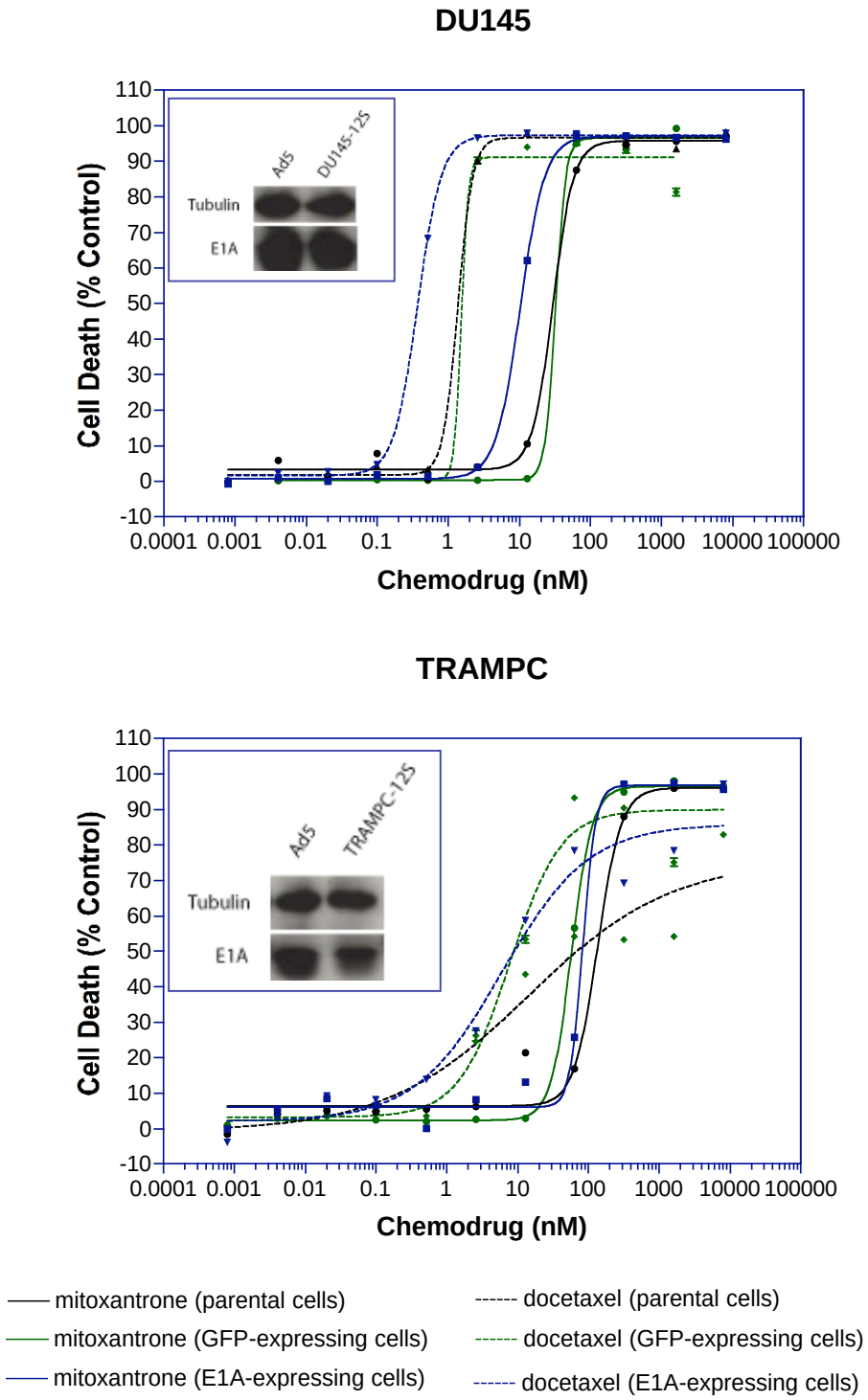


**Fig. 26**. Dose-response studies comparing E1A or GFP expressing DU145 and TRAMPC cells with their respective parental cell lines. A shift of the curve to the left when E1A was expressed indicated a sensitisation effect to the drugs, observed for mitoxantrone and docetaxel in both cell lines. E1A expression was confirmed by western blotting.

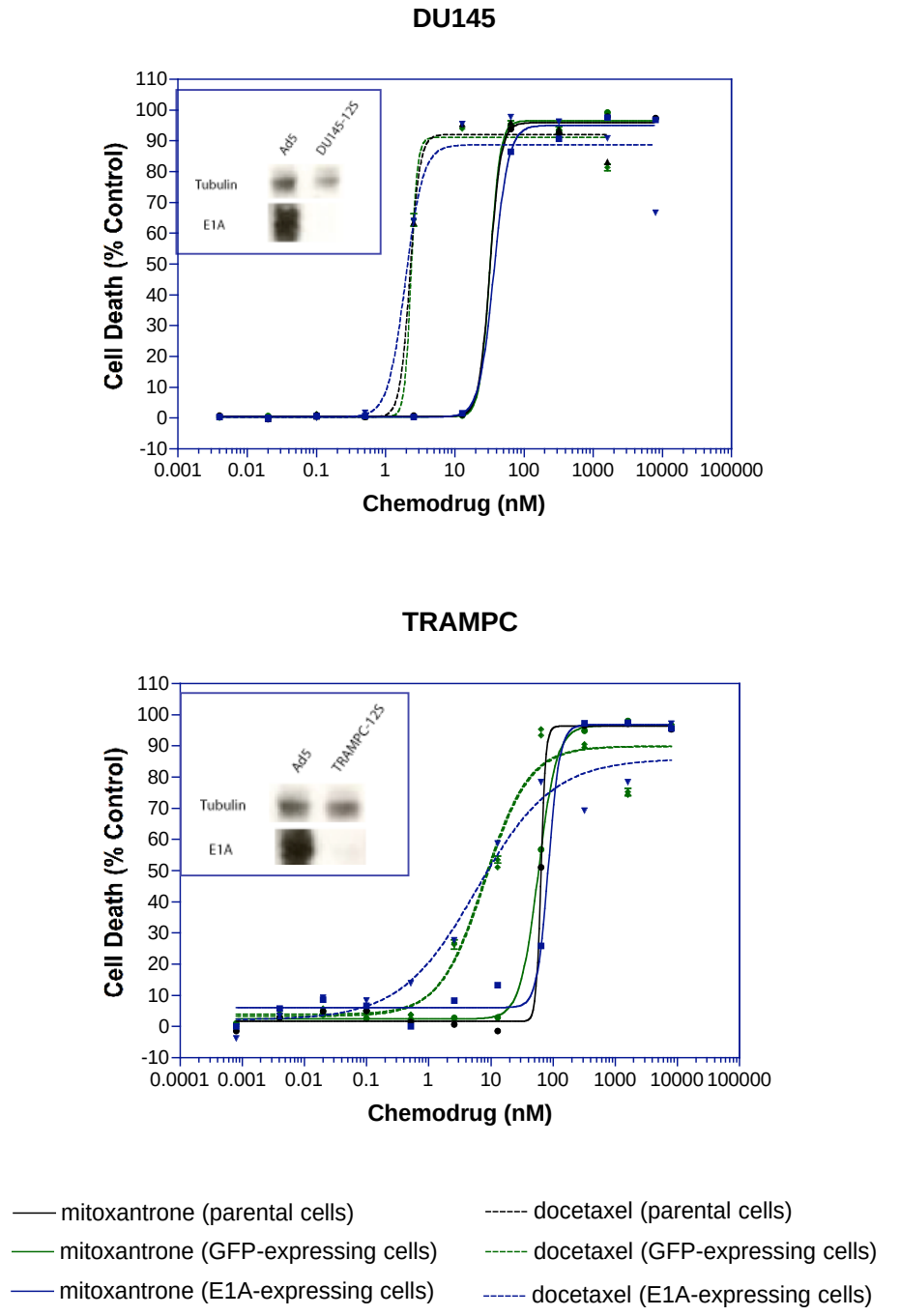


**Fig. 27.** Sensitisation was not observed after one passage of the retrovirus infected cells. E1A-expression was lost, even though puromycin resistance was maintained, resulting in lack of sensitisation.

# Chapter 5

## *Use of replication-deficient E1A-mutant adenoviruses for expression of the E1A gene in prostate cancer cell lines.*

Since transfection and retroviral transduction failed to successfully maintain E1A expression in the prostate cancer cell lines in a reproducible manner, a different approach was necessary. One idea was to use replication-defective adenoviruses as gene-transfer vectors, expressing the various E1A gene deletions but lacking the E1B and E3 genes. This would allow to study the role of E1A expression in the absence of other viral proteins involved in cell killing or cycle regulation, hence minimizing viral replication. The pAdEasy-1 vector enabled the construction of adenovirus vectors that lacked E1B and E3 genes and expressed the gene of interest under control of the CMV promoter.

## 5.1 Construction and characterisation of a replication deficient adenovirus expressing E1A-12S protein.

First, the E1A-12S cDNA, described in the previous chapter, was cloned into a pShuttle-CMV plasmid and then recombined with the pAd-Easy-1 plasmid as described in Materials and Methods, section 2.2.2.3. This generated pAdE1A-12S plasmids that were linearised and transfected into JH293 cells in order to produce the recombined AdE1A-12S virus. The virus was further expanded to larger quantities using the HEK293 cells as the producer and packaging cells.

Viral DNA was extracted to check the correct insertion of E1A and the absence of E1B and E3 by PCR (Fig. 28). E1A was sequenced to ensure that no recombination had occurred during the production of the virus with the cellular genome. The sequence data showed perfect homology with the E1A-12S cDNA sequence previously described in the literature. Details of the sequencing data can be found in the Appendix (Chapter 9). Amplification was observed with the E3 primers in the pAdE1A-12S plasmid. The bigger band was extracted and sequenced. A BLAST search showed 100% homology with the sequence of the pAdEasy-1 plasmid. The other bands were considered non-specific amplification.

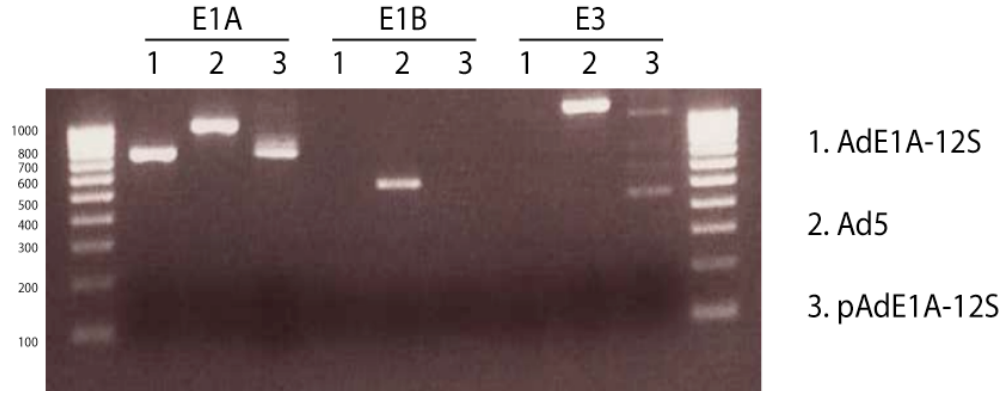


**Fig. 28.** PCR of E1A, E1B and E3 viral genes. The AdE1A-12S virus did not have E1B and E3 as expected and the E1A was smaller in size than in the Ad5 wild type virus since Ad5 carries the complete gene, coding for the additional E1A-13S protein. The bigger band observed in pAdE1A-12S with the E3 primers correspond to a sequence present in the pAdEasy-1 plasmid used to genereate pAdE1A-12S. the other bands are non-specific amplification.

### 5.1.1 Expression of E1A in AdE1A-12S infected cells was confirmed by western blotting.

In order to use AdE1A-12S as a vector to express E1A in prostate cancer cell lines, the level and timing of expression should be similar to that of the intact Ad5 and was subsequently evaluated.

22Rv1, PC3 and DU145 cells were infected with Ad5 or AdE1A-12S at 10, 100 and 1000 ppc and proteins were harvested after 24h. Expression of E1A-12S in AdE1A-12S infected cells was confirmed by western blotting (Fig. 29). Levels of the E1A protein were similar in Ad5 and AdE1A-12S infected cells after 24h of infection.

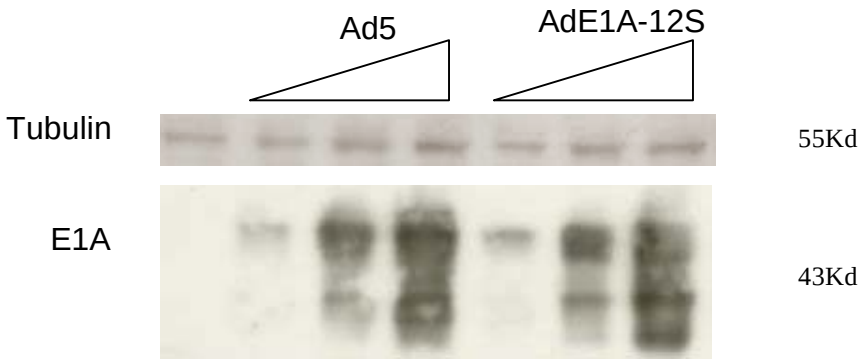


**Fig. 29.** Expression levels of E1A in DU145 cells by AdE1A-12S virus were similar to that of Ad5. Cells were infected with 10, 100 or 1000 ppc and proteins were harvested 24h post-infection. Same results were observed in PC3 and 22Rv1 cells (not shown).

### 5.1.2 Cytotoxicity of the AdE1A-12S virus was attenuated compared to Ad5.

Toxicity of the AdE1A-12S virus was compared to that of Ad5 to evaluate the effect that the absence of E1B and E3 had on viral toxicity. Dose-response studies with the AdE1A-12S mutant and Ad5 were performed in the human prostate cancer cell lines 22Rv1, DU145 and PC3. $EC_{50}$ values were determined 6 days after infection (Fig. 30). Lack of E1A-13S, E1B and E3 genes in AdE1A-12S significantly attenuated the potency of the 12S-mutant compared to intact Ad5 in the three cell lines tested. Infection of PC3 cells with AdE1A-12S resulted in an $EC_{50}$ value of 17000 ppc, while the value for Ad5 was 110 ppc. A similar attenuation was observed in DU145 cells, with $EC_{50}$ values of 1600 and 2 ppc for AdE1A-12S and Ad5 respectively (Fig. 30.B). The attenuation in viral toxicity was not as great in 22Rv1 cells as in the other cell lines. $EC_{50}$ value for Ad5 was 1 ppc, while the value for AdE1A-12S was 30 ppc. However, these cells were also more sensitive to infection with the *dl*312 mutant, with an $EC_{50}$ value for this virus of 1220 ppc while $EC_{50}$ value in DU145 and PC3 was higher than $1x10^5$ ppc. It is possible that 22Rv1 cells were very sensitive to viral infection and that viral entry into the cell triggered a cell death mechanism, in addition to E1A expression and/or viral replication.

We observed an attenuation of toxicity when E1B and E3 genes were not expressed. Nevertheless, the AdE1A-12S virus was more potent than the E1A-deleted mutant *dl*312 in all cell lines; this indicated that cell death was induced by E1A expression. We next analysed replication of AdE1A-12S to elucidate if the observed toxicity was due only to E1A expression or to potential replication of the virus.

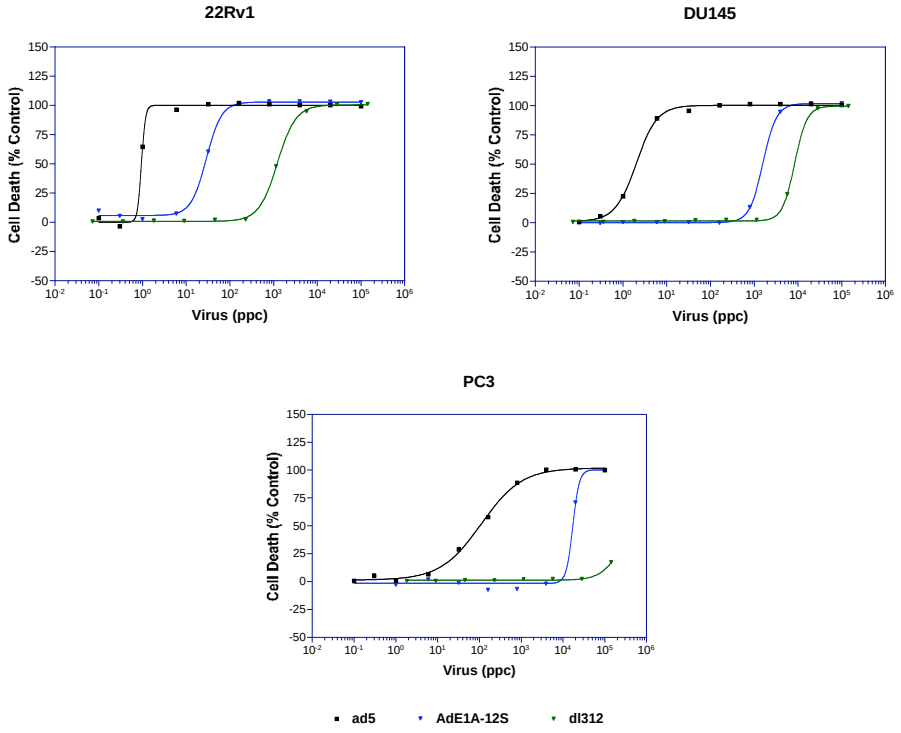


| | EC50 values (ppc) | | |
|---|---|---|---|
| | **Ad5** | **AdE1A-12S** | ***dl*312** |
| **22Rv1** | 1 | 30 | 1220 |
| **DU145** | 2 | 1600 | 8500 |
| **PC3** | 110 | 17000 | >100000 |

**Fig. 30.** Representative dose-response assays in 3 human prostate cancer cell lines treated with serial dilutions of AdE1A-12S (blue), Ad5 (black) or *dl*312 (green) (A) with $EC_{50}$ values calculated (B). AdE1A-12S virus showed less toxicity than Ad5 in the cell lines tested, but it was more cytotoxic than the *dl*312 mutant. Representative dose-response curves from 3 independent experiments.

### 5.1.3 The AdE1A-12S virus failed to replicate in human prostate cancer cell lines.

One explanation for the observed attenuation of cytotoxicity in the tested cell lines could be poor replication of the AdE1A-12S virus. Therefore, replication of this virus was investigated in the human cell lines used above. Replication was not detected after 48h of infection in 22Rv1, DU145 or PC3 cells (Fig. 31). It was therefore concluded that expression of E1A-12S protein was not sufficient to support replication of the E1B and E3 deleted AdE1A-12S mutant and consequently replication was not a cause of the observed cytotoxicity.

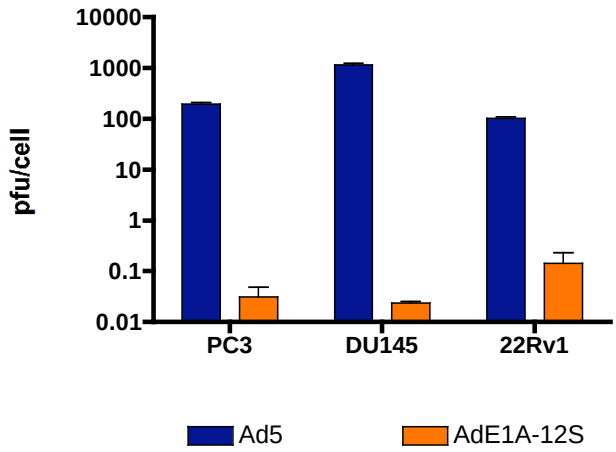


**Fig. 31.** The AdE1A-12S virus failed to replicate in the three human prostate cancer cell lines. Cells were infected with 100 ppc of Ad5 or AdE1A-12S for 2h. Media and cells were collected 48h post-infection and $TCID_{50}$ assays were done to determine viral replication. Data represent the averages of 3 independent experiments with standard deviation.

### 5.1.4 Greater synergistic interactions were achieved with AdE1A-12S than with Ad5 in combination with cytotoxic drugs.

#### 5.1.4.1 Further enhancement of synergistic interactions with AdE1A-12S and mitoxantrone, a DNA-damaging agent.

PC3 and DU145 cells were treated with different combination ratios of mitoxantrone with AdE1A-12S, Ad5 or *dl*1520 in synergy assays as described in Chapter 3. $EC_{50}$ values for virus, mitoxantrone and the combinations were calculated and isobolograms were constructed to quantify the level of synergy through determination of combination indexes (CI).

Synergistic interactions were higher in combinations of mitoxantrone with AdE1A-12S than with Ad5 or the E1B-55kd deleted *dl*1520 in DU145 cells. With Ad5 only the combination ratios at low ppc/nM resulted in two CI values lower than 0.8 (Fig. 32). Values were close to 0.8 for all combinations with Ad5, showing a trend towards synergy in these cells. The *dl*1520 mutant showed better synergy than Ad5 with two combinations resulting in clear synergistic interactions with mitoxantrone, although the combination at the lowest ratio was antagonistic. However, infection with the AdE1A-12S virus resulted in synergistic cell death in combination with mitoxantrone at three of the four ratios tested, with CI values below 0.7. At the highest ratio tested, an additive interaction was observed, with a CI value of 0.84.

In PC3 cells, the *dl*1520 virus showed synergistic interactions with mitoxantrone at all four test ratios also resulting in the lowest CI values (Fig. 33). The AdE1A-12S virus showed synergistic interactions at three of the ratios with an additive effect observed at the lowest ratio tested, CI value of 0.81.

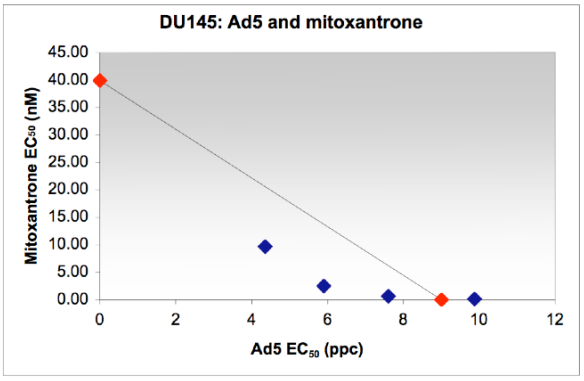


| ratio (ppc/nM) | Combination index |
|---|---|
| 0.50 | 0.73 |
| 2.50 | 0.72 |
| 12.50 | 0.86 |
| 62.50 | 1.10 |

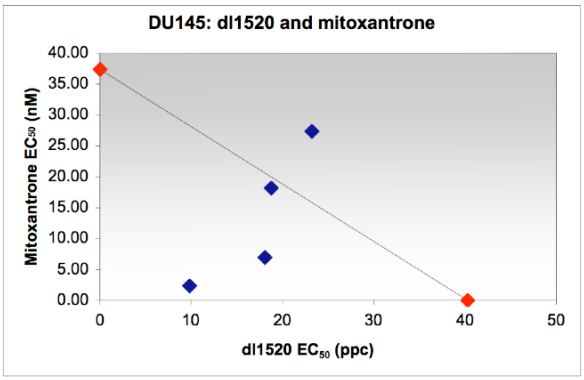


| ratio (ppc/nM) | Combination index |
|---|---|
| 0.50 | 1.31 |
| 2.50 | 0.95 |
| 12.50 | 0.63 |
| 62.50 | 0.31 |

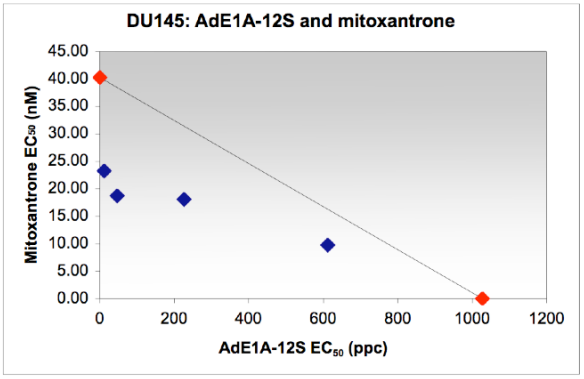


| ratio (ppc/nM) | Combination index |
|---|---|
| 0.50 | 0.59 |
| 2.50 | 0.51 |
| 12.50 | 0.67 |
| 62.50 | 0.84 |

**Fig. 32.** DU145 cells were treated with mitoxantrone in combination with Ad5, *dl*1520 or AdE1A-12S viruses at four different constant ratios as described in materials and methods. Isobolograms were constructed and combination indexes (CI) calculated for each ratio are shown in tables next to each isobologram. The AdE1A-12S virus showed better synergistic interactions with mitoxantrone than the *dl*1520 mutant. Ad5 showed weak synergistic interactions with the drug, resulting in CI values close to 0.8. Representative data of 2 independent experiments.

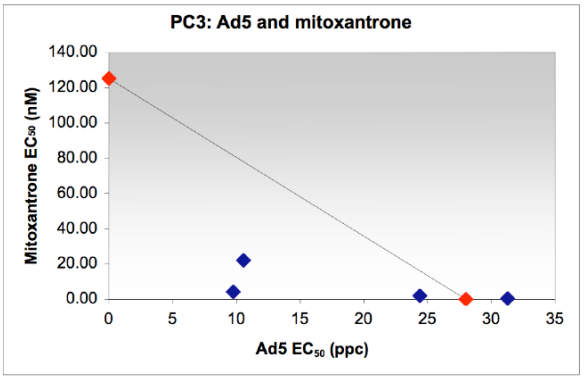


| ratio (ppc/nM) | CI |
|---|---|
| 0.50 | 0.55 |
| 2.50 | 0.38 |
| 12.50 | 0.89 |
| 62.50 | 1.12 |

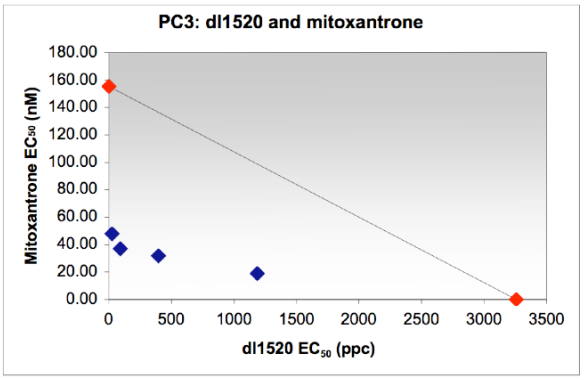


| ratio (ppc/nM) | CI |
|---|---|
| 0.50 | 0.32 |
| 2.50 | 0.27 |
| 12.50 | 0.33 |
| 62.50 | 0.49 |

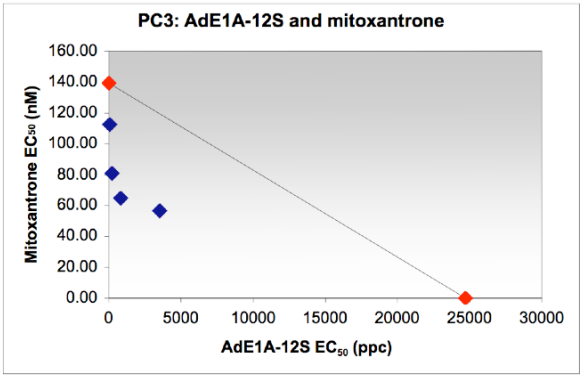


| ratio (ppc/nM) | CI |
|---|---|
| 0.50 | 0.81 |
| 2.50 | 0.59 |
| 12.50 | 0.50 |
| 62.50 | 0.55 |

**Fig. 33.** Analysis of synergistic interactions between mitoxantrone and Ad5, *dl*1520 or AdE1A-12S at four different ratios in PC3 cells. Isobologram analysis of the combinations is shown for each virus and their respective CI values shown in adjacent tables. The *dl*1520 mutants showed best interactions with the drug, resulting in lower CI values. The AdE1A-12S virus also showed better synergistic interactions than Ad5. Data is representative of 2 independent experiments.

The CI values for the other ratios varied between 0.49, at 12.5 ppc/nM, and 0.59 at 62.5 ppc/nM. Similar to the observations in DU145 cells, in PC3 cells Ad5 also showed less synergistic effects than the other two mutants. For Ad5 the interactions with mitoxantrone were additive at the two highest ratios tested and synergistic at the lowest ratios. Good synergy resulted from combination of Ad5 and mitoxantrone at a ratio of 2.5 ppc/nM, with a CI value of 0.38.

More efficient synergistic interactions were observed with the AdE1A-12S virus than with the *dl*1520 mutant and Ad5; the AdE1A-12S was the only virus that showed synergistic interactions at the four ratios tested in DU145 cells; in PC3 cells, this virus showed an effect similar to the *dl*1520 mutant and always better than Ad5. The absence of replication did not seem to influence an efficient synergistic interaction between AdE1A-12S and mitoxantrone.

#### 5.1.4.2 Synergistic interactions with docetaxel, a microtubule stabilising chemotherapeutic drug, were observed with AdE1A-12S but not with Ad5.

DU145 and PC3 cells were also treated with combinations of docetaxel and AdE1A-12S, *dl*1520 or Ad5. The aim was to determine if synergy was observed with viruses in combination with a drug that acts through mechanisms that do not involve direct DNA damage as opposed to mitoxantrone.

Ad5 failed to act synergistically with docetaxel in DU145 in three out of the four ratios tested (Fig. 34). Minor synergistic interactions were observed at the lowest ratio (0.5 ppc/nM), resulting in a CI value of 0.76. Synergy was higher with docetaxel and the *dl*1520 mutant with one of the ratios resulting in a CI value of 0.6, indicating a synergistic interaction. Two of the other three ratios tested showed CI values just below 0.8, while at the highest ratio (62.5 ppc/nM) the combination of drug and virus only resulted in additive effects. However, all four

combination ratios of docetaxel and AdE1A-12S virus resulted in CI values lower than 0.8, indicating that docetaxel and this virus acted in synergy at all combination ratios tested.

Results in PC3 were similar to those in DU145 cells; Ad5 only showed a weak synergistic interaction at a ratio of 0.5ppc/nM, with a CI of 0.71 (Fig. 35). The interactions between Ad5 and the drug were additive at the other ratios tested. The results for the combination of the *dl*1520 mutant with docetaxel were similar to those with Ad5; the interactions observed were only additive, although the CI value for the ratio 12.5 ppc/nM was 0.74 and could be considered an indication of a weak synergistic interaction. Combination of docetaxel with AdE1A-12S resulted in improved synergistic interactions compared to the other two viruses tested; with additive interactions at the lowest ratio, 0.5 and synergy at the higher ratios.

This data indicated that synergistic interactions with mitoxantrone and docetaxel were stronger with AdE1A-12S than with Ad5 and the *dl*1520 mutant. The value of the CIs also indicated that viral infection resulted in better synergy in combination with mitoxantrone, a DNA-damaging agent, than with docetaxel, a microtubule-stabilising agent. The higher synergy with the AdE1A-12S virus could have been due to the increase of supra-additive interactions between the drug and E1A, constantly expressed in infected cells due to CMV promoter regulation. Expression of E1A in Ad5 infected cells varies during the viral cycle; the different E1A proteins are differentially expressed during the cycle and consequently might have influenced the synergistic interaction between E1A and the drugs.

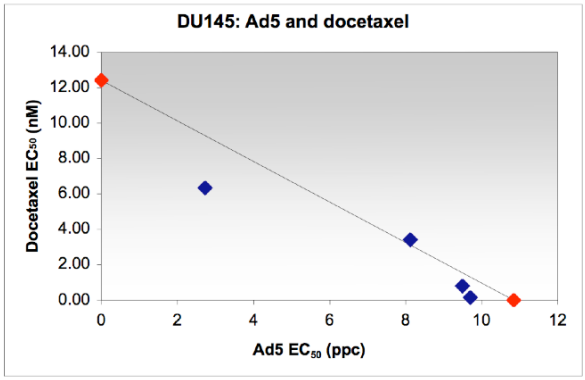


| ratio (ppc/nM) | Combination index |
|---|---|
| 0.50 | 0.76 |
| 2.50 | 1.03 |
| 12.50 | 0.94 |
| 62.50 | 0.91 |

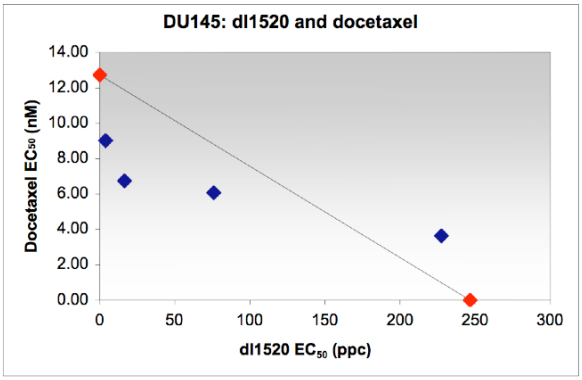


| ratio (ppc/nM) | Combination index |
|---|---|
| 0.50 | 0.73 |
| 2.50 | 0.60 |
| 12.50 | 0.78 |
| 62.50 | 1.21 |

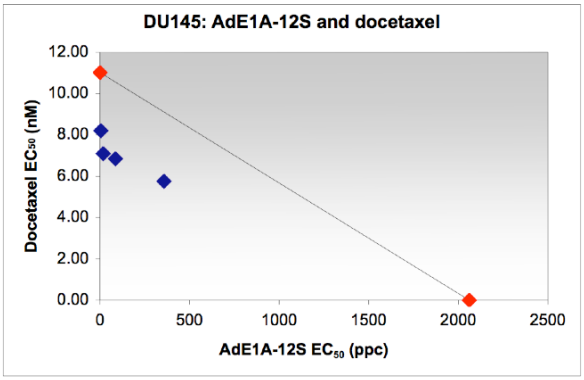


| ratio (ppc/nM) | Combination index |
|---|---|
| 0.50 | 0.75 |
| 2.50 | 0.65 |
| 12.50 | 0.66 |
| 62.50 | 0.70 |

**Fig. 34.** DU145 cells were treated with docetaxel in combination with Ad5, *dl*1520 or AdE1A-12S at four different ratios. Isobolograms of the combinations were constructed and CI values for each ratio are shown in adjacent tables. Weak synergistic interactions were observed with AdE1A-12S at all ratios; the *dl*1520 mutant showed synergistic interactions, but not with all combination ratios tested. Combination of Ad5 and docetaxel resulted in additive effects at all ratios tested. Data representative of 2 independent experiments.

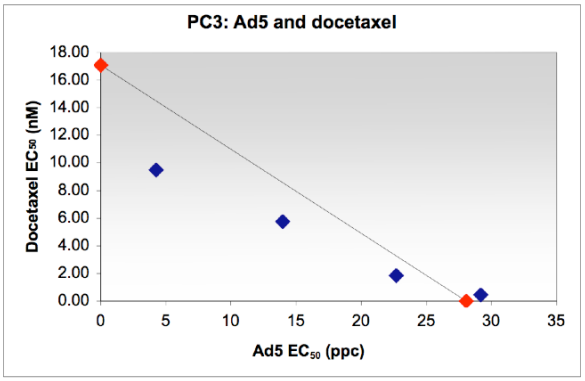


| ratio (ppc/nM) | CI |
|---|---|
| 0.50 | 0.71 |
| 2.50 | 0.83 |
| 12.50 | 0.92 |
| 62.50 | 1.07 |

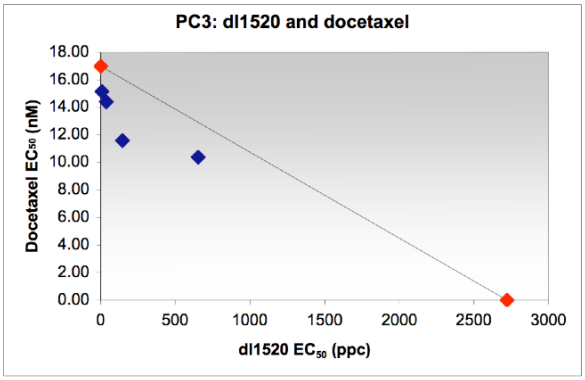


| ratio (ppc/nM) | CI |
|---|---|
| 0.50 | 0.90 |
| 2.50 | 0.86 |
| 12.50 | 0.74 |
| 62.50 | 0.85 |

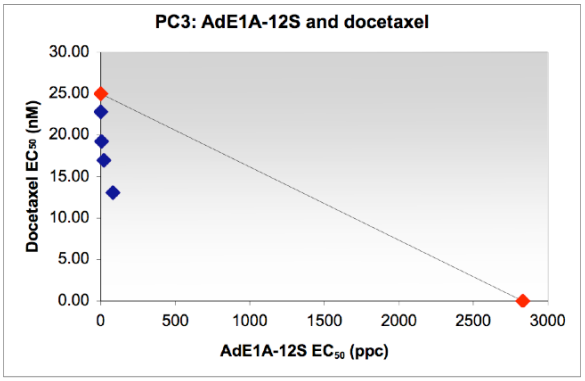


| ratio (ppc/nM) | CI |
|---|---|
| 0.50 | 0.91 |
| 2.50 | 0.77 |
| 12.50 | 0.69 |
| 62.50 | 0.55 |

**Fig. 35.** Isobolographic analysis of interaction between docetaxel and Ad5, *dl*1520 or AdE1A-12S at four different ratios in PC3 cells. CI values for each combination are shown in tables next to the isobolograms. Better synergistic interactions were observed with docetaxel in combination with AdE1A-12S virus than with *dl*1520 and Ad5 that showed weak synergy only at one of the combination ratios tested. Data is representative of 2 independent experiments.

## 5.2 Construction of new replication-defective AdE1A12S-deletion mutants.

The AdE1A-12S virus proved to be an efficient vector to express E1A and study its interactions with chemotherapy in prostate cancer cell lines, in the absence of other viral proteins. Because of the promising results with the AdE1A-12S mutant new viruses were generated; we selected E1A mutants with deletions in the N-terminus (E1A-1102), the CR1 domain (E1A-1104) and the CR2 domain (E1A-1108) in order to identify regions that were critical for sensitisation. These deletions were identical to those in the replication competent viruses tested in chapter 3. These mutants were chosen as each one has a deletion in highly conserved regions of known function for E1A; the E1A-1102 mutant is deleted in the N-terminus, so it does not bind to p400 but can interact with p300. The E1A-1104 mutant is deleted in the p300-binding region of E1A; the E1A-1108 mutant was chosen as it is the mutant with the bigger deletion in the CR2 region (as compared to E1A-922-947 or other mutants). Hence, each mutant lacks the binding site for one major cellular pathway (p400, p300 or pRb) but not the others. Gene splicing by overlapping extension PCR (SOEing PCR) was used to generate the selected E1A-mutants as described in materials and methods section 2.2.2.4, and new viruses were constructed as described for the AdE1A-12S virus in this chapter.

### 5.2.1 Expression of E1A proteins by the newly constructed AdE1A12S-deletion mutants.

Expression of E1A proteins by the newly generated replication defective adenoviruses was confirmed by western blotting. DU145 cells were infected with

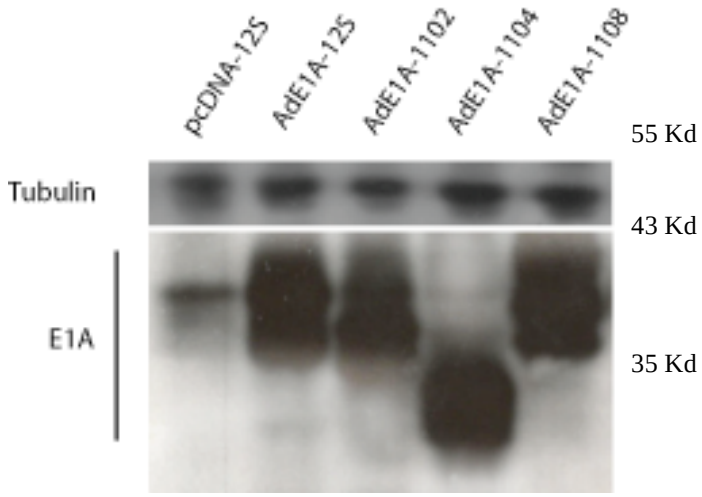


**Fig. 36.** Expression of E1A-12S by the newly generated AdE1A-12S-deletion mutant adenoviruses in DU145 was confirmed by western blotting. Cells were infected with 10 ppc and proteins were harvested 24h later; all E1A proteins expressed by the different mutants were similar in size, with the exception of E1A-1104.

100 ppc of each virus and proteins were harvested 24h post-infection. E1A proteins expressed by the different mutants were similar in size to E1A-12S, with the exception of the E1A expressed by AdE1A-1104 infection that was smaller than the other E1A-mutant proteins (Fig. 36).

### 5.2.2 The AdE1A-1104 mutant showed attenuated cytotoxicity.

Prostate cancer cell lines were treated with increasing doses of each virus to determine differences in E1A12S-induced toxicity for the newly constructed mutants. We observed no replication with the AdE1A-12S mutant virus, hence toxicity was due to the effects of E1A on the cells. Therefore, differences among the newly constructed viruses would be indicative of the efficiency of each E1A-12S mutant to induce cell death.

22Rv1, DU145 and PC3 cells were treated with serial dilutions of each virus followed by calculation of $EC_{50}$ values 6 days post-infection, as described in Materials and Methods (Fig. 37). Differently from the data in Fig. 30 the $EC_{50}$

values for the AdE1A-12S virus were significantly lower. The reason for this difference was the change in assays for viral particle determination. For the viruses used in Fig. 30, viral content was determined by the traditional optical density assay (described in Materials and Methods) since Ad5 and dl312 viruses were previously quantified by this method after production. However, in this and all future studies, virus was quantified by the more sensitive pico-green technology that consistently resulted in lower particle values (vp/ml) and hence a lower $EC_{50}$ value in dose-response assays.

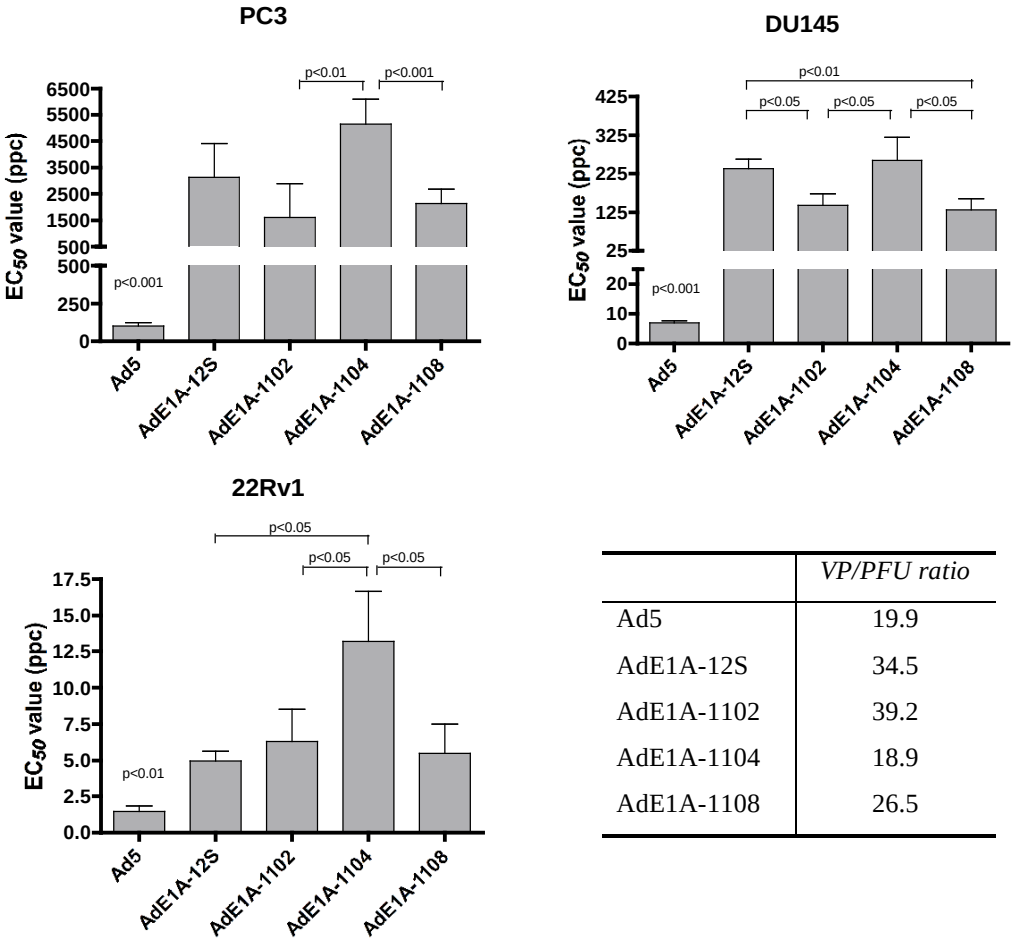


| | *VP/PFU ratio* |
|---|---|
| Ad5 | 19.9 |
| AdE1A-12S | 34.5 |
| AdE1A-1102 | 39.2 |
| AdE1A-1104 | 18.9 |
| AdE1A-1108 | 26.5 |

**Fig. 37.** Cytotoxicity of the new E1A-expressing replication-defective adenoviral vectors was assessed in human prostate cancer cell lines. Dose-response curves were constructed and $EC_{50}$ values calculated 6 days after infection. As observed previously for the AdE1A-12S virus, potency of the new viruses was attenuated compared to Ad5. The AdE1A-1104 virus showed the highest $EC_{50}$ values in the 3 cell lines tested. The vp/pfu ratio, shown in table, varied between 19.9 for Ad5 to 39.2 for AdE1A-1102; these differences were not sufficient to account for the attenuation in toxicity. Data represent averages of 3 independent experiments with standard deviations. T-test statistical analysis showed that cytotoxicity for all AdE1A-mutant viruses was significantly attenuated compared to Ad5 ($p<0.001$ in PC3 and DU145; $p<0.01$ in 22Rv1)

PC3 cells were the most resistant to viral toxicity, as previously observed with replication selective viruses. The AdE1A-1102 and AdE1A-1108 mutants were more potent than AdE1A-12S, while potency for the AdE1A-1104 mutant was attenuated compared to AdE1A-12S (Fig. 37). All replication defective viruses were at least 100 fold less toxic than Ad5. A similar trend was observed in DU145 cells with AdE1A-1102 and AdE1A-1108 showing a lower $EC_{50}$ value than AdE1A-12S. AdE1A-1104 had a similar potency to the E1A-12S expressing adenovirus. As observed in PC3 cells, all newly generated viruses were at least 50 times less potent than the replicating Ad5. These differences between Ad5 and replication-defective viruses were not as pronounced in the 22Rv1 cells (Fig. 37) in which AdE1A-12S, with an $EC_{50}$ value of 5 ppc, was the most potent of the newly constructed viruses, while the value for Ad5 was 1.4 ppc. The AdE1A-1102 and AdE1A-1108 viruses had similar potency to AdE1A-12S, while the AdE1A-1104 mutant was attenuated, with an EC50 value of 13 ppc.

These data suggest that the deleted region in the E1A-1104 mutation was involved in E1A-induced cell death in prostate cancer cell lines. In addition, the mutations in E1A-1102 and E1A-1108 appeared to still maintain potency at a level similar to that of wild type E1A or even increased the potency as observed in the PC3 cells.

### 5.2.3 Significantly attenuated replication of the new E1A-12S-deletion mutants.

Human prostate cancer cell lines were infected for 2 hours with 100 ppc of the replication-selective viruses previously used in chapter 3 (*dl*1102, *dl*1104, *dl*1108) and the replication-defective mutants (see above) expressing the

corresponding E1A deletions in the 12S-protein. Replication of adenoviruses was determined 48 hours post-infection. The replication-selective adenoviruses replicated as efficiently as Ad5 in PC3 and DU145 cells (Fig. 38). However, in the 22Rv1 cells the *dl*1102 and *dl*1104 mutants were less efficient at replicating compared to Ad5 and the *dl*1108 mutant viruses. Infection with Ad5 resulted in 1070 ± 88 pfu/cell after 48 hours, while the *dl*1102 and *dl*1104 viruses only produced 745 ± 34 and 624 ± 85 pfu/cell respectively, statistically significant compared to Ad5 ($p<0.05$).

Absence of E1B and E3 in the newly generated mutant viruses resulted in low replication as observed previously for the AdE1A-12S virus (Fig. 31). Replication was not detectable (<1pfu/cell) with the AdE1A-12S and AdE1A-1104 viruses in any of the tested cell lines (Fig. 38). The AdE1A-1102 and AdE1A-1108 mutants showed poor replication that resulted in low levels of particle production, approximately 50 pfu/cell in PC3 and 22Rv1 cells and 100 pfu/cell in DU145 cells. Nevertheless, the poor replication observed for these two mutants was significantly reduced to that of Ad5, with $p<0.01$ in all the three cell lines (Fig. 38).

Viral genome amplification was also determined as an indirect measure of viral replication by qPCR. RNA was extracted from prostate cancer cell lines 3, 24, 48 and 72 hours after infection, as described in materials and methods (section 2.5.1). Hexon DNA copy number was quantified and expressed as a ratio of hexon copy number 3h post-infection (as a measure of viral infection in each sample) (Fig. 39).

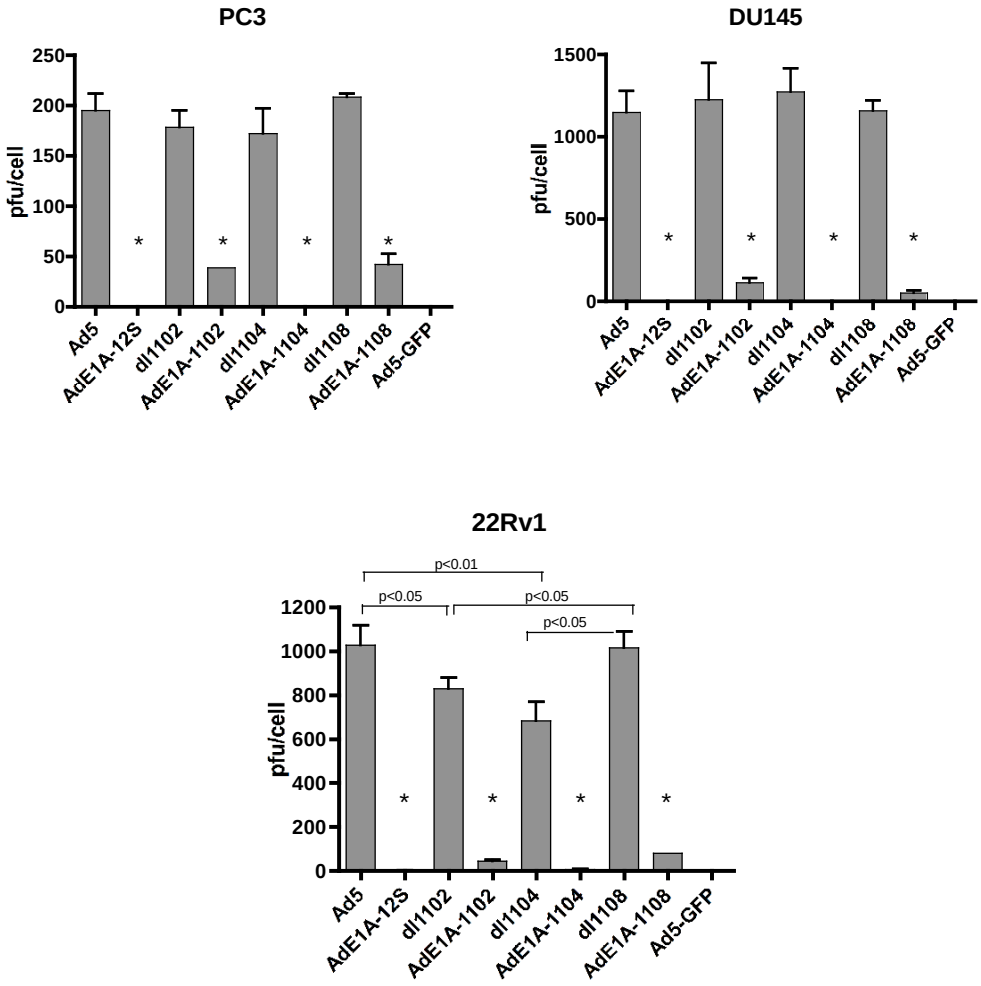


**Fig. 38.** Replication of the new AdE1A12S-deletion mutants and the corresponding replicating viruses. The $TCID_{50}$ assay was used to assess replication in human prostate cancer cell lines 48h post-infection. Replication could not be detected for the AdE1A-12S and the AdE1A-1104 viruses while the AdE1A-1102 and AdE1A-1108 mutants showed low levels of replication in PC3 cells although, at lower levels than the replicating equivalents *dl*1102 and *dl*1108. Replication-selective mutants replicated as efficiently as Ad5 in DU145 and PC3 cells; replication of dl1102 and dl1104 viruses in 22Rv1 cells was less efficient than that of Ad5. Data represent averages with standard errors of 3 independent experiments. All AdE1A-mutants were significantly deficient in replication compared to their respective replicating viruses, $p<0.001$, t-test (*)

Similar to the results from $TCID_{50}$ assays, the increase in hexon DNA copies over time was higher in DU145 and 22Rv1 than in PC3 cells after Ad5 infection (Fig. 39). The newly generated viruses AdE1A-mutants showed defective replication in the three prostate cancer cell lines tested; the weak replication observed for the AdE1A-1102 and AdE1A-1108 mutants by $TCID_{50}$ correlated with a small increase in hexon copy number observed by qPCR, while no increase in hexon was observed for AdE1A-12S and AdE1A-1104 viruses. However, the small increases were never comparable with the increase in hexon copy number observed with the replicating mutants *dl*1102 and *dl*1108 (Fig. 39). The replicating viruses showed an attenuated replication in 22Rv1 but not in DU145 cells, in agreement with the previous observations by $TCID_{50}$. The *dl*1104 and *dl*1102 mutants showed attenuated replication in PC3 cells at 48h, although hexon DNA in *dl*1102 infected cells was increased at 72h to levels similar to Ad5 and the *dl*1108 mutant (Fig. 39). Hexon expression was also detected at the protein level in prostate cancer cells infected with the AdE1A-1102 and AdE1A-1108 mutants (Fig. 43).

Taken together, we concluded from the $TCID_{50}$ assay and qPCR data that AdE1A-mutants were replication defective and that cell death induced by these viruses was caused by the expression of their respective E1A proteins. Detection of hexon by western blotting (Fig. 43) and the small amount of replication observed for AdE1A-1102 and AdE1A-1108 mutants could be due to impurity of the viruses due to recombination with cellular DNA from the packaging cell line HEK293, resulting in intact E1A and/or E1B that were below the detection limit for both PCR and sequencing. Despite showing traces of hexon protein and attenuated replication, toxicity of the AdE1A-12S mutant viruses was greatly attenuated compared to Ad5 and very similar to the potency of the AdE1A-12S virus. This suggests that the recombination that might have occur during the production process was low and that the replication observed is not enough to

induce changes in the potency of these viruses. Further plaque-purification is necessary to isolate viruses free from recombination.

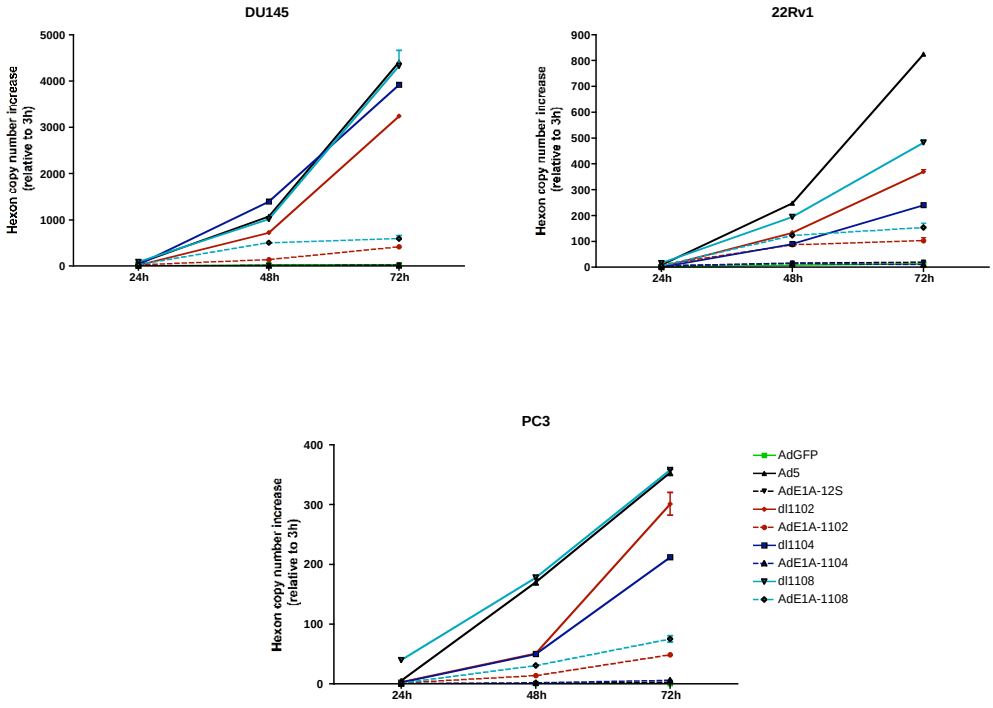


**Fig. 39.** Viral DNA, determined as hexon DNA copies, increased over time after infection with replication-selective E1A-mutant viruses but not with their newly generated replication deficient equivalents. Hexon DNA was quantified by qPCR at 24, 48 and 72h and standardised to hexon copy number 3h post-infection for each sample. As observed by $TCID_{50}$, AdE1A-mutants showed defective replication in prostate cell lines compared to their equivalent *dl*-mutants. Weak increase in hexon copy number was observed with AdE1A-1102 and AdE1A-1108 mutants, but never to levels similar to *dl*1102 or *dl*1108. Data represent averages and standard errors of 2 independent experiments.

# Chapter 6

## *Combination of cytotoxic drugs and replication deficient E1A-expressing adenovirus mutants in prostate cancer cell lines.*

### 6.1 Binding to p300 is necessary for chemosensitisation of prostate cancer cell lines by E1A.

We determined in the previous chapter that the replication deficient AdE1A-12S mutants were good vectors for the expression of E1A proteins in prostate cancer cell lines. We also observed that synergistic interactions with the cytotoxic agents were more efficient with AdE1A-12S than with Ad5. Next we tested if any of the deletions in E1A expressed by these viruses had attenuated sensitising effects in combination with mitoxantrone or docetaxel.

Human prostate cancer cell lines were treated with increasing concentrations of mitoxantrone or docetaxel in the presence or absence of a fixed dose of viral particles; $EC_{50}$ values for each drug were calculated. Different doses of virus were chosen to determine whether the amount of virus used could have different effects in combination with the cytotoxic drugs. $EC_{50}$ values for each drug were calculated 6 days after infection and drug addition as described in materials and methods.

DU145 cells were treated with drugs in combination with 10 or 100 ppc of each replication-defective E1A12S-mutant adenovirus. The non-replicating AdGFP virus used as a control did not sensitise DU145 cells to either mitoxantrone or docetaxel, indicating that E1A expression was causing the drug sensitisation (Fig. 40.A). Sensitisation by the AdE1A-mutants was observed at both viral concentrations although cell death induced by 100 ppc was significantly higher than for 10 ppc (Fig. 40.B). Infection with 100 ppc induced a high percentage of cell death except with the AdE1A-1104 mutant. AdE1A-1108 mutant at 100 ppc induced a 70% cell death as single treatment, while AdE1A-1102 induced a 55% and AdE1A-12S virus almost 40% (Fig. 40.B). It is possible that such high percentage of cell death could have affected $EC_{50}$ value calculations of the combination with drugs. Even though values were corrected for virus-induced cell death, high cell death implied that few cells remained viable and calculations could be affected. At 10 ppc, the AdE1A-1108 mutant induced less than 20% cell death, while AdE1A-1102 only caused 4%. The other viruses tested did not induce cell death.

Sensitisation was more efficient with mitoxantrone than with docetaxel, suggesting that the degree of sensitisation by E1A expression was dependent on the mechanism of action for each drug. This effect was better observed at the highest viral dose used although cell death induced by virus alone also contributed

to the enhancement. All E1A-mutant viruses tested induced a decrease in the $EC_{50}$ value for both drugs at the highest viral dose tested (Fig. 40.B).

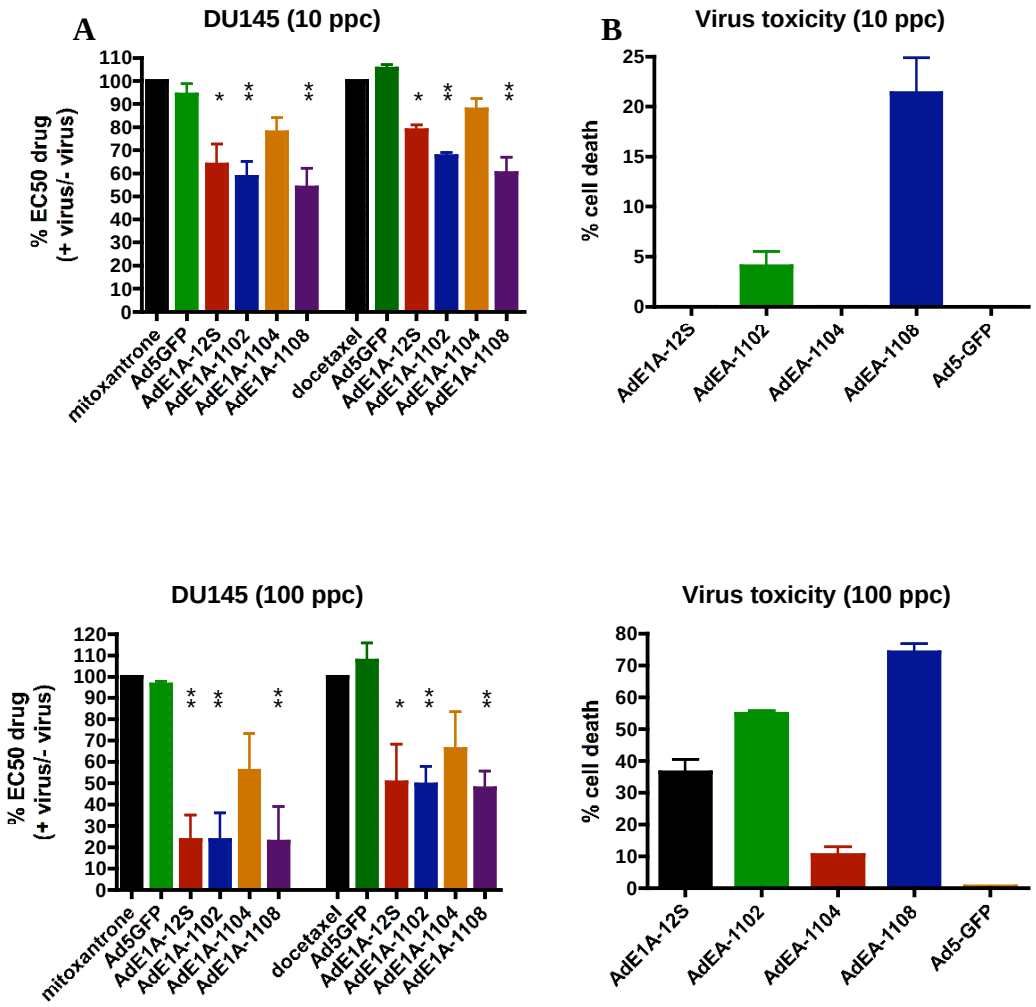


**Fig. 40.** Sensitisation to mitoxantrone and docetaxel in DU145 cells by AdE1A-mutant viruses. Dose-response curves to the drugs were constructed and $EC_{50}$ values were determined and compared to that of drugs alone, expressed as % of EC50 for drug alone. Sensitisation was observed both at 10 and 100 ppc. The reduction in EC50 value for the AdE1A-1104 virus was not statistically significant at any dose used (A). Sensitisation was greater with 100 ppc although virus-induced cell death was very high at this concentration (B). Data represents the average and standard deviation of 5 independent experiments, with t-test statistical analysis comparing each combination of drug and virus to drug alone, $P<0.05$ (*) and $P<0.01$ (**).

However, the AdE1A-1104 mutant failed to decrease the value for either drug to a degree statistically significant. There were no differences between the AdE1A-12S, AdE1A-1102 and AdE1A-1108 mutants at 100 ppc, although the two E1A mutant viruses were slightly more efficient at sensitising DU145 cells than the AdE1A-12S virus when 10 ppc were used (Fig. 40.A).

Three viral concentrations were tested in combination with mitoxantrone and docetaxel for similar studies in the PC3 cells. The observed degree of sensitisation correlated with increasing viral dose. As observed in DU145 cells, PC3 cells were more efficiently sensitised to mitoxantrone than to docetaxel (Fig. 41.A). The AdE1A-1104 mutant was the least effective at inducing sensitisation to the drugs. This virus failed to sensitise PC3 cells to docetaxel at any viral concentration tested. It induced a small reduction in $EC_{50}$ value for mitoxantrone only statistically significant at 50 ppc (Fig. 41.A). None of the tested viruses sensitised PC3 cells to docetaxel at 10 ppc. All mutants, with the exception of AdE1A-1104, significantly reduced the $EC_{50}$ value for this drug when 100 ppc were used (Fig. 41.A). There were no differences between AdE1A-12S, AdE1A-1102 and AdE1A-1108 at this dose in combination with docetaxel. Sensitisation to mitoxantrone was observed at all three viral doses with these viruses. AdE1A-12S virus reduced the $EC_{50}$ value for this drug by 40% at all doses: 10, 50 and 100 ppc. The E1A-mutant viruses AdE1A-1102 and AdE1A-1108 were as efficient as AdE1A-12S. The AdE1A-1102 mutant was more efficient at 10 ppc, with a 50% reduction of $EC_{50}$ for mitoxantrone at this viral dose. The AdE1A-1108 mutant was the best of the viruses tested at sensitising PC3 cells to mitoxantrone at the highest viral concentration of 100 ppc (Fig. 41.A).

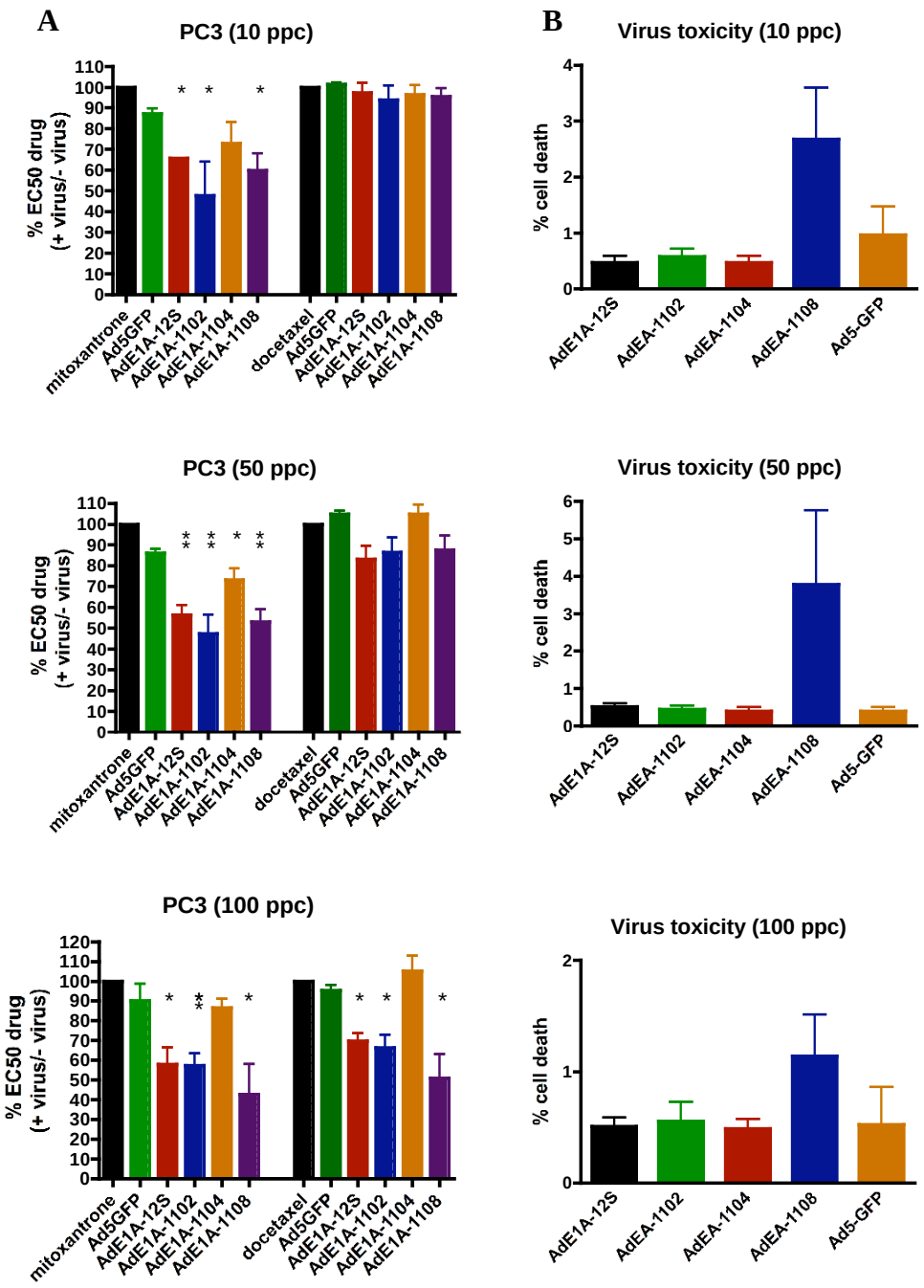


**Fig. 41.** Sensitisation to mitoxantrone and docetaxel by AdE1A-mutants in PC3 cells. Serial dilution of the drugs were combined with 10, 50 or 100 ppc of each virus. $EC_{50}$ values were calculated and expressed as percentages of the value for each drug alone (A). None of the viral doses used induced significant cell death in PC3 cells (<6%) (B). Sensitisation to mitoxantrone was observed with the three viral concentrations for all E1A-expressing viruses with the exception of AdE1A-1104 that only showed statistically significant sensitisation at 50 ppc ($P<0.05$). Sensitisation to docetaxel was proportional to viral dose although it only reached statistical significance at 100 ppc with all mutants, with the exception of AdE1A-1104. Histograms represent an average of 3 experiments with standard deviation and t-test statistical analysis; $P<0.05$ (*), $P<0.01$ (**).

In the 22Rv1 cells a lesser degree of sensitisation to mitoxantrone or docetaxel was observed with the new AdE1A12S-mutants in agreement with previous findings using the corresponding replication-selective mutants (Fig. 14). Sensitisation to docetaxel was only observed at 10 ppc, the highest of the three viral concentrations tested (Fig. 42.A). The $EC_{50}$ value for docetaxel was reduced only by 20% with the AdE1A-12S virus, the only virus to show a statistically significant reduction at this dose. Sensitisation to mitoxantrone at the highest viral dose showed the same trend as in DU145 and PC3 cells; the AdE1A-1104 virus also failed to sensitise 22Rv1 cells to mitoxantrone even at 10 ppc while the AdE1A-1102 and AdE1A-1108 mutants reduced the $EC_{50}$ value by 45% and 30% respectively (Fig. 42.A). The most efficient virus at this dose was the AdE1A-12S, with a 60% reduction in $EC_{50}$ value for mitoxantrone. The lower viral doses used, 1 and 2.5 ppc, did not induce cell death in 22Rv1 during the length of the assay (Fig. 42.B). However, only the AdE1A-12S virus was able to sensitise 22Rv1 cells to mitoxantrone at the lowest dose. Good senstitisation to mitoxantrone was observed with 2.5 ppc; at this dose, AdE1A-1102 and AdE1A-1108 viruses reduced the $EC_{50}$ value for mitoxantrone to the same level as the AdE1A-12S virus, to 60% of that of mitoxantrone alone (Fig. 42.A).

The data from the different cell lines strongly indicated that the E1A-1104 protein was not able to sensitise prostate cancer cell lines to the cytotoxic agents currently used in the clinic. We also concluded that sensitisation was more efficient when viruses were combined with DNA-damaging agents like mitoxantrone than with cytoskeleton disrupting agents like docetaxel. It is possible that the mechanism by which E1A sensitises cells to drug involves pathways more closely related to DNA-damage than to microtubule organisation and therefore better sensitisation is achieved in combination with agents such as mitoxantrone.

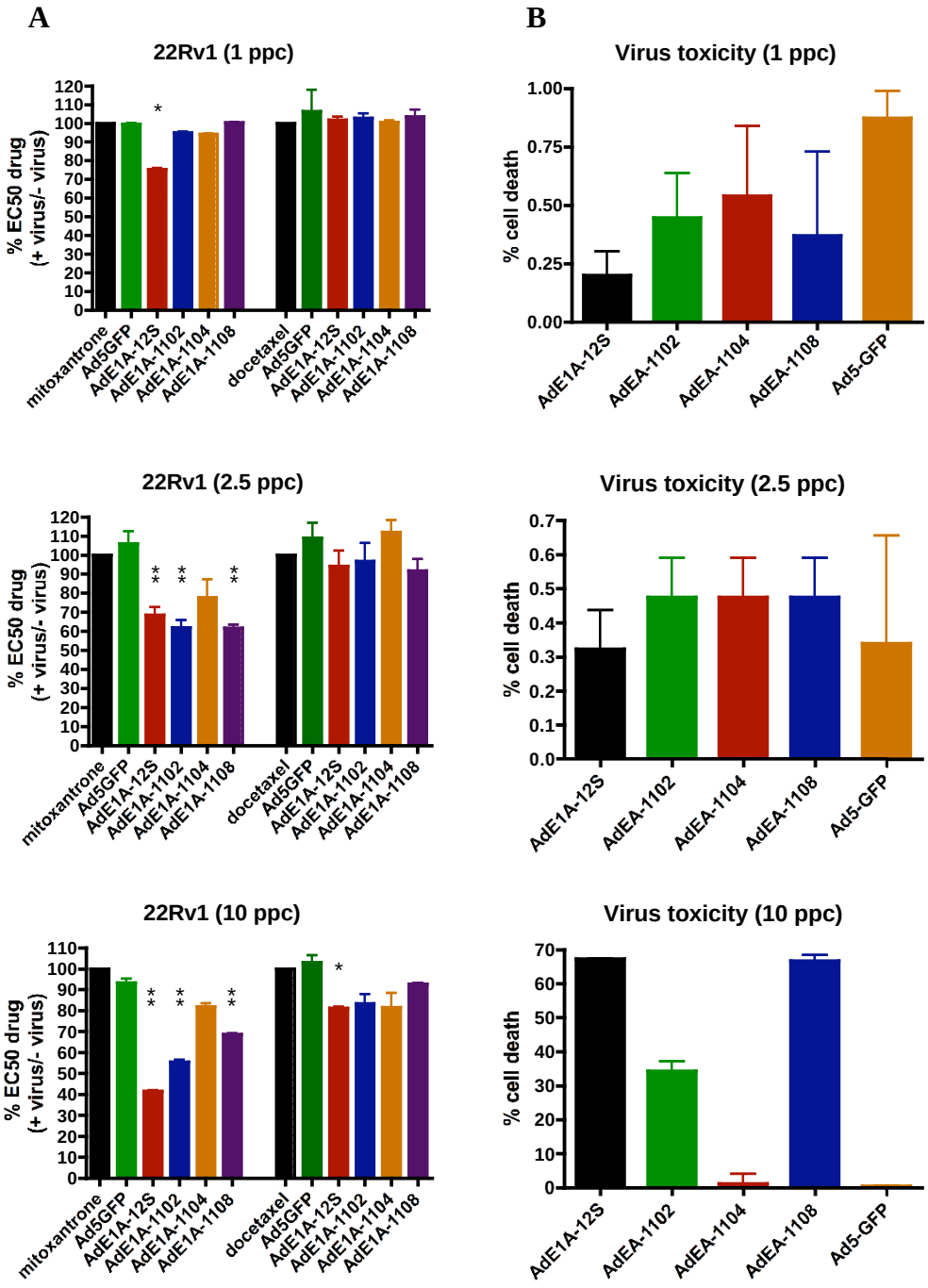


**Fig. 42.** Sensitisation to mitoxantrone and docetaxel by AdE1A-mutants in 22Rv1 cells. Each drug was combined with 1, 2.5 and 10 ppc and $EC_{50}$ values were calculated and expressed as percentages of the $EC_{50}$ values for each drug alone (A). Sensitisation was proportional to viral dose. Statistically significant reduction in EC50 values at the lower viral dose was only observed for the AdE1A-12S virus in combination with mitoxantrone ($P<0.05$). Sensitisation to mitoxantrone was observed for the other mutants at higher doses, with the exception of the AdE1A-1104 virus, that failed to sensitise 22Rv1 to this drug. Statistically significant sensitisation to docetaxel was only observed in combination with the AdE1A-12S virus at 10 ppc. However, cell death induced by virus alone at this concentration was too high (B). Data represent the averages of 3 independent experiments with SD and t-test; $P<0.05$ (*), $P<0.01$ (**).

In addition, the degree of sensitisation varied among cell lines, suggesting that the individual status of each cell line and their gene mutations could play a role in determining the efficiency of sensitisation by E1A proteins.

## 6.2 Expression of E1A increased in cells treated with mitoxantrone.

Previous experiments with replication-selective adenoviruses demonstrated increased E1A expression in the presence of mitoxantrone in chapter 3. Infection with GFP-expressing virus also demonstrated an increase in the number of infected cells in combination with mitoxantrone. Hence, E1A expression was assessed after infection with the new replication-defective E1A12S-expressing viruses in the presence or absence of the drug.

PC3, DU145 and 22Rv1 cells were treated with 100, 10 or 2.5 ppc respectively in the presence or absence of mitoxantrone at 50 nM. This concentration was selected based on previous qPCR data shown in chapter 3, showing a significant increase in E1A mRNA with this concentration of drug. Analysis of E1A proteins by western blotting showed an increase in E1A expression when cells were treated in combination with the drug. This increase in expression was observed at 24h in the three cell lines tested when virus was present throughout the experiment (Fig. 43). However, increase of E1A for all viral mutants in combination with drug was only observed in DU145 cells; the PC3 cell line showed small increases in E1A during combination treatments, only detectable for the AdE1A-1104 mutant. Similarly, increase in E1A levels in 22Rv1-infected cells was only observed for the AdE1A-1108 mutant virus (Fig. 43).

In addition, we also detected hexon expression after infection with AdE1A-1102 and AdE1A-1108 mutant viruses, indicating that late genes were expressed by these viruses, what could explain the observed reduced replication previously described in Fig. 38.

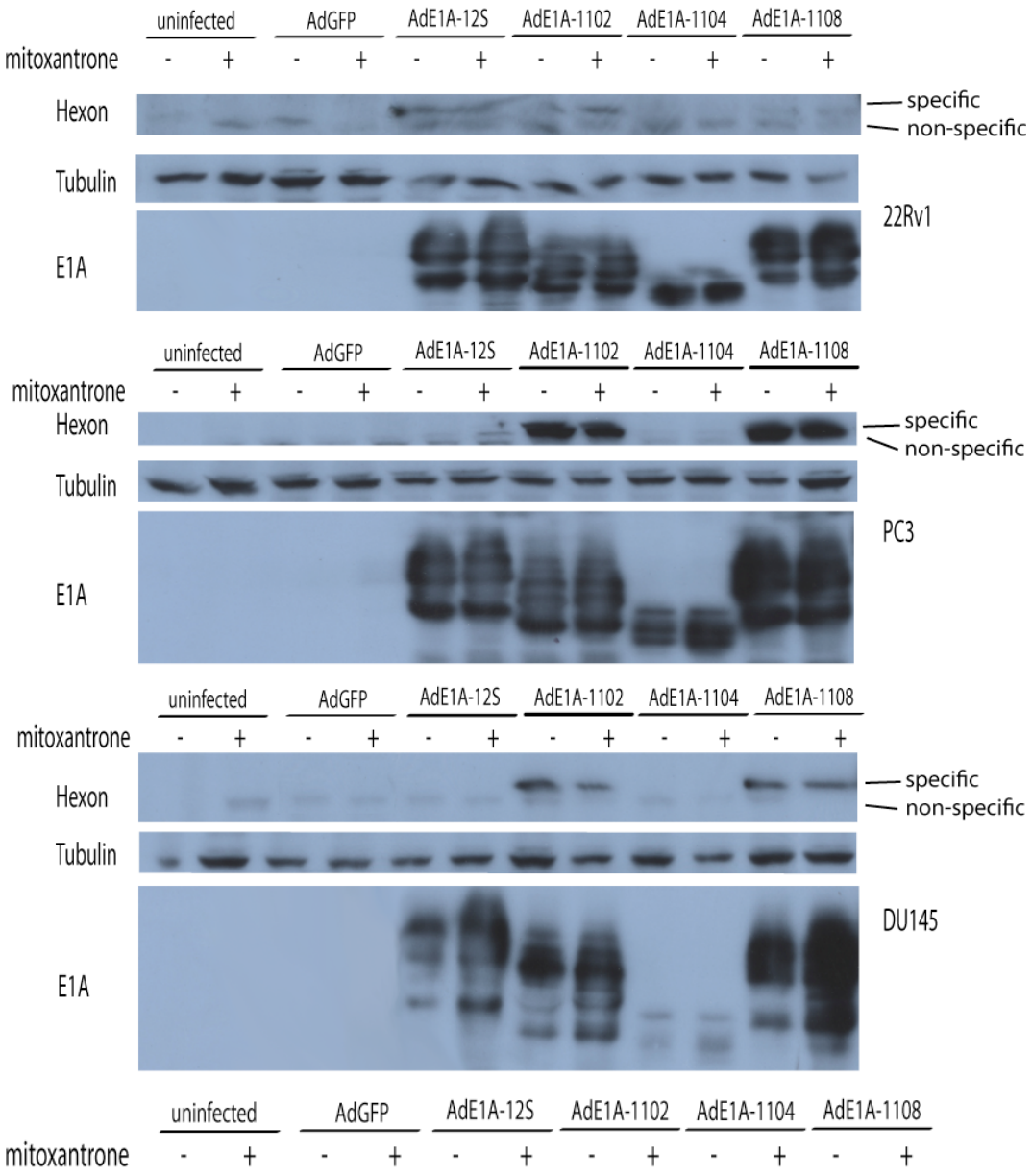


**Fig. 43.** Changes in E1A expression after 24h of infection in the absence or presence of mitoxantrone at 50 nM. E1A levels increased for all mutants in the presence of drug in DU145 infected cells, while smaller increases in E1A levels were detected for AdE1A-1104 in PC3 and for AdE1A-1108 in 22Rv1 cells. Hexon was detected after infection with AdE1A-1102 and AdE1A-1108. Virus and drug were present throughout the experiment.

The observed increase in E1A expression could have been caused by an increase in infection by the AdE1A-12S virus or by an enhancement in viral gene transcription from the CMV promoter. An increase in GFP-expressing cells was observed when prostate cancer cells were infected with non-replicating AdGFP (Fig. 18). This was only observed when the virus was present throughout the experiment as opposed to being removed after 2h. Levels of E1A mRNA were quantified by RT-qPCR to verify that the effects seen with the AdGFP virus could also be observed with the AdE1A-12S mutant. 22Rv1, PC3 and DU145 cells were infected with AdE1A-12S virus in the presence or absence of mitoxantrone under two different conditions. In one set of cells, virus was removed from samples after two hours of infection; in another set, virus was left in the media during the length of the assay, as described previously for the AdGFP virus (Fig. 18). Levels of E1A mRNA were lower in cells infected for only 2h than for 24h as expected (Fig. 44). In 22Rv1 and PC3 cells treated with mitoxantrone after infection, E1A mRNA levels were similar to those in cells without drug treatment although reproducibly small increases in E1A mRNA with mitoxantrone were seen. However, mitoxantrone increased the levels of E1A mRNA in DU145 cells.

When AdE1A-12S was present in the medium throughout the study (24h) the levels of E1A mRNA were higher, as more cells were infected during the length of the assay (Fig. 44). Differences in mRNA expression between cells treated with virus alone or in combination with mitoxantrone were significant in the three cell lines tested. The smallest effect was observed in 22Rv1 cells, with twice more expression of E1A mRNA in cells treated with a combination of virus and drug. This increase was higher in PC3 and DU145 cells, in which expression of viral mRNA was 3.5 and 12 times higher, respectively, than in cells treated with virus only (Fig. 44).

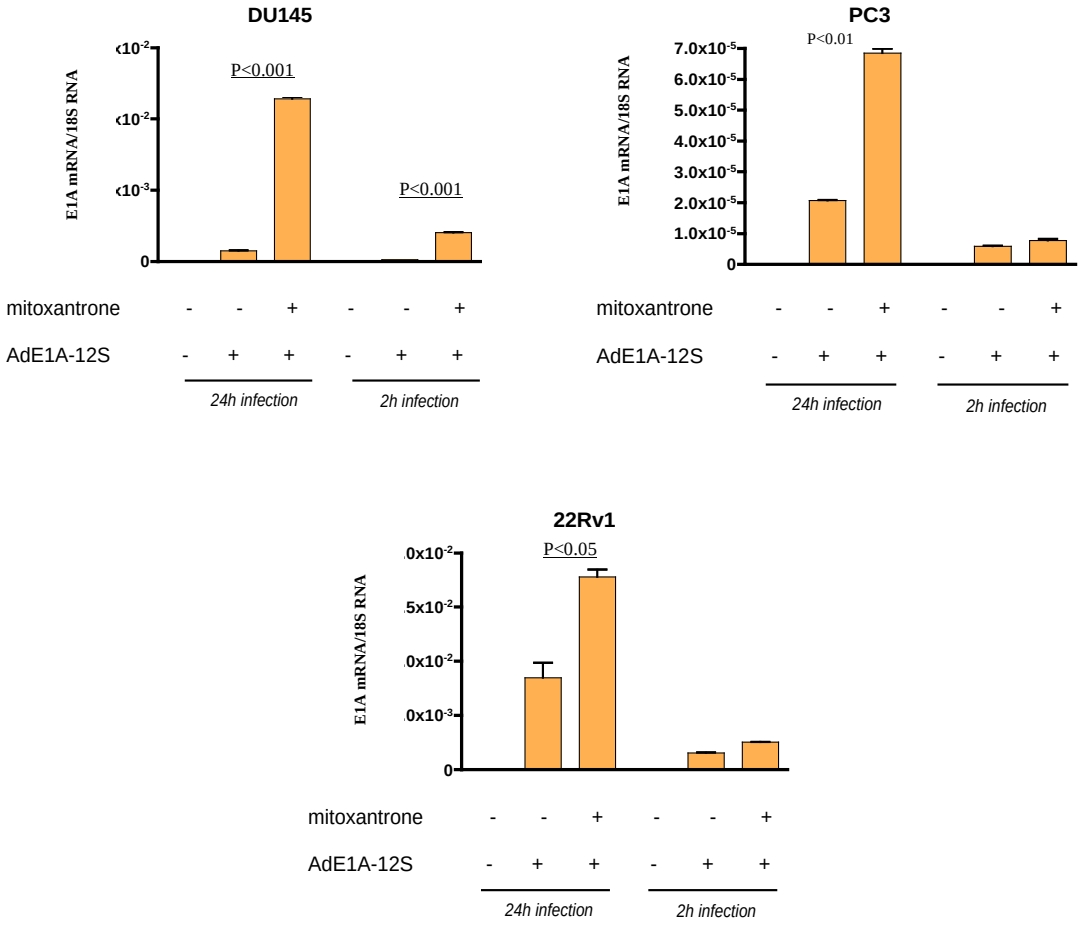


**Fig. 44.** E1A mRNA levels in prostate cancer cell lines after infection with AdE1A-12S in the presence or absence of mitoxantrone at 50 nM. Cells were treated with virus and mitoxantrone for 24h in one condition; in a second condition, virus was replaced by medium only or containing mitoxantrone after 2h of infection. E1A mRNA level only increased significantly when virus and mitoxantrone were present for 24h, but not when virus was removed. Data represent the averages of 2 independent experiments with standard deviations.

The smaller increases in E1A mRNA levels in 22Rv1 and PC3 cells compared to that in DU145 cells could explain the increase at the protein level that was clearly observed in DU145 cells but not in PC3 and 22Rv1 cells (Fig. 43).

This data, together with data from chapter 3, showed that mitoxantrone induced an increase in E1A expression. This was likely to occur due to an increase in infectability over time since no significant increase was observed when virus was removed from the cells after 2h.

## 6.3 The AdE1A-1104 mutant adenovirus failed to induce changes in cell cycle.

It is well known that E1A can induce S-phase in infected cells as a mechanism to achieve efficient viral replication while the cytotoxic drug mitoxantrone induces G2/M cell cycle arrest. We aimed to determine the effects on the cell cycle when the AdE1A-mutants were combined with mitoxantrone and whether potential changes correlated with the sensitising abilities of each mutant previously observed Fig. 40, Fig. 41 and Fig. 42.

Cell cycle progression was analysed in the three human prostate cancer cell lines to investigate changes in the cycle under combination of mitoxantrone at 50 nM with the different E1A-expressing replication-defective adenovirus mutants. Viral doses were selected based on sensitisation studies: 2.5 ppc were used for 22Rv1, 10 ppc for DU145 and 100 ppc for PC3 cells. Those were the doses that showed best sensitisation with minimal virus-induced cell death. Cells were treated with mitoxantrone, virus or in combinations for 24, 48 and 72 hours.

Propidium iodide and flow cytometry were used to quantify the number of cells in each phase of the cell cycle.

E1A expression at the viral doses used did not induce cell cycle changes in any of the cell lines tested. Replication-defective adenoviruses induced only small changes in the population of cells in each phase of the cell cycle that were never significative.

The effect of mitoxantrone on cell cycle progression varied among cell lines. The drug induced an increase in the sub G1 population and a decrease in the S-phase population in the 22Rv1 cells over time (Fig. 48). In the PC3 cells the drug initially increased the percentage of cells in S-phase but lwere later arrested in the G2/M phase. Mitoxantrone reduced the percentage of PC3 cells in G1-phase compared to untreated cells and increased the G2/M population from 22% in untreated cells to 56% at 72h (Fig. 45). Combination of mitoxantrone with replication-defective viruses showed more cells in G2/M phase than treatment with mitoxantrone alone in PC3 (Fig. 46 and Fig. 47) and 22Rv1 cells (Fig. 50 and Fig. 49), an increase that was only observed for those viruses that could sensitise the prostate cancer cells to mitoxantrone, the AdE1A-12S, AdE1A-1102 and AdE1A-1108 mutants. The AdE1A-1104 mutant and AdGFP used as control virus, did not induce changes in phase distribution resulting in the same profile as mitoxantrone alone at all time points.

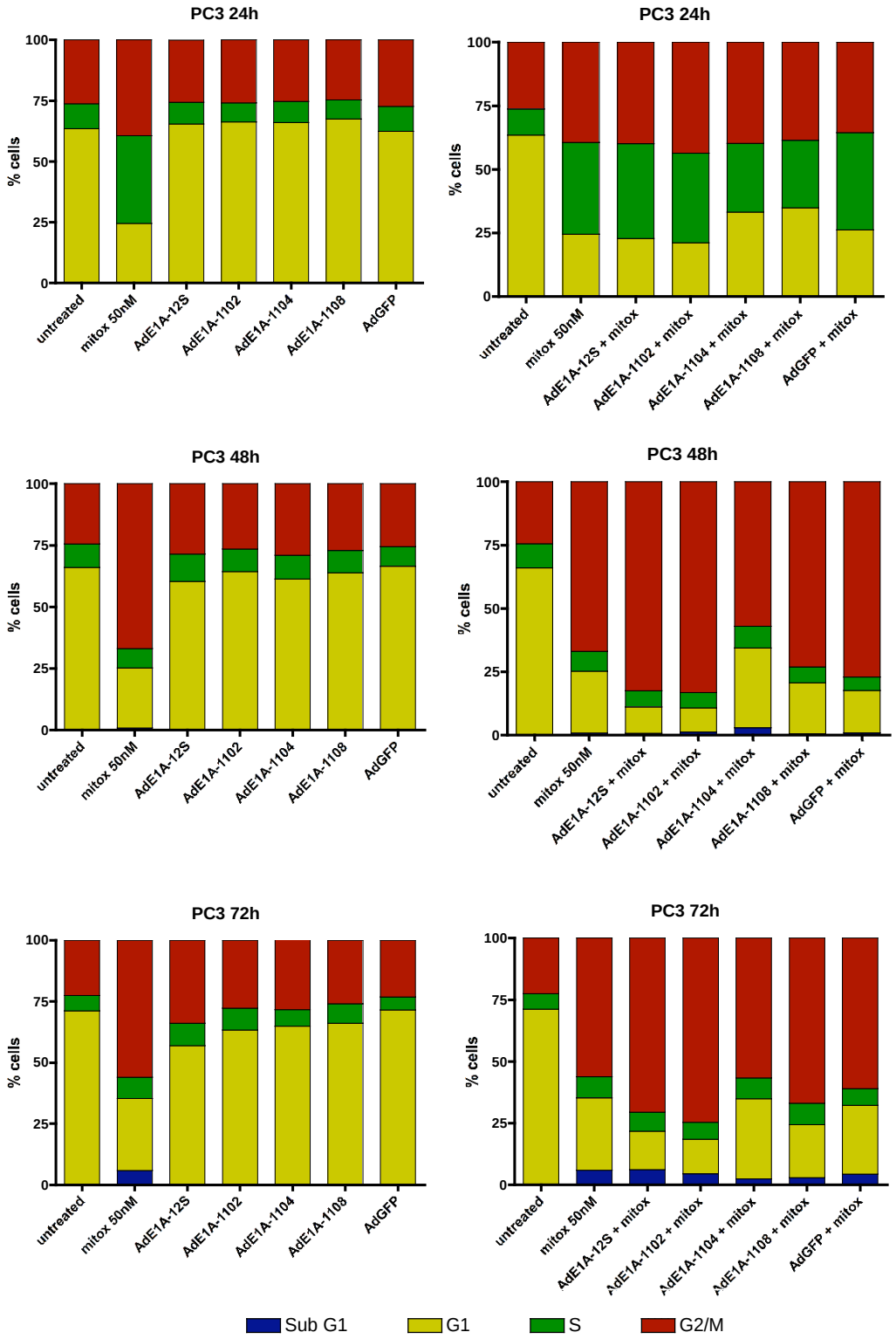


**Fig. 45.** Cell cycle analysis of PC3 cells at 24, 48 and 72h after treatment with viruses, mitoxantrone or combination of both. Viral infection did not induce changes in cell cycle at the doses used; mitoxantrone induced a progression in S-phase at early time points that resulted in G2/M arrest at 72h. E1A-mutant viruses that successfully sensitise PC3 cells to mitoxantrone increased the percentage of cells in G2/M after 72h in combination with the drug, while AdE1A-1104 and the negative control virus AdGFP showed a similar profile to mitoxantrone alone when combined with this drug. Data are representative of 3 independent experiments.

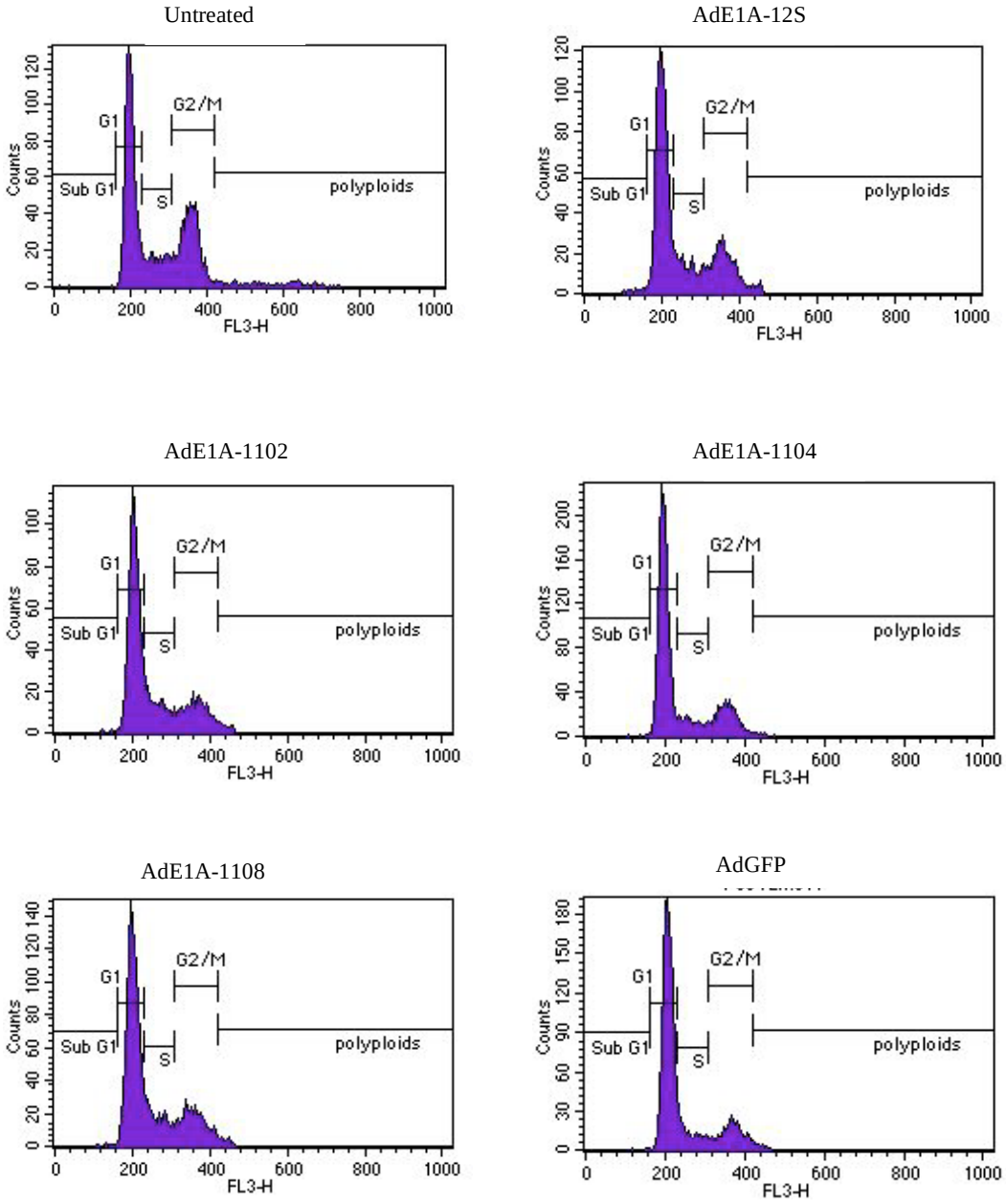


**Fig. 46.** Analysis of cell cyle in PC3 cells 72h after infection with AdE1A-12S-mutants or AdGFP. This is a representative example of how the different cell cycle phases were gated in untreated cells to determine the percentage of cells in each phase after infection with viruses. Infection of PC3 cells at 100 ppc had no effects on cell cycle with any of the viruses used.

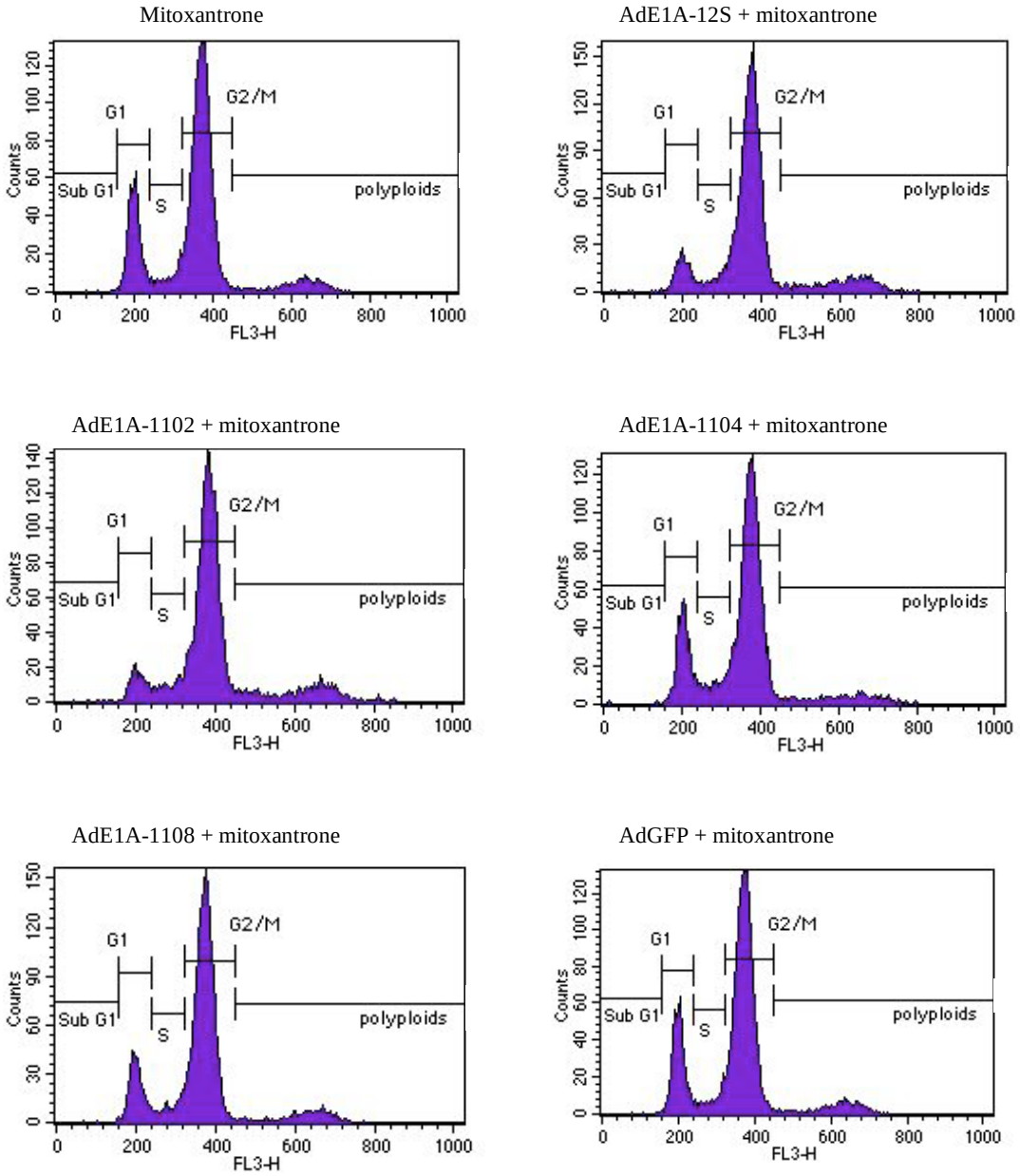


**Fig. 47.** Flow cytometry analysis of PC3 cells after 72h of treatment with mitoxantrone alone or in combination with AdE1A-12S-mutants. Each phase was determined in cells treated with the drug alone and used to determine the proportion of cells in each phase after combination of drug and viruses. We observed a decrease in G1 after combination of mitoxantrone with AdE1A-12S, AdE1A-1102 and AdE1A-1108 viruses, compared to drug alone or in combination with AdE1A-1104 or AdGFP.

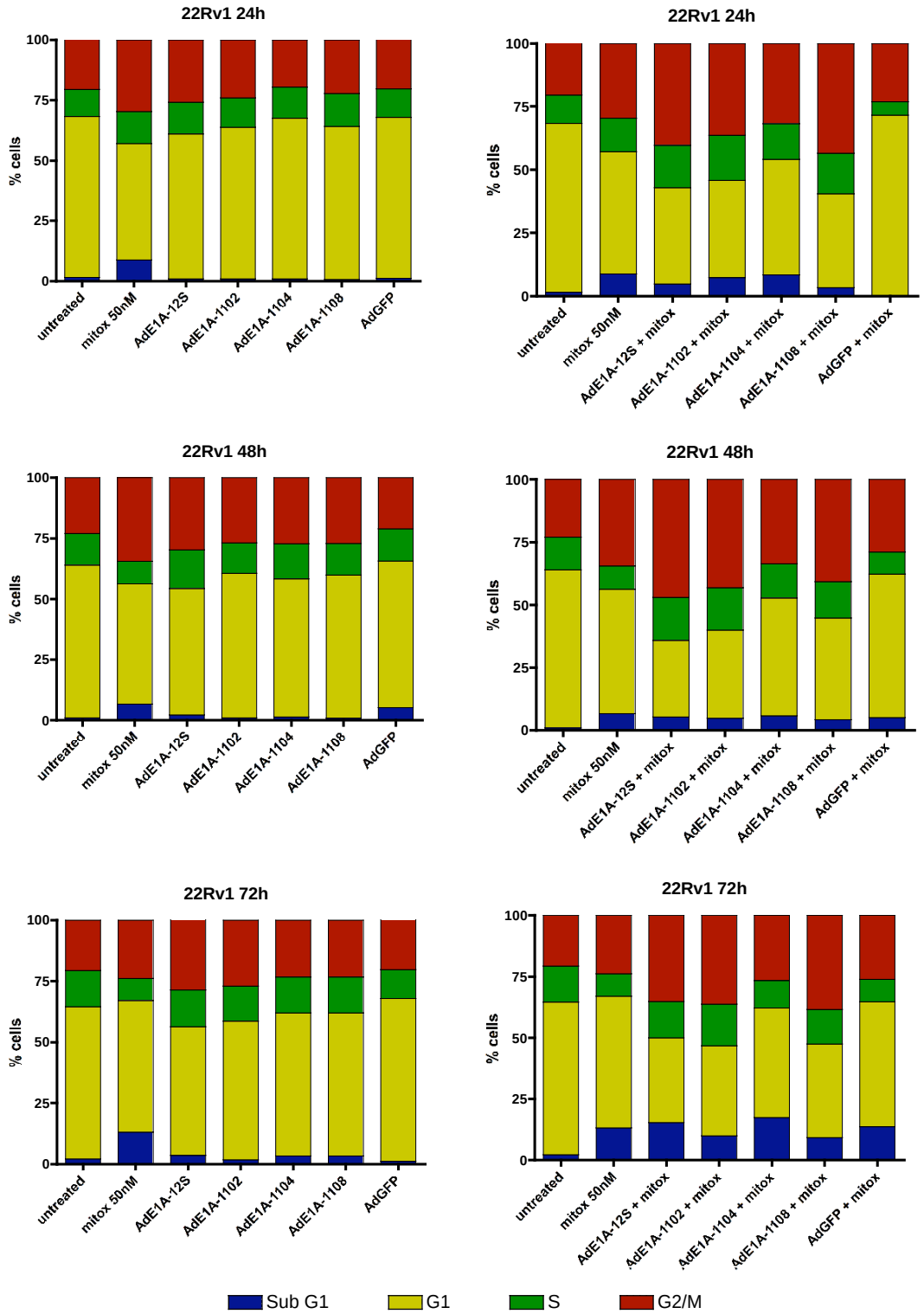


**Fig. 48.** Cell cycle analysis of 22Rv1 cells after treatment with mitoxantrone, AdE1A-mutant viruses or a combination of both agents. Similar to the results obtained in PC3 cells, viruses alone did not induce changes in cell cycle, but AdE1A-12S, AdE1A-1102 and AdE1A-1108 increased the percentage of cells in G2/M when combined with mitoxantrone after 72h. AdE1A-1104 and AdGFP, unable to sensitise cells to the drug, failed to induce changes in cell cycle in combination with mitoxantrone, compared to the dug alone. Data representative of 3 independent experiments.

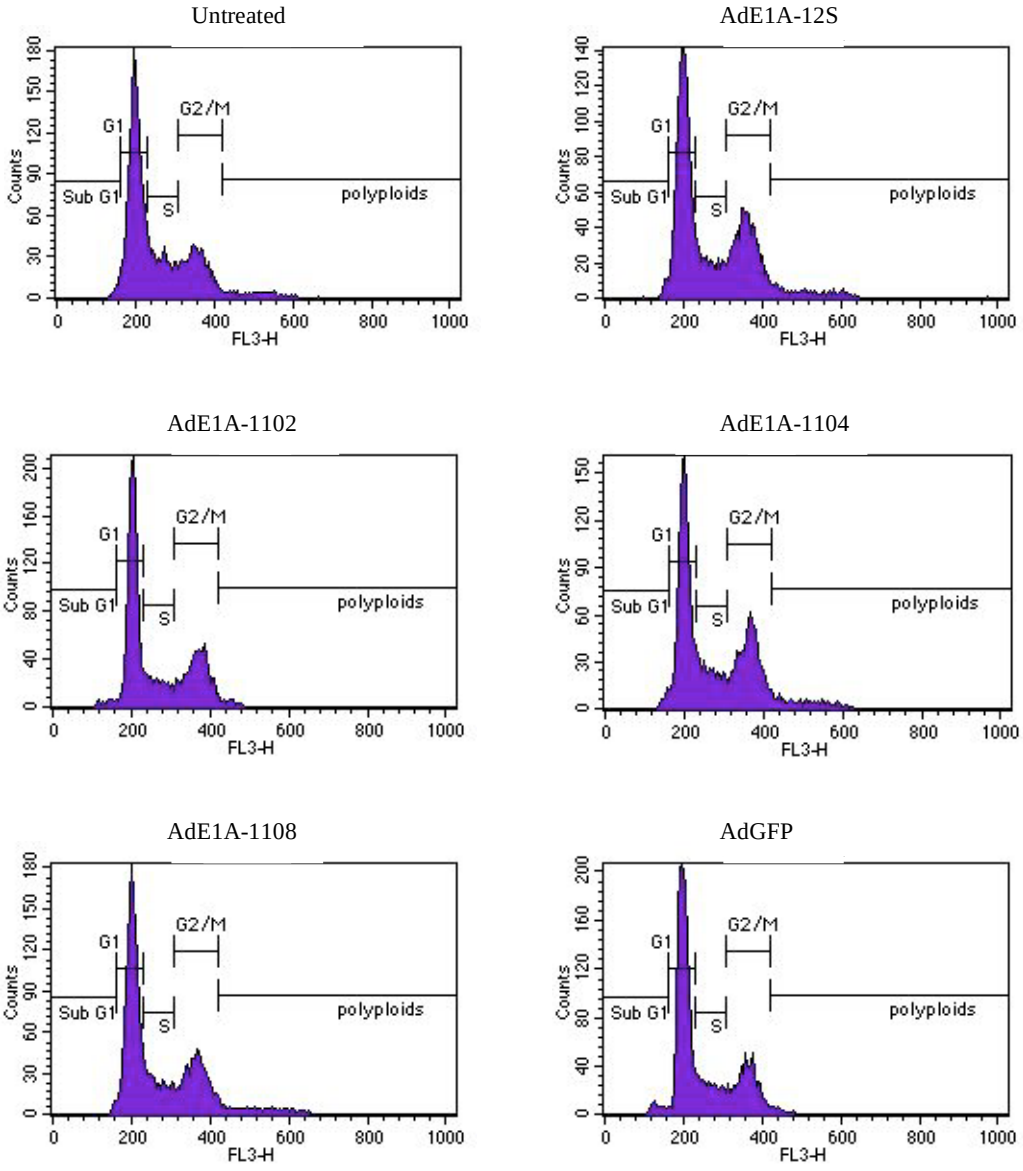


**Fig. 49.** Flow cytometry analysis of 22Rv1 cells after 72h of treatment with AdE1A-12S-mutants or AdGFP. Different cell cycle phases were gated in untreated cells and those gates were used to determine the percentage of cells in each phase for samples treated with viruses. No significant changes were observed with any of the viruses used at 2.5 ppc.

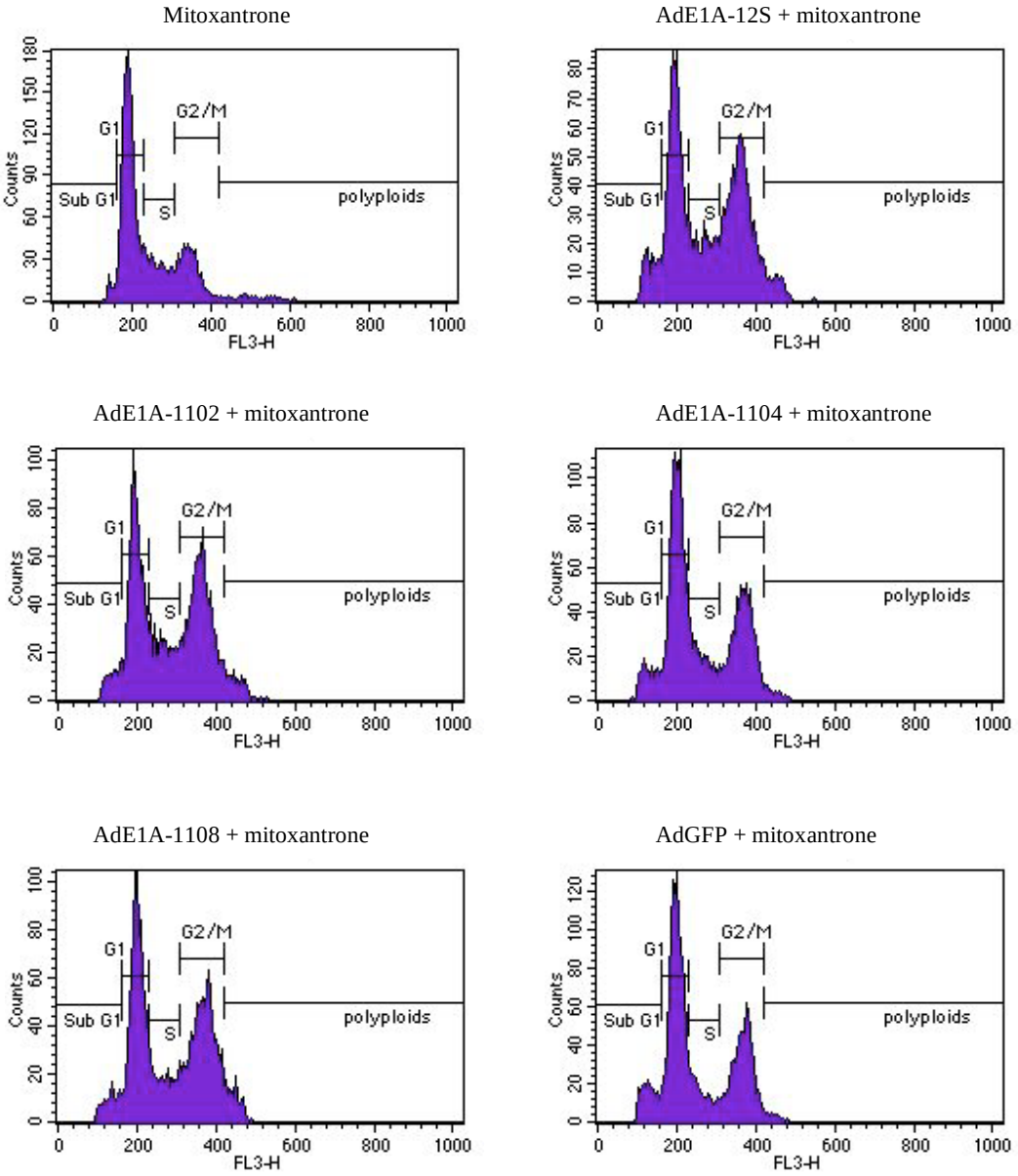


**Fig. 50.** Flow cytometry analysis of cell cycle in 22Rv1 cells 72h after treatment. This is a represenatative example showing how the different cycle phases were gated for 22Rv1 cells treated with mitoxantrone in the presence or absence of mitoxantrone. An increase in G2/M was observed with mitoxantrone combined wit AdE1A-12S, AdE1A-1102 and AdE1A-1108 viruses, compared to mitoxantrone alone. AdE1A-1104 and AdGFP combination with the drug resulted in a cell cycle profile similar to that of mitoxantrone alone.

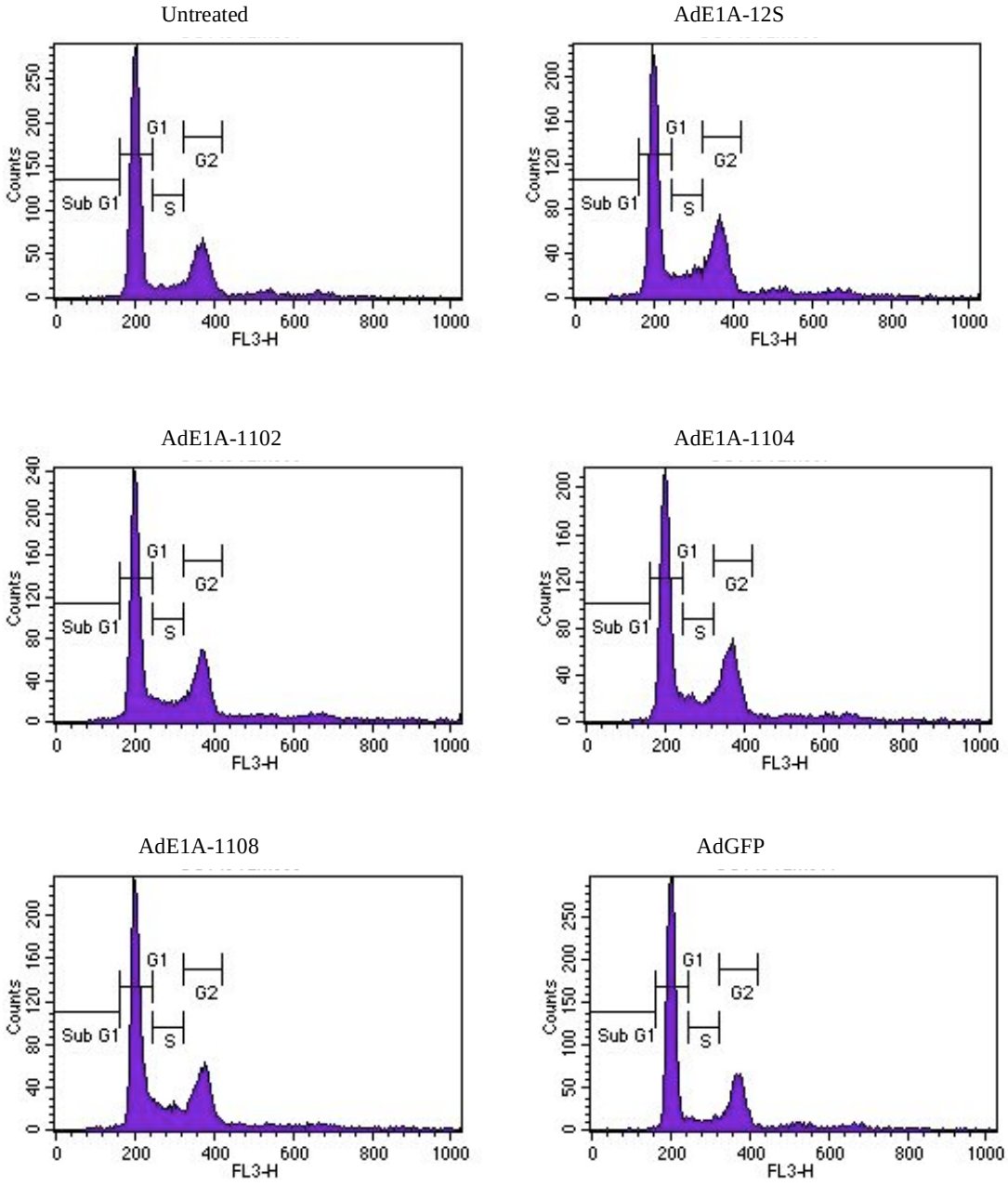


**Fig. 51.** Cell cycle analysis of DU145 cells treated with 10 ppc of each AdE1A-mutant and AdGFP during 48h. Expression of E1A-deletion mutants did not have an effect in cell cycle of these cells at the dose used. Representative data of 3 independent experiments.

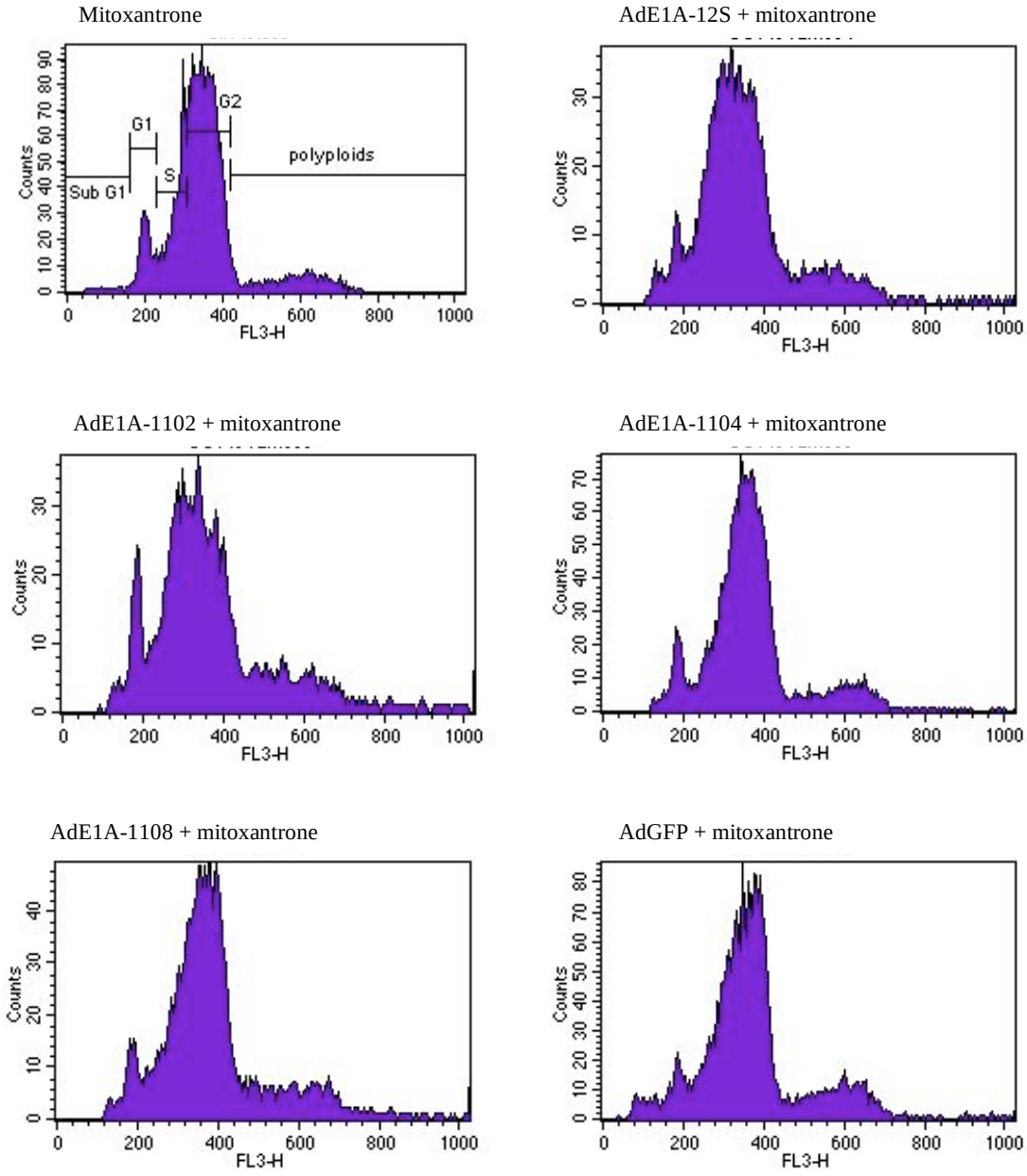


**Fig. 52.** Mitoxantrone alone or in combination with AdE1A-mutant viruses induced an arrest in G2/M phase in DU145 cells after 48h of treatment. Combination of mitoxantrone with viruses induced a greater arrest in G2/M and the formation of polyploidy; it was not possible to accurately identify each cell cycle phase in the profiles obtained after combination treatments. The AdE1A-12S and AdE1A-1102 mutants showed a greater number of cells cycling towards the G2/M than the other mutants. AdE1A-1104, AdE1A-1108 and AdGFP viruses showed a similar profile, although polyploidy was higher in cells treated with AdE1A-1108 than with AdE1A-1104 or AdGFP in combination with mitoxantrone. Data representative of 3 independent experiments.

In DU145 cells, as observed for the other prostate cell lines, viral infection did not affect the percentages of cells in each cell cycle phase (Fig. 51). However, changes induced by mitoxantrone in combination with viruses were greater than expected. The drug alone induced an arrest in the G2/M phase; the combination with viruses induced the formation of polyploidy and arrest in G2/M, although cells appeared to be in a transition between S-phase and G2/M, so accurate gating of the cells was not possible (Fig. 52). The AdE1A-12S and AdE1A-1102 viruses in combination with mitoxantrone induced a greater effect on the cell cycle in DU145 cells, while AdE1A-1104 and AdGFP showed similar profiles to that of mitoxantrone alone. The AdE1A-1108 virus induced changes in cell cycle in a similar manner as AdE1A-1104 although the percentage of polyploidy was greater for AdE1A-1108 than for AdE1A-1104.

These data showed that E1A mutants that successfully sensitised cells to mitoxantrone increased the percentage of cells in G2/M phase. Mitoxantrone induced G2/M arrest, so it is likely that enhanced cell killing by combination of drug and viruses enhanced the effects of the drug in these cells, inducing greater G2/M arrest. Supporting this hypothesis, viruses that did not sensitise prostate cancer cells to mitoxantrone did not induce a change in cell cycle profiles compared to the drug alone.

## 6.4 Mitochondrial membrane potential only changed in cells that were sensitised to cell death in response to the combination treatments.

Loss of potential of the mitochondrial membrane (mitochondrial depolarisation = $\Delta\Psi$) is associated with early induction of apoptosis. It is also known that E1A expression induces apoptosis hence, a possible mechanism of sensitisation by E1A to drugs could be through increased apoptotic activity. Cells were treated with all the replication-defective E1A-expressing mutant viruses in the presence or absence of mitoxantrone, at the concentrations described for the cell cycle analysis, followed by analysis of mitochondrial membrane potential by flow cytometry using TMRE and DAPI staining (Fig. 53.A). The newly generated replication-defective adenoviruses did not induce apoptosis at the concentrations tested in any of the cell lines used (Fig. 53.B). Mitoxantrone treatment increased the percentage of cells in early apoptosis; a higher percentage of apoptotic cells was observed after 24h in 22Rv1 cells, after 48h in DU145 and PC3 cells (Fig. 53.B). The effects of the combination of mitoxantrone with each E1A- mutant virus were similar in DU145 and PC3 cells. Ad5-GFP and AdE1A-1104 mutants failed to increase the percentage of cells undergoing apoptosis.

On the other hand, AdE1A-12S, AdE1A-1102 and AdE1A-1108 viruses almost doubled the number of apoptotic cells when combined with the drug. In DU145 cells, the AdE1A-12S virus was the most efficient of the three viruses in enhancing apoptosis, followed by the AdE1A-1108 and AdE1A-1102 mutants. In PC3 cells the AdE1A-1108 mutant induced the highest increase in apoptosis, starting at 72h (Fig. 53.B).

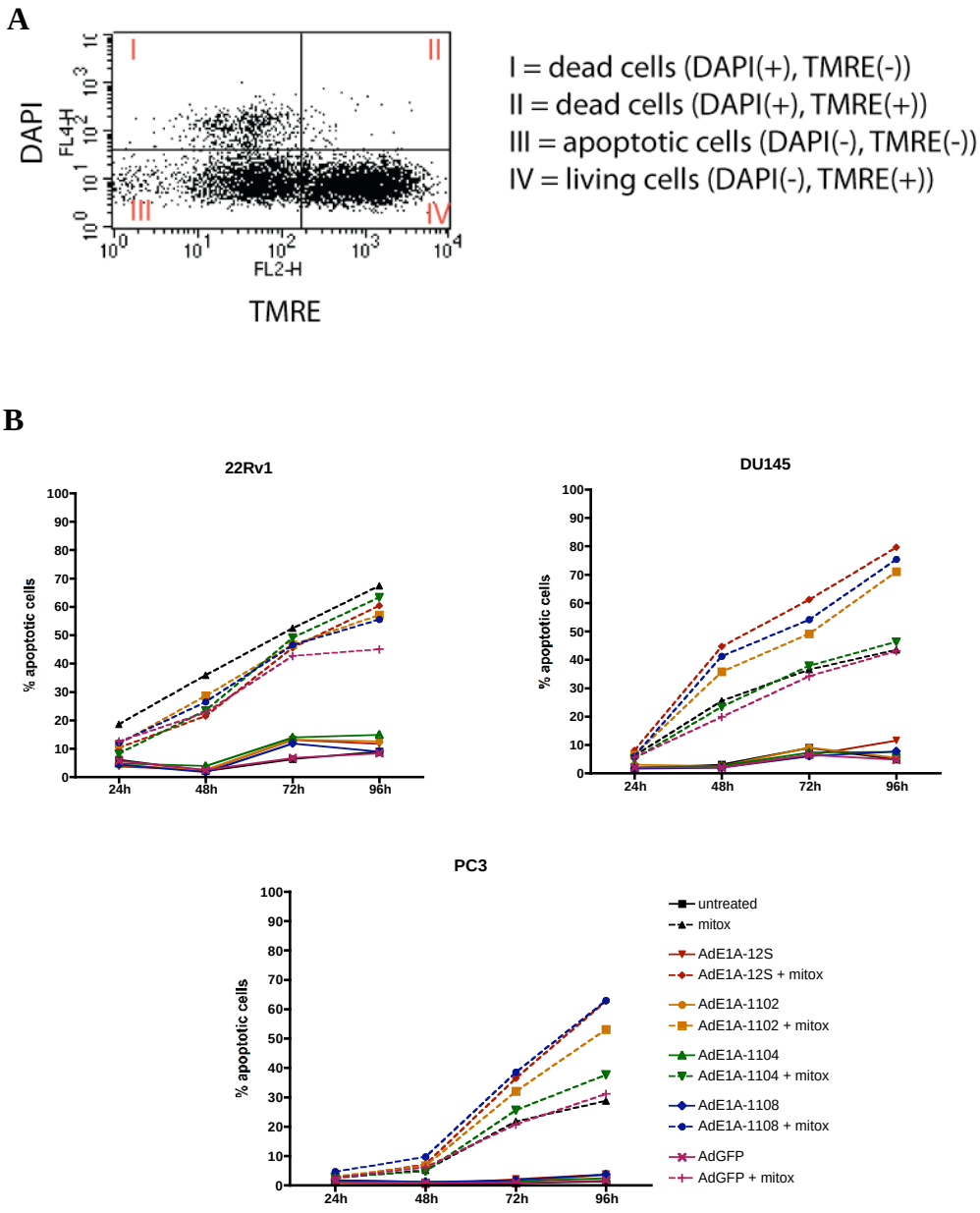


**Fig. 53.** Mitochondrial membrane depolarisation was assessed by a TMRE flow cytometry assay as an indication of activation of early apoptotic processes. Cells were treated with 2.5 ppc (22Rv1 cells), 10 ppc (DU145 cells) or 100 ppc (PC3 cells) in the absence or presence of mitoxantrone at 50 nM. A) Flow cytometry analysis of DU145 cells after mitoxantrone treatment. Cells were divided into four quadrants, according to DAPI and TMRE staining. Quadrants I and II represent dead cells; quadrant III represent cells undergoing early apoptotic events; living cells are gated in quadrant IV. B) Viral infection did not induce apoptosis in human prostate cancer cells but viruses that sensitised cells to mitoxantrone increased the number of pro-apoptotic cells in combination with this drug compared to drug alone. Combination of mitoxantrone with AdE1A-1104 or AdGFP did not induce an increase in the percentage of pro-apoptotic cells in DU145 and PC3 cells although an increase in apoptosis was observed with AdE1A-1104 in combination with mitoxantrone in 22Rv1 cells. Representative data of 3 independent experiments.

Combination of viruses and mitoxantrone did not increase the percentage of proapoptotic cells in 22Rv1. Mitoxantrone showed the same level of apoptosis induction alone as in combination with any of the viruses tested. This data was in agreement with previous observations, suggesting that this cell line was less sensitive to E1A-mediated sensitisation to cytotoxic drugs.

We observed that those viruses able to sensitise prostate cancer cell lines to mitoxantrone induced an increase in the percentage of proapoptotic cells in combination to mitoxantrone in comparison to the drug alone. This suggested that the supra-additive cell death observed in combination treatment could be due to an upregulation of proapoptotic pathways and that binding of E1A to p300 is critical to induce these pathways since AdE1A-1104 has no effect on $\Delta\Psi$ in combination with mitoxantrone.

## 6.5 Inhibition of caspases resulted in increased survival and reduction of sensitisation to mitoxantrone by E1A.

TMRE analysis showed that early activation of apoptosis was increased with the AdE1A-12S mutants that successfully sensitised prostate cancer cell lines to mitoxantrone. To further investigate the role of apoptosis in sensitisation, human prostate cancer cell lines were treated with the pan-caspase inhibitor z-VAD-FMK together with mitoxantrone and the AdE1A-mutant viruses, alone or in combination.

When the caspase inhibitor was added to cells treated with mitoxantrone and viruses the supra-additive effects of the combinations were inhibited in all cell lines (Fig. 54). The addition of inhibitor to cells treated with mitoxantrone alone also resulted in an increase of $EC_{50}$ value for the drug.

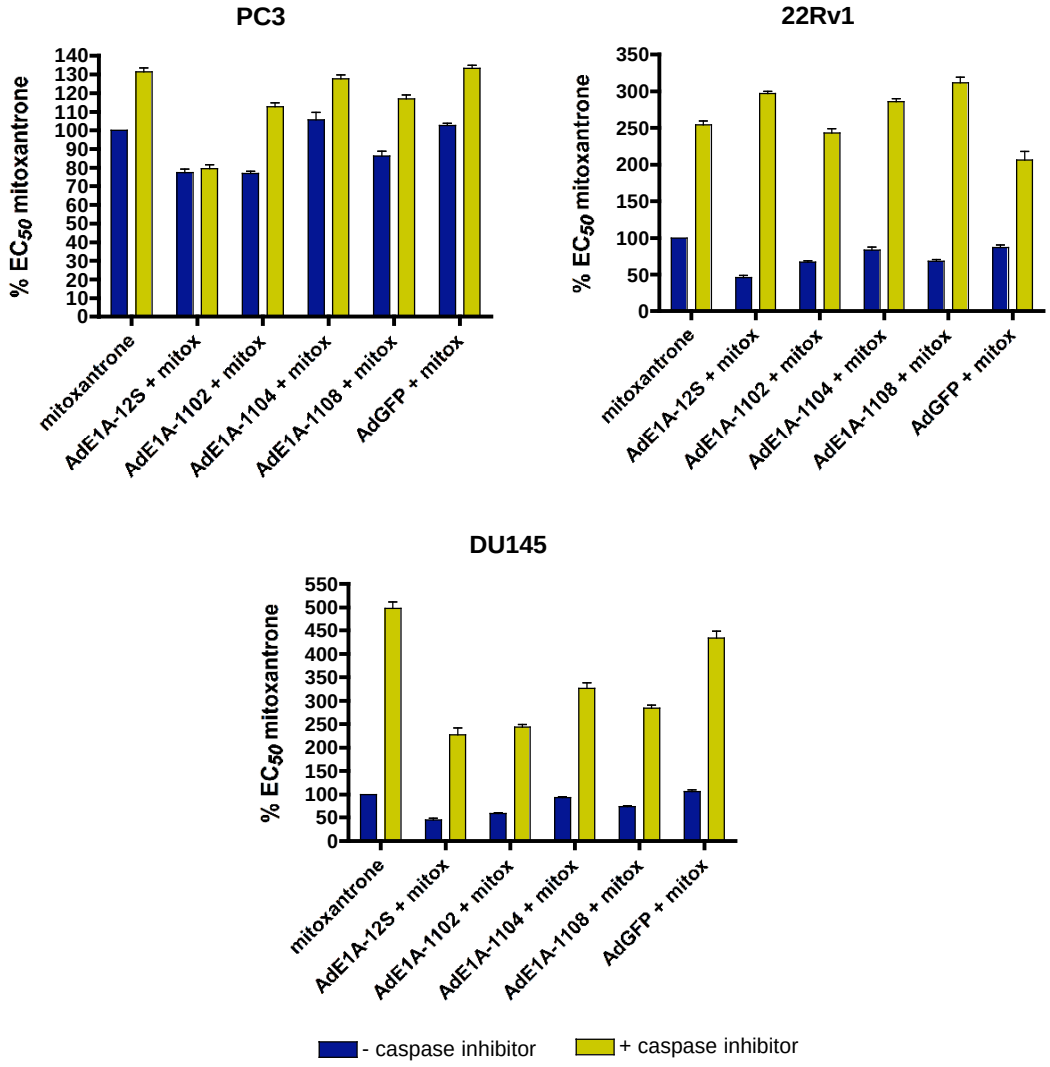


**Fig. 54.** Caspase inhibition by z-VAD-FMK at 25 μM protected human prostate cancer cell lines to mitoxantrone-induced cell death and reversed sensitisation by E1A-expressing viruses. Cells were treated with increasing concentrations of mitoxantrone in combination with each virus (2.5 ppc for 22Rv1, 10 ppc for DU145 and 100 ppc for PC3 cells) in the presence or absence of the caspase inhibitor. $EC_{50}$ values for mitoxantrone were calculates and expressed as a percentage of the $EC_{50}$ value for mitoxantrone alone. Bars represent the average and standard error of 2 independent experiments.

When mitoxantrone and viruses were combined the $EC_{50}$ value for the drug was reduced as seen previously (Fig. 40, Fig. 41, Fig. 42). However, when the caspase inhibitor was added the $EC_{50}$ values increased for all combinations, preventing sensitisation.

The increase in $EC_{50}$ value was different for each cell line. The PC3 cells showed the smallest increase in $EC_{50}$ of the three cell lines tested. The increase in $EC_{50}$ value in this cell lines was not higher than 40% in any combination and there was no increase in $EC_{50}$ value for mitoxantrone in combination with AdE1A-12S virus (Fig. 54). In 22Rv1 cells the $EC_{50}$ value for mitoxantrone was similar for the combinations with each virus in the presence of inhibitor, between 2.5 and 3 times the $EC_{50}$ value of mitoxantrone alone for all combinations. DU145 cells showed a big increase in $EC_{50}$ value for mitoxantrone when the inhibitor was combined with the drug up to 5 times higher in the presence of inhibitor (Fig. 54). There was also an increase in the $EC_{50}$ for all the combinations when treated with the inhibitor although, not as high as for the drug alone, with exception of the combination of mitoxantrone with AdGFP. Caspase inhibition increased survival in all condition; however, this increase was not as high for combination treatments as for durg alone. Therefore, E1A-mediated sensitisation was not uniquely caspase sensitive; other caspase independent mechanisms might be involved in sensitisation of prostate cancer cells by E1A.

## 6.6 Virus-induced cell death decreased after treatment with a caspase inhibitor.

The expression of E1A-12S by the replication-defective viruses at the doses used during sensitisation studies did not induce apoptosis, as determined by TMRE analysis. However, it is known that high expression of E1A can induce

apoptotic responses. Additional dose-response studies to the mutant viruses were performed in the presence or absence of the pan-caspase inhibitor to examine the potential activation of apoptotic pathways.

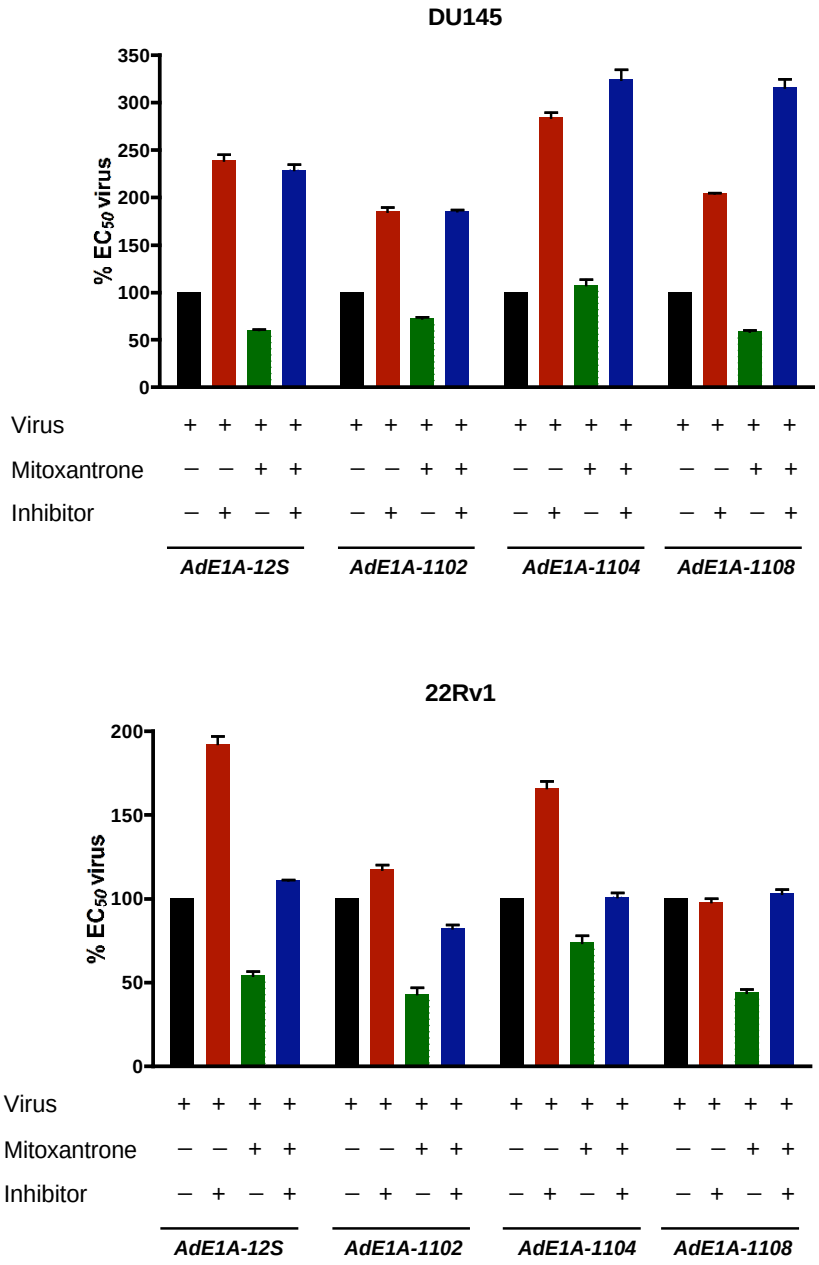


**Fig. 55.** Inhibition of caspase activity protected DU145 and 22Rv1 from virus-induced cell death and reversed mitoxantrone sensitisation to viral toxicity. Dose-response curves to each virus were constructed in the presence or absence of mitoxantrone at 50nM, z-VAD-FMK caspase inhibitor at 25 μM or both. $EC_{50}$ values were expressed as a percentage of $EC_{50}$ value for each virus alone. Presence of inhibitor protected DU145 cells to virus induced cell death by all viruses tested (red bars). An increase in $EC_{50}$ value in the presence of caspase inhibitor was only observed for AdE1A-12S and AdE1A-1104 viruses in 22Rv1 cells. The caspase inhibitor reversed sensitisation to virus by mitoxantrone, resulting in $EC_{50}$ values similar to virus and inhibitor in DU145 cells and to virus alone in 22Rv1 cells. Data represent averages with standard errors of 2 independent experiments.

In addition, cells were also treated with the viruses in the presence of 50nM of mitoxantrone, to determine whether an increase in $EC_{50}$ values would be observed in response to caspase inhibitor, similar to the findings with the mitoxantrone $EC_{50}$ values.

The $EC_{50}$ value for each virus tested increased in DU145 cells in the presence of inhibitor (Fig. 55), indicating that expression of E1A induced caspase activation. The addition of mitoxantrone reduced the $EC_{50}$ value for the virus in the absence of caspase inhibitor with the exception of the AdE1A-1104 virus. The addition of caspase inhibitor to the combinations of viruses and drug resulted in an increase of the $EC_{50}$ value for the virus to a value similar to the $EC_{50}$ value of the virus alone with inhibitor, except for the AdE1A-1108 virus that showed a greater increase (Fig. 55).

The effects observed in the 22Rv1 cells were different from those in the DU145 cells. The $EC_{50}$ values only increased for the AdE1A-12S and AdE1A-1104 viruses in the presence of caspase inhibitor while remaining the same for the AdE1A-1102 and AdE1A-1108 mutants (Fig. 55). $EC_{50}$ values for all viruses were reduced in the presence of mitoxantrone at 50 nM, indicating that mitoxantrone induced sensitisation to viral toxicity of all mutants. Addition of caspase inhibitor to the combinations resulted in increased $EC_{50}$ values compared to the combination treatment without inhibitor.

The values increased to a value similar to the $EC_{50}$ value of the virus alone, but never reached the $EC_{50}$ value of the virus in the presence of inhibitor, as observed in DU145 cells.

## 6.7 Expression of proteins involved in apoptosis changed during combination treatments.

The data presented supported the hypothesis of enhancement of apoptosis as a possible mechanism for chemo-sensitisation. Therefore, expression of proteins involved in apoptosis should be detectable by western blotting. Protein expression was analysis in the human prostate cancer cell lines PC3, DU145 and 22Rv1. Cells were treated with viruses and mitoxantrone in combination as previously described for the TMRE studies. Proteins were harvested 48h after treatment. Activation of caspase 3 was first analysed since previous data using a pan-caspase inhibitor showed inhibition of sensitisation. Pro-caspase 3 was expressed in all three cells lines in its inactive configuration, as pro-caspase 3 of 34 Kd. Cleaved caspase 3 was only detected at low levels in 22Rv1 cells (Fig. 56). Mitoxantrone as single treatment did not induced cleavage of caspase 3 at 48h in this cell line. Treatment with each AdE1A-12S mutant alone showed higher levels of cleaved protein than untreated cells. An increase in activated cleaved caspase was detected when mitoxantrone was combined with all mutants. Activation of caspase 3 was not detected in DU145 and PC3 cell with any treatment.

Expression of p53 was also analysed. Changes in p53 could only be studied in 22Rv1 cells since these cells express wild type p53. PC3 cells do not express p53 and DU145 cells express a non-functional p53 mutant. Expression of p53 in DU145 did not change with any treatment, showing levels of expression similar to untreated cells with any virus or combination with mitoxantrone (data not shown). Higher levels of p53 were observed 48h after cells were treated with mitoxantrone in 22Rv1 cells (Fig. 56). Infection with the replication defective adenoviruses also induced p53 expression, although AdE1A-1104 infection showed lower p53 levels than infection with the other mutants. This could suggest

a role of p300/CBP interaction with E1A in p53 stabilisation. AdGFP infection also increased p53 levels. Combination of mitoxantrone and viruses further increased the levels of p53 compared to virus or drug alone. The Bcl-2 protein was also detected in 22Rv1 cells expressed at high levels in untreated cells. Treatment with mitoxantrone induced a decrease of Bcl-2 that was also observed when viruses and drug where combined, with the exception of the AdE1A-1104 virus. Infection with this virus decreased BCL-2 expression, but it increased when this mutant was combined with mitoxantrone.

Another protein involved in cell cycle, p21, was studied in 22Rv1 cells. Although expression of this protein was high in untreated cells levels were

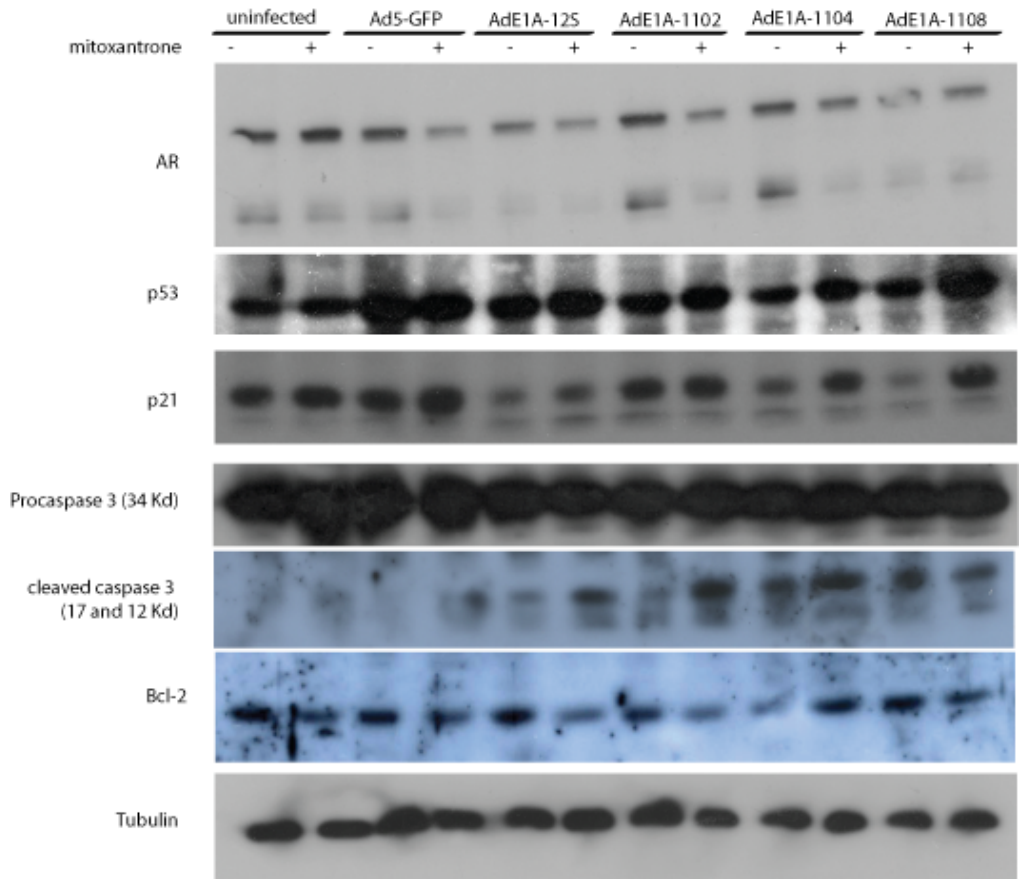


**Fig. 56.** Changes in expression of proteins regulating cell cycle and apoptosis in 22Rv1 cells. Cells were treated with mitoxantrone at 50 nM and AdE1A-mutants at 2.5 ppc for 48h.

increased 48h after treatment with mitoxantrone (Fig. 56). Infection of 22Rv1 cells with virus lowered the levels of p21 with the exception of AdE1A-1102. Combination of mitoxantrone and viruses resulted in levels of p21 similar to those of drug alone, with the exception of AdE1A-12S; p21 levels with this virus and mitoxantrone were higher than with virus alone but lower than the expression induced by mitoxantrone alone (Fig. 56).

It is known that E1A can antagonise the androgen receptor (AR); therefore, we analysed changes in the receptor levels to elucidate whether there was a relationship between E1A sensitisation and AR expression. The AdE1A-1102 and AdE1A-1104 mutants failed to downregulate AR expression, while the other E1A-mutant viruses decreased its expression. The AdE1A-1102 mutant successfully sensitised cells to mitoxantrone, indicating that AR interactions with E1A might not be involved in chemosensitisation.

# Chapter 7

## *Discussion*

The data presented in this thesis showed that interactions of the CR1 of E1A are essential for E1A-mediated chemosensitisation of prostate cancer cells. In addition, we also reported that deletion of the CR1 containing the p300-binding region attenuated viral potency, while modifications of the pRb binding site did not affect the toxicity, viral replication or E1A-mediated sensitisation of adenovirus. Sensitisation to mitoxantrone was also dependent on the status of the mutations within each cell line, as not all cell lines tested showed equal semnsitivity to mitoxantrone or docetaxel. We also observed that other viral genes could be involved in the sensitisation, as combination of drugs with viruses unable to bind p300/CBP resulted in sensitisation. However, the use of replication

deficient E1A-expressing viruses showed that E1A-mediated sensitisation requires the region binding to p300/CBP at the CR1. This could require interactions with p300/CBP or other unkown interactions with cellular proteins within the CR1 of E1A. The data indicates that E1A regions interacting with p300/CBP within CR1 should not be deleted for the design of adenoviral vectors for the treatment of prostate cancer.

Deletions of viral genes to confer cancer specificity to adenoviruses have been widely described (35, 44, 137, 142). The first adenovirus to be characterised was the dl1520 mutant, also known as ONYX-015 (183, 184). This virus did not express the E1B-55K protein that interacts with p53 to block p53-dependent apoptosis (41, 213). Hence, the hypothesis was that this virus would only be able to replicate in cells with mutated non-functional p53, a mutation of high occurrence in cancer cells. It was later shown by several groups that cancer specificity was not dependent on the p53 status of the tumour (185, 214, 215). In addition, deletion of the E1B-55K gene significantly attenuated viral potency (215, 216). Replicating adenoviruses with small deletions in E1A similar to those tested in this thesis were considered a promising alternative to achieve cancer selectivity without compromising viral toxicity. The replication selective viral mutants used in this thesis have been previously described (4, 139, 146). E1A mutations did not attenuate viral toxicity to levels similar to that of the *dl*1520 mutant. In fact, all replicating E1A-mutant adenoviruses tested in this thesis were as potent as Ad5, with the exception of the *dl*1101 and the *dl*1104 mutants that were attenuated compared to Ad5.

The attenuation observed for the *dl*1101 and *dl*1104 mutants could not be explained by a higher vp/pfu ratio, as all viruses tested showed similar ratios and consequently the specific deletions in E1A were responsible for the attenuated viral toxicity. These viruses are not able to bind p300/CBP complexes that are involved in activation of genes that regulate cell cycle progression and

differentiation (4, 146). In addition, the E1A-1101 protein does not bind the 26S proteasome (115), that results in longer half-life of this protein and failure to inhibit proteasomal degradation of cellular proteins such as p53. In fact, the *dl*1101 mutant does not stabilise p53, so no accumulation of p53 is observed in cells infected with this virus (100). This is because E1A must bind p300 to stabilise p53, so viruses unable to bind p300 fail to stabilise p53. Other reports have shown that E1A proteins produced by the *dl*1104 mutant are not stable and in consequence they are targeted for proteasomal degradation faster than wild type E1A (143). Even though we did not investigate protein stability or proteasomal degradation of E1A proteins in this thesis, we observed that levels of E1A-1104 expressed by a replication deficient virus were lower than those of the other E1A mutants tested. Although protein stability and proteasomal activity are important factors during adenoviral replication, attenuation of toxicity of these two viruses is likely caused by the loss of binding to p300/CBP complexes.

E1A-mediated transcriptional repression is essential for viral replication as it allows viral transcription and represses the expression of cellular genes that could interfere with the viral life cycle. Transcriptional repression by E1A-12S requires binding of E1A to p300 (93). Transient expression of p300 in combination with E1A does not completely restore transcriptional activity. More detailed studies have shown that both E1A-1101 and E1A-1104 fail to repress cellular transcription (92, 94). Single point mutations in amino acid residues 53 to 56, not present in E1A-1104, were sufficient to lose E1A binding to p300/CBP and transcriptional repression activity (93), suggesting that binding to p300/CBP is required to repress transactivation. Binding to p300 is also required to stabilise p53 and to induce p53-dependent apoptosis (3, 42). Disruption of MDM2-p53 complexes and acetylation of pRb by p300 are known to stabilise p53 and inhibit its degradation (78). We observed that replication of the *dl*1104 mutant in prostate cancer cell lines was influenced by their p53 status in the cells. This virus produced similar yields to Ad5 in the p53-null PC3 cell line and in DU145, which

expresses a non-functional p53. However, replication of this mutant in the p53 wild type cell line 22Rv1 was significantly reduced. These data is in agreement with the hypothesis that p53 stabilisation through p300 is an important requirement for efficient viral replication, although this interaction is not required in p53 negative cells (217, 218). In the presence of functional p53, E1A interactions with p300/CBP repress p53-dependent transcription. Transcriptional activation by p53 possibly induces the expression of pro-apoptotic genes that could decrease the efficiency of viral replication. In contrast, a deletion in the CR2 had no effect in either viral toxicity or replication of the virus. We also determined the level of replication of *dl*1102, *dl*1104 and *dl*1108 mutants in PC3, DU145 and 22Rv1 cells both by the $TCID_{50}$ method followed by viral genome quantification by qPCR, obtaining similar results. While these mutant viruses showed similar levels of replication in PC3 and DU145 cells, differences were observed in 22Rv1 cells. Viruses with mutations in the N-terminus of E1A, *dl*1102 and *dl*1104, showed an attenuated replication compared to Ad5 or the *dl*1108 mutant. The attenuation was more significant for the *dl*1104 mutant, indicating the importance of E1A-p300 interactions for viral replication. We also showed that disruption of pRb-E2F complexes by E1A does not play a role in adenoviral replication in prostate cell lines, as the *dl*1108 mutant was as effective as Ad5 in the three cell lines. It is possible that cellular mutations already present in these cell lines are sufficient to mimic the function of pRb-E1A interactions in the context of infection, while the repression of the transactivating activity of p300 is still a requirement for viral replication and toxicity.

During viral infection, p300 stabilises p53 and prevents its degradation, a function that has been demonstrated to play an important role in viral replication (3). Failure to stabilise p53 and inhibit its degradation through p300-E1A interactions could explain the attenuation in replication in *dl*1104. In addition, 22Rv1 was the only AR-positive cell line; there are reports that demonstrate a negative interaction between E1A and AR, with consequences for p300 activity

(25, 203). These reports showed that E1A represses AR-dependent transcription by indirect competition with AR activators. In addition AR negatively regulates p300, necessary for efficient virus-mediated entry into S-phase. Hence, AR interacts negatively with E1A and reduces viral replication. That hypothesis could also explain the attenuation of this virus and the lack of sensitisation in combination with chemotherapy, subject that will be discuss later in this chapter.

The murine cell lines TRAMPC and RM1 showed high resistance to viral toxicity as previously shown in numerous publications that murine cells were not as permissive to human Ad5 infection as human cells (219, 220). *In vitro* studies in several murine cell lines have shown good E1A expression after adenoviral infection followed by efficient viral DNA synthesis (219, 220). However, there are reports that late structural proteins were not efficiently expressed in murine cell lines and consequently viral assembly did not occur in these cells (219, 220). Although we did not further investigate viral gene expression and replication in the two murine cell lines tested, our data showed that Ad5 failed to replicate in murine prostate cancer cells. Detection of GFP in these cells after infection with a non-replicating GFP-expressing adenovirus, AdGFP, excluded the hypothesis that viral internalisation and transport to the nucleus was ablated in the murine cells. Although TRAMPC and RM1 cells were poorly infectable by AdGFP, poor infectability alone could not explain the complete lack of replication. The human PC3 cells showed similar low infectability to the TRAMPC and RM1 cells but Ad5 could efficiently replicate in these cells in contrast to the murine cells. Our studies showed that Ad5 could infect the murine cell lines but viral replication was impaired. However, these data do not elucidate whether lack of replication was due to lower expression of late viral proteins or reduced packaging of viral particles, as previously suggested.

In the context of adenoviral infection of prostate cancer cells, effects on androgen receptor and its interactions with E1A must also be considered. An

adenoviral mutant expressing a fusion protein E1A-AR was described as an alternative for targeting prostate cells and overcome AR-mediated decreases in viral replication (203). Our data showed that the AR positive 22Rv1 cell line was more sensitive to viral toxicity than DU145 and PC3 cells that are both AR negative. However, infection of 22Rv1 cells was more efficient than that of PC3 cells, possibly explaining the differences in toxicity. DU145 cells showed similar levels of infection to those for 22Rv1 cells, and differences in toxicity between these two cell lines were not as dramatic as those observed for PC3 cells. AR expression was determined after infection with replication deficient E1A-expressing viruses in the 22Rv1 cells. We observed that AdE1A-12S decreased AR expression, in agreement with previous studies showing negative regulation of AR by E1A (203). We also found that E1A deletions in the N-terminal region (AdE1A-1102 and AdE1A-1104 viruses) failed to downregulate AR expression in 22Rv1 cells. A correlation between downregulation of AR and viral toxicity was not observed since the replication-selective *dl*1102 mutant induced cell death to levels similar to those of Ad5. In addition, AdE1A-1102, replication deficient, showed similar toxicity to that of AdE1A-12S. We concluded that attenuated of toxicity of the E1A-1104 expressing viruses, both replicating and non-replicating, was not due to interactions with AR but to a failure to interact with p300/CBP.

Loss of AR expression has been associated with cancer progression and resistance to therapy; several groups have shown that this process might involve up-regulation of Bcl-2 in the absence of AR (7, 24, 203). We observed that the AR-negative cell line PC3 was more resistant to chemotherapy than 22Rv1 cells. However, 22Rv1 and DU145 showed similar resistance to both mitoxantrone and docetaxel. In addition, Bcl-2 was not detectable at basal levels in DU145 in spite of not expressing AR (205), indicating that sensitivity to cytotoxic drugs in prostate cancer cells might not only be associated with loss of AR and up-regulation of Bcl-2. Even though we did not observe a correlation between downregulation of AR and viral toxicity, it is possible that AR status plays a role

in sensitisation of prostate cancer cells to chemotherapy. Interestingly, AR regulation is associated with p300 expression; down-regulation of p300 in prostate cancer cells depends on the presence of functional AR (25). As the disease progresses, AR decreases and p300 increases, inducing transcriptional activation of survival genes (24, 25). It has been reported that loss of AR activity increased p300 expression resulting in failure to arrest cells in G2/M (203). We observed that the population of 22Rv1 cells arrested in G2/M after mitoxantrone treament was not as pronounced as in PC3 cells, possibly due to a reduction in AR expression that was observed after mitoxantrone treatment could have induced p300 activity that would interfere with the regulation of the G2/M checkpoint. Hence only E1A proteins able to bind p300 would be able to induce a further increase of cells in G2/M. In AR negative cells, like PC3 cells, this androgen-dependent regulation is absent, possibly contributing to a higher cycle arrest by mitoxantrone.

We constructed replication-deficient adenoviruses expressing different E1A-mutant proteins in order to identify the effect of E1A expression in the absence of other viral genes. Adenoviruses used as vectors for transient or stable transfection of the cancer prostate cell lines was not successful. Prostate cancer cell lines have previously been shown to be difficult to transfect (221). We also observed that transfection efficiencies was not higher than 30% with most of the reagents tested, even the Mirus TransIT reagent, specifically designed to transfect prostate cells. The great cell death rate observed during transfection and the loss of E1A expression after passaging the cells made it necessary to find alternative expression vectors. Cell death and loss of E1A expression was probably due to two reasons, the effects of the transfection reagents on the cells and E1A-induced cell death. In addition, transfected cells had a doubling time that was longer than untreated cells. Even though we observed good sensitisation by E1A-12S in transiently transfected cells, the problems associated with the expression system

made the assays unreliable. Similar effects were observed when retroviruses were used although we did not further explore why prostate cancer cell lines were so poorly transducible by retroviruses.

The use of replication deficient adenoviruses was a good alternative to induce E1A expression in prostate cancer cell lines. The use of replication deficient mutants lacking proteins involved in cell death inhibition or induction such as E1B or ADP respectively facilitated the study of E1A effects on cell death and chemosensitisation. In addition, expression of other viral early genes such as E4, are expected to be low as the E1A gene used for the construction of these viruses was based on E1A-12S cDNA, hence lacking the transactivation domain located in the CR3, only present in E1A-13S (42, 92). The time course and level of expression of E1A was comparable to that of Ad5-infected cells. An additional advantage was that expression lasted longer due to the regulation by the CMV promoter and not by a viral promoter that could be repressed during progression of the viral cycle. The sensitivity of all three human prostate cancer cell lines to these viruses correlated with that of the replicating viruses, with PC3 cells being the most resistant to viral toxicity and the 22Rv1 cells the most sensitive. Similar to replication-selective viruses, the E1A-1104 expressing virus was less cytotoxic while the other mutants had similar toxicity. In any case, $EC_{50}$ values for these viruses were higher than for Ad5 and replication studies using the $TCID_{50}$ method confirmed that AdE1A-mutants failed to replicate in the cell lines. This indicated that E1A-mediated apoptosis was most likely the cause of cell death. However, qPCR analysis of hexon DNA amplification showed that the amounts of hexon increased over time for AdE1A-1102 and AdE1A-1108 viruses. It is possible that some recombination occurred during the production of these viruses, integrating E1B and possibly other E1A sequences in some viral particles. The recombination was low as E1A sequencing of these viruses showed that they were both expressing the correct E1A gene respectively, and E1A-13S sequences were not detected. To corroborate these results, we checked the presence of E1A in our

virus stocks. E1B was amplified at very low levels in these viruses when more than 35 PCR cycles were used. Recombination with the packaging cell line HEK293 is a difficult problem to avoid for replication-defective viruses; further purification of viruses or alternative production techniques might be necessary for other experimental settings or in a clinical trial situation, but we did not observe any effect on cell death or replication at the viral concentration used for our sensitisation studies. In addition, we can confirm that recombination was minimal, as otherwise the replicating properties of recombined viruses would have given a much lower $EC_{50}$ value as a result of replication and spread to neighbouring cells.

Since E1A expression has been associated with the induction of apoptosis (131, 222), we hypothesised that cell death observed with the AdE1A-mutant viruses was due to activation of apoptosis. Our toxicity data for replication deficient viruses in Chapter 5 indicate that E1A-mediated apoptosis is highly dependent on binding to p300/CBP, but not to pRb. E1A-mediated induction of apoptosis might be impaired due to the instability of this mutant protein, as previously discussed, or due to a lack of the repressional activity of E1A-p300/CBP complexes. E1A-mediated apoptosis was thought to occur through activation of p53 after release of E2F (75, 78, 223). However, other studies have shown that induction of apoptosis by E1A can be p53-independent in pRb positive and negative cells (26, 83, 138). The proposed mechanism for E1A induced apoptosis involves activation of PUMA by p53-independent pathways (85). Sp1 and different isoforms of p73 have been described as positive regulators of PUMA in p53-null cell lines (224, 225). PUMA is activated by p73 in a process that requires activation of Sp1, known to interact with p300. In addition p73 is regulated by Abl, although it can also be phosphorylated by Scr, known to interact with CR2 (130). It is possible that apoptosis can be induced by mechanisms involving p300 and/or pRb binding of E1A and that the pathway triggered after E1A expression depends on host balance of the proteins related to these pathways.

The mechanisms involved in E1A-mediated apoptosis could also be responsible for the sensitising properties of E1A proteins to chemotherapy and radiotherapy. We studied combination of viruses with two different drugs commonly used in prostate cancer treatment, mitoxantrone and docetaxel. These drugs have different mechanisms of action; mitoxantrone binds to DNA and inhibits topoisomerase II, while docetaxel is a microtubule-binding agent. There is extended evidence that E1A can sensitise cancer cells to DNA damaging agents (89, 147, 150, 151, 157, 225-227); however, reports of interactions between E1A proteins and drugs with alternative mechanisms are contradictory. Our data showed that sensitisation of prostate cancer cell lines was efficient to both drugs used, although sensitisation to mitoxantrone was in all cases greater than to docetaxel. The interactions between virus and drugs were also cell line dependent but was not related to sensitivity to chemotherapy. PC3 cells were more resistant to both drugs and viruses than the other cell lines tested and yet showed better synergistic interactions in combination studies with replication selective adenoviruses and mitoxantrone. In contrast, antagonistic interactions were observed in 22Rv1 cells, despite being more sensitive to virus and drug toxicity when administered alone.

Sensitisation was also dependent on the doses of both virus and drugs since no sensitisation was observed in 22Rv1 and PC3 cells when fixed concentrations of viruses and mitoxantrone were used but strong reduction of $EC_{50}$ value for the drug was observed in combination with fixed concentrations of virus in both cell lines. Nevertheless, viral toxicity was higher than expected in the 22Rv1 cell line, possibly because these cells were already very sensitive to viral infection and small changes in viral dilutions or the cellular status at the time of infection could influence the final toxicity outcome. In contrast, TRAMPC cells could be successfully sensitised when treated with two fixed concentrations of both drug and viruses, despite a lack of significant synergistic interactions or reduction of EC50 value for the drug in other combination assays.

Interestingly, the combination of Ad5 with mitoxantrone and docetaxel significantly affected viral gene expression. Hexon expression could be detected by western blot at 24h only in combination treatment of Ad5 and docetaxel in DU145 and PC3 cells and also with mitoxantrone in PC3 cells but not in cells treated only with the virus. In addition, E1A mRNA levels increased in combination with mitoxantrone in PC3 cells. Infection with a non-replicating AdGFP virus showed that the number of infected cells increased significantly after 24h in the presence of mitoxantrone at 50 nM only when virus was not removed. Therefore we hypothesised that mitoxantrone increased the infection rate over time. A 2h infection with AdGFP did not change the percentage of infected cells, meaning that when using a replicating virus such as Ad5, once the first replication cycle is complete and new viral particles are released, more cells will be infected or a higher number of particles will enter each cell. However, we did not observe an increase in replication in the presence of drug. Further experiments are needed to fully understand the increase in infectability without an increase in replication, but we could hypothesise that the toxicity of the drug reduces the number of cells in which replication can occur. Hence, despite increasing the infectability of the cells, there would be less living cells available for further viral infection and replication. This would be further enhanced by the sensitising and bystander effects of E1A that in turn would sensitise both infected and uninfected cells to the actions of the drug. It is also possible that the molecular changes after drug treatment affect viral packaging or other late processes.

Changes in E1A expression after viral infection in combination with mitoxantrone were very significant when using replication defective viruses expressing E1A. We observed a higher expression of E1A when virus was not removed. When we compared E1A mRNA levels in these samples with those infected with AdE1A-12S virus for 2h, we observed that E1A mRNA levels only

increased if the virus was not removed after 2h. Because AdE1A-12S did not replicate, we concluded that mitoxantrone induced an increase in infectivity over time that could not be observed if virus was removed, as previous infectivity assays describe. This indicates that mitoxantrone increased viral uptake by the cells; changes induced by mitoxantrone that favour infectivity must take more than two hours to occur.

Other members of our team have reported that CAR levels are induced after mitoxantrone or docetaxel treatment, while integrin expression did not change (S. Radhakrishnan, manuscript in preparation). This unpublished data is in agreement with the increase in infection described in this thesis. These findings could have relevance in the administration of combination therapies as they suggest that pre-treatment with mitoxantrone or docetaxel could improve the infectivity of prostate cancer cells. This could also improve sensitisation to the drug by E1A, as higher E1A expression would induce sensitisation the drug through bystander effects. Members of our team have shown that pre-treatment of cancer cells with mitoxantrone did not induce better synergistic interactions or influenced viral replication (S. Radhakrishnan, manuscript in preparation). However, we must consider that pre-treatment with mitoxantrone also induced cell death, so even if treated cells were more infectable the number of viable cells prone to infection was reduced by the action of the drug.

Our results with replication-defective adenoviruses expressing E1A-mutant proteins showed that E1A-1104 protein failed to sensitise prostate cancer cells to mitoxantrone or docetaxel. This mutant was also unable to induce and increase G2/M arrest or changes in mitochondrial membrane potential in combination with mitoxantrone compared to drug alone. Cell death observed during these sensitisation studies was caused by induction of apoptosis, as demonstrated by an increase in pro-apoptotic cells by TMRE staining. In addition, inhibition of caspase activity protected prostate cancer cell lines to mitoxantrone-

induced cell death and to viral sensitisation. Based on the expression profiles of the cell lines used, we hypothesise that induction of apoptosis was independent of p53 status in PC3 and DU145 cells but not in 22Rv1 since this is the only cell line expressing functional wild type p53. In this cell line, total p53 levels were increased after infection with the replication defective E1A-expressing mutants AdE1A-12S and AdE1A-1102, both able to bind pRb and p300/CBP. However, increases in p53 were not as high with the AdE1A-1108 and AdE1A-1104 and it is likely that these mutants did not stabilise p53 as efficiently as AdE1A-12S or AdE1A-1102. E1A interactions with pRb can upregulate p53, so less p53 could be expected after expression of E1A-1108, and a second interaction of E1A with p300/CBP further stabilises p53 (83, 99, 100, 223). Possibly, E1A-1104 and E1A-1108 are less effective at stabilising p53 due to the deletions in the binding site of either cellular factor. The p53-antagonist Bcl-2 protein was decreased in the presence of mitoxantrone and when combined with all mutants with the exception of AdE1A-1104. The lack of sensitisation by the AdE1A-1104 virus in this cell line could partially be due to Bcl-2 antiapoptotic properties. It is possible that the downregulation of antiapoptotic proteins like Bcl-2 is involved in sensitisation; the E1A-1104 was not able to downregulate the levels of Bcl-2 in the presence of mitoxantrone, partially explaining why we did not observed supra-additive effects after the combination of this mutant with the drug.

Toxicity of AdE1A-12S mutant viruses was due to activation of apoptosis, as inhibition of caspases significantly attenuated viral toxicity. However, the viral doses used for sensitisation studies did not induce apoptosis and mitochondrial depolarisation, therefore we suggest that E1A expression upregulated mitoxantrone-induced apoptosis. The main cellular proteins involved in E1A-mediated regulation are pRb and p300/CBP. We did not find any relationship between the pRb pathway and the enhancement of apoptosis during combination treatments, not only because the AdE1A-1108 virus does not bind pRb, but also because good sensitisation was observed in DU145 despite the lack

of pRb expression in this cell line. Sensitisation by E1A-12S was thought to be dependent on pRb binding and consequent release of E2F (138). This would activate several transcription factors, resulting in p53-dependent apoptosis. Previous studies showed that induction of apoptosis by E1A-12S and sensitisation to chemotherapy and radiotherapy were independent of binding to pRb (126). Additional studies demonstrated that even though dissociation of pRb-E2F complexes is mainly through E1A sequestering of pRb, transcriptional activation of E2F1 is also dependent on binding to the N-terminus of CBP. E1A can also stimulate E2F1 transcription by directing CBP to the E2F promoter although this activation has only been demonstrated *in vitro* (103). Regulation of E2F1 transcriptional activity is regulated by acetylation mainly by CBP and, to a lesser extent by p300, through a mechanism that is negatively regulated by pRb (103). E2F release from pRb has also been described after expression of E4-6/7 adenoviral proteins (47).

Binding of p300/CBP to E1A is also known to be the mechanism responsible for the observed downregulation of p21 induction after p53 stabilisation, proposed by some groups as a mechanism for the induction of apoptosis in DNA-damaged cells (42, 89). Our data, however, demonstrate that it is possible to enhance drug-mediated apoptosis independently of p21 inactivation in prostate cancer cell lines. E1A can regulate p21 activity by direct or indirect interactions with TRRAP and p400 (106). We observed that p21 levels did not decrease after infection with AdE1A-1102 that is unable to bind p400 although no effect on sensitisation was detected. We should consider that p21 is mainly involved in cell cycle arrest and senescence (41) by inhibiting cyclin E/cdk2 (103). This cannot be considered a survival mechanism since under those conditions survival pathways are inhibited and cell viability is compromised. Another issue to consider when investigating apoptosis induction is the host status. Interaction of p400 and myc have been reported to induce apoptosis (113), however, myc is commonly deregulated in cancer cells and so is the regulation of

cyclin dependent kinases controlling cell cycle checkpoints (228). More importantly, E1A expression also influences expression of cyclins and cdks to force entry into S-phase (3, 42, 222). Cyclin E/cdk2 are negative regulators of p300, providing a checkpoint that regulates the G1/S transition (103). Interestingly, other groups have proposed that cyclin E/cdk2 can phosphorylate CBP and increase HAT activity, as observed when bound to E1A (103).

It was suggested that p400 binding was required for sensitisation, as myc–defective cell could be lines less efficiently sensitised by E1A, due to reduced expression of caspase-7 (113). However, myc expression is regulated by E1A through p400 interaction, possibly to overcome cycle arrest (42). Myc expression is often deregulated in cancer cells, so E1A interaction with p300/CBP and p400 might be more important to control the different cell cycle checkpoints after infection than interactions with p400.

In order to postulate a hypothesis that is in agreement with our observations, we must consider the effects of the drugs on the prostate cancer cells tested and how sequestering of p300 by E1A can enhance them. Mitoxantrone is a drug classified as a topoisomerase II inhibitor and a DNA-intercalating agent that induces DNA damage by DNA double strand break (13). There is evidence that E1A can regulate the activity of the topoisomerase II promoter in E1A-expresing cells (229) and that topoisomerase I is increased in cells infected with *dl*922-947 or Ad2 (230). In addition, exogenous expression of topoisomerase II can sensitise cells to topoisomerase II inhibitors such as etoposide (231). It is then likely that E1A-sensitisation of prostate cancer cells to mitoxantrone was caused by upregulation of topoisomerase II after infection and that the process requires binding of E1A to p300/CBP. The use of the topoisomerase II inhibitor TAS-103 in a range of cancer cell lines showed that susceptibily to this inhibitor was dependent on p300 expression and that over-

expression of p300 sensitised these cell lines to TAS-103 but not to cisplatin (232).

One protein that has been described to play a role in topoisomerase II transcriptional activation and E1A expression is p38 (233). This protein belong to the family of mitogen-activated protein kinases, involved in both proliferative and apoptotic activities. Inhibition of p38 by the specific inhibitor SB203580 correlated with a decrease in topoisomerase II expression (233). Activation of p38 also occured during late G2/M phase by topoisomerase II and histone deacetylase activity, inducing the inhibition of the cdc25B phosphatase and phosphorylation of cdc2; this results in a decrease of cyclin A/cdk2 and arrest in G2/M (234, 235). It is well known that E1A alters host HDAC activity and mitoxantrone inhibits topoisomerase II (13), hence it is reasonable that during combination therapies of these two agent we observe G2/M arrest as a consequence of p38 phosphorylation and a decrease in p300 activity. Our data showed that when sensitisation to mitoxantrone was successful with replication-deficient viruses, a higher proportion of cells were arrested in G2/M. In contrast, AdE1A-1104 in combination with the drug showed the same cell cycle profile as cells treated only with mitoxantrone. It is possible then that E1A-p300/CBP complexes increase HAT activity, accompanied by a repression in HDACs, to stimulate p38-dependent G2/M arrest. Failure of the E1A-1104 protein to sequester p300/CBP would result in a failure to overcome G2/M arrest, as we have observed. When it comes to cell cycle analysis, we must also consider the effects that E1A could have in progression through it; it is well established that E1A promotes entry into S phase, and alters the cyclin/cdks balance to favour viral replication (3, 41, 42, 222); those effects could interfere with the arrest induced by mitoxantrone. However, no effect on the cell cycle was observed under the condition used in this thesis, so we conclude that alteration in cell cycle distribution is a consequence of drug treatment and E1A-mediated sensitisation to this treatment.

Combination of replication deficient adenoviruses expressing E1A-mutant proteins with mitoxantrone in the presence of the broad pan-caspase inhibitor z-VAD-FMK resulted in abrogation of E1A-mediated sensitisation and protection against mitoxantrone-induced cell death. Similar effects were observed when a sub-optimal concentration of the drug was combined with different viral concentrations. This suggested a strong interaction of the caspase pathway in the cell death observed. However, cleavage of caspase-3 was weakly observed in 22Rv1 cells and not detected in DU145 and PC3 cells, even though procaspase-3 levels were slightly decreased. It would be interesting to detect caspase-3 activation by more sensitive methods, such as flow cytometry with specific antibodies, to further elucidate the involvement of caspase-3 in mitoxantrone-induced cell death. The levels of active caspase-3 detected in 22Rv1 cells were similar in all combinations, including the sensitisation-deficient mutant AdE1A-1104. However, the changes in mitochondrial transmembrane potential strongly suggest that this mutant failed to increase the proapoptotic effects of mitoxantrone. Low levels of transmembrane potential lead to cytochrome c release and consequent caspase activation, leading to apoptosis (236). However, mitochondrial transmembrane potential can be altered by other mechanisms, such as increases in K+ permeability not related to apoptosis (236).

We should consider the possibility that mitochondrial activation of apoptosis could be both caspase dependent and independent; recent findings have shown that apoptosis induced after excision of chromatin loop domains upregulates caspase-independent apoptosis, involving topoisomerase II, p38 and mitochondrial loss of potential (235). In this model, DNA cleavage would activate p38 that would induce BAX translocation to the mitochondrial membrane, reducing its permeability. This would favour the release of apoptosis inducing factor (AIF) and the formation of a positive feedback loop with topoisomerase II, inducing apoptosis in a caspase-independent manner. This would also allow the release of cyt c and activation of caspase-dependent apoptotic pathways that

would work in parallel with caspase-independent pathways. These researchers proposed a model in which caspase-dependent apoptosis is dispensable in the apoptotic pathway associated with the excision of DNA loop domains, but not when internucleosomal DNA fragmentation occurs. Interestingly, caspase-2 is regulated by topoisomerase I and II and it is involved in G2/M checkpoint arrest (237, 238), although it has been shown to have both pro- and anti-apoptotic effects, which could partially explain the antagonism observed between topoisomerase II inhibitors and other chemotherapeutic agents (14).

The antiapoptotic Akt protein, also known as PKB, is also involved in p38 regulation (156). Decreased Akt phosphorylation has been demonstrated after chemotherapy-induced apoptosis with agents like cisplatin and taxol (155, 156, 205). In all cases, downregulation of Akt correlates with activation of p38, PARP cleavage and caspase activation. Akt activity is downregulated by removal of phosphate groups by PTEN and PP2A/C, both enzymes having recognised tumour-suppressive functions (155). Good correlation has been observed between PTEN/Akt status of prostate cancer cell lines and their resistance to chemotherapy (205); PC3 cells express non-functional PTEN and have been described to be more resistant to taxol and cisplatin than other cell lines (205). Our data with docetaxel and mitoxantrone is in agreement with this hypothesis, as PC3 cells were more resistant to these agents than the other cell lines tested.

Other groups have shown that upregulation of PP2A/C is required for chemosensitisation and that its activity is significantly increased in E1A stable-transfected cell lines (155). However, these changes in host proteins that induce chemosensitisation are not similar in the context of a replicating adenovirus. Even though PP2A/C and p38 activation and subsequent Akt dephosphorylation have been documented in E1A-transfected cells, opposite results were observed when replicating viruses were used (239). E4-ORF1 and E4-ORF4 viral genes can actually control activation of the MEK/ERK pathway and replication seems to be

dependent on it (47, 51, 240); use of ERK inhibitors results in decrease of replication in Ad5-infected cells. Control of this pathway is probably upstream of ERK, as the E4-ORF4 region can specifically bind to PP2A and reduce its functions, hence increasing activated Akt and ERK1/2 that will activate the mTOR and MAKP signally pathway (240). Viral mutants unable to bind PP2A failed to phosphorylate p70S6K, downstream of ERK, impairing S-phase entry. Under this condition, viral protein expression and viral production was decreased by 50% (240). Involvement of ERK1/2 in viral replication could partially explain the resistance observed in PC3 to viral toxicity and replication, as p-ERK1/2 is not detected in PC3 cells (205). Lack of p-ERK in these cell lines could also account for the sensitisation observed in spite of their known resistance to chemotherapy, as lack of activated ERK would have a downstream effect on p38, increasing its activity.

MAPK is also relevant in p300/CBP upregulation of HAT activity. CBP is associated in vivo with ERK1 and phosphorylated by ERK2 to induce HAT activity, possibly mediating the ability of CBP to mediate the transcriptional activity of Elk1 (103). There is also strong evidence of increased phosphorylation of p38 in E1A-expressing cell lines that promotes phosphorylation by activated p38 of several transcription factors that bind to p300/CBP and E1A, such as CREB, Sp1, c-Fos, c-Jun and Elk-1 (241, 242). E1A and E4 possibly regulate the activity of all these transcription factors to ensure efficient viral replication (47).

It seems as if E1A-induced changes in cellular pathways are different and opposite to viral replication; one example of this is the strong induction of proapoptotic signals observed during E1A expression, including p53 stabilisation and p21 activation. However, these alterations are later counteracted by other viral genes such as E1B. A similar mechanism could involved the MAPK family of proteins; E1A could induce activation of MAPK-dependent pro-apoptotic signalling in a similar fashion to p53 stabilisation, to repress other cellular

pathways that might reduced efficiency of replication. At the same time, the balance of E1A-12S and E1A-13S levels could be important, as E1A-12S lacks the transactivation domain and hence is involved in transcriptional repression, while E1A-13S favours transcription (93, 243). The CR3 domain, unique in E1A-13S protein, binds to several transcription factors to allow successful transcription of viral proteins and the host proteins needed for viral cycle progression. This domain might actually be essential for efficient activation of the MEK/ERK pathway, as other groups have shown that the induction of Akt phosphorylation and PI3K pathway is only observed in E1A-13S-transformed cells, but not when E1A-12S was used (244). If E1A-12S expression maintain p-Akt at lower levels than E1A-13S, then E1A-mediated sensitising combination therapies should be designed with E1A-12S viruses for those drugs affecting this cellular pathway.

Interestingly we observed that synergistic interactions between mitoxantrone and AdE1A-12S obtained lower CI values than combinations of the drug with Ad5. Taking into account that combinations with a replicating virus also resulted in virus-induced cell death, we expected synergy with a non-replicating virus to be less efficient *in vitro*. The results observed could be explained by several factors. First, the replication deficient virus only expressed E1A-12S, inducing a stronger transcriptional repression than Ad5. Secondly, E1A-12S was constantly expressed after infection while E1A in Ad5-infected cells was expressed in the context of viral cycle progression. Last, we must also take into consideration that the bystander effects of E1A expressed by AdE1A-12S were possibly greater due to constant strong expression in infected cells. In order to obtain a low CI value both virus and drug must work in synergy with one another; in most cases when replicating viruses were used, EC50 value decrease for the drug was observed, but virus dose-response curve were less affected in each combination. This indicates that viral toxicity is not greatly affected by combination with drugs, but viral proteins sensitised cancer cells to the apoptotic actions of the chemotherapy.

The improvement in the synergistic interactions was greater for mitoxantrone than for docetaxel, possibly because E1A can better sensitise cells to apoptotic pathways that are upregulated by mitoxantrone but not by docetaxel. Docetaxel is a taxane that bind to ß-tubulin monomers by stabilising microtubules and arresting their depolymerisation (17). This leads to inactivation of Bcl-2 and apoptosis. It has also been proposed that docetaxel induces cell death through a mechanism different from apoptosis termed mitotic catastrophe that is dependent on caspase-2 activation (17, 238, 245). If docetaxel-inducted cell death was triggered by the same caspases as mitoxantrone, we would expect similar sensitisation to the taxane as to the DNA-damaging agent. Although we observed sensitisation to docetaxel, the viral concentration needed was higher than for mitoxantrone. In addition, synergy between AdE1A-12S and docetaxel was not as efficient as with mitoxantrone. We also observed that E1A-1104 failed to sensitise prostate cancer cells to docetaxel. So it is possible that the mechanisms underlying E1A-mediated sensitisation are similar for both DNA-damage and cytostatic agents and that both agents activated similar proapoptotic proteins that target different signalling pathways. Maybe this only applies to mitoxantrone, as one report indicates that mitoxantrone could inhibit microtubule assembly in addition to its known DNA-damaging properties, being a drug that works by two distinctive mechanisms (15). Caspase-2 would be a good candidate to regulate the apoptotic processes with both drugs; apoptosis induced by cytoskeletal disruption is highly dependent on caspase-2 activation of the mitochondrial apoptotic pathway, as caspase-$2^{-/-}$ cells are resistant to taxane-induced cell death (245). This would induce translocation of Bax, release of cyt c and upregulation of caspase 10, 9, 8 and 3, as described after docetaxel or taxol treatment. Topoisomerase II inhibitors, on the other hand, can activate caspase-2 dependent apoptotic pathways in both a cytochrome c dependent and independent manner (235). We hypothesise that E1A can upregulate both mechanisms, although it might be more efficient at sensitising cells to drugs affecting apoptosis involving

DNA-damage. In addition, little is known about the effects in tubulin and cytoskeleton during combination treatments; tubulin expression is downregulated after adenovirus infection and tubulin specific chaperones are upregulated (246), possibly promoting tubulin degradation. In addition, the cytoskeleton shows changes in configuration after infection that could alter, positively or negatively, the effects of cytostatic agents.

These findings have implications in the future design of adenoviral vectors for prostate cancer therapy. The E1A mutations chosen to design new viruses should retain the CR1 region binding to p300/CBP in order to maintain the sensitising potential of E1A, in addition to retaining the same toxicity as Ad5 in cancer cells. On the other hand, viruses unable to bind the pRb family members are a better option, as they maintained sensitising potential and viral toxicity similar to Ad5. These results also suggest that the use of DNA-damaging agents in combination with adenovirus therapy may be more efficient than the use of cytostatic drugs, as these did not synergise with viral therapy as efficiently as DNA-damaging agents. We also showed that mitoxantrone treatment increased the infectability of the cells, and future work will aim to investigate the advantages of drug treatment prior to adenoviral infection, in order to maximise the number of infected cells. Further research will also aim to elucidate the role of other viral genes in sensitisation; a careful examination of the effects of viral gene expression on chemosenstitisation would lead to the construction of much more efficient viruses for the use in the clinic.

# Chapter 8

## *Future directions*

The data discussed in this thesis show that binding to p300/CBP is essential to efficiently sensitise prostate cancer cell lines to both mitoxantrone and docetaxel. The great number of differences in the survival and apoptotic pathways in the cell lines tested helped us identify that E1A binding to p300/CBP sensitised prostate cells by p53 and pRb independent mechanisms. Further research is needed to identify the molecular mechanisms of the observed sensitisation. The molecular changes after drug treatment must be better understood, together with the involvement of p300/CBP. Based on the literature and the available evidence discussed in the previous chapter, the effects of the combination treatment on certain promoters, like the topoisomerase II promoter, involves cofactors such as Sp1 that are modified and regulated both by p300/CBP and the p38 pathway, also suggested to be involved in sensitisation. It would be interesting to use new E1A mutants deleted in the CR1 domain binding to pRb, to fully understand the involvement of pRb in sensitisation of pRb-positive cells and alternative mechanisms of sensitisation in cells with mutated pRb. Understanding how E1A regulates the transcription of cellular factors could also determine why

sensitisation to mitoxantrone was more effective than to docetaxel. As discussed previously, this could be due to a double sensitisation by E1A in combination with mitoxantrone, both at apoptotic pathways and at the promoter level of genes that are not affected by docetaxel treatment. The identification of the mechanisms of sensitisation to DNA-damaging and cytoskeleton disruption agents could lead to the discovery of common targets of E1A and the design of therapies that maximise sensitisation by targeting those proteins.

The cancer specificity of the E1A-deletion mutants should be further analysed. The data in this thesis has focused on the sensitising abilities of the different E1A mutations. However, in order to use these findings for the construction of new viruses, we must assess the impact of the E1A modifications on replication and toxicity in normal cells. We observed that E1A-1102 and E1A-1108 retained the sensitising ability of wild type E1A, but further research should elucidate whether one of these mutations confers better cancer selectivity in the context of a replicating virus. Replication and toxicity of the replication selective E1A-mutant adenoviruses used in this thesis should be evaluated; this would allow the determination of the optimal E1A mutation for the construction of new replicating viruses for prostate cancer treatment. In addition, the sensitising abilities of these E1A-mutant proteins should also be compared *in vivo*. The use of the replication deficient viruses in animal models night not result in significant tumour regression, since these viruses do not replicate and viral particles could also be rapidly cleared. However, in combination with chemotherapy, we might obtain interesting results even in the absence of replication as previously shown (145). We must consider these viruses as a tool to understand the effects of E1A both *in vitro* and *in vivo*, rather than good candidates for the use in the clinic. Nevertheless, new evidence from *in vivo* studies together with data from normal cells would be useful to finally choose the best E1A mutations for evaluation in the clinic.

New replication-selective adenoviruses could then be constructed expressing the selected E1A mutant. In addition, the same mutant could be inserted as a transgene to obtain expression of E1A at a late phase of infection. We observed that synergy with both docetaxel and mitoxantrone was more efficient with AdE1A-12S than with replication competent viruses. This suggest that a constant expression of the E1A mutant, not controlled by the self-regulation of E1A during the early phase of infection, might be more efficient at sensitising prostate cancer cells. Hence, the expression of E1A as a transgene could improve the sensitising efficiency of replicating viruses. The construction of viruses overexpressing E1A would imply new research to fully determine the consequences of E1A expression as a transgene. These viruses should be characterised: analyse the effect of E1A in replication, their toxicity and sensitising abilities *in vivo* and *in vitro*, compared to the already available E1A-mutated replication selective and defective viruses.

The data presented in this thesis and the future work that would arise from it will contribute to a more efficient design of adenoviruses for the treatment of prostate cancer, maximising toxicity, selective replication and sensitising potential.

# Chapter 9

# *Appendix*

## 9.1 PCR verification of the viruses used in this thesis.

The following figures show the PCR products of E1A, E1B and E3 in the viruses used in this thesis. E1A was amplified in all viruses to check size compared to Ad5 E1A. An E1B fragment was amplified to check presence of this gene in the replication competent viruses and its absence in the AdE1A-mutant viruses. In addition, the deletion in the *dl*1520 mutant is reflected by a small size of the amplified product. Amplification of E1B in AdE1A-1102, AdE1A-1104 and AdE1A-1108 was observed after 35 cycles of PCR. The band obtained was fainter than that obtained for the replication competent viruses. It is possible that recombination between the viral plasmid and the HEK293 cells genome took place, resulting in a small proportion of virus carrying E1B. The AdE1A-1102 and AdE1A-1108 viruses showed defective replication and a toxicity similar to AdE1A-12S, what suggests that if recombination took place, it only resulted in a minor proportion of virus carrying E1B. A fragment of the E3 gene was also amplified to check the absence in the AdE1A-mutants.

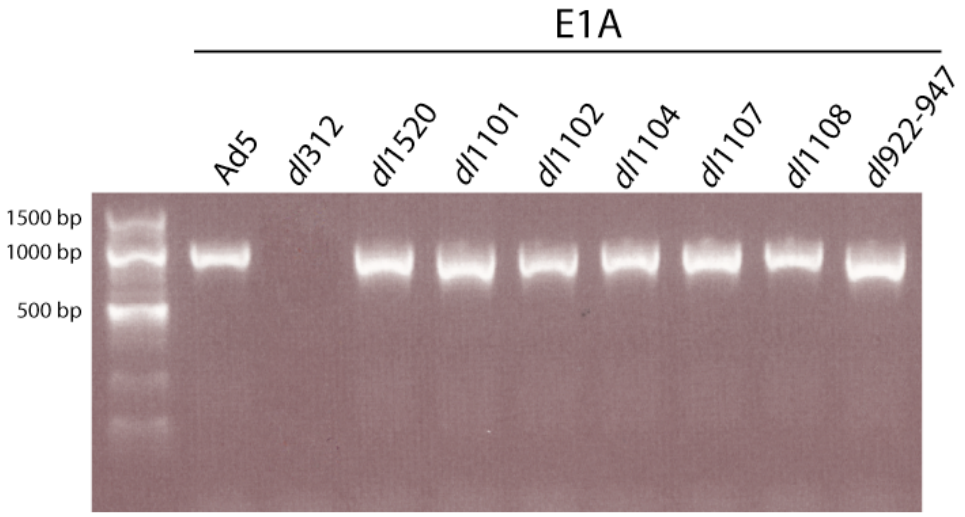


**Fig. 57.** E1A PCR amplification for each replication competent E1A-mutant vadenovirus. As expected, the *dl*312 mutant did not show any band for E1A and the mutant viruses showed bands smaller than that of Ad5, as these mutants only expressed the E1A-12S protein and not E1A-13S. PCR was run as described in materials and methods using primers for the whole E1A gene; the sequence of the primers can be found in the materials and methods chapter.

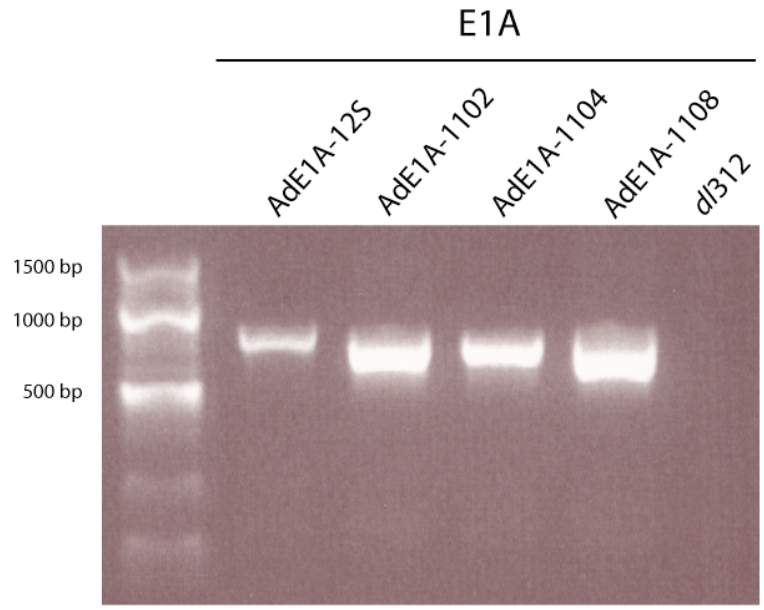


**Fig. 58**. E1A amplification on AdE1A-mutant viruses. The AdE1A-12S virus contained a bigger E1A fragment, as it carried the whole E1A-12S cDNA without any deletions. The E1A DNA amplified on the other viruses was slightly smaller than the band for AdE1A-12S. This indicated the absence of the deleted region, what was also confirmed by sequencing.

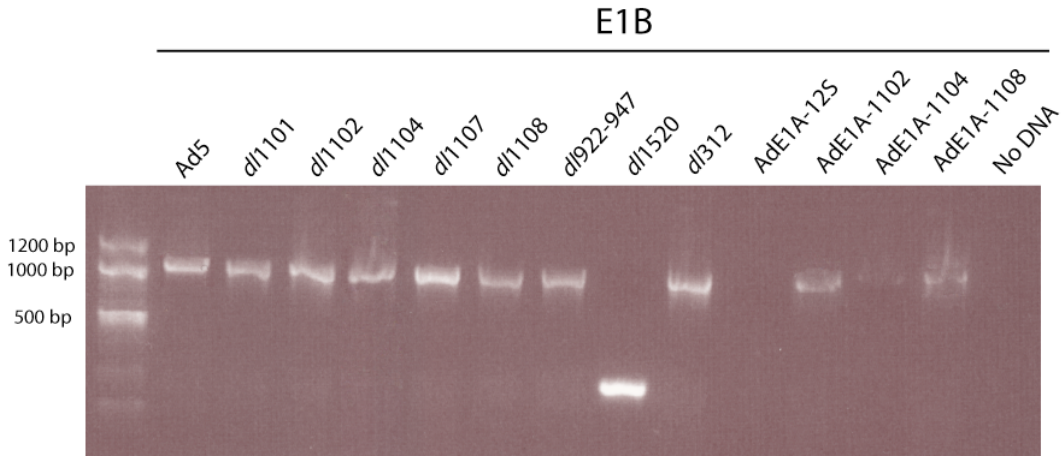


**Fig. 59.** E1B amplification. Primer set 6, described in materials and methods, was used to detect the presence of the E1B gene in each virus used. All replication competent viruses contained the E1B gene. The *dl*1520 mutant showed a smaller band than Ad5, as it is deleted in the E1B-55K gene. E1B was not present in the AdE1A-12S virus; amplification was observed in the other AdE1A-mutant viruses. This could be due to recombination with the cellular genome during the production of the viruses, resulting in a small proportion of viruses containing E1B. The bands for E1B in these viruses were faint compared to their replication compentent equivalents, indicating, that presence of E1B is reduced to a small proportion of virus.

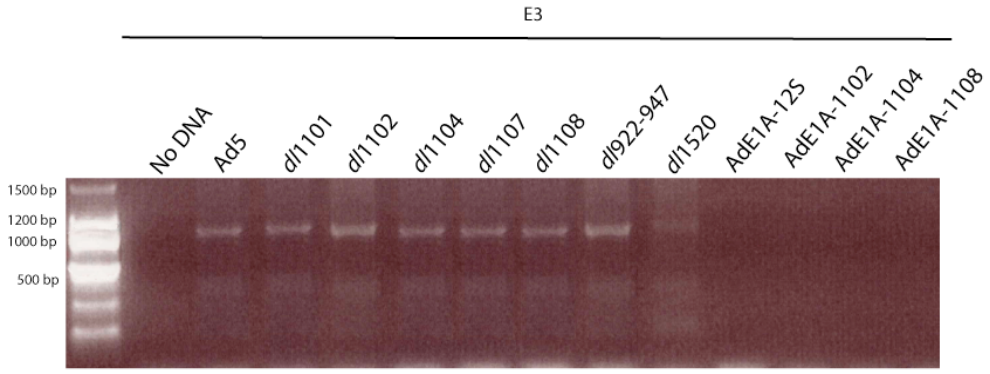


**Fig. 60.** E3 amplification for each virus used. E3 was amplified using the primer set 7 described in the materials and methods chapter. E3 was detected in all replication competent viruses but not in the replication deficient AdE1A-mutant viruses.

## 9.2 Sequence verification of the E1A mutant cDNAs used in this thesis.

All E1A cDNAs used in this thesis were sequenced by the Genome Centre (Institute of Cancer). First, the E1A-12S cDNA sequence was compared to the consensus sequence of E1A-13S cDNA, to observe the lack of the region corresponding to the CR3 (Fig. 61). All E1A-mutant sequences were aligned against the consensus sequence for E1A-12S cDNA. The E1A-1102 mutation lacked 30 nucleotides corresponding to amino acids residues 26 to 35 (Fig. 62); E1A-1104 also showed the correct deletion of 39 nucleotides (Fig. 63) and E1A-1108 lacked the 12 nucleotides that code for the amino acid residues 124 to 127 (Fig. 64).

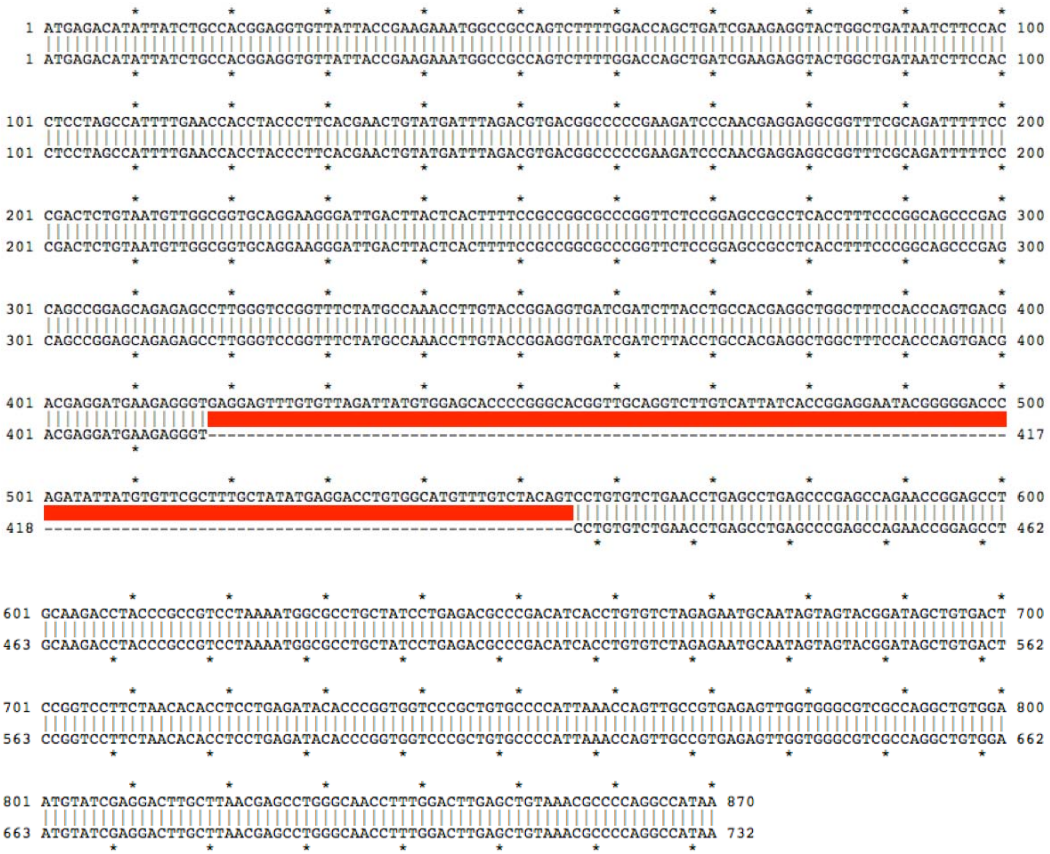

**Fig. 61.** Alignment of the E1A-12S cDNA obtained to construct the AdE1A-12S virus to the consensus sequence of E1A-13S.

**Fig. 62.** Alignment of E1A-12S sequence (on top) against the sequence of the E1A-1102 mutant used in this thesis (bottom sequence). The deleted region in the E1A-1102 mutant corresponded to the deletion of residues 26 to 35, indicating that the E1A-1102 constructed would produce the correct mutant protein.


**Fig. 63.** Alignment of E1A-12S (top) against the E1A-1104 constructed (bottom). The deletion in E1A-1104 corresponded to the sequence coding for amino acid residues 48 to 60, verifying the identity of the E1A-1104 mutant.

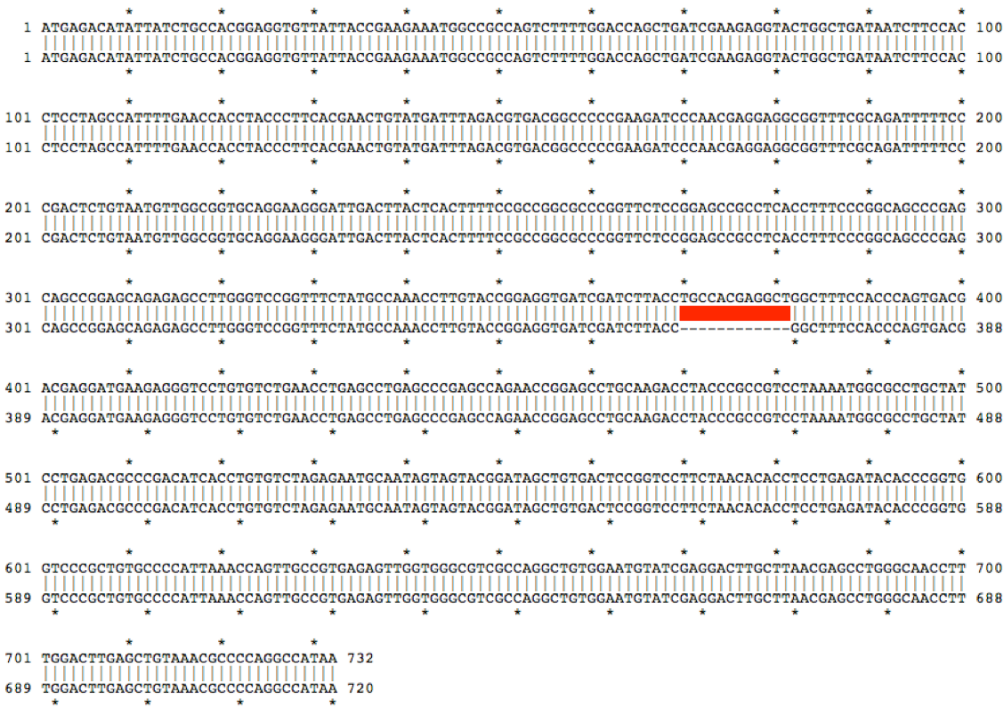


**Fig. 64.** Alignment of E1A-12S (top) against E1A-1108 (bottom). The small deleteion observed in the E1A-1108 cDNA constructed corresponded to the residues missing in the E1A-1108 consensus sequence.

# *REFERENCES*


1.Shenk E. *Adenoviridae*: The viruses and Their Replication. Fields Virology. fourth edition ed: Lippincott Williams & Wilkins; 2001. p. 2265-300.

2.Russell WC. Update on adenovirus and its vectors. J Gen Virol 2000;81:2573-604.

3.Gallimore PH, Turnell AS. Adenovirus E1A: remodelling the host cell, a life or death experience. Oncogene 2001;20:7824-35.

4.Mymryk JS. Database of mutations within the adenovirus 5 E1A oncogene. Nucleic Acids Res 1998;26:292-4.

5.Kanerva A, Hemminki A. Modified adenoviruses for cancer gene therapy. Int J Cancer 2004;110:475-80.

6.CRUK. Cancer statistics.

7.Suzuki H, Ueda T, Ichikawa T, Ito H. Androgen receptor involvement in the progression of prostate cancer. Endocr Relat Cancer 2003;10:209-16.

8.Schulz WA, Burchardt M, Cronauer MV. Molecular biology of prostate cancer. Mol Hum Reprod 2003;9:437-48.

9.SN R. The Prostate Book: Sound Advise on Symptoms and Treatment. 3rd Edition ed: W. W. Norton & Co; 2001.

10.Amirghofran Z, Monabati A, Gholijani N. Androgen receptor expression in relation to apoptosis and the expression of cell cycle related proteins in prostate cancer. Pathol Oncol Res 2004;10:37-41.

11.Berges RR, Furuya Y, Remington L, English HF, Jacks T, Isaacs JT. Cell proliferation, DNA repair, and p53 function are not required for programmed death of prostatic glandular cells induced by androgen ablation. Proc Natl Acad Sci U S A 1993;90:8910-4.

12.Kemppainen JA, Langley E, Wong CI, Bobseine K, Kelce WR, Wilson EM. Distinguishing androgen receptor agonists and antagonists: distinct

mechanisms of activation by medroxyprogesterone acetate and dihydrotestosterone. Mol Endocrinol 1999;13:440-54.

13.Fox EJ. Mechanism of action of mitoxantrone. Neurology 2004;63:S15-8.

14.Solier S, Lansiaux A, Logette E, et al. Topoisomerase I and II inhibitors control caspase-2 pre-messenger RNA splicing in human cells. Mol Cancer Res 2004;2:53-61.

15.Ho CK, Law SL, Chiang H, Hsu ML, Wang CC, Wang SY. Inhibition of microtubule assembly is a possible mechanism of action of mitoxantrone. Biochem Biophys Res Commun 1991;180:118-23.

16.Ehninger G, Schuler U, Proksch B, Zeller KP, Blanz J. Pharmacokinetics and metabolism of mitoxantrone. A review. Clin Pharmacokinet 1990;18:365-80.

17.Fabbri F, Amadori D, Carloni S, et al. Mitotic catastrophe and apoptosis induced by docetaxel in hormone-refractory prostate cancer cells. J Cell Physiol 2008;217:494-501.

18.NICE. Docetaxel for the treatment of hormone-refractory metastatic prostate cancer: National Institute for Heatlh and Clinical Excellence; 2006.

19.Nupponen NN, Kakkola L, Koivisto P, Visakorpi T. Genetic alterations in hormone-refractory recurrent prostate carcinomas. Am J Pathol 1998;153:141-8.

20.Agus DB, Cordon-Cardo C, Fox W, et al. Prostate cancer cell cycle regulators: response to androgen withdrawal and development of androgen independence. J Natl Cancer Inst 1999;91:1869-76.

21.Claudio PP, Zamparelli A, Garcia FU, et al. Expression of cell-cycle-regulated proteins pRb2/p130, p107, p27(kip1), p53, mdm-2, and Ki-67 (MIB-1) in prostatic gland adenocarcinoma. Clin Cancer Res 2002;8:1808-15.

22.Fusi A, Procopio G, Della Torre S, et al. Treatment options in hormone-refractory metastatic prostate carcinoma. Tumori 2004;90:535-46.

23.Balk SP, Knudsen KE. AR, the cell cycle, and prostate cancer. Nucl Recept Signal 2008;6:e001.

24.Linja MJ, Porkka KP, Kang Z, et al. Expression of androgen receptor coregulators in prostate cancer. Clin Cancer Res 2004;10:1032-40.

25.Heemers HV, Sebo TJ, Debes JD, et al. Androgen deprivation increases p300 expression in prostate cancer cells. Cancer Res 2007;67:3422-30.

26.Steiner MS, Wang Y, Zhang Y, Zhang X, Lu Y. p16/MTS1/INK4A suppresses prostate cancer by both pRb dependent and independent pathways. Oncogene 2000;19:1297-306.

27.Horwitz MS. Adenoviruses. Fields Virology. fourth edition ed: Lippincott Williams & Wilkins; 2001. p. 2265-300.

28.Davison AJ, Benko M, Harrach B. Genetic content and evolution of adenoviruses. J Gen Virol 2003;84:2895-908.

29.Hawkins LK, Lemoine NR, Kirn D. Oncolytic biotherapy: a novel therapeutic plafform. Lancet Oncol 2002;3:17-26.

30.Wold WS, Doronin K, Toth K, Kuppuswamy M, Lichtenstein DL, Tollefson AE. Immune responses to adenoviruses: viral evasion mechanisms and their implications for the clinic. Curr Opin Immunol 1999;11:380-6.

31.Law LK, Davidson BL. What does it take to bind CAR? Mol Ther 2005;12:599-609.

32.Lacher MD, Tiirikainen MI, Saunier EF, et al. Transforming growth factor-beta receptor inhibition enhances adenoviral infectability of carcinoma cells via up-regulation of Coxsackie and Adenovirus Receptor in conjunction with reversal of epithelial-mesenchymal transition. Cancer Res 2006;66:1648-57.

33.Bilbao R, Srinivasan S, Reay D, et al. Binding of adenoviral fiber knob to the coxsackievirus-adenovirus receptor is crucial for transduction of fetal muscle. Hum Gene Ther 2003;14:645-9.

34.Wickham TJ, Mathias P, Cheresh DA, Nemerow GR. Integrins alpha v beta 3 and alpha v beta 5 promote adenovirus internalization but not virus attachment. Cell 1993;73:309-19.

35.Wang Y, Thorne S, Hannock J, et al. A novel assay to assess primary human cancer infectibility by replication-selective oncolytic adenoviruses. Clin Cancer Res 2005;11:351-60.

36.Dechecchi MC, Tamanini A, Bonizzato A, Cabrini G. Heparan sulfate glycosaminoglycans are involved in adenovirus type 5 and 2-host cell interactions. Virology 2000;268:382-90.

37.Bao Y, Peng W, Verbitsky A, et al. Human coxsackie adenovirus receptor (CAR) expression in transgenic mouse prostate tumors enhances adenoviral delivery of genes. Prostate 2005;64:401-7.

38.van't Hof W, Crystal RG. Manipulation of the cytoplasmic and transmembrane domains alters cell surface levels of the coxsackie-adenovirus receptor and changes the efficiency of adenovirus infection. Hum Gene Ther 2001;12:25-34.

39.Wang X, Bergelson JM. Coxsackievirus and adenovirus receptor cytoplasmic and transmembrane domains are not essential for coxsackievirus and adenovirus infection. J Virol 1999;73:2559-62.

40.Waddington SN, McVey JH, Bhella D, et al. Adenovirus serotype 5 hexon mediates liver gene transfer. Cell 2008;132:397-409.

41.Berk AJ. Recent lessons in gene expression, cell cycle control, and cell biology from adenovirus. Oncogene 2005;24:7673-85.

42.Frisch SM, Mymryk JS. Adenovirus-5 E1A: paradox and paradigm. Nat Rev Mol Cell Biol 2002;3:441-52.

43.Cuconati A, White E. Viral homologs of BCL-2: role of apoptosis in the regulation of virus infection. Genes Dev 2002;16:2465-78.

44.Liu TC, Kirn D. Viruses with deletions in antiapoptotic genes as potential oncolytic agents. Oncogene 2005;24:6069-79.

45.Blanchette P, Kindsmuller K, Groitl P, et al. Control of mRNA export by adenovirus E4orf6 and E1B55K proteins during productive infection requires E4orf6 ubiquitin ligase activity. J Virol 2008;82:2642-51.

46.White E, Cipriani R. Role of adenovirus E1B proteins in transformation: altered organization of intermediate filaments in transformed cells that express the 19-kilodalton protein. Mol Cell Biol 1990;10:120-30.

47.O'Connor RJ, Hearing P. The E4-6/7 protein functionally compensates for the loss of E1A expression in adenovirus infection. J Virol 2000;74:5819-24.

48.Moore M, Horikoshi N, Shenk T. Oncogenic potential of the adenovirus E4orf6 protein. Proc Natl Acad Sci U S A 1996;93:11295-301.

49.Lavoie JN, Nguyen M, Marcellus RC, Branton PE, Shore GC. E4orf4, a novel adenovirus death factor that induces p53-independent apoptosis by a pathway that is not inhibited by zVAD-fmk. J Cell Biol 1998;140:637-45.

50.Branton PE, Roopchand DE. The role of adenovirus E4orf4 protein in viral replication and cell killing. Oncogene 2001;20:7855-65.

51.Shtrichman R, Kleinberger T. Adenovirus type 5 E4 open reading frame 4 protein induces apoptosis in transformed cells. J Virol 1998;72:2975-82.

52.Higashino F, Aoyagi M, Takahashi A, et al. Adenovirus E4orf6 targets pp32/LANP to control the fate of ARE-containing mRNAs by perturbing the CRM1-dependent mechanism. J Cell Biol 2005;170:15-20.

53.Harada JN, Shevchenko A, Pallas DC, Berk AJ. Analysis of the adenovirus E1B-55K-anchored proteome reveals its link to ubiquitination machinery. J Virol 2002;76:9194-206.

54.Cascallo M, Gros A, Bayo N, Serrano T, Capella G, Alemany R. Deletion of VAI and VAII RNA genes in the design of oncolytic adenoviruses. Hum Gene Ther 2006;17:929-40.

55.Doronin K, Toth K, Kuppuswamy M, Ward P, Tollefson AE, Wold WS. Tumor-specific, replication-competent adenovirus vectors overexpressing the adenovirus death protein. J Virol 2000;74:6147-55.

56.Wang Y, Hallden G, Hill R, et al. E3 gene manipulations affect oncolytic adenovirus activity in immunocompetent tumor models. Nat Biotechnol 2003;21:1328-35.

57.Zhang X, Mullbacher A, Braithwaite AW. Down-regulation of E1a expression by E3 gene products in group C adenoviruses. Immunol Cell Biol 1992;70 ( Pt 1):65-71.

58.Zhang X, Bellett AJ, Hla RT, Voss T, Mullbacher A, Braithwaite AW. Down-regulation of human adenovirus E1a by E3 gene products: evidence for translational control of E1a by E3 14.5K and/or E3 10.4K products. J Gen Virol 1994;75 ( Pt 8):1943-51.

59.Subramanian T, Vijayalingam S, Chinnadurai G. Genetic identification of adenovirus type 5 genes that influence viral spread. J Virol 2006;80:2000-12.

60.Carmody RJ, Maguschak K, Chen YH. A novel mechanism of nuclear factor-kappaB regulation by adenoviral protein 14.7K. Immunology 2006;117:188-95.

61.Routes JM, Metz BA, Cook JL. Endogenous expression of E1A in human cells enhances the effect of adenovirus E3 on class I major histocompatibility complex antigen expression. J Virol 1993;67:3176-81.

62.Routes JM, Cook JL. Resistance of human cells to the adenovirus E3 effect on class I MHC antigen expression. Implications for antiviral immunity. J Immunol 1990;144:2763-70.

63.Ulfendahl PJ, Linder S, Kreivi JP, et al. A novel adenovirus-2 E1A mRNA encoding a protein with transcription activation properties. EMBO J 1987;6:2037-44.

64.Stephens C, Harlow E. Differential splicing yields novel adenovirus 5 E1A mRNAs that encode 30 kd and 35 kd proteins. EMBO J 1987;6:2027-35.

65.Nevins JR, Ginsberg HS, Blanchard JM, Wilson MC, Darnell JE, Jr. Regulation of the primary expression of the early adenovirus transcription units. J Virol 1979;32:727-33.

66.Nevins JR. Regulation of early adenovirus gene expression. Microbiol Rev 1987;51:419-30.

67.Schaeper U, Subramanian T, Lim L, Boyd JM, Chinnadurai G. Interaction between a cellular protein that binds to the C-terminal region of adenovirus E1A (CtBP) and a novel cellular protein is disrupted by E1A through a conserved PLDLS motif. J Biol Chem 1998;273:8549-52.

68.Pelka P, Ablack JN, Fonseca GJ, Yousef AF, Mymryk JS. Intrinsic structural disorder in adenovirus E1A: a viral molecular hub linking multiple diverse processes. J Virol 2008;82:7252-63.

69.Spindler KR, Berk AJ. Rapid intracellular turnover of adenovirus 5 early region 1A proteins. J Virol 1984;52:706-10.

70.Zhang Q, Yao H, Vo N, Goodman RH. Acetylation of adenovirus E1A regulates binding of the transcriptional corepressor CtBP. Proc Natl Acad Sci U S A 2000;97:14323-8.

71.Moran B, Zerler B. Interactions between cell growth-regulating domains in the products of the adenovirus E1A oncogene. Mol Cell Biol 1988;8:1756-64.

72.Avvakumov N, Sahbegovic M, Zhang Z, Shuen M, Mymryk JS. Analysis of DNA binding by the adenovirus type 5 E1A oncoprotein. J Gen Virol 2002;83:517-24.

73.Corbeil HB, Branton PE. Functional importance of complex formation between the retinoblastoma tumor suppressor family and adenovirus E1A proteins as determined by mutational analysis of E1A conserved region 2. J Virol 1994;68:6697-709.

74.Dyson N, Guida P, McCall C, Harlow E. Adenovirus E1A makes two distinct contacts with the retinoblastoma protein. J Virol 1992;66:4606-11.

75.Fattaey AR, Harlow E, Helin K. Independent regions of adenovirus E1A are required for binding to and dissociation of E2F-protein complexes. Mol Cell Biol 1993;13:7267-77.

76.McCabe MT, Azih OJ, Day ML. pRb-Independent growth arrest and transcriptional regulation of E2F target genes. Neoplasia 2005;7:141-51.

77.Seifried LA, Talluri S, Cecchini M, Julian LM, Mymryk JS, Dick FA. pRB-E2F1 complexes are resistant to adenovirus E1A-mediated disruption. J Virol 2008;82:4511-20.

78.Helt AM, Galloway DA. Mechanisms by which DNA tumor virus oncoproteins target the Rb family of pocket proteins. Carcinogenesis 2003;24:159-69.

79.Nemajerova A, Talos F, Moll UM, Petrenko O. Rb function is required for E1A-induced S-phase checkpoint activation. Cell Death Differ 2008;15:1440-9.

80.Alevizopoulos K, Sanchez B, Amati B. Conserved region 2 of adenovirus E1A has a function distinct from pRb binding required to prevent cell cycle arrest by p16INK4a or p27Kip1. Oncogene 2000;19:2067-74.

81.Barbeau D, Charbonneau R, Whalen SG, Bayley ST, Branton PE. Functional interactions within adenovirus E1A protein complexes. Oncogene 1994;9:359-73.

82.Parreno M, Garriga J, Limon A, et al. E1A blocks hyperphosphorylation of p130 and p107 without affecting the phosphorylation status of the retinoblastoma protein. J Virol 2000;74:3166-76.

83.Sherr CJ, McCormick F. The RB and p53 pathways in cancer. Cancer Cell 2002;2:103-12.

84.Deng J, Kloosterbooer F, Xia W, Hung MC. The NH(2)-terminal and conserved region 2 domains of adenovirus E1A mediate two distinct mechanisms of tumor suppression. Cancer Res 2002;62:346-50.

85.Klanrit P, Flinterman MB, Odell EW, et al. Specific isoforms of p73 control the induction of cell death induced by the viral proteins, E1A or apoptin. Cell Cycle 2008;7:205-15.

86.Zhao X, Gschwend JE, Powell CT, Foster RG, Day KC, Day ML. Retinoblastoma protein-dependent growth signal conflict and caspase activity are required for protein kinase C-signaled apoptosis of prostate epithelial cells. J Biol Chem 1997;272:22751-7.

87.Mal A, Chattopadhyay D, Ghosh MK, Poon RY, Hunter T, Harter ML. p21 and retinoblastoma protein control the absence of DNA replication in terminally differentiated muscle cells. J Cell Biol 2000;149:281-92.

88.Keblusek P, Dorsman JC, Teunisse AF, Teunissen H, van der Eb AJ, Zantema A. The adenoviral E1A oncoproteins interfere with the growth-inhibiting effect of the cdk-inhibitor p21(CIP1/WAF1). J Gen Virol 1999;80 ( Pt 2):381-90.

89.Chattopadhyay D, Ghosh MK, Mal A, Harter ML. Inactivation of p21 by E1A leads to the induction of apoptosis in DNA-damaged cells. J Virol 2001;75:9844-56.

90.Jarrard DF, Sarkar S, Shi Y, et al. p16/pRb pathway alterations are required for bypassing senescence in human prostate epithelial cells. Cancer Res 1999;59:2957-64.

91.Egan C, Jelsma TN, Howe JA, Bayley ST, Ferguson B, Branton PE. Mapping of cellular protein-binding sites on the products of early-region 1A of human adenovirus type 5. Mol Cell Biol 1988;8:3955-9.

92.Boyd JM, Loewenstein PM, Tang Qq QQ, Yu L, Green M. Adenovirus E1A N-terminal amino acid sequence requirements for repression of transcription in vitro and in vivo correlate with those required for E1A interference with TBP-TATA complex formation. J Virol 2002;76:1461-74.

93.Loewenstein PM, Arackal S, Green M. Mutational and functional analysis of an essential subdomain of the adenovirus E1A N-terminal transcription repression domain. Virology 2006;351:312-21.

94.Wang HG, Rikitake Y, Carter MC, et al. Identification of specific adenovirus E1A N-terminal residues critical to the binding of cellular proteins and to the control of cell growth. J Virol 1993;67:476-88.

95.Pelka P, Ablack JN, Torchia J, Turnell AS, Grand RJ, Mymryk JS. Transcriptional control by adenovirus E1A conserved region 3 via p300/CBP. Nucleic Acids Res 2009;37:1095-106.

96.Song CZ, Tierney CJ, Loewenstein PM, et al. Transcriptional repression by human adenovirus E1A N terminus/conserved domain 1 polypeptides in vivo and in vitro in the absence of protein synthesis. J Biol Chem 1995;270:23263-7.

97.Turnell AS, Mymryk JS. Roles for the coactivators CBP and p300 and the APC/C E3 ubiquitin ligase in E1A-dependent cell transformation. Br J Cancer 2006;95:555-60.

98.Rasti M, Grand RJ, Mymryk JS, Gallimore PH, Turnell AS. Recruitment of CBP/p300, TATA-binding protein, and S8 to distinct regions at the N terminus of adenovirus E1A. J Virol 2005;79:5594-605.

99.O'Connor MJ, Zimmermann H, Nielsen S, Bernard HU, Kouzarides T. Characterization of an E1A-CBP interaction defines a novel transcriptional adapter motif (TRAM) in CBP/p300. J Virol 1999;73:3574-81.

100.Querido E, Teodoro JG, Branton PE. Accumulation of p53 induced by the adenovirus E1A protein requires regions involved in the stimulation of DNA synthesis. J Virol 1997;71:3526-33.

101.Chiou SK, White E. p300 binding by E1A cosegregates with p53 induction but is dispensable for apoptosis. J Virol 1997;71:3515-25.

102.Putzer BM, Stiewe T, Parssanedjad K, Rega S, Esche H. E1A is sufficient by itself to induce apoptosis independent of p53 and other adenoviral gene products. Cell Death Differ 2000;7:177-88.

103.Goodman RH, Smolik S. CBP/p300 in cell growth, transformation, and development. Genes Dev 2000;14:1553-77.

104.Green M, Panesar NK, Loewenstein PM. The transcription-repression domain of the adenovirus E1A oncoprotein targets p300 at the promoter. Oncogene 2008;27:4446-55.

105.Sundqvist A, Sollerbrant K, Svensson C. The carboxy-terminal region of adenovirus E1A activates transcription through targeting of a C-terminal binding protein-histone deacetylase complex. FEBS Lett 1998;429:183-8.

106.Samuelson AV, Narita M, Chan HM, et al. p400 is required for E1A to promote apoptosis. J Biol Chem 2005;280:21915-23.

107.Zhao LJ, Subramanian T, Chinnadurai G. Inhibition of transcriptional activation and cell proliferation activities of adenovirus E1A by the unique N-terminal domain of CtBP2. Oncogene 2008;27:5214-22.

108.Bruton RK, Pelka P, Mapp KL, et al. Identification of a second CtBP binding site in adenovirus type 5 E1A conserved region 3. J Virol 2008;82:8476-86.

109.Martens JH, Verlaan M, Kalkhoven E, Dorsman JC, Zantema A. Scaffold/matrix attachment region elements interact with a p300-scaffold attachment factor A complex and are bound by acetylated nucleosomes. Mol Cell Biol 2002;22:2598-606.

110.Lang SE, Hearing P. The adenovirus E1A oncoprotein recruits the cellular TRRAP/GCN5 histone acetyltransferase complex. Oncogene 2003;22:2836-41.

111.Baluchamy S, Sankar N, Navaraj A, Moran E, Thimmapaya B. Relationship between E1A binding to cellular proteins, c-myc activation and S-phase induction. Oncogene 2007;26:781-7.

112.Chan HM, Narita M, Lowe SW, Livingston DM. The p400 E1A-associated protein is a novel component of the p53 --> p21 senescence pathway. Genes Dev 2005;19:196-201.

113.Tworkowski KA, Chakraborty AA, Samuelson AV, et al. Adenovirus E1A targets p400 to induce the cellular oncoprotein Myc. Proc Natl Acad Sci U S A 2008;105:6103-8.

114.Flinterman MB, Mymryk JS, Klanrit P, et al. p400 function is required for the adenovirus E1A-mediated suppression of EGFR and tumour cell killing. Oncogene 2007;26:6863-74.

115.Turnell AS, Grand RJ, Gorbea C, et al. Regulation of the 26S proteasome by adenovirus E1A. Embo J 2000;19:4759-73.

116.Rasti M, Grand RJ, Yousef AF, et al. Roles for APIS and the 20S proteasome in adenovirus E1A-dependent transcription. EMBO J 2006;25:2710-22.

117.Swaffield JC, Melcher K, Johnston SA. A highly conserved ATPase protein as a mediator between acidic activation domains and the TATA-binding protein. Nature 1995;374:88-91.

118.Hateboer G, Gennissen A, Ramos YF, et al. BS69, a novel adenovirus E1A-associated protein that inhibits E1A transactivation. EMBO J 1995;14:3159-69.

119.Isobe T, Uchida C, Hattori T, Kitagawa K, Oda T, Kitagawa M. Ubiquitin-dependent degradation of adenovirus E1A protein is inhibited by BS69. Biochem Biophys Res Commun 2006;339:367-74.

120.Moran E, Zerler B, Harrison TM, Mathews MB. Identification of separate domains in the adenovirus E1A gene for immortalization activity and the activation of virus early genes. Mol Cell Biol 1986;6:3470-80.

121.Pereira DS, Rosenthal KL, Graham FL. Identification of adenovirus E1A regions which affect MHC class I expression and susceptibility to cytotoxic T lymphocytes. Virology 1995;211:268-77.

122.Jelinek T, Pereira DS, Graham FL. Tumorigenicity of adenovirus-transformed rodent cells is influenced by at least two regions of adenovirus type 12 early region 1A. J Virol 1994;68:888-96.

123.Zhao B, Ricciardi RP. E1A is the component of the MHC class I enhancer complex that mediates HDAC chromatin repression in adenovirus-12 tumorigenic cells. Virology 2006;352:338-44.

124.Deol P, Zaiss DM, Monaco JJ, Sijts AJ. Rates of processing determine the immunogenicity of immunoproteasome-generated epitopes. J Immunol 2007;178:7557-62.

125.Routes JM, Ryan JC, Ryan S, Nakamura M. MHC class I molecules on adenovirus E1A-expressing tumor cells inhibit NK cell killing but not NK cell-mediated tumor rejection. Int Immunol 2001;13:1301-7.

126.Cook JL, Krantz CK, Routes BA. Role of p300-family proteins in E1A oncogene induction of cytolytic susceptibility and tumor cell rejection. Proc Natl Acad Sci U S A 1996;93:13985-90.

127.Kretsovali A, Agalioti T, Spilianakis C, Tzortzakaki E, Merika M, Papamatheakis J. Involvement of CREB binding protein in expression of major histocompatibility complex class II genes via interaction with the class II transactivator. Mol Cell Biol 1998;18:6777-83.

128.Ruley HE. Adenovirus early region 1A enables viral and cellular transforming genes to transform primary cells in culture. Nature 1983;304:602-6.

129.Ruppert JM, Vogelstein B, Kinzler KW. The zinc finger protein GLI transforms primary cells in cooperation with adenovirus E1A. Mol Cell Biol 1991;11:1724-8.

130.Fischer RS, Quinlan MP. Expression of the pRb-binding regions of E1A enables efficient transformation of primary epithelial cells by v-src. J Virol 1998;72:2815-24.

131.Deng J, Xia W, Hung MC. Adenovirus 5 E1A-mediated tumor suppression associated with E1A-mediated apoptosis in vivo. Oncogene 1998;17:2167-75.

132.Yoo GH, Hung MC, Lopez-Berestein G, et al. Phase I trial of intratumoral liposome E1A gene therapy in patients with recurrent breast and head and neck cancer. Clin Cancer Res 2001;7:1237-45.

133.Frisch SM. E1a induces the expression of epithelial characteristics. J Cell Biol 1994;127:1085-96.

134.Moran E, Grodzicker T, Roberts RJ, Mathews MB, Zerler B. Lytic and transforming functions of individual products of the adenovirus E1A gene. J Virol 1986;57:765-75.

135.Haley KP, Overhauser J, Babiss LE, Ginsberg HS, Jones NC. Transformation properties of type 5 adenovirus mutants that differentially express the E1A gene products. Proc Natl Acad Sci U S A 1984;81:5734-8.

136.Hortobagyi GN, Ueno NT, Xia W, et al. Cationic liposome-mediated E1A gene transfer to human breast and ovarian cancer cells and its biologic effects: a phase I clinical trial. J Clin Oncol 2001;19:3422-33.

137.Kirn D. Replication-selective oncolytic adenoviruses: virotherapy aimed at genetic targets in cancer. Oncogene 2000;19:6660-9.

138.Samuelson AV, Lowe SW. Selective induction of p53 and chemosensitivity in RB-deficient cells by E1A mutants unable to bind the RB-related proteins. Proc Natl Acad Sci U S A 1997;94:12094-9.

139.Heise C, Hermiston T, Johnson L, et al. An adenovirus E1A mutant that demonstrates potent and selective systemic anti-tumoral efficacy. Nat Med 2000;6:1134-9.

140.Fueyo J, Alemany R, Gomez-Manzano C, et al. Preclinical characterization of the antiglioma activity of a tropism-enhanced adenovirus targeted to the retinoblastoma pathway. J Natl Cancer Inst 2003;95:652-60.

141.Sauthoff H, Pipiya T, Heitner S, et al. Impact of E1a modifications on tumor-selective adenoviral replication and toxicity. Mol Ther 2004;10:749-57.

142.Howe JA, Demers GW, Johnson DE, et al. Evaluation of E1-mutant adenoviruses as conditionally replicating agents for cancer therapy. Mol Ther 2000;2:485-95.

143.Jiang H, Alemany R, Gomez-Manzano C, et al. Downmodulation of E1A protein expression as a novel strategy to design cancer-selective adenoviruses. Neoplasia 2005;7:723-9.

144.Kim J, Kim JH, Choi KJ, Kim PH, Yun CO. E1A- and E1B-Double mutant replicating adenovirus elicits enhanced oncolytic and antitumor effects. Hum Gene Ther 2007;18:773-86.

145.Leitner S, Sweeney K, Oberg D, et al. Oncolytic adenoviral mutants with E1B19K gene deletions enhance gemcitabine-induced apoptosis in pancreatic carcinoma cells and anti-tumor efficacy in vivo. Clin Cancer Res 2009;15:1730-40.

146.Shisler J, Duerksen-Hughes P, Hermiston TM, Wold WS, Gooding LR. Induction of susceptibility to tumor necrosis factor by E1A is dependent on binding to either p300 or p105-Rb and induction of DNA synthesis. J Virol 1996;70:68-77.

147.Cook JL, Miura TA, Ikle DN, Lewis AM, Jr., Routes JM. E1A oncogene-induced sensitization of human tumor cells to innate immune defenses and chemotherapy-induced apoptosis in vitro and in vivo. Cancer Res 2003;63:3435-43.

148.Martin-Duque P, Sanchez-Prieto R, Romero J, et al. In vivo radiosensitizing effect of the adenovirus E1A gene in murine and human malignant tumors. Int J Oncol 1999;15:1163-8.

149.Hayashi N, Asano K, Suzuki H, et al. Adenoviral infection of survivin antisense sensitizes prostate cancer cells to etoposide in vivo. Prostate 2005;65:10-9.

150.Lee WP, Tai DI, Tsai SL, et al. Adenovirus type 5 E1A sensitizes hepatocellular carcinoma cells to gemcitabine. Cancer Res 2003;63:6229-36.

151.Chang CY, Lin YM, Lee WP, Hsu HH, Chen EI. Involvement of Bcl-X(L) deamidation in E1A-mediated cisplatin sensitization of ovarian cancer cells. Oncogene 2006;25:2656-65.

152.Liao Y, Zou YY, Xia WY, Hung MC. Enhanced paclitaxel cytotoxicity and prolonged animal survival rate by a nonviral-mediated systemic delivery of E1A gene in orthotopic xenograft human breast cancer. Cancer Gene Ther 2004;11:594-602.

153.Ueno NT, Yu D, Hung MC. Chemosensitization of HER-2/neu-overexpressing human breast cancer cells to paclitaxel (Taxol) by adenovirus type 5 E1A. Oncogene 1997;15:953-60.

154.Yoon AR, Kim JH, Lee YS, et al. Markedly Enhanced Cytolysis by E1B-19kD-Deleted Oncolytic Adenovirus in Combination with Cisplatin. Hum Gene Ther 2006.

155.Liao Y, Hung MC. A new role of protein phosphatase 2a in adenoviral E1A protein-mediated sensitization to anticancer drug-induced apoptosis in human breast cancer cells. Cancer Res 2004;64:5938-42.

156.Liao Y, Hung MC. Regulation of the activity of p38 mitogen-activated protein kinase by Akt in cancer and adenoviral protein E1A-mediated sensitization to apoptosis. Mol Cell Biol 2003;23:6836-48.

157.Lehmann BD, McCubrey JA, Jefferson HS, Paine MS, Chappell WH, Terrian DM. A dominant role for p53-dependent cellular senescence in radiosensitization of human prostate cancer cells. Cell Cycle 2007;6:595-605.

158.Qiu W, Wu J, Walsh EM, et al. Retinoblastoma protein modulates gankyrin-MDM2 in regulation of p53 stability and chemosensitivity in cancer cells. Oncogene 2008;27:4034-43.

159.Couzin-Frankel J. Genetics. The promise of a cure: 20 years and counting. Science 2009;324:1504-7.

160.Pearson H. Human genetics: One gene, twenty years. Nature 2009;460:164-9.

161.Edelstein ML, Abedi MR, Wixon J. Gene therapy clinical trials worldwide to 2007--an update. J Gene Med 2007;9:833-42.

162.Blaese RM, Culver KW, Miller AD, et al. T lymphocyte-directed gene therapy for ADA- SCID: initial trial results after 4 years. Science 1995;270:475-80.

163.Hacein-Bey-Abina S, von Kalle C, Schmidt M, et al. A serious adverse event after successful gene therapy for X-linked severe combined immunodeficiency. N Engl J Med 2003;348:255-6.

164.Raper SE, Chirmule N, Lee FS, et al. Fatal systemic inflammatory response syndrome in a ornithine transcarbamylase deficient patient following adenoviral gene transfer. Mol Genet Metab 2003;80:148-58.

165.Martin Duque MP, Sanchez-Prieto R, Lleonart M, Ramon y Cajal S. Perspectives in gene therapy. Histol Histopathol 1998;13:231-42.

166.Patel P, Ashdown D, James N. Is gene therapy the answer for prostate cancer? Prostate Cancer Prostatic Dis 2004;7 Suppl 1:S14-9.

167.Lichtenstein DL, Wold WS. Experimental infections of humans with wild-type adenoviruses and with replication-competent adenovirus vectors: replication, safety, and transmission. Cancer Gene Ther 2004;11:819-29.

168.Alexander BL, Ali RR, Alton EW, et al. Progress and prospects: gene therapy clinical trials (part 1). Gene Ther 2007;14:1439-47.

169.Aiuti A, Bachoud-Levi AC, Blesch A, et al. Progress and prospects: gene therapy clinical trials (part 2). Gene Ther 2007;14:1555-63.

170.Arlen PM, Gulley JL, Parker C, et al. A randomized phase II study of concurrent docetaxel plus vaccine versus vaccine alone in metastatic androgen-independent prostate cancer. Clin Cancer Res 2006;12:1260-9.

171.St George JA. Gene therapy progress and prospects: adenoviral vectors. Gene Ther 2003;10:1135-41.

172.Liu TC, Kirn D. Systemic efficacy with oncolytic virus therapeutics: clinical proof-of-concept and future directions. Cancer Res 2007;67:429-32.

173.Vorburger SA, Hunt KK. Adenoviral gene therapy. Oncologist 2002;7:46-59.

174.Hoffmann D, Wildner O. Restriction of adenoviral replication to the transcriptional intersection of two different promoters for colorectal and pancreatic cancer treatment. Mol Cancer Ther 2006;5:374-81.

175.Schmitz M, Graf C, Gut T, et al. Melanoma cultures show different susceptibility towards E1A-, E1B-19 kDa- and fiber-modified replication-competent adenoviruses. Gene Ther 2006;13:893-905.

176.Bauerschmitz GJ, Guse K, Kanerva A, et al. Triple-targeted oncolytic adenoviruses featuring the cox2 promoter, E1A transcomplementation, and serotype chimerism for enhanced selectivity for ovarian cancer cells. Mol Ther 2006;14:164-74.

177.Campos SK, Barry MA. Current advances and future challenges in Adenoviral vector biology and targeting. Curr Gene Ther 2007;7:189-204.

178.Kawakami Y, Li H, Lam JT, Krasnykh V, Curiel DT, Blackwell JL. Substitution of the adenovirus serotype 5 knob with a serotype 3 knob enhances multiple steps in virus replication. Cancer Res 2003;63:1262-9.

179.Wang H, Liu Y, Li Z, et al. In vitro and in vivo properties of adenovirus vectors with increased affinity to CD46. J Virol 2008;82:10567-79.

180.Volk AL, Rivera AA, Kanerva A, et al. Enhanced adenovirus infection of melanoma cells by fiber-modification: incorporation of RGD peptide or Ad5/3 chimerism. Cancer Biol Ther 2003;2:511-5.

181.Lord R, Parsons M, Kirby I, et al. Analysis of the interaction between RGD-expressing adenovirus type 5 fiber knob domains and alphavbeta3 integrin reveals distinct binding profiles and intracellular trafficking. J Gen Virol 2006;87:2497-505.

182.Korokhov N, Mikheeva G, Krendelshchikov A, et al. Targeting of adenovirus via genetic modification of the viral capsid combined with a protein bridge. J Virol 2003;77:12931-40.

183.Ries S, Korn WM. ONYX-015: mechanisms of action and clinical potential of a replication-selective adenovirus. Br J Cancer 2002;86:5-11.

184.Bischoff JR, Kirn DH, Williams A, et al. An adenovirus mutant that replicates selectively in p53-deficient human tumor cells. Science 1996;274:373-6.

185.Goodrum FD, Ornelles DA. p53 status does not determine outcome of E1B 55-kilodalton mutant adenovirus lytic infection. J Virol 1998;72:9479-90.

186.Cherubini G, Petouchoff T, Grossi M, Piersanti S, Cundari E, Saggio I. E1B55K-deleted adenovirus (ONYX-015) overrides G1/S and G2/M checkpoints and causes mitotic catastrophe and endoreduplication in p53-proficient normal cells. Cell Cycle 2006;5:2244-52.

187.Hann B, Balmain A. Replication of an E1B 55-kilodalton protein-deficient adenovirus (ONYX-015) is restored by gain-of-function rather than loss-of-function p53 mutants. J Virol 2003;77:11588-95.

188.Kirn D. Clinical research results with dl1520 (Onyx-015), a replication-selective adenovirus for the treatment of cancer: what have we learned? Gene Ther 2001;8:89-98.

189.Kirn D, Martuza RL, Zwiebel J. Replication-selective virotherapy for cancer: Biological principles, risk management and future directions. Nat Med 2001;7:781-7.

190.Mulvihill S, Warren R, Venook A, et al. Safety and feasibility of injection with an E1B-55 kDa gene-deleted, replication-selective adenovirus (ONYX-015)

into primary carcinomas of the pancreas: a phase I trial. Gene Ther 2001;8:308-15.

191.Nemunaitis J, Ganly I, Khuri F, et al. Selective replication and oncolysis in p53 mutant tumors with ONYX-015, an E1B-55kD gene-deleted adenovirus, in patients with advanced head and neck cancer: a phase II trial. Cancer Res 2000;60:6359-66.

192.Nemunaitis J, Senzer N, Sarmiento S, et al. A phase I trial of intravenous infusion of ONYX-015 and enbrel in solid tumor patients. Cancer Gene Ther 2007;14:885-93.

193.Opyrchal M, Aderca I, Galanis E. Phase I clinical trial of locoregional administration of the oncolytic adenovirus ONYX-015 in combination with mitomycin-C, doxorubicin, and cisplatin chemotherapy in patients with advanced sarcomas. Methods Mol Biol 2009;542:705-17.

194.Zhang Z, Li M, Wang H, Agrawal S, Zhang R. Antisense therapy targeting MDM2 oncogene in prostate cancer: Effects on proliferation, apoptosis, multiple gene expression, and chemotherapy. Proc Natl Acad Sci U S A 2003;100:11636-41.

195.Zhang M, Mukherjee N, Bermudez RS, et al. Adenovirus-mediated inhibition of survivin expression sensitizes human prostate cancer cells to paclitaxel in vitro and in vivo. Prostate 2005;64:293-302.

196.Ahn M, Lee SJ, Li X, et al. Enhanced combined tumor-specific oncolysis and suicide gene therapy for prostate cancer using M6 promoter. Cancer Gene Ther 2009;16:73-82.

197.Freytag SO, Stricker H, Peabody J, et al. Five-year follow-up of trial of replication-competent adenovirus-mediated suicide gene therapy for treatment of prostate cancer. Mol Ther 2007;15:636-42.

198.Freytag SO, Movsas B, Aref I, et al. Phase I trial of replication-competent adenovirus-mediated suicide gene therapy combined with IMRT for prostate cancer. Mol Ther 2007;15:1016-23.

199.Yu DC, Chen Y, Dilley J, et al. Antitumor synergy of CV787, a prostate cancer-specific adenovirus, and paclitaxel and docetaxel. Cancer Res 2001;61:517-25.

200.Dilley J, Reddy S, Ko D, et al. Oncolytic adenovirus CG7870 in combination with radiation demonstrates synergistic enhancements of antitumor efficacy without loss of specificity. Cancer Gene Ther 2005;12:715-22.

201.Lee SJ, Zhang Y, Lee SD, et al. Targeting prostate cancer with conditionally replicative adenovirus using PSMA enhancer. Mol Ther 2004;10:1051-8.

202.Small EJ, Carducci MA, Burke JM, et al. A phase I trial of intravenous CG7870, a replication-selective, prostate-specific antigen-targeted oncolytic adenovirus, for the treatment of hormone-refractory, metastatic prostate cancer. Mol Ther 2006;14:107-17.

203.Hoti N, Li Y, Chen CL, et al. Androgen receptor attenuation of Ad5 replication: implications for the development of conditionally replication competent adenoviruses. Mol Ther 2007;15:1495-503.

204.Okegawa T, Li Y, Pong RC, Bergelson JM, Zhou J, Hsieh JT. The dual impact of coxsackie and adenovirus receptor expression on human prostate cancer gene therapy. Cancer Res 2000;60:5031-6.

205.Skjoth IH, Issinger OG. Profiling of signaling molecules in four different human prostate carcinoma cell lines before and after induction of apoptosis. Int J Oncol 2006;28:217-29.

206.Kaighn ME, Narayan KS, Ohnuki Y, Lechner JF, Jones LW. Establishment and characterization of a human prostatic carcinoma cell line (PC-3). Invest Urol 1979;17:16-23.

207.Stone KR, Mickey DD, Wunderli H, Mickey GH, Paulson DF. Isolation of a human prostate carcinoma cell line (DU 145). Int J Cancer 1978;21:274-81.

208.Sramkoski RM, Pretlow TG, 2nd, Giaconia JM, et al. A new human prostate carcinoma cell line, 22Rv1. In Vitro Cell Dev Biol Anim 1999;35:403-9.

209.Nakanishi H, Taylor RM, Hawkins AL, Griffin CA, Martin GR, Passaniti A. Establishment of hormone-dependent and hormone-independent carcinoma cell lines with different metastatic potentials from spontaneous mammary tumors in aged Wistar rats. Int J Cancer 1994;58:592-601.

210.Foster BA, Gingrich JR, Kwon ED, Madias C, Greenberg NM. Characterization of prostatic epithelial cell lines derived from transgenic adenocarcinoma of the mouse prostate (TRAMP) model. Cancer Res 1997;57:3325-30.

211.Maizel JV, Jr., White DO, Scharff MD. The polypeptides of adenovirus. I. Evidence for multiple protein components in the virion and a comparison of types 2, 7A, and 12. Virology 1968;36:115-25.

212.O'Reilly DR ML, Luckow VA. Virus Methods. Baculovirus Expression Vectors: A laboratory Manual: Oxford University Press; 1994. p. 132-4.

213.Debbas M, White E. Wild-type p53 mediates apoptosis by E1A, which is inhibited by E1B. Genes Dev 1993;7:546-54.

214.Ries SJ, Brandts CH, Chung AS, et al. Loss of p14ARF in tumor cells facilitates replication of the adenovirus mutant dl1520 (ONYX-015). Nat Med 2000;6:1128-33.

215.O'Shea CC, Johnson L, Bagus B, et al. Late viral RNA export, rather than p53 inactivation, determines ONYX-015 tumor selectivity. Cancer Cell 2004;6:611-23.

216.Zheng X, Rao XM, Gomez-Gutierrez JG, Hao H, McMasters KM, Zhou HS. Adenovirus E1B55K region is required to enhance cyclin E expression for efficient viral DNA replication. J Virol 2008;82:3415-27.

217.Sang N, Severino A, Russo P, et al. RACK1 interacts with E1A and rescues E1A-induced yeast growth inhibition and mammalian cell apoptosis. J Biol Chem 2001;276:27026-33.

218.Miura TA, Cook JL, Potter TA, Ryan S, Routes JM. The interaction of adenovirus E1A with p300 family members modulates cellular gene expression to reduce tumorigenicity. J Cell Biochem 2007;100:929-40.

219.Duncan SJ, Gordon FC, Gregory DW, et al. Infection of mouse liver by human adenovirus type 5. J Gen Virol 1978;40:45-61.

220.Oualikene W, Gonin P, Eloit M. Short and long term dissemination of deletion mutants of adenovirus in permissive (cotton rat) and non-permissive (mouse) species. J Gen Virol 1994;75 ( Pt 10):2765-8.

221.Read ML, Singh S, Ahmed Z, et al. A versatile reducible polycation-based system for efficient delivery of a broad range of nucleic acids. Nucleic Acids Res 2005;33:e86.

222.White E. Regulation of the cell cycle and apoptosis by the oncogenes of adenovirus. Oncogene 2001;20:7836-46.

223.Moran E. Interaction of adenoviral proteins with pRB and p53. FASEB J 1993;7:880-5.

224.Ming L, Sakaida T, Yue W, Jha A, Zhang L, Yu J. Sp1 and p73 activate PUMA following serum starvation. Carcinogenesis 2008;29:1878-84.

225.Flinterman M, Guelen L, Ezzati-Nik S, et al. E1A activates transcription of p73 and Noxa to induce apoptosis. J Biol Chem 2005;280:5945-59.

226.Itamochi H, Kigawa J, Kanamori Y, et al. Adenovirus type 5 E1A gene therapy for ovarian clear cell carcinoma: a potential treatment strategy. Mol Cancer Ther 2007;6:227-35.

227.Liu TC, Wang Y, Hallden G, et al. Functional interactions of antiapoptotic proteins and tumor necrosis factor in the context of a replication-competent adenovirus. Gene Ther 2005;12:1333-46.

228.Blagosklonny MV, Pardee AB. The restriction point of the cell cycle. Cell Cycle 2002;1:103-10.

229.Zhou Z, Guan H, Kleinerman ES. E1A specifically enhances sensitivity to topoisomerase IIalpha targeting anticancer drug by up-regulating the promoter activity. Mol Cancer Res 2005;3:271-5.

230.Gomez-Manzano C, Alonso MM, Yung WK, et al. Delta-24 increases the expression and activity of topoisomerase I and enhances the antiglioma effect of irinotecan. Clin Cancer Res 2006;12:556-62.

231.Asano T, An T, Mayes J, Zwelling LA, Kleinerman ES. Transfection of human topoisomerase II alpha into etoposide-resistant cells: transient increase in sensitivity followed by down-regulation of the endogenous gene. Biochem J 1996;319 ( Pt 1):307-13.

232.Torigoe T, Izumi H, Wakasugi T, et al. DNA topoisomerase II poison TAS-103 transactivates GC-box-dependent transcription via acetylation of Sp1. J Biol Chem 2005;280:1179-85.

233.Yamochi T, Aytac U, Sato T, et al. Regulation of p38 phosphorylation and topoisomerase IIalpha expression in the B-cell lymphoma line Jiyoye by CD26/dipeptidyl peptidase IV is associated with enhanced in vitro and in vivo sensitivity to doxorubicin. Cancer Res 2005;65:1973-83.

234.Johnson CA, Padget K, Austin CA, Turner BM. Deacetylase activity associates with topoisomerase II and is necessary for etoposide-induced apoptosis. J Biol Chem 2001;276:4539-42.

235.Solovyan VT. Characterization of apoptotic pathway associated with caspase-independent excision of DNA loop domains. Exp Cell Res 2007;313:1347-60.

236.Marcelli M, Marani M, Li X, et al. Heterogeneous apoptotic responses of prostate cancer cell lines identify an association between sensitivity to staurosporine-induced apoptosis, expression of Bcl-2 family members, and caspase activation. Prostate 2000;42:260-73.

237.Norbury CJ, Zhivotovsky B. DNA damage-induced apoptosis. Oncogene 2004;23:2797-808.

238.Troy CM, Ribe EM. Caspase-2: vestigial remnant or master regulator? Sci Signal 2008;1:pe42.

239.Schumann M, Dobbelstein M. Adenovirus-induced extracellular signal-regulated kinase phosphorylation during the late phase of infection enhances viral protein levels and virus progeny. Cancer Res 2006;66:1282-8.

240.O'Shea C, Klupsch K, Choi S, et al. Adenoviral proteins mimic nutrient/growth signals to activate the mTOR pathway for viral replication. Embo J 2005;24:1211-21.

241.Chang L, Karin M. Mammalian MAP kinase signalling cascades. Nature 2001;410:37-40.

242.Hazzalin CA, Mahadevan LC. MAPK-regulated transcription: a continuously variable gene switch? Nat Rev Mol Cell Biol 2002;3:30-40.

243.Bellett AJ, Jackson P, David ET, Bennett EJ, Cronin B. Functions of the two adenovirus early E1A proteins and their conserved domains in cell cycle alteration, actin reorganization, and gene activation in rat cells. J Virol 1989;63:303-10.

244.Shimwell NJ, Martin A, Bruton RK, et al. Adenovirus 5 E1A is responsible for increased expression of insulin receptor substrate 4 in established adenovirus 5-transformed cell lines and interacts with IRS components activating the PI3 kinase/Akt signalling pathway. Oncogene 2009;28:686-97.

245.Ho LH, Read SH, Dorstyn L, Lambrusco L, Kumar S. Caspase-2 is required for cell death induced by cytoskeletal disruption. Oncogene 2008;27:3393-404.

246.Zhao H, Granberg F, Pettersson U. How adenovirus strives to control cellular gene expression. Virology 2007;363:357-75.